Understanding the role of Cripto in female reproduction

By

Shiva Shafiei

Division of Experimental Medicine

McGill University

Montreal, QC, Canada

January 2020

A thesis submitted to McGill University in partial fulfillment of the requirements of the degree of Doctor of Philosophy

Abstract

Pregnancy is a crucial component of mammalian reproduction comprised of complex sequential events such as implantation, decidualization, placentation and eventually parturition. Perturbation of these events can lead to different clinical issues including infertility and pregnancy complications such as preeclampsia, intrauterine growth restriction (IUGR) and preterm birth. While the major physiological events associated with reproduction have been characterized, there are still many molecular pathways that have yet to be fully elucidated in order to open new avenues toward overcoming and managing these reproductive issues.

Cripto is a member of the epidermal growth factor-Cripto1/FRL1/Cryptic protein family and plays a critical role in embryonic development, stem cell maintenance and tumor progression through TGFβ-dependent and independent pathways. Several studies have suggested that Cripto may also have a role in female reproduction and pregnancy maintenance, but its specific role remains elusive.

In this study we showed the spatiotemporal localization pattern of Cripto in the uterus and at the maternal-fetal interface during the course of mouse pregnancy. We defined that depending on gestational age, different cell types produce Cripto including uterine luminal epithelium, uterine stroma, decidual cells, uterine immune cells, embryonic trophectoderm, spongiotrophoblast cells and labyrinth sinusoidal giant cells.

As Cripto null Knockout (KO) is embryonic lethal, we created a conditional KO (cKO) mouse model in which Cripto was deleted only in the reproductive tissues using a Cre-loxP system. Pregnancy rate and number of pups per litter were evaluated as general fertility indices. We observed a significant decrease in pregnancy rate and litter size with loss of uterine Cripto indicating that Cripto cKO females are subfertile. Although the pre-implantation period was normal in Cripto cKO females, we showed that 20% of cKO females fail to establish pregnancy and an additional 20% of females undergo full litter loss after implantation between day 5.5 postcoitum (d5.5pc) and d8.5pc. During this period, loss of uterine Cripto resulted in impaired uterine decidualization, remodeling and luminal closure and was accompanied by significant

downregulation of Bmp2, Wnt4 and several components of Notch signaling pathway which all are known to be important factors in uterine remodeling and decidualization.

We also found that loss of maternal Cripto in uterine stromal, epithelial and decidual cells during early pregnancy eventually results in defective placentation, altered immune cell composition at maternal-fetal interface, decreased vascularization within maternal decidua and more interestingly in the placental labyrinth and leads to fetal IUGR and fetal death. We further demonstrated that components of the VEGF and Notch signaling pathways are down-regulated in Cripto cKO decidua and placenta potentially contributing to defects in the development of the vasculature at maternal-fetal interface.

In summary, we have shown that maternal Cripto plays critical roles during pregnancy and its loss results in implantation failure, defective uterine remodeling and luminal closure during peri-implantation period, impaired uterine decidualization, as well as severe placentation defects leading to subfertility, IUGR and fetal death.

Resume

La grossesse est une composante cruciale de la reproduction des mammifères, composée d'événements séquentiels complexes tels que l'implantation, la décidualisation, la placentation et finalement la parturition. La perturbation de ces événements peut entraîner différents problèmes cliniques, notamment de l'infertilité et des complications de grossesse dont la pré-éclampsie, le retard de croissance intra-utérin (RCIU) et la naissance prématurée. Bien que les principaux événements physiologiques associés à la reproduction ont été caractérisés, il reste encore de nombreuses voies moléculaires à élucider pour identifier de nouvelles voies pour surmonter et gérer ces problèmes de reproduction.

Cripto est un membre de la famille des facteurs de croissance épidermiques - Cripto1 / FRL1 / Cryptic - et joue un rôle essentiel dans le développement embryonnaire, le maintien des cellules souches et la progression des tumeurs par des voies TGFβ-dépendantes et indépendantes. Plusieurs études ont suggéré que Cripto pourrait également avoir un rôle dans la reproduction féminine et le maintien de la grossesse, mais son rôle spécifique n'est pas encore évident.

Dans cette étude, nous avons montré le schéma de localisation spatio-temporelle de Cripto dans l'utérus et à l'interface mère-fœtus au cours de la grossesse de la souris. Nous avons défini qu'en fonction de l'âge gestationnel, différents types de cellules produisent Cripto, notamment l'épithélium luminal utérin, le stroma utérin, les cellules déciduales, les cellules immunitaires utérines, le trophectoderme embryonnaire, les cellules spongiotrophoblastes et les cellules géantes sinusoïdales du labyrinthe.

Puisque le modèle murin Cripto knock-out nul (KO) est mortel pour l'embryon, nous avons créé un modèle de souris KO conditionnel (cKO) dans lequel Cripto a été supprimé uniquement dans les tissus reproducteurs à l'aide d'un système Cre-loxP. Le taux de gestation et le nombre de souriceaux par portée ont été évalués en tant qu'indices de fertilité générale. Nous avons observé une diminution significative du taux de gestation et de la taille des portées avec la perte de Cripto utérin, ce qui indique que les femelles Cripto cKO sont sous-fertiles. Bien que la

période préimplantatoire soit normale chez les femelles Cripto cKO, nous avons montré que 20% des femelles cKO ne parviennent pas à établir une grossesse et que 20% additionnels des femelles subissent une perte complète de la portée après l'implantation entre le 5ème jour du post-coïtum (d5,5pc) et le d8,5pc. Au cours de cette période, la perte de Cripto utérin a entraîné une altération de la décidualisation, du remodelage et de la fermeture luminale de l'utérus et s'est accompagnée d'une baisse significative de la régulation de Bmp2, de Wnt4 et de plusieurs composantes de la voie de signalisation Notch qui sont toutes reconnues comme des facteurs importants du remodelage et de la décidualisation utérine.

Nous avons également constaté que la perte de Cripto maternel dans les cellules stromales, épithéliales et déciduales de l'utérus en début de grossesse finit par entraîner le développement d'un placenta défectueux, une altération de la composition des cellules immunitaires à l'interface mère-fœtus, une diminution de la vascularisation de la décidue maternelle et, plus de façon encore plus intéressante, dans le labyrinthe placentaire, et conduit à un RCIU fœtal et à la mort fœtale. Nous avons également démontré que les composantes des voies de signalisation VEGF et Notch sont régulées négativement dans les décidues Cripto cKO et dans le placenta, ce qui peut contribuer à des défauts dans le développement de la vascularisation à l'interface materno-fœtale.

En résumé, nous avons montré que le Cripto maternel joue un rôle essentiel pendant la grossesse et que sa perte entraîne un échec de l'implantation, un remodelage utérin défectueux et une fermeture luminale pendant la période de péri-implantation, une altération de la décidualisation utérine, ainsi que de graves défauts de placentation entraînant une sous-fertilité, un RCIU et la mort du fœtus.

Contribution to Original Knowledge

Before our study, limited information was available in the literature related to Cripto and its role in female reproduction. It was shown that Cripto mRNA is consistently detected in endometrial samples from healthy women during the menstrual cycle. Furthermore, the expression of Cripto was seen to be dysregulated in specific human placental and endometrial pathologies. The specific role of maternal Cripto in female reproduction and pregnancy had remained elusive however, as no study had yet been conducted that presents an in-depth analysis of its function in the endometrium.

Our study was the first that utilized a uterine-specific conditional knockout mouse model of Cripto to investigate whether it was a key contributing component in physiologic events of mouse pregnancy such as implantation, uterine decidualization and placentation.

In this study, we have shown the spatiotemporal localization pattern of Cripto in the uterus and at the maternal-fetal interface during the course of mouse pregnancy for the first time. We have defined that depending on gestational age, different cell types produce Cripto including uterine luminal epithelium, uterine stroma, decidual cells, uterine immune cells, embryonic trophectoderm, trophoblast giant cells, spongiotrophoblast cells and labyrinth sinusoidal giant cells. Our study is the first to show that maternal Cripto is required for proper implantation, uterine remodeling and luminal closure, uterine decidualization, as well as placental development.

We have introduced a mouse model to better understand regulation of female reproduction by TGF-β related signaling which also can be considered a good tool to study pathogenesis of pregnancy related issues in humans, aiming towards the development of new treatments for female infertility.

Acknowledgment

Many thanks to my supervisor Dr. Daniel Dufort for giving me the opportunity to be a student in his lab. I greatly appreciate his guidance, patience, support, kindness and more than everything else, the trust that he shows in his students assuring them of their capabilities.

I would also like to thank the members of my thesis committee, Dr. Aimee Ryan, Dr. Indra Gupta and Dr. Bertrand Jean-Claude for their valuable advice and help in the progress of this project.

During my PhD studies over the past 5 years, I have had the pleasure to meet and work with great people, many of them now are my best friends. Dear Taghreed Ayash, Omar Farah, Lisa Starr and Roxane Assaf, thank you for your friendship and your support and thank you for being really cool and fun!

I would like to thank all previous and current members of Dufort lab as well as my friends in other labs at the RI-MUHC : Natasha Mokhtarian, Parinaz Kazemian, Karl-Frédéric Vieux, Luz Esther Ramos Ballesteros, Sibat Anam, Herthana khan, Marie-Helen Godin-Page, Sarah Yull, Mansuba Rana, Karen Carvaleho, , Touhid Al-Rashid and Allyssa Hooper.

I would like to specially thank my dear friends Aida Kasaei and Laleh Abbassi who are like dear members of family to me. Thank you for always being there, in good days and bad.

I have lived far from family for several years in order to complete my studies, but the love and support of my parents Hamideh and Rafie, my sister Shabnam and my brother Nima does not know distance. Love you more than anything else in the world. I would like to dedicate this thesis to my beloved parents as a small sign of gratitude for their unconditional support and encouragement in achieving my goals in life.

Table of Contents

List of Figures and Tables

List of Figures

CHAPTER 1 - BACKGROUND

CHAPTER 2 - Manuscript I

CHAPTER 3 - Manuscript II

List of Tables

Publications and Contribution of Authors

1- **Shiva Shafiei**, Omar Farah and Daniel Dufort. “Maternal Cripto is required for proper uterine decidualization and peri-implantation uterine remodeling”. Manuscript submitted in *Biology of Reproduction*. (Chapter 2: Manuscript I)

The candidate, Shafiei S, performed all the experiments presented in this manuscript except for what is described below. Farah O, performed embryo flushing on day2.5pc and d3.5pc (included in Table 1). Shafiei S, performed the data analysis and figure preparation for all experiments and wrote the primary draft of the manuscript. Farah O. and Dufort D. contributed to editing the manuscript.

2- **Shiva Shafiei** and Daniel Dufort. “Maternal Cripto is critical for proper development of placental vasculature by affecting the level of VEGF and Notch signaling pathway components”. Manuscript in preparation (Chapter 3: Manuscript II)

The candidate, Shafiei S, performed all the experiments presented in this manuscript. Shafiei S, also performed the data analysis and figure preparation for all experiments and wrote the primary draft of the manuscript. Dufort D. contributed to editing the manuscript.

3- Nicole Lustgarten Guahmich, Greg Farber, **Shiva Shafiei**, Dylan Richard McNally, David Redmond, Eleni Kallinos, Heidi Stuhlmann, Daniel Dufort, Daylon James Carl Blobel. “Endothelial deletion of ADAM10, a key regulator of Notch signaling, causes impaired decidualization and reduced fertility in female mice”. Manuscript submitted in *Angiogenesis*.

The candidate, Shafiei S, performed the “Artificial Induction of Decidualization” experiment, presented as Figure 3 in this manuscript. Shafiei S, also assisted in editing the manuscript.

List of Abbreviations

ActRII activin receptor type II

ALK activin receptor-like kinase

AKT protein kinase B

Ang-1 Angitensin-1

Ang-2 Angiotensi-2

BSA bovine serum albumin

BMP bone morphogenetic protein

CR1 Cripro-1

CFC1 Cryptic

CREB cAMP response element-binding protein

CCL chemokine c-c motif ligand

CD cluster of differentiation

χ2 Chi-square

COX cyclooxygenase

c-myc transcriptional regulator Myc-like

CSL proteins acronym for CBF-1/RBPJ-κ in Homo sapiens/Mus musculus respectively, Suppressor of Hairless in Drosophila melanogaster, Lag-1 in Caenorhabditis elegans

cPLA2α cytosolic phospholipase A2α

COUP-TFII chicken ovalbumin upstream promoter transcription factor-2

Dsh Dishevelled

DAB dolichos biflorus agglutinin

DCs dendritic cells

Dll-1 delta like canonical Notch ligand 1

Dll-4 delta like canonical Notch ligand 4

EGF epidermal growth factor

ERK extracellular signal-regulated kinase

EBAF endometrial bleeding associated factors

EGF-CFC epidermal growth factor-Cripto1, FRL1, Cryptic

E2 Estrogen

ER Endoplasmic reticulum

ErbB1 Epidermal growth factor receptor

ErbB4 Erb-b2 receptor tyrosine kinase 4

ES cells embryonic stem cells

Esx-1 extraembryonic, spermatogenesis, homeobox 1

FGF Fibroblast growth factor

FSH Follicle stimulating hormone

FSHR Follicle stimulating hormone receptor

Fzd Frizzled

FRL1 FRIGIDA like 1

GDF1 growth and differentiation factors 1

GDF3 growth and differentiation factors 3

GDF9 growth differentiation factor 9

GnRH gonadotropin releasing hormone

GPI glycosylphosphatidylinositol

GE Glandular epithelium

GSK3 Glycogen synthase kinase 3

gp130 glycoprotein 130

Hand2 heart- and neural crest derivatives-expressed protein 2

Hes-1 hes family bHLH transcription factor 1

Hey-1 hairy/enhancer-of-split related with YRPW motif 1

Hey-2 hairy/enhancer-of-split related with YRPW motif 2

HIF-1α hypoxia inducible factor 1 subunit alpha

HRP horseradish peroxidase

Hh Hedgehog

Hoxa10 Homeobox A10

Hoxa11 Homeobox A11

HUVECs human umbilical endothelial cells

HSPG heparan sulfate proteoglycan

HBEGF heparan-binding epidermal growth factor-like growth factor

Ihh Indian Hedgehog

IL-1β interleukin 1 beta

iPSCs induced pluripotent stem cells

IUGR intrauterine growth restriction

ICM inner cell mass

IL interleukin

IFN-g interferon-gamma

KLF5 Kruppel-like factor 5

LH luteinizing hormone

LPS lipopolysaccharide A

LE Luminal Epithelium

LH Luteinizing hormone

LIF Leukemia inhibitory factor

LRP 5 low-density lipoprotein receptor-related protein 5

LPA3 lysophosphatidic acid receptor 3

LRP 6 low-density lipoprotein receptor-related protein 6

MAPK mitogen activated protein kinase

MCP-1 macrophage chemoattractant protein-1

MMP matrix metalloproteinase

Msx1 Muscle segment homeobox 1

MT1-MMP membrane type-1 matrix metallopeptidase (also known as matrix metalloproteinase 14)

NF-kB nuclear factor-Kappa B

NO nitric oxide

NK natural killer (cells)

Nkx2-5 NK2 homeobox 5

pNK cells or cNK cells peripheral or conventional natural killer (cells)

PBS phosphate-buffered saline

PBST phosphate buffered saline with 0.1% Tween-20

PCR polymerase chain reaction

PI3K phosphatidylinositol 3-kinase

P4 Progesterone

PGs Prostaglandins

PLC Phospholipase-C

Ptc Patched

Ptgs Prostaglandin-endoperoxide synthase

PPAR-δ peroxisome proliferators–activating receptor δ

PIGF phosphatidylinositol glycan anchor biosynthesis

P-SMAD phosphorylated-SMAD

PFA paraformaldehyde

PR progesterone receptor

ROCK Rho-associated kinase

Rbpj recombination signal binding protein for immunoglobulin kappa J region

RXR retinoid X receptor

RT-PCR real time polymerase chain reaction

SMAD sma-and mad-related

SEM standard error of the mean

SGK1 serum and glucocorticoid-inducible kinase 1

STAT3 signal transducer and activator of transcription 3

Tcf/Lef T-cell factor/lymphoid enhancer factor

Tpbpa trophoblast specific protein alpha

TGFβ transforming growth factor β

TNFα tumor necrosis factor alpha

TGC trophoblast giant cells

TDGF-1 teratocarcinoma-derived growth factor-1

Tie-2 TEK receptor tyrosine kinase

uNK uterine natural killer (cells)

uPA plasminogen activator, urokinase

uPAR plasminogen activator, urokinase receptor

VEGF vascular endothelial growth factor

VEGFR vascular endothelial growth factor receptor

WNT wingless-Type MMTV integration site family

Chapter I: BACKGROUND

1) Introduction

Reproduction is a fundamental evolutionary process necessary to sustain life. It can be either asexual, when a new organism is produced only from genetic materials of an individual; or sexual, where two individuals merge their genome to create an offspring (Dey, Lim et al. 2004).

During evolution, viviparity is a landmark. It means development of the embryo inside the body of the parent and eventually birth of the live progeny. A type of viviparity is the mammalian reproduction which is a very complex process and needs to be tightly regulated for the support of the mammalian superior offspring. This process begins with the union of a sperm and an egg (ovum) during fertilization. The one-cell fertilized egg, called zygote at this time, goes through several mitotic cell divisions, forming the embryo and then a more differentiated stage named blastocyst. A highly complex reciprocal interaction between the blastocyst and maternal uterine wall initiates the process of implantation. With the implantation of the blastocyst into uterine wall, pregnancy is established (Wang and Dey 2006).

Pregnancy is a crucial component of mammalian reproduction comprising of complex sequential events such as implantation, decidualization, placentation and eventually parturition (Dey, Lim et al. 2004, Wang and Dey 2006). Perturbation of these events can lead to different clinical issues in humans such as infertility, or pregnancy complications like preeclampsia, intrauterine growth restriction (IUGR) and preterm birth (Wang and Dey 2006). While the major physiological events associated with reproduction have been characterized, there are still many molecular pathways that have yet to be fully uncovered in order to open new windows toward overcoming and managing these reproductive issues (Dey, Lim et al. 2004). Limitations in *in vivo*

research on uterine-embryo interactions in humans has led to relying primarily on animal models, such as the mouse, to identify the molecular mechanisms that facilitate uterine receptivity, embryo implantation, uterine decidualization and placental development (Cha, Sun et al. 2012).

In the beginning of this chapter, major physiologic events of mammalian pregnancy are described. Then the focus of this chapter will be on Cripto, a member of EGF-CFC protein family. Biological functions of Cripto, its interaction with different cell signaling pathways and finally the available information about its possible roles in female reproduction will be described.

2) Female reproductive system in mammalians

The female reproductive tract in mammalians is composed of two ovaries, two oviducts, a uterus, cervix and vagina (Figure 1.1). Each ovary is connected to an oviduct (termed fallopian tube in humans). In humans, the uterus is a hollow pear-shaped organ connected to the fallopian tubes proximally and connected to the cervix distally. In many mammals however, the oviducts are linked to two separate uterine horns that join at the utero-cervical junction. The cervix and the vagina form the birth canal from which the fully developed fetus is born (Rendi, Muehlenbachs et al. 2011). Oocyte (female gamete) maturation and ovulation, spermatozoa (male gamete) transportation, and finally fertilization all happen within the female reproductive tract. In addition, uterus in particular, provides a hospitable environment for the implanting embryo to develop and grow until the time of delivery through birth canal at parturition (Robboy, Kurita et al. 2017).

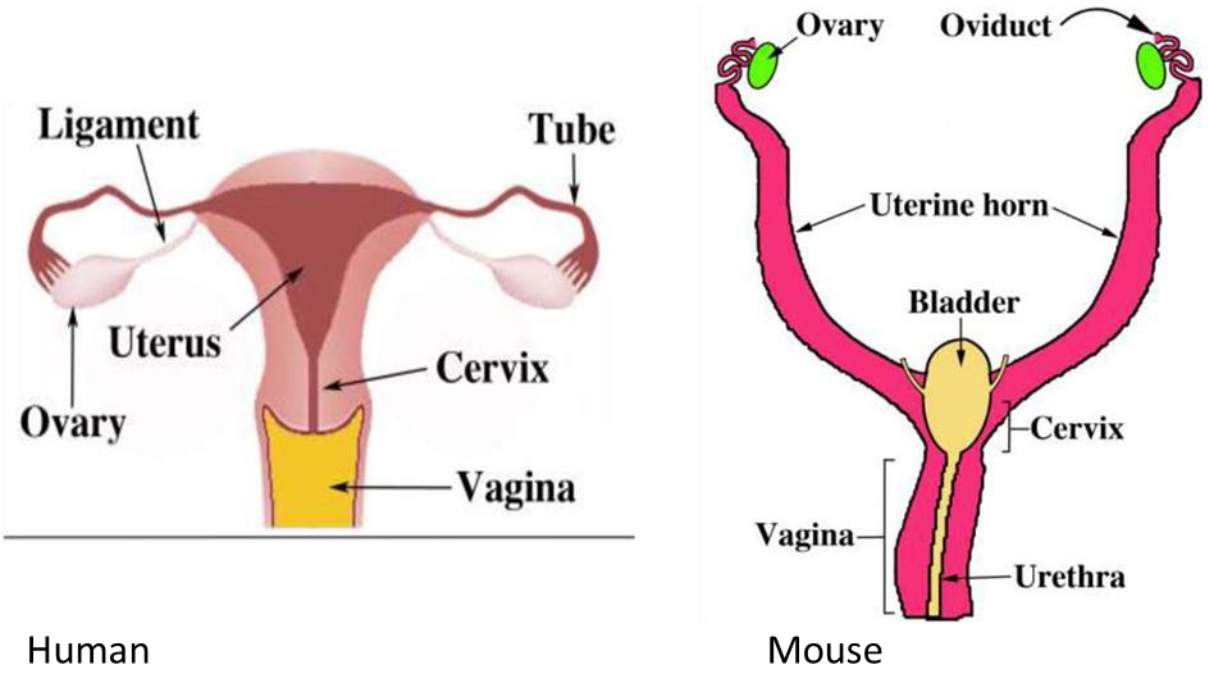

Figure 1.1. Diagrams of female genital tract in human and mouse. Adapted from (Robboy, Kurita et al. 2017).

3) Folliculogenesis, Ovulation and Fertilization

Immature primary oocytes are surrounded by a single layer of flat squamous somatic cells called granulosa cells. This spherical structure is called primordial follicle. At puberty a cohort of primordial follicles are recruited and start to grow. When the single layer of granulosa cells become cuboidal, the follicle is called a primary follicle. Granulosa cells in primary follicles proliferate, subsequently the follicle and oocyte grow in size, the zona pellucida forms around the oocyte and theca cells surround the growing granulosa cells. These changes result in the formation of the secondary follicles (Rimon-Dahari, Yerushalmi-Heinemann et al. 2016). In the tertiary stage follicle (i.e. antral follicle), a fluid filled cavity called antrum forms within the follicle, adjacent to the oocyte. Under the effect of follicle stimulating hormone (FSH) from the

anterior pituitary gland, several tertiary follicles grow rapidly until the largest one becomes the dominant follicle and enters the preovulatory stage and the remaining follicles undergo regression and apoptotic atresia (Rimon-Dahari, Yerushalmi-Heinemann et al. 2016). Unlike humans where there is usually only one preovulatory follicle in each cycle, in litter-bearing species such as the mouse, multiple preovulatory follicles are formed and they have multiple ovulations in each reproductive cycle (Fortune 1994).

In response to luteinizing hormone (LH) from anterior pituitary gland, preovulatory follicles produce increasing amounts of estrogen (E2) which eventually triggers a surge in the secretion of FSH and LH from the anterior pituitary gland. The LH surge results in proteolytic changes in the preovulatory follicular which ends in the rupture of the follicle and release of the maturing oocyte in the abdominal cavity adjacent to the infundibulum of the oviduct. This process is called Ovulation (Rimon-Dahari, Yerushalmi-Heinemann et al. 2016). Following ovulation and release of the oocyte, the remnants of follicle(s) transform into temporary endocrine gland called corpus luteum (plural: corpora lutea). Corpus luteum produces progesterone which is essential for preparation of uterine environment for embryo survival, implantation and maintenance of pregnancy (Fortune 1994).

Ovulated oocyte(s) will be collected by the fimbriae projections of the oviduct infundibulum. The ampullae of the oviduct is where the oocyte will encounter the spermatozoa and fertilization will take place (Demott and Suarez 1992).

4) Uterine histological structure

Uterus is the part of the female reproductive tract in which fetus resides, develops and grows throughout the pregnancy till the right time for birth. In both mouse and human, uterus is composed of an outer muscular compartment termed the myometrium and an internal compartment which is called the endometrium (Rendi, Muehlenbachs et al. 2011). The endometrium lines the uterine inner cavity which is referred to as lumen. The endometrium itself is consisted of three different cell types: the uterine stroma (mainly comprised of fibroblastic stromal cells), endometrial glands and the innermost layer, the luminal epithelium which is a single layer of columnar epithelial cells that directly line the uterine lumen (Figure 1.2).

During the menstrual cycle in human and estrous cycle in mouse, the endometrium undergoes dynamic structural changes in preparation for a potential pregnancy. These cyclic structural changes can be divided into 2 phases: proliferative and secretory. During the proliferative phase (also called follicular phase), under the effect of increasing levels of ovarian estrogen, luminal epithelium, glandular epithelium, stromal cell as well as vascular endothelium proliferate extensively (Wang and Dey 2006). After ovulation, the secretory phase (also called luteal phase) begins where the estrogen-primed endometrium responds to progesterone from corpus luteum by producing and secreting different factors into uterine lumen which renders the uterine fluid hospitable for blastocyst survival and later implantation (Wang and Dey 2006). During the secretory phase in human, some pre-decidual changes take place around the uterine spiral arterioles (described later). At the end of the cycle, corpus luteum regresses and the decline in

progesterone levels results in the shedding of endometrium (menstruation in humans) and a new cycle begins.

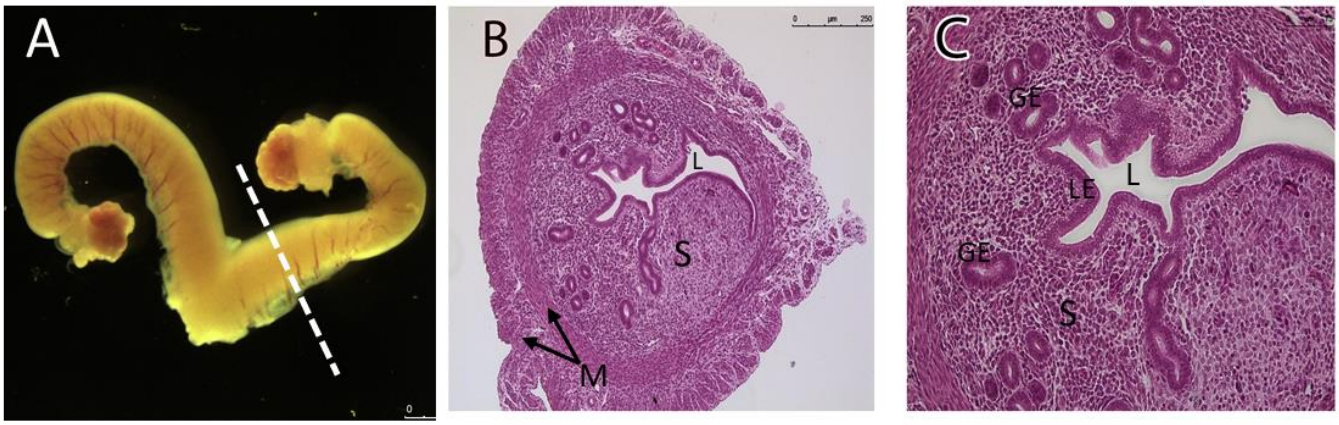

Figure 1.2. Wholemount (A) and transverse sections (B and C) of the mouse uterus. GE: glandular epithelium, L: lumen, LE: luminal epithelium, M: myometrium, S: stroma. B and C, adapted and modified from (Farah, Biechele et al. 2018).

5) Uterine receptivity

Based on the sensitivity of the uterus to implantation and the correlation of this sensitivity with ovarian hormones, three uterine phases have been classified: pre-receptive, receptive, and nonreceptive (refractory) phases (Psychoyos 1973, Dey, Lim et al. 2004)(Figure 1.3). For establishment of pregnancy in mammalians, the uterus needs to enter a specific state where conditions are provided for embryo-uterine communications and initiation of the process of implantation. This state is called the period of uterine receptivity (receptive phase) and lasts only for a limited duration. During the period of receptivity, uterine environment is suitable for supporting blastocyst growth, attachment and eventually implantation (Psychoyos 1973, Yoshinaga 1988, Paria, Huet-Hudson et al. 1993, Dey, Lim et al. 2004). Studies have shown that

ovarian progesterone (and estrogens in some species) along with cytokines, growth factors, transcription factors, lipid mediators and morphogens (produced locally within the uterus) are involved in the process of uterine receptivity (Dey, Lim et al. 2004, Wang and Dey 2006).

The harmonized activity of progesterone and estrogen in mice regulates proliferation and differentiation of uterine cells in a spatiotemporal manner which defines the uterine receptive state for implantation (Huet-Hudson, Andrews et al. 1989). On day 1 of pregnancy in mice (the day of vaginal plug observation), the estrogen released from the preovulatory follicles results in proliferation of uterine epithelial cells (luminal and glandular epithelium). With ovulation and declining of ovarian hormones on day 2, these epithelial cells stop proliferation. With formation of corpora lutea and consequently increasing levels of progesterone from day 3 of pregnancy, stromal cell proliferation initiates and becomes further stimulated by a transient ovarian estrogen secretion on morning of day 4 of pregnancy (Huet-Hudson, Andrews et al. 1989).

In the mouse, uterus is considered pre-receptive on day 1–3 of pregnancy (or pseudopregnancy) whereas it becomes fully receptive on day 4. The chance of implantation declines after day 4, (Song, Lim et al. 2002) and the uterus becomes completely refractory to implantation by day 6 (Figure 1.3).

The Menstrual cycle in humans begins with menses (day 1 of cycle, defined as day minus 14 in Figure 1.3) which is also the start of the proliferative (follicular) phase. During the proliferative phase, under the effect of increasing estrogen levels from growing ovarian follicles, proliferation of the epithelium, stroma and vascular endothelium leads to regeneration of the endometrium. Most of developing endometrial glands become highly coiled during the late

proliferative phase. Ovulation which takes place on day 14 of the menstrual cycle (defined as day 0 in Figure 1.3) defines the end of proliferative (follicular) phase and the start of secretory (luteal) phase (Cha, Sun et al. 2012). In the early secretory (luteal) phase, the corpus luteum is formed from the ruptured follicle and progesterone production commences. In preparation for implantation, the endometrium thickens, glands become secretory and stromal cell around the endometrial spiral arteries (pre-decidualization) and endometrium differentiate and become edematous (Hess, Nayak et al. 2006). During the mid-luteal phase (cycle days 20–24, defined as day 7-10 in Figure 1.3), rising estrogen levels overlapped with high progesterone levels, define the window of receptivity in humans. If at this time, no embryo is present in the uterus, the receptive phase will terminate and uterus enters the refractory phase, followed by regression of corpus luteum, decline of ovarian steroids and restart of the cycle by menstruation on cycle day 0/28 (defined as day 14 in Figure 1.3). On the other hand, implantation of blastocyst, which secretes human chorionic gonadotropin (hGC), prevents the corpus luteum regression, therefore, the progesterone levels are maintained high and the pregnancy is supported (Cha, Sun et al. 2012).

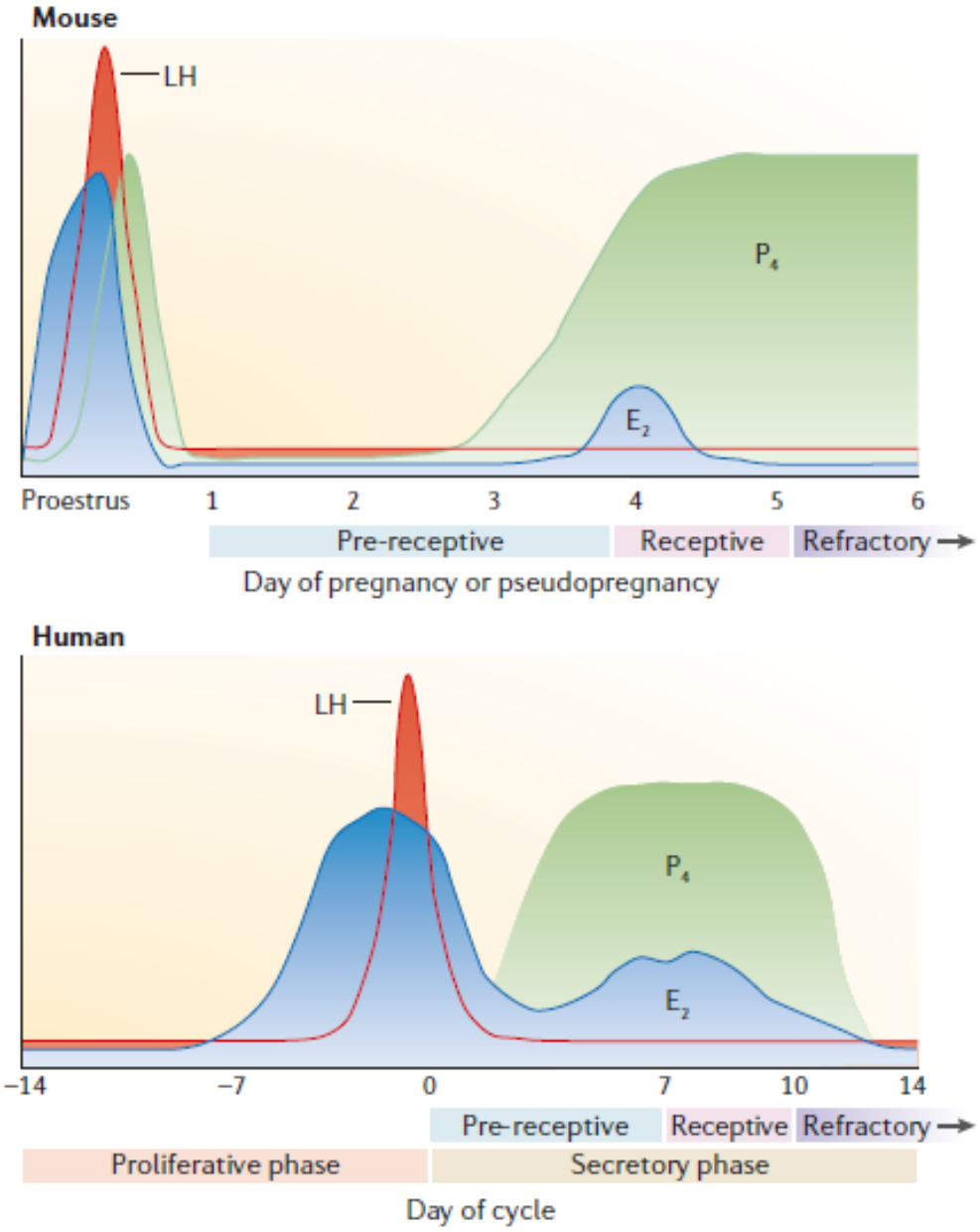

Figure 1.3. The window of uterine receptivity in mice and humans. Adapted from (Wang and Dey 2006).

6) Implantation

The process of embryo implantation is classified into three stages: apposition, adhesion, and invasion (Dey, Lim et al. 2004). During apposition, the embryonic trophectoderm and uterine luminal epithelium align in very close contact without actual attachment. Apposition is followed by the adhesion (attachment) stage where cell surface molecular changes in embryonic trophectoderm and uterine luminal epithelium result in intimate association of these two cell types. At this time, blastocysts cannot be retrieved by flushing the uterine lumen. In invasion stage, the embryonic trophectoderm invades the luminal epithelium and the embryo penetrates the uterine wall, triggering the differentiation of stromal cells to decidual cells (described later) (Dey, Lim et al. 2004). Before the start of apposition stage, a global edema is observed in the uterine stroma of mammals (specially in rodents). This stromal edema leads to the closure of the uterine lumen (described with more details later), resulting in microvilli interdigitation of the trophectoderm and the luminal epithelia (i.e. apposition), followed by closer contact between them in adhesion (attachment) reaction. The first sign of the attachment reaction in the process of implantation appears in the mouse on the evenings of day 4 and in humans approximately on day 8 of pregnancy (Das, Wang et al. 1994, Fazleabas 2007).

7) Uterine luminal closure and embryo orientation

The two poles of the vertical axis of the uterine horn are called mesometrial pole (where the mesometrium, an extension of peritoneum, is attached to the uterus) and anti-mesometrial

pole (the opposite side of mesometrium insertion) (Figure 1.4). During implantation in rodents, blastocysts demonstrate a very consistent orientation in relation to uterine axes. The blastocyst locates at the anti-mesometrial pole of the uterine lumen and at this location, embryonic pole of blastocyst (inner cell mass (ICM)) is facing the mesometrial pole of the uterus (ASSHETON 1894, Wimsatt 1975, Rossant and Tam 2004). As a result, the ICM-abembryonic axis of the rodent blastocyst always coincides with the uterine mesometrial-antimesometrial (M-AM) axis (Wang and Dey 2006). The embryonic orientation at implantation also sets the basis for the future uterus-embryo orientation during post-implantation stages (Smith 1980) when the uterine shape is transformed by the special pattern of stromal decidualization (Smith 1985). Although these morphological features are well characterized, the precise molecular mechanisms that direct the proper embryonic orientation at implantation and later coordinated pattern of uterine stromal decidualization, are still mainly understudied (Wang and Dey 2006, Cha, Sun et al. 2012, Chen, Zhang et al. 2013).

Before embryo attachment to the luminal epithelium, the endometrium experiences extensive changes under the effect of ovarian progesterone and estrogen resulting in regulated stromal edema (Tranguch, Smith et al. 2006, Zhang, Lin et al. 2013) (Figure 1.4). The general irregular shape of the uterine lumen alters from having many randomly oriented epithelial folds, to a very regulated slit-like structure, where its long axis is oriented in a M-AM direction. This transformation in the shape of uterine lumen is called “luminal closure” (Tranguch, Cheung-Flynn et al. 2005, Wang and Dey 2006, Zhang, Lin et al. 2013) (Figure 1.4). Luminal closure provides an initial directional guide which directs the appropriate embryo alignment at the time of implantation, and therefore, sets the base for the later uterus-embryo orientation as well.

Pre-implantation luminal closure in mice is seen on day 4 of pregnancy (day 1 is observation of vaginal plug) and is achieved by a progesterone dominated uterine environment accompanied with a small surge of pre-implantation estrogen secretion (Dey, Lim et al. 2004). The failure of normal luminal closure results in the loss of orientational clues for the embryo within the uterine lumen, potentially leading to the formation of random and incorrect embryo orientation at implantation (Figure 1.4).

After implantation, the closely regulated pattern of stromal decidual remodeling and vasculature development within the implantation site (both described later) may also play a dynamic role in the ultimate establishment of uterine boundary and embryo-uterine alignment optimization which are necessary for embryo survival (Paria, Ma et al. 2001, Daikoku, Song et al. 2004).

As mentioned before, the molecular mechanisms controlling embryo orientation are not well understood. Notch-pathway dependent mechanisms have been shown to be involved in proper luminal closure before embryo-uterine attachment and orientation of uterine-embryonic axis at post-implantation stages (Zhang, Kong et al. 2014). Also at post-implantation stages, regulation of uterine Mmp2 (matrix metalloproteinase 2) expression by Notch signaling pathway ensures the normal decidual remodeling (Zhang, Kong et al. 2014). Uterine Msx1 has also been reported to be important in proper luminal closure and its deletion from the uterus results in the presence of extra uterine crypts for blastocyst attachment and increased pregnancy loss during mid-gestation (Daikoku, Cha et al. 2011).

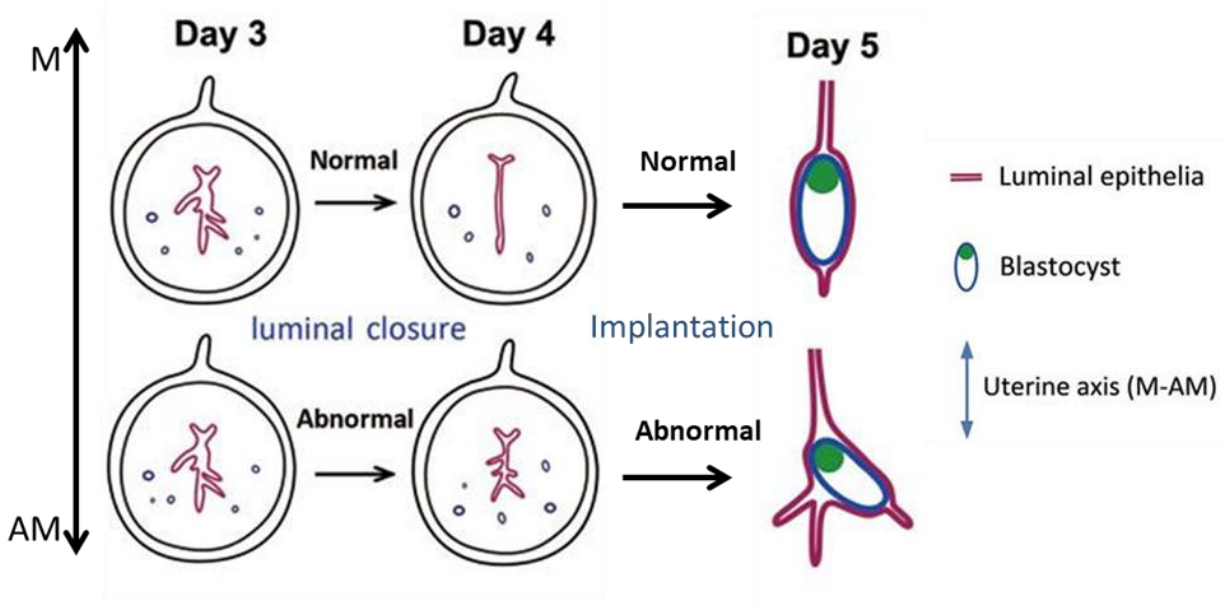

Figure 1.4. Diagram illustrating the process of luminal closure and embryo orientation with respect to uterine Mesometrial-Antimesometrial (M-AM) axis. On day 3 uterine lumen has an irregular shape but on day 4, the process of luminal closure results in the formation of a single slit-like luminal crypt which is oriented in M-AM direction and directs the position of embryo implantation. If luminal closure is defective, there will be multiple branches of luminal crypts and embryo may randomly implant in one of these extra luminal crypts, resulting in abnormal embryo orientation within the uterus (adapted and modified from (Zhang, Kong et al. 2014)).

8) Uterine Decidualization

In human and mouse pregnancy, implantation starts with the attachment of the embryos to the uterine luminal epithelium following by blastocyst trophoblast invasion into the uterine endometrial stroma. Under the control of the ovarian steroid hormones, estrogen and progesterone, the stromal cells adjacent to the implanting embryo experience a major transformation known as decidualization. Uterine stromal decidualization is highly essential for successful implantation and progress of pregnancy. This process includes morphologic,

biochemical and functional changes in endometrial stromal cells driven mainly by the estrogen and progesterone receptors (Ramathal, Bagchi et al. 2010).

In the mouse, blastocysts travel through the oviduct and enter the uterus on day 4 of pregnancy (Paria, Huethudson et al. 1993). As mentioned previously, the blastocyst attachment to the luminal epithelium at the anti-mesometrial pole of the uterus and then penetration into the uterine wall triggers the process of decidualization (Wang and Dey 2006). In mouse, between days 5 and 6 of pregnancy, stromal cells immediately surrounding the implanting blastocyst stop proliferating and go through terminal differentiation into decidual cells. This specific area at every implantation site is called the primary decidual zone (PDZ) which is nonvascular and epithelioid in nature. Stromal cells adjacent to the PDZ keep proliferating and then differentiate into decidual cells making the secondary decidual zone (SDZ). The SDZ is completely developed by day 7 of pregnancy and is defined with terminally differentiated decidual cells which are polyploid and have one or two large nuclei (mono- or bi-nucleated decidual cells) (Tan, Raja et al. 2002). Cellular polyploidy is a unique process in which cells undergo several rounds of DNA replication without cell division (Edgar and Orr-Weaver 2001). It is suggested that decidual cell polyploidy restricts their life span to tolerate the trophoblast invasion/expansion necessary for the support of the growing embryo (Sachs and Shelesnyak 1955, Ansell, Barlow et al. 1974). Terminal differentiation of the decidual cells starts at anti-mesometrial pole in decidual cells surrounding the implanted embryo, while the mesometrial stromal cells are still proliferating to later differentiate and give rise to decidual cells. Mesometial pole decidual cells, which are smaller and less differentiated in general, are critical for proper placentation later in the course of pregnancy (described later) (Dey, Lim et al. 2004).

In pseudo-pregnant mice (i.e. mice mated with vasectomized males), corpora lutea form normally and therefore the effect of ovarian steroid hormones on the uterine environment is maintained, similar to normal pregnancy. During the receptive phase (day 1–4), the receptivity of the pseudo-pregnant uterus to implantation is very similar to normal pregnancy, and blastocyst transfer into the uterine lumen results in normal implantation reactions and consequent decidualization. While blastocysts are the normal triggers of decidualization in mice, several nonspecific stimuli can also initiate the decidual cell reaction in pseudo-pregnant or hormonally prepared uteri. These nonspecific triggers can be infusion of oil or air into uterine lumen, or a mechanical stimuli such as the trauma caused by inserting a needle into uterine lumen (Dey, Lim et al. 2004).

Several roles have been defined for decidual cells including production and secretion of growth factors and cytokines which are involved in support of growing embryo, modulation of immunological state of implantation site and regulation of trophoblast invasion (Ramathal, Bagchi et al. 2010). Another role for decidual cells is believed to be the support of maternal blood vessel formation (described later) at the implantation site to facilitate blood perfusion and nourishment of the developing embryo during early pregnancy (Ni and Li 2017).

In humans, preparation of uterine endometrium for potential pregnancy takes place in every menstrual cycle after ovulation during the late secretory phase. This preparation includes the decidualization of endometrial stroma which first starts in stromal cells surrounding the endometrial spiral arteries (Maruyama and Yoshimura 2008). These differentiated decidual cells, which are larger and rounder than the stromal cells, have unique biochemical and cellular

characteristics and are critical for the support of embryo implantation. Therefore, endometrial decidualization in humans is a prerequisite for successful implantation and pregnancy. If embryo implantation takes place, stromal decidualization expands beyond the spiral arteries surroundings and continues until the maternal decidual compartment is completely formed (Ramathal, Bagchi et al. 2010).

Although the morphologic and developmental transformations that define different stages of embryo implantation and decidualization have been described in both humans and mice, the precise molecular pathways that control the process of decidualization are not well known. Different research groups through their studies have identified several growth factors, cytokines, cytokine receptors, morphogens and transcription factors which are thought to be implicated in establishment of early pregnancy by regulation of uterine receptivity, implantation and decidualization under the control of ovarian steroid hormones (Paria, Reese et al. 2002, Dey, Lim et al. 2004, Lim and Wang 2010, Cha and Dey 2014). Some of these factors are summarized in Figure 1.5 explaining when and in which compartment of the uterus these factors are expressed (Adapted from (Cha and Dey 2014)). For instance, in mouse, Cox2 is expressed by uterine luminal epithelium (LE) early post-mating (day 1), then by LE and uterine stromal at the time of implantation and post-implantation period (day 4-8). Loss of Cox2 in the mouse uterus results in failures in ovulation, fertilization, implantation and decidualization (Lim, Paria et al. 1997, Lim, Gupta et al. 1999). Bmp2 is expressed by uterine stroma and decidual cells starting from early post-implantation period and targeted deletion of Bmp2 from the mouse uterus leads to infertility due to decidualization failure (Lee, Jeong et al. 2007). Another example is Wnt4, expressed by uterine stroma and decidual cells starting from early post-

implantation period. Targeted deletion of Wnt4 from the mouse uterus leads to subfertility due to impaired implantation and decidualization (Franco, Dai et al. 2011).

Figure 1.5. A schematic diagram showing the distinctive and overlapping expression of several transcription factors, morphogens, cytokines and signaling molecules in the **mouse uterus** during pre-implantation period (day 1, 2 and 3), around the time of implantation (day 4) and decidualization period (day 5, 6, 7 and 8). Key signaling pathways for uterine receptivity, implantation, and decidualization in the context of cell types and temporal expression are illustrated. LE, luminal epithelium (blue); GE, glandular epithelium (yellow); LE + GE (green); S, stroma (pink); LE + stroma (purple). Adapted from (Cha and Dey 2014).

Periimplantation gene expression in the uterus

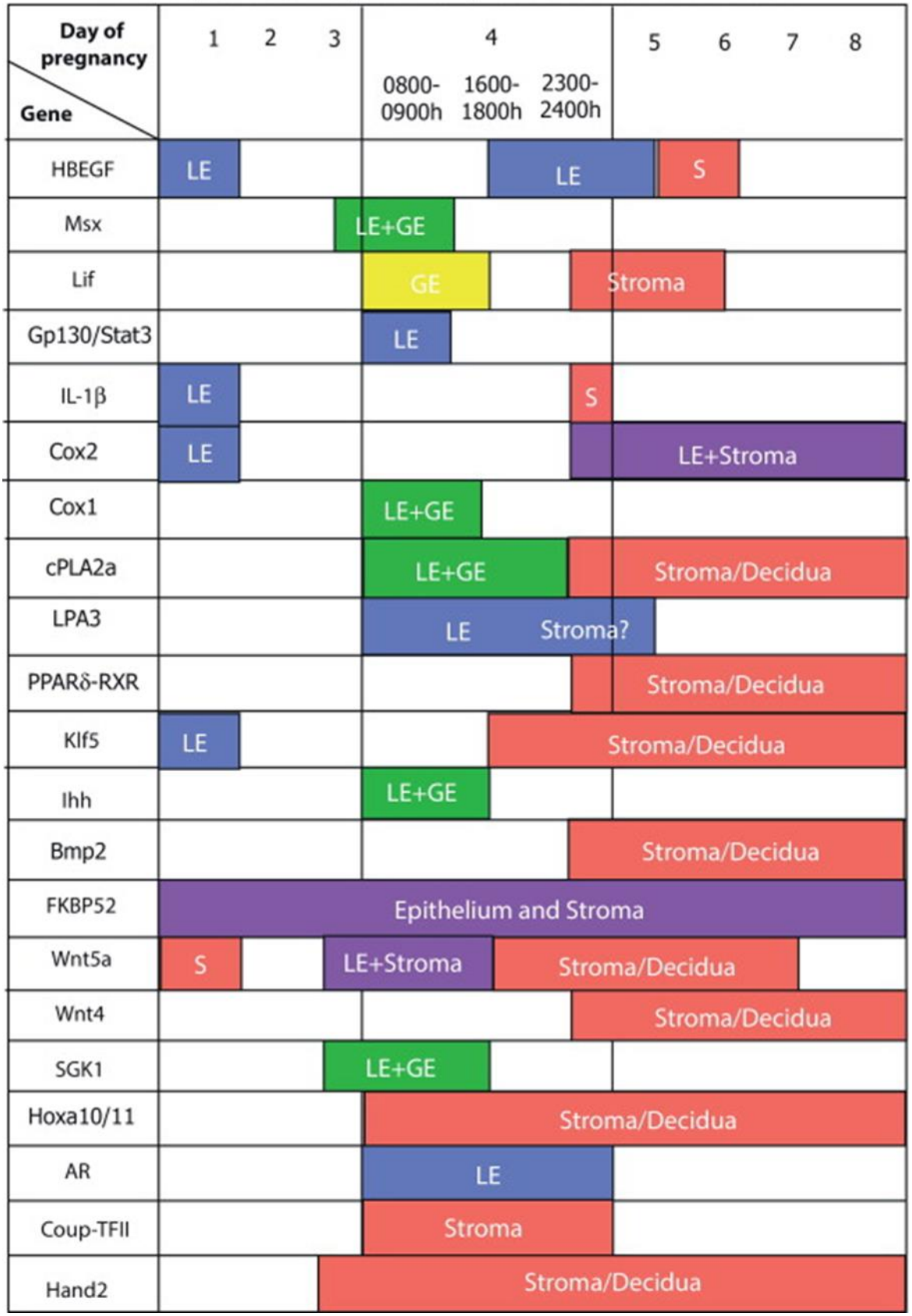

9) Angiogenesis at the implantation sites

Angiogenesis is the process of new vascular structure formation from existing vasculature. Proper angiogenesis within the uterine endometrium is a critical event required for successful embryo implantation, maintenance of early pregnancy and later placental development. Within the pregnant uterus, angiogenesis happens simultaneously with embryo implantation and stromal cell decidualization (Wang and Dey 2006, Plaisier 2011, Cha, Sun et al. 2012).

As mentioned previously, in both mice and humans, the uterine decidua is responsible for the support of the growing embryo during early pregnancy before development of placenta. The decidua provides a scaffold for the developing decidual vascular plexus after implantation. This decidual vascular plexus acts as the first exchange system between the embryo and the maternal blood circulation and is vital for pregnancy maintenance prior to formation of placenta (Rockwell, Pillai et al. 2002, Sengupta, Lalitkumar et al. 2007, Douglas, Tang et al. 2009). Insufficient decidual vascular development in mice leads to pregnancy loss by mid-gestation (Douglas, Tang et al. 2009, Kim, Park et al. 2013). Similarly, inadequate decidual vascularization in humans is associated with infertility as the result of implantation failure and first trimester miscarriages (Torry, Leavenworth et al. 2007, Chen, Man et al. 2017). Insufficient decidual vascular development in humans can also lead to pregnancy complications such as preeclampsia and intrauterine growth restriction because of abnormal placenta formation and function (Maynard, Epstein et al. 2008, Plaisier 2011).

Estrogen and progesterone from the ovaries regulate endometrial stromal decidualization and decidua formation; however, molecular signaling pathways responsible for regulation of

decidual angiogenesis are not yet completely defined. It is believed that implantation site angiogenesis is greatly influenced by vascular endothelial growth factor (VEGF) and angiopoietins (Wang and Dey 2006). It has been shown in mice and non-human primates, that activation of VEGF receptors (VEGFR) by VEGF results in increased uterine vascular permeability and decidual angiogenesis which are essential for embryo implantation (Rabbani and Rogers 2001, Rockwell, Pillai et al. 2002, Sengupta, Lalitkumar et al. 2007). As Prostaglandins (PGs) are known to be involved in angiogenesis in other systems, they are also believed to contribute to angiogenesis in the uterus during pregnancy. In fact, in a study by Matsumoto and colleagues, it was shown that COX2-derived PGs noticeably affect uterine angiogenesis during decidualization through regulation of VEGF and angiopoietin signaling pathways (Matsumoto, Ma et al. 2002).

Besides VEGF signaling, the other well-known regulator of angiogenesis during development and adult life is the Notch signaling pathway. Interaction between VEGF and Notch signaling pathways is known to coordinate angiogenesis both during embryo/fetus development and in the postnatal period (Hellstrom, Phng et al. 2007, Lobov, Renard et al. 2007, Shawber, Funahashi et al. 2007, Harrington, Sainson et al. 2008). Recent studies have also suggested the involvement of Notch1, Notch4, Dll4, and Jagged-1 during decidual angiogenesis and early placentation. It has been shown that Dll4/Notch1 pathway plays a key role in regulating the VEGF/VEGF receptor 2 (VEGFR2) driven decidual angiogenesis (Garcia-Pascual, Ferrero et al. 2014, Shawber, Lin et al. 2015).

The close association between the decidual cells and the developing vascular network in the implantation site suggests that critical regulatory factors originated from stromal/decidual cells

are involved in uterine angiogenesis. Connexins are proteins that form transmembrane channels for direct intercellular communication (Kumar and Gilula 1996). It has been shown that Connexin 43 (Cx43), which is a gap junction element and its expression is regulated by estrogen in the stromal cells of pregnant mouse uterus, greatly influences communication between decidual cells and developing blood vessels during decidualization (Laws, Taylor et al. 2008). A conditional Cx43 knockout mouse was generated by Law and Colleagues to study the role of Cx43 in decidualization (Laws, Taylor et al. 2008). These conditional knockout mice showed impaired stromal differentiation in response to an artificial trigger of decidualization. Furthermore, the absence of the Cx43 gap junctions in these mice caused them to fail to adequately develop the decidual vascular network needed to maintain pregnancy which was accompanied by lack of endothelial cell proliferation and dysregulation of key angiogenic factors, such as VEGF and angiopoietins 2 and 4. *In vitro,* siRNA-mediated knockdown of Cx43 in human endometrial stromal cells (hESC), also resulted in impaired decidualization and gap junction communication. These findings support the idea that gap junctions between decidualizing stromal cells (such as Cx43) most likely control the paracrine secretions of these cells. Among these paracrine factors, some might influence the endothelial cells proliferation and migration, therefore regulating the formation of new blood vessel in the uterus during early pregnancy (Laws, Taylor et al. 2008, Ramathal, Bagchi et al. 2010).

10) Placentation

Mammalian fetal growth and survival is dependent on the placenta which acts as the interface between the maternal and fetal blood circulation for the exchange of nutrients, gas and fetal wastes (Watson and Cross 2005). The placenta forms a barrier that protects the fetus against the maternal immune system. Furthermore, the placenta is the source of hormones that change maternal physiology required for adaptation to pregnancy (Cross, Simmons et al. 2003).

10-1) Development and structure of placenta in mouse and human

Although there are some differences in the details of the human and mouse placental structures, the overall architecture of placenta and the molecular mechanisms controlling placental development are very similar (Rossant and Cross 2001). This similarity has led to the increasing use of mouse models for studying the essential elements of placental development. It can be said that placental development in mice begins as early as the blastocyst stage at embryonic day (E) 3.5 when the embryonic cells are allocated either to the trophectoderm layer or to the inner cell mass (Figure 6) (Watson and Cross 2005). On E4.5, the trophectoderm cells which are not in contact with the inner cell mass (called the mural trophectoderm), differentiate into trophoblast giant cells (analogous to human extravillous cytotrophoblast cells) (Rossant and Cross 2001). In these giant cells, DNA replication continues without cell division (endoreduplication) resulting in polyploidy. The extraembryonic ectoderm and the ectoplacental cone which are diploid cell types, arise from the polar trophectoderm (those cells of the trophectoderm layer which are immediately adjacent to the inner cell mass) (Rossant and Cross 2001) (Figure 1.6). Later, the extraembryonic ectoderm will give rise to the

trophoblast cells of the chorion layer and eventually, the labyrinth. The ectoplacental cone develops into a layer called the spongiotrophoblast which structurally supports the developing labyrinth. The spongiotrophoblast is a compact layer of cells located between the labyrinth and the outer giant cell layer and is equivalent to the column cytotrophoblast of the human placenta (Rossant and Cross 2001). later during the pregnancy, a group of trophoblast cells, called glycogen trophoblast cells, start to differentiate within the spongiotrophoblast layer and invade the maternal decidua (Adamson, Lu et al. 2002).

At E8.0, extraembryonic mesoderm (allantois) extends from the posterior end of the embryo and later at E8.5, in a process called chorioallantoic attachment (or fusion), merges with the chorion (Cross, Simmons et al. 2003) (Figure 1.6). Shortly after, the chorion starts to fold toward mesometrial pole, eventually forming the chorionic villi which creates spaces for the allantois-derived fetal blood vessels to grow into (Cross, Simmons et al. 2003). Concomitantly, the differentiation of chorionic villi trophoblast cells into labyrinth cell types, begins. Syncytiotrophoblasts are multinucleated cells that surround the endothelium of the fetal capillaries within the labyrinth and are formed by the fusion of trophoblast cells (see Figure 7). The maternal blood sinuses within the labyrinth are lined by a mononuclear trophoblast cell type. The labyrinth trophoblast cells, and fetal vasculature together form the structure of the highly branched mouse placental labyrinth villi (comparable with human chorionic villi). The Labyrinth grows and becomes more extensively branched with the progression of pregnancy until birth which in mice is between E18.5 to 19.5 (Adamson, Lu et al. 2002). Labyrinth of the placenta is the placental compartment where the maternal and fetal blood are in very close proximity for the purpose of nutrients, gas and fetal waste transport. The countercurrent

direction of maternal and fetal blood flow within the labyrinth maximizes the efficiency of this transport (Adamson, Lu et al. 2002). Any developmental defect such as aberrant or inadequate vascularization, branching, or dilation of the labyrinth, can result in impaired placental perfusion and insufficient oxygen and nutrient diffusion which negatively affects the fetal growth and survival (Pardi, Marconi et al. 2002).

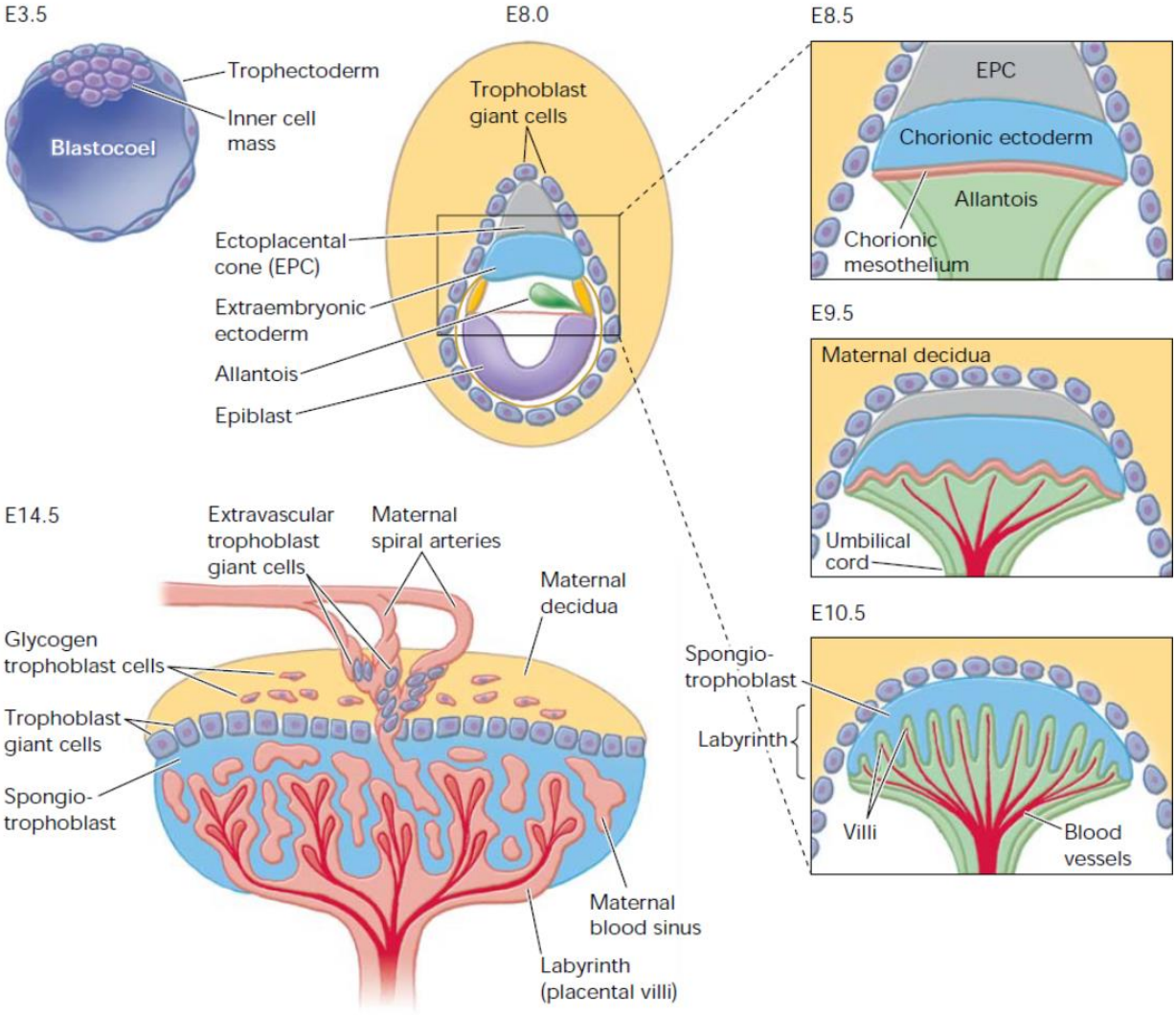

Figure 1.6. Development of the placenta in the mouse. Trophectoderm of the blastocyst (embryonic day (E) 3.5) is the origin of the extraembryonic lineages. Chorioallantoic attachment takes place on E8.0, which is followed by labyrinth branching morphogenesis to form the villi

(E8.5–10.5). The mature placenta (E14.5) is consisted of three layers: the maternal decidua, the fetal spongiotrophoblast, and the fetal labyrinth. Adapted from (Watson and Cross 2005).

As mentiond above, Trophoblast giant cells in rodent's placenta are similar to invasive extravillous cytotrophoblast cells in humans (Figure 7). The distinctive feature of trophoblast giant cells is polyploidy (Zybina and Zybina 1996), as a result of DNA endoreduplication (MacAuley, Cross et al. 1998). Polyploidy is also observed in human extravillous cytotrophoblasts (Berezowsky, Zbieranowski et al. 1995); however, this polyploidy tends to be limited to 4–8 N in contrast to rodents which can be up to 1024 N (Zybina and Zybina 1996). Although the exact role of polyploidy is not known, it has been proposed that it can be involved in the high level of protein production/secretion in TGCs, or contribute to very fast tissue growth with less amount of energy as TGCs have a short life span (Hu and Cross 2010, Fox and Duronio 2013). Polyploidy in TGCs is different from what is seen in syncytiotrophoblast cells, as the latter is the result of trophoblast cell fusion and the formation of a multi-nucleated syncytium where each nucleus remains diploid (2N) (Figure 1.7).

The extent of uterine invasion and the factors secreted by the invasive and endocrine trophoblast cells is different between species. Trophoblast giant cells and glycogen trophoblast cells of rodents invade several hundred microns into the uterus (Adamson, Lu et al. 2002), which compared to the extravillous cytotrophoblast cells of human is rather a short distance. On the other hand, similar cell adhesion molecules and extra cellular matrix degrading

proteinases, which are involved in trophoblast invasion in humans, are also expressed by mouse trophoblast giant cells (Cross, Werb et al. 1994).

The role of the spongiotrophoblast layer of the rodent placenta (also called junctional zone), is not well established. However, some cells in the spongiotrophoblast layer (and also in their precursor, the ectoplacental cone) are able to give rise to giant cells. Considering this characteristic, the spongiotrophoblasts are analogous to column cytotrophoblast cell (Figure 1. 7) of the human placenta which give rise to invasive trophoblasts (i.e. extravillous cytotrophoblasts).

The function of labyrinth layer of the mouse placenta is totally analogous to the chorionic villi of the human placenta (Rossant and Cross 2001). The uterine endometrial epithelium is eliminated at maternal-fetal interface in both rodents and primates. This phenomenon results in direct contact of trophoblast cells with maternal blood (hemochorial placenta). Fetal endothelial cells, a layer of mononuclear trophoblasts and one (in primates) or two (in rodents) layer(s) of syncytial trophoblasts lie between maternal and fetal blood cells within the placental villi (Figure 1.7) (Cross, Baczyk et al. 2003).

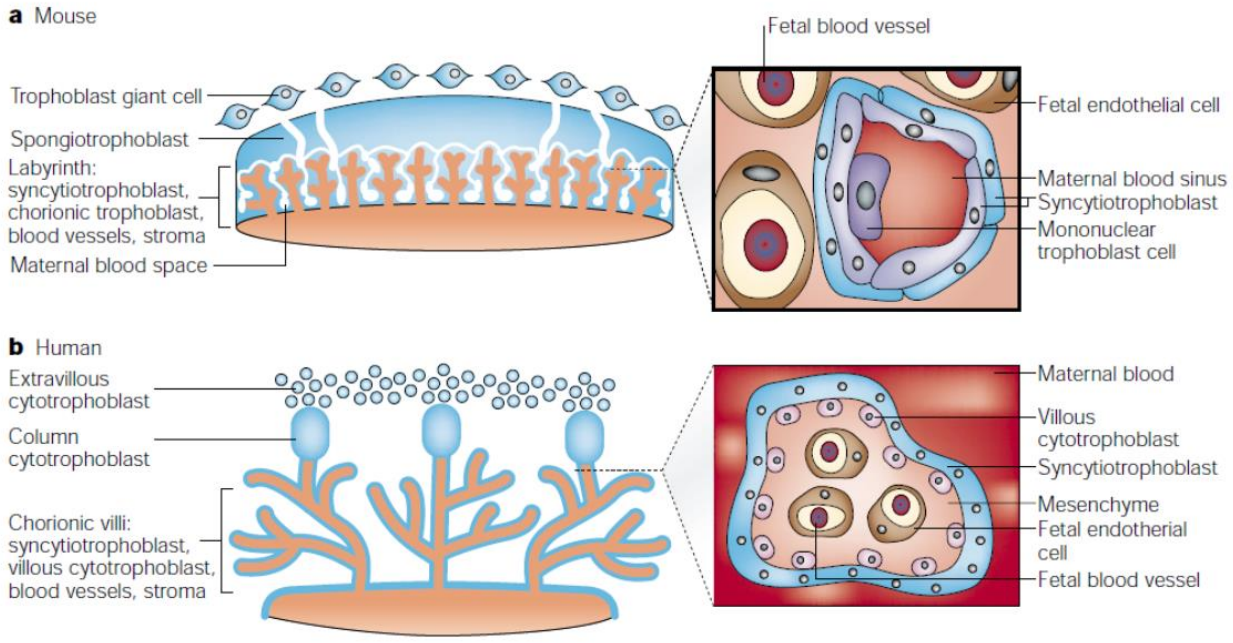

Figure 1.7. Comparative anatomy of the mouse and human placenta. Schematic structure of the mouse placenta (a) and human placenta (b). Trophoblast-originated structures are depicted in blue and mesoderm-derived tissues are shown in orange. The insets in each section details the number and type of cell layers separating maternal and fetal blood. Adapted from (Rossant and Cross 2001)

10-2) Remodeling of maternal vasculature

Uterine blood supply is provided by uterine arteries that enter the uterus from uterine mesometrium. After crossing the myometrium, every uterine artery branches into several spiral arteries in the maternal decidua. These spiral arteries are the source of maternal blood delivered to the placenta (Adamson, Lu et al. 2002). The characteristic feature of the hemochorial type placenta is the elimination of maternal endothelial cells and their replacement by fetal trophoblast cells. This means that the maternal vasculature in the

placenta are lined by fetal trophoblast cells and not the endothelial cells. This replacement is observed starting from the level of spiral arteries, then in all the subsequent maternal vasculature network, up to the last level of trophoblast lined vessels which are those veins that carry nutrient- and oxygen-depleted blood out of the placenta joining the uterine veins (Rai and Cross 2014). Trophoblast invasion into maternal vasculature begins around E8.5 in mice where spiral artery trophoblast giant cells (SpA-TGC) invade into the lumen of the arteries and replace the endothelial lining. In humans, within first 12 weeks of pregnancy, extravillous cytotrophoblast cells start to invade the spiral arteries (Rossant and Cross 2001, Cross, Hemberger et al. 2002, Harris 2010).

Besides endothelial cell replacement by trophoblast cells, another feature of spiral arteries in normal pregnancies is the lack of vascular wall smooth muscles which makes these vessels very dilated. This phenomenon is referred to as “arterial remodeling” of pregnancy. Spiral artery remodeling is thought to occur due to trophoblast cell invasion. In normal pregnancies in humans, extravillous cytotrophoblast cells are observed within and around the remodeled spiral arteries (Ashton, Whitley et al. 2005, Whitley and Cartwright 2009). Interestingly, ablation of SpA-TGCs in mice results in failure of the spiral arteries dilation which shows that SpA-TGCs are in fact required for the process of spiral artery remodeling (Hu and Cross 2011).

Uterine natural killer cells (uNK cells, described later) are also believed to play a part in spiral artery remodeling as they are observed around the spiral arteries in human placenta (Hazan, Smith et al. 2010, Robson, Harris et al. 2012) and also uNK cell deficient mice have shown vascular remodeling defects (Croy, Ashkar et al. 2000, Greenwood, Minhas et al. 2000). More

recent studies suggest that both SpA-TGCs and uNK cells are involved and their interaction is essential in the regulation of spiral artery remodeling (Chakraborty, Rumi et al. 2011).

Loss and replacement of endothelial and smooth muscle cells of the spiral artery wall which results in the dilation of the artery, is suggested to be based on degradation of the extracellular matrix that supports these cells. Loss of supporting extracellular matrix can eventually lead to endothelial and smooth muscle cells aberrant function or apoptosis. Studies have shown the up-regulation of some matrix metalloproteinase in the mouse trophoblast cells that are differentiating into TGCs (Armant and Kameda 1994, Whiteside, Jackson et al. 2001, Lei, Hohn et al. 2007). Similarly, it has been shown that in human pregnancy, along with the invasion of extravillous trophoblast cells into the uterine decidua, signs of extracellular matrix loss appears (Rai and Cross 2014). Uterine NK cells may also be involved in extracellular matrix degradation because they have been shown to produce several proteases (Harris 2010). The trophoblast cells might also be able to induce vascular endothelial and smooth muscle cell apoptosis either by secretion of apoptosis associated cytokines and growth factors or by direct cell–cell contact signal (Whitley and Cartwright 2009).

Different subtypes of TGCs line the maternal blood space in the mouse placenta. These subtypes are classified based on their location, developmental origin, function, and their differential expression of Prolactin related hormones (Simmons, Fortier et al. 2007, Gasperowicz, Surmann-Schmitt et al. 2013). Despite their different gene expression patterns, all various TGC subtypes look similar in morphology where they have a large polyploid nucleus,

large cytoplasm and extensive golgi and endoplasmic reticulum (Bevilacqua and Abrahamsohn 1988, Zybina and Zybina 1996).

In the human placenta, the characteristics of extravillous cytotrophoblast cells which invade the arteries, are well studied (Zhou, Genbacev et al. 2003). However, there is little known about the features of extravillous cytotrophoblast cells that line the intervillous space and venous outflow of human placenta (Rai and Cross 2014).

10-3) Immune cells at the maternal-fetal interface during placentation

Maternal immune cells residing within the uterine decidua are important players in regulating the interactions of maternal and fetal originated cells within placenta. The balanced composition of these immune cells and their specific functions are essential not only for proper development and function of placenta, but also in preventing the maternal immune system from attacking the placenta as a foreign organ. In addition, these immune cells within the maternal decidua are important in defeating placental infections (Erlebacher 2013).

In humans, immune cells infiltrate the endometrium after ovulation. With no implantation, the number of endometrial immune cells decline during menstruation. In case of fertilization and implantation, the number of immune cells increases within decidua until up to the 20th week of pregnancy (van den Heuvel, Chantakru et al. 2005). In the first trimester, 30% of stromal cells in the human uterus are leukocytes (Bulmer, Morrison et al. 1991). The decidual immune cell composition during this period is: uNK cells (~70%), macrophages (~20%) (Trundley and Moffett 2004, Bulmer, Williams et al. 2010) and T cells (~10–20%). Dendritic cells (DCs), B cells,

and NKT cells are rare (Bulmer, Williams et al. 2010). Recruitment and initiation of human uNK cell differentiation, which happens in every menstrual cycle, is regulated by uterine stromal cells in response to ovarian hormones and does not need exposure to semen components or trophoblast-derived factors (Henderson, Saunders et al. 2003). After fertilization and implantation, in addition to ovarian hormones, trophoblasts-derived cytokines and chemokines are thought to also play a role in the recruitment of uNK cells and macrophages to implantation sites (Hanna, Wald et al. 2003, Wu, Jin et al. 2005, Fest, Aldo et al. 2007).

It is believed that uterine decidual cells and uNK cells have extensive interactions that are highly critical for proper regulation of developing implantation site. An example of these interactions is the production of interleukin 15 (IL-15) by decidual cells which is an essential growth factor for uNK cells. The expression of IL-15 in decidual cells is controlled by leukemia inhibitory factor (LIF) from uterine stromal cells and luminal epithelium and also by ovarian progesterone (Shuya, Menkhorst et al. 2011, Vacca, Mingari et al. 2013).

Uterine NK cells are the source of different growth factors, angiogenic factors, chemokines, cytokines and proteases, including VEGF, Ang-1, Ang-2, TIE-2, PlGF, uPA, uPAR and MT1-MMP (see Abbreviations section) (Albertsson, Kim et al. 2000, Lash, Schiessl et al. 2006, Naruse, Lash et al. 2009). In addition to modulation of maternal immune system, uNK cells are proposed to be involved in uterine stromal decidualization, regulation of trophoblast invasion, maternal vascular remodeling and induction of apoptosis in endovascular cytotrophoblasts (EVT) (Plaisier 2011).

Uterine NK cells are also the main leukocytes of the mouse decidua, for example they make up 75% of all uterine immune cells on day 8.5 of pregnancy. With embryo implantation and start of uterine stromal decidualization in mice, the number of immune cells within the implantation site starts to increase noticeably from gestational (pregnancy) day 5.5 (gd5.5), peaking around gd12.5. This increase is specially the result of a drastic rise in the number of uNK cells (Croy, Zhang et al. 2010). In mice, the initial localization of uNK cells is to the decidua basalis (uterine decidua on the mesometrial pole of the implantation site that is the site for later placental development) (Croy, Zhang et al. 2010). Around gd6.5 (beginning of mid-gestation) a pregnancy specific structure develops between the two layers of myometrium on the mesometrial side of each implantation site and lasts until around gd15. This structure which is called the mesometrial lymphoid aggregate of pregnancy (MLAp) and surrounds the major vessels entering and leaving each implantation site, is also mostly composed of uNK cells (Zhang, Chen et al. 2012). uNK cells are highly proliferative in the early decidua which at least partly contributes to their drastic increase in number. By mid-pregnancy (dg8.5-dg9.5), uNK cells in the decidua basalis stop proliferation but the MLAp uNK cells still continue to divide (Paffaro, Bizinotto et al. 2003, Croy, Chen et al. 2012). After mid-pregnancy, the number of uNK cells starts to drop such that at the time of parturition, 90% of the peak numbers of uNK cells are already lost and the rest will be shed at birth with the placenta (Peel 1989, Delgado, McBey et al. 1996). By flow cytometry (Yadi, Burke et al. 2008), periodic acid–Schiff (PAS) staining and reactivity with Dolichos biflorus agglutinin (DBA) lectin (Paffaro, Bizinotto et al. 2003, Zhang, Yamada et al. 2009), different subsets have been defined for mouse uNK cells. PAS-positive, DBA-negative uNK cells are the main type during early pregnancy. However, PAS-positive, DBA-

positive cells, which have distinct appearance and functions compared to blood and splenic NK cells, become more abundant with the advancement of the pregnancy and by mid-gestation comprise around 90% of the total uNK cell population. These cells have high angiogenic activities within the maternal-fetal interface (Chen, Zhang et al. 2012, Degaki, Chen et al. 2012, Lima, Croy et al. 2012). The PAS-positive, DBA-negative uNK cell subset produces interferon-gamma (IFN-g) which is a critical cytokine required for spiral artery remodeling (discussed earlier) (Chen, Zhang et al. 2012). Despite their name, neither mouse nor human uNK cells display any cytotoxic activities (Lima, Croy et al. 2012, Felker, Chen et al. 2013) (Kopcow, Allan et al. 2005).

The other important immune cells at maternal-fetal interface during mouse and human pregnancy are Macrophages. During the first trimester of human pregnancy, 10% of the immune cells within uterine decidua are macrophages. They act as immunosuppressive modulators, have phagocytic functions and also are implicated in control of placental growth (Bulmer, Pace et al. 1988). IL-10 produced by uNK cells and decidual cells along with decidual cell-originated CSF1 (a specific growth factor for macrophages) are thought to be involved in regulating decidual macrophage differentiation and anti-inflammatory function (Lin, Mosmann et al. 1993, Qiu, Zhu et al. 2009, Thaxton and Sharma 2010, Svensson, Jenmalm et al. 2011). Although it is not known whether decidual macrophages can in turn modulate functions of uNK cells, the close physical proximity of both these immune cell types to the remodeling spiral arterioles in humans, is suggestive of the reciprocal interaction between them at least in the context of placental vascular remodeling (Erlebacher 2013)(Figure 1.8).

Uterine dendritic cells (uDCs) are also present at the implantation site with low frequency. These antigen-presenting cells are capable of modulating implantation site angiogenesis by producing angiogenic growth factors and chemokines. Uterine NK cell-derived signals are important for maturation of uDCs and consequently their proangiogenic and antiangiogenic actions (Barrientos, Tirado-Gonzalez et al. 2009).

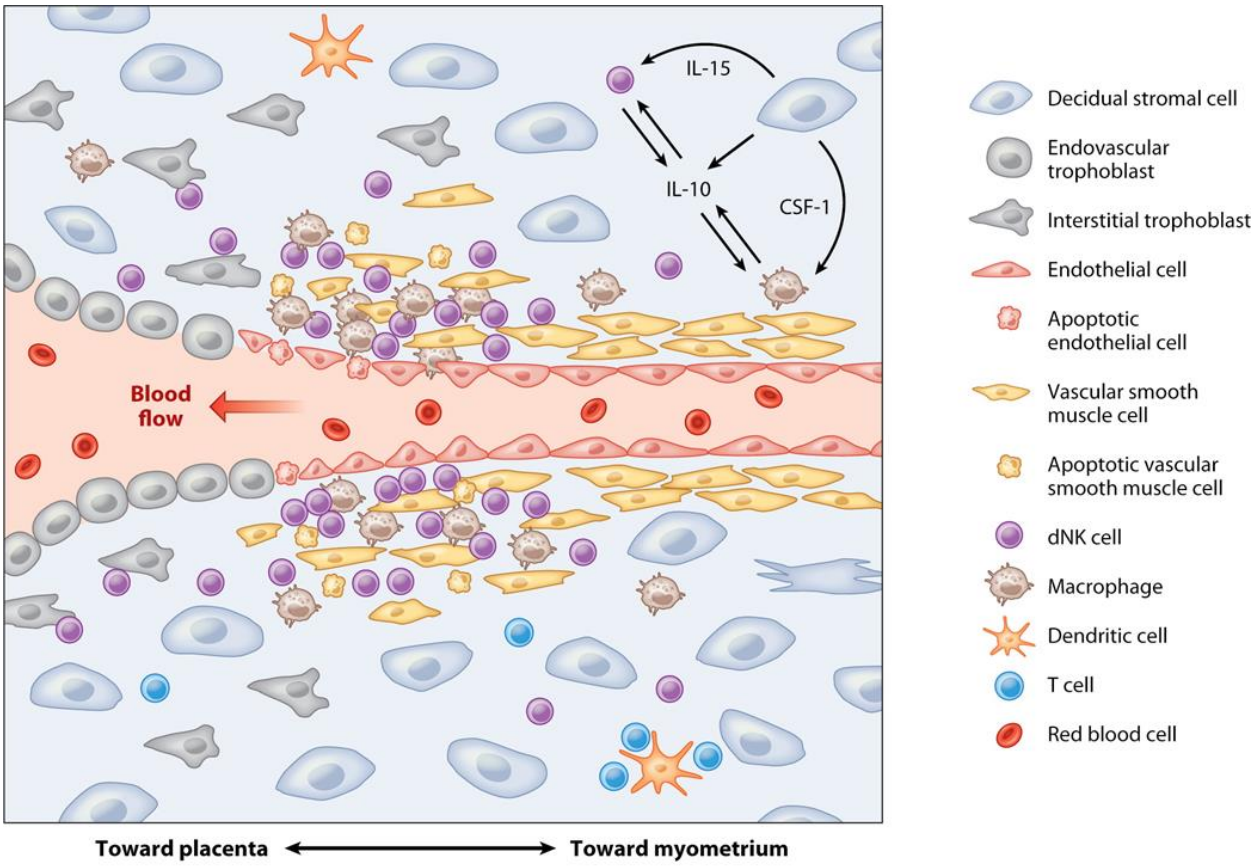

Figure 1.8. Schematic illustration of the main cell components of human decidua during first trimester of pregnancy. In the first phase of remodeling of spiral arteriols while the vascular smooth muscle cells and endothelial cells separate and degenerate, decidual natural killer (dNK) cells and macrophages are gathered around the vessel wall. Then the vessel is invaded by a subset of extravillous trophoblasts termed endovascular trophoblasts. Those extravillous trophoblasts that remain within the decidual stroma are called interstitial trophoblasts. Some cytokines and their potential cellular sources and target cell types are also shown here. Adapted from (Erlebacher 2013)

10-5) placental defects and pregnancy complications

Defects in placental development, such as abnormalities in villi/labyrinth morphogenesis, compromised trophoblast differentiation or invasion and impaired remodeling of maternal vasculature, can result in pregnancy loss or serious pregnancy complications including intra-uterine growth restriction (IUGR) and pre-eclampsia (Rossant and Cross 2001).

Pre-eclampsia, a pregnancy related disease that affects 3–5% of pregnant women, is a leading cause of maternal and neonatal mortality and morbidity. Pre-eclampsia is associated with compromised differentiation and invasion of extravillous cytotrophoblast cells and impaired vascular remodeling of maternal spiral arteries which results in placental insufficiency because of reduced placental blood flow (Fisher 2004). However, because of the very complex nature of this disease, it is often difficult to the determine the primary underlying defect with high certainty (Cross 2010).

When defective placentation is the underlying cause of the first trimester miscarriages or severe IUGR cases, the placental defect is usually related to reduced branching of the chorionic villi and its vasculature (Rossant and Cross 2001). IUGR affects 4–7% of births and is associated with increased neonatal morbidity and mortality. Maternal smoking, fetal chromosomal abnormalities, infectious diseases as well as defective placental development can lead to fetal IUGR. Assessment of placentas from human IUGR fetuses revealed considerably lower number of capillaries within the placental villi compared to normal pregnancy. The area of capillaries was also significantly decreased in these IUGR placentas (Krebs, Macara et al. 1996). These vascular deficiencies are suggested to be the result of decreased expression of angiogenic

factors leading to decreased vascular branching and angiogenesis within the placental villi (Kingdom and Kaufmann 1997, Plaisier 2011).

12) Cripto: Introduction

Human Cripto-1 (CR-1), which is also named teratocarcinoma-derived growth factor-1 (TDGF-1), is a member of the Epidermal Growth Factor-CRIPTO/FRL1/CRYPTIC protein family (EGF-CFC protein family)(Saloman, Bianco et al. 2000). Orthologous genes have been identified in chicken (Colas and Schoenwolf 2000), zebrafish (Zhang, Talbot et al. 1998), mouse (Cr-1) (Dono, Scalera et al. 1993) and Xenopus (FRL1)(Kinoshita, Minshull et al. 1995). Mouse Cryptic (Cfc1) and human Cryptic (CFC1) are genes related to Cripto-1 (Shen, Wang et al. 1997, Bamford, Roessler et al. 2000, Shen and Schier 2000, de la Cruz, Bamford et al. 2002). Cripto-1 was initially isolated from human NTERA-2 and mouse F9 undifferentiated teratocarcinoma cells (Ciccodicola, Dono et al. 1989). EGF-CFC protein family members are composed of an NH2-terminal signal peptide, a modified EGF-like domain, a conserved cysteine-rich region (CFC motif) and a short hydrophobic COOH-terminus that has sequences for glycosylphosphatidylinositol (GPI) attachment and cleavage (Minchiotti, Parisi et al. 2000) (Figure 1.9). All EGF-CFC proteins have a site for O-linked fucosylation within the EGF-like domain. This fucosylation site is required for the EGF-CFC protein to function as the co-receptors of the TGF-ß protein family members, i.e. Nodal, growth and differentiation factors 1 and 3 (GDF1/3) (Schiffer, Foley et al. 2001, Yan, Liu et al. 2002). EGF-CFC proteins are mostly cell membrane-associated glycoproteins that are composed of 171 to 202 amino acids with molecular weights between18 to 21 kDa. However,

the molecular weight can vary greatly because of the presence of multiple glycosylation sites. Mouse and human Cripto-1 proteins are mostly reported to be 24, 28 and 36 kDa in size but the range is from 14 to 60 kDa with differential glycosylation at N- and O-linked asparagine and serine residues (Strizzi, Bianco et al. 2005). The mouse and human Cripto-1 protein can be released from cell membrane attachment as a soluble form by treatment of cells with phosphatidylinositol-specific phospholipase C (PI-PLC) (Minchiotti, Parisi et al. 2000) or GPI-phospholipase D which remove the GPI anchor (Watanabe, Hamada et al. 2007). These soluble forms are reported to have biological activities (Strizzi, Bianco et al. 2005). All known biological activities of Cripto-1 protein is conserved as long as the peptide still has its intact EGF domain and CFC domain (Minchiotti, Manco et al. 2001, Yan, Liu et al. 2002). Several studies have shown the presence of both Cripto-1 forms (cell membrane-associated and soluble) *in vivo* and also in multiple cell lines, suggesting that Cripto-1 can function both as a coreceptor in cis and as ligand in trans mechanisms (Yan, Liu et al. 2002). However, the biological functions which are possibly activated differentially by the soluble Cripto-1 versus cell-associated form, are not yet defined (Minchiotti, Manco et al. 2001, Yan, Liu et al. 2002).

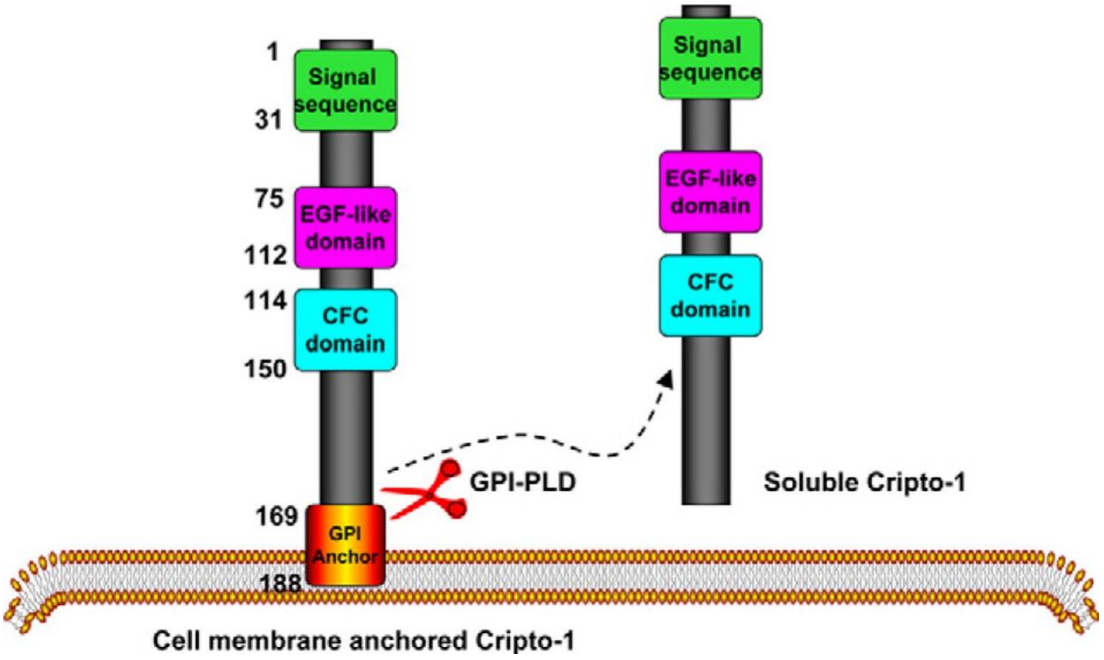

Figure 1.9. Schematic diagram of human Cripto-1 protein (amino acids 1-188). Cripto-1 is a GPI-anchored membrane protein that can be cleaved by glycosylphosphatidylinositol phospholipase (GPI-PLD) and released into the supernatant of the cells as a soluble protein. Adapted from (Bianco, Rangel et al. 2010).

During mouse embryonic development, Cripto-1 is first detected in the inner cell mass and extraembryonic trophoblast cells of the day 4 blastocyst. The highest Cripto-1 expression is observed during gastrulation in the epiblast cells which are going through epithelial to mesenchymal transition (EMT) to migrate and give rise to the mesoderm and endoderm layers of the gastrula. It has been shown that during embryogenesis, Cripto-1 is involved in the formation of the primitive streak, anterior/posterior axis patterning, mesoderm and endoderm cell allocation during gastrulation, and establishment of left/right asymmetry of developing organs (Meno, Ito et al. 1997, Ding, Yang et al. 1998). Cripto-1 null knockout mouse embryos die between day 7.5 to 10.5 of embryogenesis because of defective gastrulation and axis

patterning (Ding, Yang et al. 1998, Xu, Liguori et al. 1999). Expression of Cripto-1 is limited to the developing heart after day 8 of embryogenesis. Interestingly, genetic studies in humans with ventricular septal defects (one of the most common congenital heart defects), are indicative of Cripro-1 involvement in the pathogenesis of this disease (Wang, Yan et al. 2011).

In adults, Cripto-1 expression is very minimal and is probably limited only to the stem cell population of adult tissues (Bianco, Rangel et al. 2010). Studies have defined Cripto-1 as an important factor in dynamics and maintenance of embryonic stem (ES) cells and induced pluripotent stem cells (iPSCs) and suggested that it can be considered as a potential stem cell marker (Bianco, Rangel et al. 2010).

Numerous studies have revealed an essential role for Cripto-1 in the etiology and progression of several types of human tumors. Cripto-1 was found to be expressed in a population of cancer stem cells (CSCs). It is also involved in epithelial-mesenchymal transition during tumorigenesis where it helps tumor cell migration, invasion and angiogenesis (Klauzinska, Castro et al. 2014). High levels of Cripto-1 expression has been detected in several types of human tumors, such as colon, gastric, pancreatic, breast, cervical, endometrial, ovarian, testis, lung, skin and bladder carcinomas (Bianco, Strizzi et al. 2005).

13) Regulation of Cripto expression

Studies have defined several regulatory mechanisms for the control of Cripto-1 expression during embryogenesis and oncogenesis (Figure 10). T-cell factor/lymphoid enhancer factor (Tcf/Lef)-binding elements and Smad-binding elements are detected in the promoter region of

the Cripto-1 gene (Hamada, Watanabe et al. 2007, Mancino, Strizzi et al. 2008) which make Cripto-1 a potential primary target gene of the Wnt/ß-catenin (Morkel, Huelsken et al. 2003) and TGF-ß superfamily signaling pathways, respectively. Hypoxia-responsive elements within the Cripto-1 promoter are also detected. During embryonic cardiac differentiation, hypoxia can directly enhance Cripto-1 expression by binding of the transcriptional factor HIF-1α to this regulatory element (Bianco, Cotten et al. 2009). In addition, Cripto-1 is a direct downstream target gene of Oct-4 and Nanog. Genome wide chromatin immunoprecipitation analysis has shown the presence of Oct-4 and Nanog binding sites within the Cripto-1 promoter region (Loh, Wu et al. 2006, Watanabe, Meyer et al. 2010).

The other factors that are suggested to directly regulate Cripto-1 expression include: Nkx2-5 by binding to Nkx2-5 binding elements within Cripto-1 promoter (up-regulation) (Behrens, Ren et al. 2012), orphan nuclear receptor germ cell nuclear factor (GCNF) by binding to a DR0 motif in the human Cripto-1 promoter (down-regulation) (Hentschke, Kurth et al. 2006), LRH-1 orphan nuclear receptor by binding to the Cripto-1 promoter to change DNA methylation status of the Cripto-1 gene (up-regulation) (Bianco, Castro et al. 2013) and finally miR-15a/16 cluster by binding to miR15a/16 binding element in the Cripto-1 mRNA 3'UTR (translational repression) (Chen, Hou et al. 2014).

14) Cripto interactions with multiple signaling pathways

Cripto-1 interacts with and/or activates several signaling pathways (Figure 1.10). It is an obligatory co-receptor for the Smad-dependent signaling of transforming growth factor-ß family members, Nodal, GDF1 and GDF3. Moreover, Cripto-1 can activate Smad-independent signaling pathways PI3K/Akt and MAPK. Cripto-1 can also enhance canonical Notch and canonical Wnt/ß-catenin signaling pathways by acting as a chaperone protein (Klauzinska, Castro et al. 2014).

Figure 1.10. Control of Cripto-1 expression and cross talk of the Cripto-1 with multiple signaling pathways. Cripto-1 promoter has Tcf/Lef binding elements which make Cripto-1 a downstream target gene of the Wnt/β-catenin canonical pathway. Hypoxia regulates Cripto-1 expression in ES cells through binding of HIF-1α to specific HREs within the Cripto-1 promoter. Activated Smad-2/Smad-3/Smad-4 complex can regulate Cripto-1 gene expression by binding to specific Smad binding elements within the Cripto-1 promoter. Oct-4 and Nanog (ES cells specific transcription factors) directly regulate Cripto-1 expression by binding to the Cripto-1 promoter. Cripto along with ALK4/7 and ActRII makes the required receptor complex for Nodal, GDF1 and GDF3 Smad-dependent signaling. Cripto-1 binds to Glypican-1 and induces activation of c-Src/MAPK/AKT pathways, leading to cell motility and EMT. Within ER/Golgi membranes, Cripto-1 directly interacts with Notch receptors and improves cleavage of the Notch extracellular domain, leading to increased activity of Notch signaling. Non-canonical Wnt11 binds to Cripto-1/Frizzled 7 (Fzd7)/Glypican-4 receptor complex and induces β-catenin stabilization. CBP: CREB binding protein; EMT indicates epithelial to mesenchymal transition; ER, endoplasmic reticulum; GDF, Growth and Differentiation Factor; HRE: hypoxia regulatory elements; LRP, low-density lipoprotein receptor-related protein; MAPK, mitogen activated protein kinase; Notch ICD, Notch intracellular domain; SBE: Smad binding elements; TBE: TCF/LEF binding elements; TCF/LEF: T-cell factor/lymphoid enhancer factor. Adapted from (Bianco, Rangel et al. 2010)

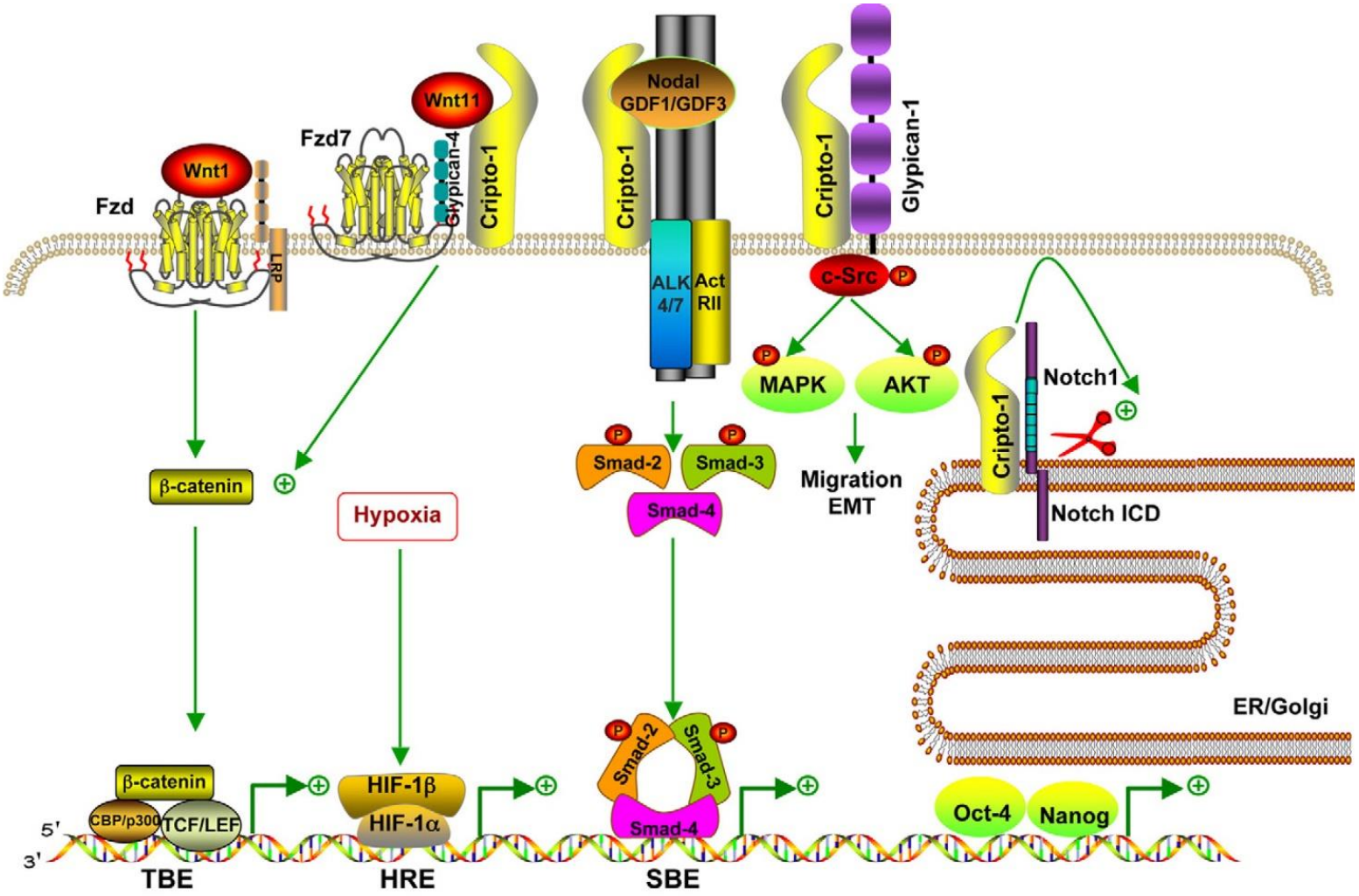

Cripto-1 promoter region

14-1) Cripto-1 and TGF-beta signaling pathway

Signaling by TGF-ß superfamily members is critical during multiple aspects of embryonic development and organogenesis such as gastrulation, correct positioning of the three main body axes, generation of organ asymmetries and organ-specific morphogenesis (Wu and Hill 2009). After embryonic life, these factors have been discovered to be involved in formation and progression of various tumors in several different tissues (Tian and Schiemann 2009, Wu and Hill 2009). The TGF-ß family includes the TGF-ßs, the bone morphogenetic proteins (BMPs), Activins, GDFs and Nodal (Wu and Hill 2009). As described earlier, by binding to specific TGF-ß binding elements within the Cripto-1 promoter, TGF-ß family members can directly regulate Cripto-1 expression (studied in human embryonal carcinoma cells and in human colon cancer cells) (Mancino, Strizzi et al. 2008).

14-1-1) Cripto-1 and Nodal

Cripto-1 can directly bind to Nodal and ALK4 and acts as the obligatory co-receptor for Nodal Smad-dependent signaling (Schier 2009). Binding of ligands (Nodal/GDF-1/GDF-3 homodimers or heterodimers) to the cell membrane associated receptor complex (composed of Cripro-1, Activin type I (ALK4 or ALK7) and Activin type II serine threonine kinase receptors), results in phosphorylation of Smad-2 and Smad-3. Phosphorylated Smad-2 and Smad-3 bind to Smad-4, creating a transcriptional complex, and translocate to the nucleus to trigger transcription of specific target genes (Schier 2009) (Figure 7). During embryogenesis, Nodal/Cripto-1 signaling is critical in the formation of the primitive streak, anterior/posterior axis specification, mesoderm and endoderm formation during gastrulation, and establishment of left/right asymmetry of developing organs (Meno, Ito et al. 1997, Ding, Yang et al. 1998).

Nodal signaling has been shown to be involved in embryo implantation, uterine decidualization, placental development and timing of parturition (Papageorgiou, Nicholls et al. 2009, Park and Dufort 2011, Park, DeMayo et al. 2012, Park and Dufort 2013, Heba, Park et al. 2015). Therefore, through its interaction with Nodal signaling, Cripto-1 could also be implicated in these reproductive processes.

14-1-2) Cripto-1 and GDF1/GDF3

Cripto-1 can also bind GDF-1 and GDF-3 and act as their required co-receptor for Smad-dependent signaling (Figure 10) (Bianco, Strizzi et al. 2005). GDF-1 and GDF-3 are co-expressed with Nodal during embryogenesis (Andersson, Bertolino et al. 2007). GDF-1 works together with Nodal during embryogenesis in establishing the Left/Right body asymmetry (Andersson, Reissmann et al. 2006). GDF-3, besides functioning as a Nodal-like ligand, is a direct BMP inhibitor in early embryos and pluripotent stem cells (Levine and Brivanlou 2006). Furthermore, GDF-3 along with Cripto-1, are specific markers for a population of uncommitted ES cells with high self-renewal capacity (Hough, Laslett et al. 2009).

14-1-3) Cripto-1 and other TGF-ß superfamily members

Lefty is a Nodal signaling inhibitor during embryogenesis which is also highly expressed in stem cells (Tabibzadeh and Hemmati-Brivanlou 2006, Bendall, Hughes et al. 2009). Lefty can bind to Cripto-1 and prevent its binding to Nodal. Furthermore, Lefty can also directly interact with Nodal, preventing Nodal binding to Cripto-1 and its receptor complex (Bianco, Strizzi et al. 2005). Cripto-1 can interact with Activin A, Activin B and TGF-ß1 and interfere with the binding

of these ligands to their receptor complexes. This interactions result in decreased TGF-ß1, Activin A and B signaling in multiple cell lines (Klauzinska, Castro et al. 2014).

14-2) Cripto-1 and Notch Signaling pathway

The Notch signaling pathway is critical during different stages of normal embryonic development and embryonic stem cell fate determination (Wang, Li et al. 2009). Notch signaling has also been implicated in dynamics of adult stem cells in several tissue types such as skin, intestines, hematopoietic and central nervous system (Wang, Li et al. 2009). Furthermore, dysregulation of Notch signaling has been reported in many types of human tumors (Wang, Li et al. 2009).

Notch genes encode for large transmembrane receptors: Notch1, Notch2, Notch3 and Notch4. Notch receptors interact with membrane-bound Notch ligands: Delta-like1 (Dll1), Delta-like3 (Dll3), Delta-like4 (Dll4), Jagged1, and Jagged2. The interaction of Notch ligands and receptors is of juxtacrine type meaning the ligand within membrane of one cell, binds to the Notch receptor on the neighboring cell membrane. The ligand-receptor bound triggers the proteolytic cleavage of the intracellular domain (ICD) of Notch receptor. This is followed by translocation of the cleaved ICD into the cell nucleus where together with CLS proteins (called CBF1 or RBPJ-k in mouse and human), it forms the required DNA binding complex, leading to transcription of downstream target genes of Notch signaling pathway such as Hes-1, Hey, NF-kB, cyclin D1, and c-myc (Wang, Li et al. 2009).

Similar to Nodal/Cripto-1 Smad-dependent signaling, Notch signaling pathway is also involved in determination of Left/Right asymmetry during embryo development (Wang, Li et al. 2009). In addition, there is a binding site for CSL proteins (Notch signaling pathway transcriptional complex) within the Nodal gene promoter. These facts suggest a cross talk of Notch signaling pathway with the Nodal/Cripto-1 signaling pathway for regulation of Left/Right asymmetry during embryogenesis (Krebs, Iwai et al. 2003, Raya, Kawakami et al. 2003) and also in development of malignancies (Postovit, Seftor et al. 2007).

In another type of Cripto-1 interaction with Notch signaling, Cripto-1 binds to Notch receptors and enhances their cleavage by protein convertases (Nagaoka, Karasawa et al. 2012). By immunoprecipitation assay, it was shown that Cripto-1 directly binds to all four mammalian Notch receptors mainly in the endoplasmic reticulum/Golgi complex (Figure 10) (Watanabe, Nagaoka et al. 2009). Cripto-1 binding to Notch1 results in localization of Notch1 in the lipid raft fraction of the endoplasmic reticulum and improves the cleavage of the Notch1 extracellular domain by a furin-like convertase. This is similar to what Cripto-1 does in the regulation of Nodal processing where it recruits proprotein convertases required for cleaving the Nodal precursor. Enhanced cleavage of Notch-1 induced by Cripto-1 binding, results in increased ligand-induced activation of Notch signaling (Watanabe, Nagaoka et al. 2009). Interestingly, knockdown of Cripto-1 expression in mouse and human embryonal carcinoma cells resulted in decreased activity of Notch signaling (Watanabe, Nagaoka et al. 2009).

With regards to female reproduction, it has been shown that Notch signaling and its components are critical for proper peri-implantation uterine remodeling and luminal closure,

uterine stromal decidualization, development of uterine vasculature at implantation sites as well as proper development of placental vasculature (Afshar, Jeong et al. 2012, Zhang, Kong et al. 2014, Kim, Huang et al. 2015, Shawber, Lin et al. 2015). Through its interactions with Notch signaling, Cripto-1 can potentially be involved in these processes as well.

14-3) Cripto-1 and Glypican-1, PI3/Akt and MAPK pathways

Cripto-1 can act as a ligand for Glypican-1. Glypican-1 is a membrane-associated heparan sulfate proteoglycan (HSPG) that has been shown to function as a coreceptor for several different growth factors such as Wnts, FGF and HBEGF (Bianco, Strizzi et al. 2003). Binding of Cripto-1 to Glypican-1 results in activation of a cytoplasmic tyrosine kinase called c-Src and subsequently activation of mitogen-activated protein kinase (MAPK) and phosphatidylinositol 3-kinase (PI3K)/Protein Kinase B (Akt) signaling pathways (Figure 10). Through these two pathways, Cripto-1 regulates/promotes cell proliferation, motility, survival, epithelial-to-mesenchymal transition (EMT), and also stimulates angiogenesis (Bianco, Strizzi et al. 2005).

Activation of MAPK and PI3K/Akt pathways by Cripto-1 was shown to be independent of Nodal and ALK4, because in EpH4 mouse mammary epithelial cells that lack ALK4 and in MC3T3-C1 osteoblast cells that lack Nodal expression, Cripto-1 was able to activate MAPK and AKT phosphorylation and activation (Bianco, Adkins et al. 2002).

By protein interaction studies, it was found that a 78 kDa Glucose Regulated Protein (GRP78) is a specific cell surface binding partner and signaling co-factor for Cripto-1 (Shani, Fischer et al. 2008, Gray and Vale 2012). In recent studies it has been suggested that Cripto-1 binding to

GRP78 might be generally required for its functions. It was shown that knocking down GRP78 or treatment with an anti-GRP78 antibody (that prevents Cripto-1 and GRP78 binding), results in the blocking of Cripto-1 effects on Activin A, Activin B, TGF-β1 and also inhibits the activation of Nodal signaling and c-Src /MAPK/ PI3K/Akt pathways by Cripto-1 (Kelber, Panopoulos et al. 2009, Miharada, Karlsson et al. 2011, Spike, Kelber et al. 2014).

14-4) Cripto-1 and Wnt signaling pathway

Canonical Wnt signaling is important for various developmental processes starting from early embryonic patterning to the development of specialized organ tissues (Yang 2012). Several studies have shown that Wnt signaling and Wnt proteins are critical for the maintenance of ES cells as well as adult tissue stem cells (stem cells in hair follicle, skin, colon crypts, hematopoietic and the nervous systems) (Nusse, Fuerer et al. 2008). In addition, activation of Wnt signaling pathway has been implicated in initiation and progress of several types of carcinomas such as skin, brain, intestine and liver (Reya and Clevers 2005, Nusse, Fuerer et al. 2008).

Wnt proteins are secreted ligands which their binding to the related cell surface receptor complex (comprised of LRP-5/6 and Frizzled family of receptors), leads to stabilization of β-catenin, the Wnt signaling pathway cytoplasmic transducer. Stabilized β-catenin translocates into the nucleus where together with Tcf/Lef and other transcriptional activators, results in expression of the target genes (Reya and Clevers 2005).

Several studies presented evidence for interaction between Cripto-1 and the canonical Wnt/β-catenin signaling pathway both through Nodal related signaling and independent of Nodal. As described earlier, canonical Wnt/β-catenin signaling pathway can directly regulate the expression of mouse and human Cripto-1 genes (Figure 10) during embryonic development and in colon carcinoma cells (Morkel, Huelsken et al. 2003). It was also shown that in β-catenin or Wnt3 null knockout mouse embryos, Cripto-1 expression is down-regulated. Wnt/β-catenin signaling was also shown to directly regulate the expression of Nodal during Left/Right axis formation in Xenopus and Chick embryos (Rodriguez-Esteban, Capdevila et al. 2001, Yokota, Kofron et al. 2003). On the other hand, Nodal/Cripto-1 signaling can activate the Wnt/β-catenin signaling through phosphorylated Smad-2 and p300 (independent of Smad-4) (Hirota, Watanabe et al. 2008).

It has been shown that Cripto-1 ortholog in Xenopus (FRL-1) can act as a co-receptor for Wnt11 in a receptor complex composed of glypican-4 and Xenopus frizzled receptor 7 (Xfz7), leading to stabilization of β-catenin and activation of canonical Wnt signaling (Figure 10) (Tao, Yokota et al. 2005). Another example of Cripto-1 and Wnt signaling interaction, is the binding of Cripto-1 to Wnt co-receptors LRP-5 and LRP-6, leading to enhancement of their binding to Wnt3a and increased activity of canonical Wnt/β-catenin signaling (Nagaoka, Karasawa et al. 2013).

The reciprocal cross talk between Cripto-1 and Wnt/β-catenin signaling pathway potentially can result in a positive feed-forward loop which in the context of tumor progression might be of great importance (Bianco, Rangel et al. 2010).

Recent studies are increasingly suggestive of critical roles for Wnt signaling in multiple reproductive events including pre-implantation embryo development, blastocyst activation for implantation, post-natal uterine development, uterine decidualization and placental development (Li, Kannan et al. 2007, Sonderegger, Pollheimer et al. 2010, Zhang and Yan 2016, Farah, Biechele et al. 2017, Farah, Biechele et al. 2017, Farah, Biechele et al. 2018). Therefore, Cripto-1 can potentially affect these reproductive events through interactions with canonical Wnt signaling.

16) Cripto and angiogenesis

In the context of tumorigenesis, evidence suggests that Cripto-1 might be involved in modulation of tumor angiogenesis. Bianco and colleagues (Bianco, Strizzi et al. 2005) showed that besides improving the proliferation, migration and invasion of human umbilical endothelial cells (HUVECs), Cripto-1 stimulates the differentiation of these cells into vascular-like structures. They also showed that enhancement of HUVECs proliferation by Cripto-1 is dose-dependent and is mediated through activation of c-Src and PI3-K/AKT signaling pathways in these cells. The angiogenic activity of Cripto-1 in endothelial cells was shown to be independent of VEGF, because in vitro use of a specific VEGF receptor inhibitor did not block the angiogenic effect of Cripto-1 on HUVECs (Bianco, Strizzi et al. 2005). Furthermore, in an in vitro system where recombinant Cripto-1 protein was able to induce formation of microvessel structures in silicone cylinders filled with Matrigel, the use of an anti-Cripto-1 monoclonal antibody for blocking Cripto activity, strongly inhibited this microvessel formation. These findings suggest

that Cripto-1 directly an regulate angiogenesis (Bianco, Strizzi et al. 2005). Likewise, Cripto-1 overexpression in MCF-7 human breast cancer cell xenografts resulted in enhancement of tumor neovascularization in vivo (Bianco, Strizzi et al. 2005).

18) Cripto and female reproduction

Most of available studies related to Cripto and its biological/pathological functions are in the context of embryo development, stem cells and oncogenesis. There is very limited information related to Cripto and its association with female reproduction and pregnancy.

18-1) Cripto expression in mammary gland during pregnancy and lactation

Cripto-1 plays an important role in development of mouse mammary gland (Kenney, Huang et al. 1995) and is expressed in the growing terminal end buds in the mammary gland of the virgin mouse. Interestingly, Cripto-1 expression in the mammary gland increases during mouse pregnancy and lactation (Kenney, Huang et al. 1995).

The presence of a 28 kDa Cripto-1 protein has been detected in Human milk (Bianco, Wechselberger et al. 2001). Furthermore, purified Cripto-1 protein from human milk stimulated the phosphorylation of MAPK in non-transformed NMuMG mouse mammary epithelial cells suggesting that Cripto-1 in human milk might be involved in regulating mammary gland development during pregnancy and lactation (Bianco, Wechselberger et al. 2001).

18-2) Cripto is detectable in the human uterus during menstrual cycle

Cripto-1 mRNA has been detected in the endometrial samples of healthy women during all stages of the menstrual cycle. This expression is moderately higher during the secretory phase of the cycle (Papageorgiou, Nicholls et al. 2009). Localization of Cripto-1 protein in human endometrium is similar to Nodal protein, meaning that Cripto protein signal is observed in luminal epithelium, glandular epithelium and endometrial stroma (Papageorgiou, Nicholls et al. 2009, Torres, Florio et al. 2009). The level of Cripto-1 protein in the luminal and glandular epithelium of human endometrium is comparable in all phases of the menstrual cycle. However, the level of Cripto-1 protein in the endometrial stroma decreases significantly during the late-secretory phase and menstruation, compared to the rest of the cycle. Cripto-1 protein also shows a distinct localization around the human uterine spiral arterioles (Papageorgiou, Nicholls et al. 2009). The expression pattern and localization of Cripto within the mouse uterus during the estrous cycle or pregnancy have not been studied yet.

18-3) Aberrant endometrial expression of Cripto in women with endometriosis

Endometriosis is an estrogen-related uterine disease that affects between 5-10 % of women. It is defined by the presence of endometrial tissue outside of the uterine cavity and can cause pelvic pain and infertility in 35-50 % of affected women. The ectopic endometrial tissue is mostly seen within the peritoneal cavity on the ovaries, fallopian tubes, uterine serosa and even intestines (Vercellini, Vigano et al. 2014). This disease is thought to be multifactorial, but the exact pathogenic mechanisms are not yet known (Burney and Giudice 2012).

Although possible involvement of Cripto-1 in pathogenesis of endometriosis has not been investigated yet, dysregulation of endometrial Cripto-1 expression in women with endometriosis has been observed in several studies. Tores and colleagues observed that while there was no difference in the level of ActRII and Nodal mRNA expression in patients with and without endometriosis, Activin A expression in eutopic endometrium of patients with endometriosis was significantly higher than in controls (7-10 folds higher $P < .001$) and Cripto-1 mRNA was prominently lower in both eutopic and ectopic endometrium of women affected by endometriosis compared with eutopic endometrium from healthy women as control (0.03 and 0.14 fold change, respectively, $P < .001$) (Torres, Florio et al. 2009). In another study, Rocha and colleagues observed a lack of endometrial cycle-related variations of Cripto-1 mRNA expression in eutopic and ectopic endometrium of women with endometriosis (Rocha, Carrarelli et al. 2011). In another study by De la Cruz and colleagues, mRNA expression, protein level and localization of some components of Nodal signaling pathway including Nodal, Cripto-1, SMAD3, pSMAD3 and SMAD4 were compared in eutopic endometrium of women with and without endometriosis. Among these factors, the only observed difference was the expression of Cripto-1 that was significantly lower (fold change 0.27, $P < .05$) in the endometriosis group compared to Control group (Dela Cruz, Del Puerto et al. 2015).

18-4) Aberrant expression of Cripto at metrnal-fetal interface in some human placental complications

Neither in humans nor in mice, the expression and spatiotemporal localization of Cripto in maternal-fetal interface during placentation and in mature placenta has been defined yet.

However, there are some studies that have showed some evidence for Cripto-1 presence at maternal-fetal interface in both biological and pathological placental conditions.

Microarray analysis of cultured mouse ectoplacental cone cells, obtained from gestational day 7.5 (a day before start of placental formation in mice), demonstrated that the Cripto-1 is expressed by these cells (Hoshida, Gorjao et al. 2007).

In humans, Bandeira and colleagues presented immunohistological evidence for Cripto-1 protein at maternal-fetal interface at 36 and 38 weeks of gestation in normal pregnancies. Cripto-1 protein was observed in extravillous cytotrophoblast cells and also in some endothelial cells or perivascular areas (Bandeira, Borbely et al. 2014). Furthermore, this study showed that in cases of placenta creta, a pathological condition in which placental villi invade excessively into maternal decidua and insert directly into the myometrium, extravillous cytotrophoblast cells express significantly higher levels of Cripto-1 protein (Bandeira, Borbely et al. 2014). Jiang *et. al.* reported similar findings where they observed significantly higher expression of Cripto-1 in placenta creta and placenta previa (a pathological condition where placenta is formed near the uterine cervix) compared to placentas from normal pregnancies. Their study also revealed that in cases of placenta creta, the level of Cripto-1 overexpression was directly associated with severity (depth) of villous invasion into uterine myometrium (Jiang, Wu et al. 2019). More studies are needed to investigate the potential role of Cripto-1 in regulation of trophoblast invasion during human and mouse placental development.

19) Rationale and Hypothesis

Pregnancy is a crucial component of mammalian reproduction comprised of complex sequential events such as implantation, decidualization, placentation and eventually parturition. Perturbation of these events can lead to different clinical issues including infertility and pregnancy complications like preeclampsia, intrauterine growth restriction (IUGR) and preterm birth. While the major physiological events associated with reproduction have been characterized, there are still many molecular pathways that have yet to be fully elucidated in order to open new windows toward overcoming and managing these reproductive issues. In vivo research limitations, especially on subjects related to uterine-embryo interactions in humans, has led researchers to rely primarily on animal models to identify the molecular mechanisms that govern reproduction (Dey, Lim et al. 2004, Wang and Dey 2006, Cha, Sun et al. 2012).

Several studies have demonstrated the involvement of different transforming growth factor-beta (TGFβ) superfamily members and their related receptors in many fundamental reproductive events including: folliculogenesis and ovulation, pre-implantation embryonic development, maternal-embryo communication during implantation, uterine decidualization, placentation, embryos patterning and gastrulation, and reproductive tract morphogenesis and function (Matzuk, Kumar et al. 1995, Dong, Albertini et al. 1996, Elvin, Clark et al. 1999, Brown, Houston-Hawkins et al. 2000, Jorgez, Klysik et al. 2004, Lee, Jeong et al. 2007, Park and Dufort 2011, Park, DeMayo et al. 2012, Zhao, Lin et al. 2012, Clementi, Tripurani et al. 2013, Nagashima, Li et al. 2013, Park and Dufort 2013, Zhang, Kong et al. 2014, Heba, Park et al. 2015,

Peng, Fullerton et al. 2015, Peng, Monsivais et al. 2015, Rodriguez, Tripurani et al. 2016, Ni and Li 2017).

Cripto is a member of the epidermal growth factor-Cripto1/FRL1/Cryptic (EGF-CFC) protein family that acts as a co-receptor in the TGF-β signaling pathways that involve Nodal, GDF1 and GDF3. CRIPTO has been shown to play a critical role in embryo development (Strizzi, Bianco et al. 2005, Jin and Ding 2013) and *Cripto* null mice are embryonic lethal (between d7.5pc and d10.5pc) because of major gastrulation and heart development defects (Ding, Yang et al. 1998). In addition to being a co-receptor in the TGF-β signaling pathway, CRIPTO can activate Smad-independent signaling elements such as PI3K/Akt and MAPK pathways and facilitate signaling through the canonical Wnt/ß-catenin and Notch/Cbf-1 signaling pathways (Klauzinska, Castro et al. 2014). Through these various mechanisms, Cripto is implicated in: early embryogenesis, embryonic stem cell maintenance, facilitating epithelial-mesenchymal transitions and significantly enhancing tumor cell migration, invasion and angiogenesis (Klauzinska, Castro et al. 2014).

Some studies in the literature suggest that, in addition to the aforementioned functions, Cripto may also have a role in female reproduction and pregnancy maintenance. *Cripto* mRNA is consistently detected in endometrial samples from healthy women during the menstrual cycle (Papageorgiou, Nicholls et al. 2009). The expression of Cripto is also dysregulated in specific human placental and endometrial pathologies i.e. placenta creta, (Bandeira, Borbely et al. 2014) and endometriosis (Dela Cruz, Del Puerto et al. 2015). The specific role of maternal Cripto in female reproduction and pregnancy remains elusive however, as no study has yet been

conducted that presents an in-depth analysis of its function in the endometrium. In this study, we utilized a uterine-specific conditional knockout of *Cripto* to investigate whether *Cripto* is a key contributing component in physiologic events of mouse pregnancy such as implantation, uterine decidualization and placentation.

We hypothesized that uterine Cripto has a major role in female fertility and maintenance of pregnancy.

20) Thesis outline

The results of our study are presented in two manuscripts in this thesis. The thesis includes 5 chapters:

Chapter 1 is ***Introduction***, Chapter 2 ***Manuscript 1***, Chapter 3 **M*anuscript 2,*** Chapter 4 ***General discussion and conclusion*** and finally Chapter 5 ***References***.

Chapter 2: MANUSCRIPT I

Title

Maternal Cripto is required for proper uterine decidualization and peri-implantation uterine remodeling

Shiva Shafiei,[1,2] Omar Farah, [1,2] Daniel Dufort [1,2,3,4]

1 Division of Experimental Medicine, McGill University Health Centre, Montreal, Canada
2 Child Health and Human Development Program, Research Institute of the McGill University Health Centre, Montreal, Canada
3 Department of Obstetrics and Gynecology, McGill University Health Centre, Montreal, Canada
4 Department of Biology, McGill University, McGill University Health Centre, Montreal, Canada

Corresponding Author: Daniel Dufort

Program Leader, Child Health and Human Development program
Director of the Division of Translational Research in OBGYN
Research Institute of the McGill University Health Centre
1001 Blvd. Décarie
CHHD EM03230
Montréal, QC, H4A 3J1
Canada
Daniel.dufort@mcgill.ca
Tel: (514) 934-1934 ext. 34743

Keywords:

Cripto, Decidualization, Implantation, Uterine remodeling, Notch signaling

:

Preface

Prior to initiation of this thesis in September 2014, there was no information about the expression of Cripto in the mouse uterus and the roles it plays during pregnancy.

In Manuscript I (Chapter 2), our experiments started with addressing ***whether Cripto is expressed in the mouse uterus during the non-pregnant state as well as during early stages of pregnancy***. As the answer was yes to both questions, we created a conditional Knockout (cKO) mouse model missing Cripto in the uterus, enabling us to study the role of uterine Cripto in physiologic events of female fertility. Fertility evaluations showed that Cripto cKO females are subfertile as they had significantly lower pregnancy rate and number of pups per litter.

Then, the rest of the experiments of the manuscript I (chapter 2) were focused on ***evaluating the critical stages of early pregnancy*** including ovulation, implantation, peri-implantation uterine remodeling and stromal decidualization in Cripto cKO females to determine the underlying causes of the observed subfertility.

Abstract

Cripto, a member of the TGFβ superfamily, encodes for a cell surface receptor whose role in embryonic development and stem cell maintenance has been studied. Cripto mRNA and protein have been detected in the human uterus at all stages of the menstrual cycle and its dysregulation has been found in placenta creta and endometriosis in humans. To date, there is not much known about Cripto's role in female reproduction. As Cripto null Knockout (KO) is embryonic lethal, we created a conditional KO (cKO) mouse model in which Cripto is deleted only in the reproductive tissues using a Cre-loxP system. Pregnancy rate and number of pups per litter were evaluated as general fertility indices. We observed a significant decrease in pregnancy rate and litter size with loss of uterine Cripto indicating that Cripto cKO females are subfertile. We showed that although the pre-implantation period is normal in Cripto cKO females, 20% of cKO females fail to establish pregnancy and an additional 20% of females undergo full litter loss after implantation between day 5.5 postcoitum (d5.5pc) and d8.5pc. By means of histology, quantitative PCR, artificial induction of decidualization, and alkaline phosphatase staining, we showed that subfertility caused by loss of uterine Cripto is due to defects in uterine decidualization, remodeling and luminal closure and is accompanied by significant down-regulation of Bmp2, Wnt4 and several components of Notch signaling pathway which all are known to be important factors in uterine remodeling and decidualization. Our study demonstrates that Cripto is expressed in the uterus during critical stages of early pregnancy and its deletion results in subfertility due to implantation failure, impaired peri-implantation uterine remodeling and impaired uterine decidualization.

Introduction

Pregnancy is a crucial component of mammalian reproduction comprised of complex sequential events such as implantation, decidualization, placentation and eventually parturition. Perturbation of these events can lead to different clinical issues including infertility and pregnancy complications like preeclampsia, intrauterine growth restriction (IUGR) and preterm birth [1-3]. While the major physiological events associated with reproduction have been characterized, there are still many molecular pathways that have yet to be fully elucidated in order to open new avenues toward overcoming and managing these reproductive issues. In vivo research limitations, especially on subjects related to uterine-embryo interactions in humans, has led researchers to rely primarily on animal models to identify the molecular mechanisms that govern reproduction [1-3].

Several studies have demonstrated the involvement of different transforming growth factor-beta (TGFβ) superfamily members and their related receptors in many fundamental reproductive events including: folliculogenesis and ovulation, pre-implantation embryonic development, maternal-embryo communication during implantation, uterine decidualization, placentation, embryos patterning and gastrulation, and reproductive tract morphogenesis and function [4-21]

Cripto is a member of the epidermal growth factor-Cripto1/FRL1/Cryptic (EGF-CFC) protein family that acts as a co-receptor in the TGF-β signaling pathways that involve Nodal, GDF1 and GDF3. Cripto has been shown to play a critical role in embryo development [22, 23] and Cripto

null mice are embryonic lethal (between d7.5pc and d10.5pc) because of major gastrulation and heart development defects [24]. In addition to being a co-receptor in the TGF-β signaling pathway, Cripto can activate Smad-independent signaling pathways such as PI3K/Akt and MAPK and facilitate signaling through the canonical Wnt/ß-catenin and Notch/Cbf-1 signaling pathways [25]. Through these various mechanisms, Cripto is implicated in: early embryogenesis, embryonic stem cell maintenance, facilitating epithelial-mesenchymal transitions and significantly enhancing tumor cell migration, invasion and angiogenesis [25]. Cripto may also have a role in female reproduction and pregnancy maintenance. Cripto mRNA is consistently detected in endometrial samples from healthy women during the menstrual cycle [26]. The expression of Cripto is also dysregulated in specific human placental and endometrial pathologies like placenta creta, [27] and endometriosis [28]. The specific role of maternal Cripto in female reproduction and pregnancy still remains elusive as no study has yet been conducted that presents an in-depth analysis of its function in the endometrium. In this study, we utilize a uterine-specific conditional knockout of Cripto to investigate whether Cripto is a key contributing component in physiologic events of mouse pregnancy such as implantation and uterine decidualization. Our results demonstrate that Cripto is expressed in the uterus during critical stages of early pregnancy and its deletion results in subfertility due to implantation failure, impaired peri-implantation uterine remodeling and impaired uterine decidualization.

Materials and methods

Generation and maintenance of Cripto cK.O Mice

Experimental protocols in this study are in accordance with regulations established by the Canadian Council on Animal Care and were reviewed and approved by the Animal Care Committee of the McGill University Health Centre. Wild-type CD1 mice were purchased from Charles Rivers Company. Mice with loxP sites flanking exon 3-5 of the Cripto gene (Criptofloxed/floxed or Cripto f/f) on a C57BL6 background were purchased from The Jackson Laboratory (Stock Number: 016539, Strain Name: STOCKTdgf1tm2.2Mms/J). The generation of these mice has been previously described [40]. Progesterone receptor-Cre mice (PgrCre/+) were generously donated by F. J. DeMayo and J. P. Lydon [40]. and maintained on a CD1 background in our lab. Both strains have previously been reported to be healthy and demonstrated normal fertility. PgrCre/+ mice have been used in numerous studies to investigate uterine-specific gene function.

Homozygous Criptof/f females were crossed with heterozygous PgrCre/+ males and the offspring were genotyped by tail snip digestion and PCR. The Cripto floxed (~ 300 bp) and Cripto wildtype (178 bp) alleles were amplified by touch-down PCR (94 °C 30 Sec, 58-55 °C 30 Sec, 72 °C 30 Sec) for 7 cycles decreasing the annealing temperature 0.5 °C in every cycle; then 30 cycles of (94 °C 30 Sec, 55 °C 30 Sec, 72 °C 30 Sec) using the following primers: Forward 5’-TGG TGA TCC AGA GTC ATT GG-3’ and Reverse 5’-GGG GTC ATT CCT CTC CTA GC-3’. The Pgr-Cre (550 bp) and Pgr-wildtype (300 bp) alleles were amplified by standard PCR (94 °C 1 min, 60 °C 1 min,

72 °C 2 min) for 30 cycles using the following primers: 5'-ATGTTTAGCTGGCCCAAATG-3'; 5'-TATACCGATCTCCCTGGACG-3'; 5'-CCCAAAGAGACACCAGGAAG-3'.

In the first generation, half of the offspring are heterozygous for both genes (Criptof/+ PgrCre/+). The heterozygous males (Criptof/+ PgrCre/+) were crossed with Criptof/f females in order to generate all required genotypes which are: Cripto conditional knockout (Cripto cK.O: Cripto f/f, PgrCre/+), Cripto conditional heterozygous (Cripto cHet: Criptof/+, PgrCre/+) and Control females (Criptof/f,Pgr +/+).

Fertility Assessments

To assess fertility, 6-8 weeks old virgin females (Control, Cripto cHet and Cripto cK.O) were mated with sexually mature fertile wild-type CD1 males. Mating was confirmed by observation of a vaginal plug. The day of vaginal plug observation was considered as day 0.5 post-coitum (d0.5pc) through the whole study. Females were separated from males after mating, kept in individual cages and monitored daily for 3 weeks. A successful pregnancy was defined by birth of live pups. The number of pups per litter and duration of pregnancy were also recorded. In a different approach, 12-weeks-old females were housed with sexually mature fertile wild-type CD1 males for a period of 5 months (1 female and 1 male in each cage). Cages were monitored regularly, and the number of litters and pups were recorded for every female in the study.

For assessment of different stages of pregnancy, the females were mated with sexually mature fertile wildtype CD1 males, then were sacrificed on specific gestational ages. Uteri were dissected and the gross morphology was assessed, photographs were taken and further required analysis was done.

Embryo flushing and collection

Control and Cripto cK.O females were mated with sexually mature fertile wildtype CD1 males and the day of vaginal plug was assigned as d0.5pc. Females were sacrificed on d2.5pc and d3.5 pc, intact reproductive tract was dissected (ovaries, oviducts and uterus). Embryos were flushed and collected from the oviducts on d2.5pc and from the uterine horns on d3.5pc.

measurements of the conceptus site size

Using ImageJ software, the area of each conceptus site was measured in the photographs taken from whole mount pregnant uteri of Control and Cripto cK.O females at different time-points of pregnancy.

Tissue processing, paraffin embedding, sectioning and H&E staining

Dissected samples were collected in PBS, fixed overnight at 4 °C in 4% paraformaldehyde (PFA)/PBS or 10% neutral buffered formalin, dehydrated in increasing ethanol series (25%, 50%, 75%, and 100%, 20 min each) and cleared in xylene (2× 15 min). The tissue was incubated overnight in melted paraffin wax (TissueTek) at 60 °C in a vacuum oven then embedded at room temperature, and the blocks were placed on a cold plate for 1 hour to solidify slowly then transferred to −20 °C freezer overnight before sectioning. Seven-micrometer sections were cut with the Leica RM2145 microtome, mounted on Fisherbrand Superfrost plus slides and dried overnight. Slides were then either used for immunofluorescence, immunohistochemistry (described later) or stained with Hematoxylin and Eosin (H&E). For H&E staining, slides were deparaffinized in xylenes (2x 5 min), rehydrated with a decreasing ethanol gradient (100%, 95%,

85%, 75%, 50%, 20%, and water, 2 min each), placed in Harris Modified Hematoxylin solution [Sigma] for 6 min and then washed in running tap water for 10 min. Sections were then decolorized with dipping in 1% acidic alcohol (1-2 seconds), placed in a 1% sodium bicarbonate bluing agent (3 seconds), before counterstaining with Eosin [Sigma] for 15 seconds. The slides were then dehydrated, cleared and mounted using Permount [Fisher Scientific].

Immunofluorescence staining

As described earlier, uteri (Non-pregnant or d0.5pc to d4.5pc pregnant) were dissected, dehydrated, cleared, embedded in paraffin blocks and sectioned. Slides were then washed in xylene (2x 10 min), rehydrated with a decreasing ethanol gradient (100%, 95%, 85%, 75%, 50%, 20%; 2 min each). Antigen retrieval was done in 10mM sodium citrate solution (+ 0.05% Tween 20, pH 6) at 95 °C for 20 min. Sections then were permeabilized with PBT (0.2% BSA, 2.5% Triton X-100 in PBS for 15 min), blocked for 1 h at room temperature (10% BSA in PBS) then incubated with the primary antibody, Cripto [Santa Cruz sc-17188; 1:100] at 4 °C overnight. Following several washes in 0.1% PBS-Tween 20, slides were incubated with the appropriate secondary antibody for 1 h at room temperature (Alexa Fluor 488, Life technologies 1:300). Slides were then washed, counterstained with DAPI (1:5000) and mounted with Mowiol 4–88 [Sigma].

Immunohistochemistry

As described earlier, uteri were dissected, dehydrated, cleared, embedded in paraffin blocks and sectioned. Slides were then washed in xylene (2x 10 min), rehydrated with a decreasing ethanol gradient (100%, 95%, 85%, 75%, 50%, 20%; 2 min each). Antigen retrieval was done in

10mM sodium citrate solution (+ 0.05% Tween 20, pH 6) at 95 °C for 20 min. Sections then were permeabilized with TBT (0.2% BSA, 2.5% TritonX-100 in TBS for 15 min), blocked for 1 h at room temperature (10% BSA in TBS). Following washes in TBS-0.025 % Tween 20 (TBST), slides were incubated with primary antibody: Cripto [Santa Cruz sc-17188; 1:50], Cox2 [Cayman, aa570-598, 1:150] or PCNA [Santa Cruz, FL-261, 1:100] at 4 °C overnight. After washes with TBST, 0.3 % H2O2 in TBS was used for blocking endogenous peroxidase activity following by incubation with an appropriate secondary HRP antibody (1:500) for 1 h at room temperature. For antigen visualization, DAB Substrate Kit (Abcam ab64238) was used based on recommended instructions provided by the manufacturer. Then Slides were counterstained with Hematoxylin solution, Gill no. 2 (Sigma-Aldrich) and mounted with Richard-Allan Scientific™ Mounting Medium (Thermo Fisher Scientific).

Artificial decidualization

Control and Cripto cK.O females were mated with vasectomized males. On d3.5pc, females were anesthetized with isoflurane and an incision was made on the lower back of the mice lateral to the midline, exposing the ovary and uterus on one side. One uterine horn was subsequently scratched along the uterine lumen on the anti-mesometrial side with a 22G needle inserted from the proximal end of the uterine horn close to the oviduct. The other horn served as an internal control. The incision was sutured, and females were allowed to recover till d7.5pc when they were sacrificed and the uterus was dissected out in order to assess the decidualization response.

Alkaline phosphatase staining

After tissue processing, paraffin embedding and sectioning, slides were deparaffinized in xylene (2x 5 min each) then rehydrated in a series of decreasing ethanol dilutions (100%, 100%, 95%, 75%, 50%, and dH2O, 2 min each). Slides were pre-incubated overnight in 1% MgCl2 in Tris-maleate buffer (100 mM Tris-Maleate, 150 mM NaCl, and 1mM MgCl2, pH 9.2) at room temperature. Slides were incubated for 2 h in alkaline phosphatese-substrate solution at room temperature (NBT 660 µl and 330 µl BCIP in 100 ml Tris-maleate buffer). Slides were then washed, counter-stained with nuclear fast red, dehydrated with series of increasing ethanol dilutions, cleared with Xylene, mounted and imaged.

Hormone analysis

Control and Cripto cK.O females were mated with sexually mature fertile wild-type CD1 males. On d7.5pc females were euthanized, blood was collected by cardiac puncture, uteri were dissected, and the pregnancy status and number of implantation sites were recorded. Serum was separated from the blood and stored at −80°C prior to being sent to Ligand Assay and Analysis Core at University of Virginia (Charlottesville, Virginia) for hormone analysis where serum Progesterone levels were measured.

Reverse transcription and Real-time PCR

RNA extraction was done using Trizol and RNeasy Mini Kit [Qiagen Cat. No. 74104]. QuantiTect Reverse Transcription Kit [Qiagen Cat. No. 205311] was then used for cDNA synthesis. Real-time PCR was performed using the Rotor-Gene SYBR Green PCR Kit [Qiagen Cat. No. 204074]

following the manufacturer's protocol. The following primers were used: Cripto (200 bp) 5'-GACCAGAAAGAACCTGCCGT -3' and 5'- AGGATAGACCCACAGTGCTCTT -3'; Hoxa10 (207 bp) 5'-CGCTACGGCTGATCTCTAGG-3' and 5'-CAGCCCCTTCAGAAAACAGT-3'; Hoxa11 (285 bp) 5'-TATAAGGGCAGCGCTTTTTG-3' and 5'-ACCTCGCTTCCTCCGACTAC-3'; Wnt4 (243 bp) 5'-AACGGAACCTTGAGGTGATG-3' and 5'-TCACAGCCACATTCTCCAG-3'; Bmp2 (95 bp) 5'-AACACTAGAAGACAGCGGGTC-3' and 5'-CTCTCTCAATGGACGTGCCC-3'; Notch4 (194 bp) 5'-TTGGCTGAGCAGAAGTCTCG-3' and 5'-CCTCACTTCTCCTGCACCTG-3'; Notch1 (371 bp) 5'-TCACTCTCACAGTTGCGACC-3' and 5'-AGTGGCCCTAATTGCCAGAC-3'; Dll4 (149 bp) 5'-TTCTTGCACGGAGAGTGGTG-3' and 5'-CAACACGACACCGGAACAAAC-3'; GAPDH (223 bp) 5'-AACTTTGGCATTGTGGAAGG-3' and 5'-ACACATTGGGGGTAGGAACA-3'; Ihh (196 bp) 5'-CTACAAGCAGTTCAGCCCCA-3' and 5'- TGAGTTCAGACGGTCCTTGC-3'; Cox2 (232 bp) 5'-GCTGTACAAGCAGTGGCAAA-3' and 5'-CCCCAAAGATAGCATCTGGA -3'.

Statistics

Data are presented as the mean ± SEM of independent samples. Statistical analysis comparing experimental groups was performed using two-tailed Student t-test for independent samples, Student t-test for correlated samples and one-way ANOVA followed by a Tukey's multiple comparison test. P-values less than 0.05 were considered statistically significant.

Results

Cripto is expressed in the uterus during the peri-implantation and early post-implantation periods.

To determine the spatiotemporal localization of CRIPTO in the wild-type mouse uterus, we performed immunofluorescence staining against CRIPTO in non-pregnant and peri-implantation stages of pregnancy (d0.5pc-d4.5pc). CRIPTO protein was sparsely observed in the non-pregnant uterus with a slight increase after mating (d0.5pc) (Figure 2.1). Protein levels significantly increased from d2.5pc onward and was prominently localized in uterine stromal cells (Figure 2.1).

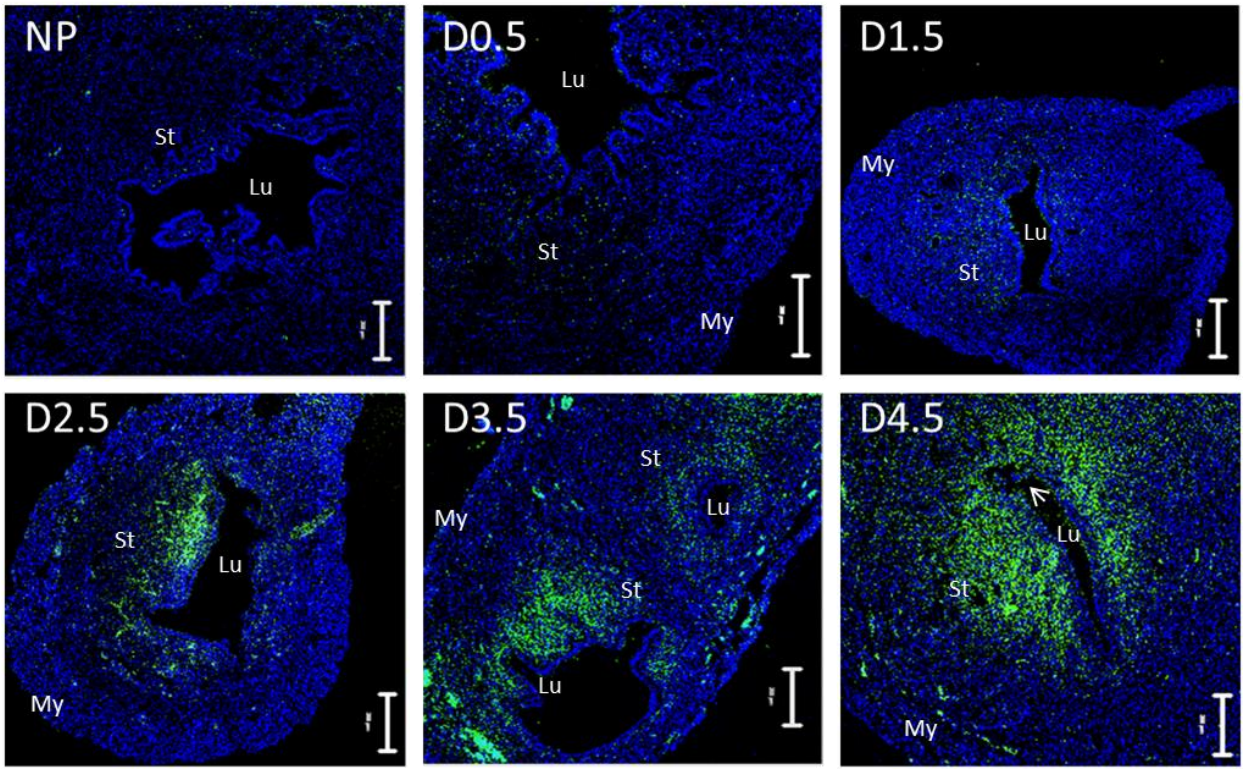

Figure 2.1. Localization of Cripto in the wild-type mouse uterus during peri-implantation period. Spatiotemporal localization of Cripto (green) in non-pregnant (NP) and 0.5 day till 4.5

days post-coitum (D0.5-D4.5pc) mouse uterus is shown by Immunofluorescence staining. Cripto protein (green) is rarely expressed in non-pregnant uterus. Its expression starts weakly after mating (d0.5pc) and increases gradually till it becomes prominent from d2.5pc onward mainly in the uterine stromal cells. Lu, lumen; My, myometrium; St, stroma; arrowhead, Embryo. (Scale bar, 200 μm)

To further characterize the pattern of CRIPTO protein localization during early pregnancy, immunohistochemistry was also performed on d1.5pc, d3.5pc and d5.5pc uteri. On d1.5pc limited Cripto localization was only observed in a few stromal cells adjacent to the luminal epithelium and in a few cells within the luminal epithelium. Other compartments of uterus did not show any Cripto localization at this time point (Figure 2.S1 A and B). Interestingly, on d3.5pc, Cripto protein levels became quite prominent in the embryo as well as in the subluminal uterine stroma and luminal epithelium only at the future implantation sites and not at the inter-implantation spaces (Figure 2.S1 C-D"). A gradient pattern of Cripto protein localization in the stromal cells at the implantation site was also observed where it was mostly visible in the stromal cells adjacent to the luminal epithelium and decreased with distance away from the lumen toward the periphery of the uterus (Figure 2.S1 C-C")

With the initiation of the implantation process on the anti-mesometrial pole of the uterus, uterine stromal cells that are closest to the site of embryo penetration, also referred to as the primary decidual zone (PDZ), undergo proliferation and differentiation and transform into uterine decidual cells, which are morphologically and functionally distinct from stromal cells. This stromal to decidual transformation then extends into the anti-mesometrial pole and advances toward the mesometrial pole which is referred as secondary decidual zone (SDZ) [29].

Our immunohistological evaluations on d5.5pc (1 day after implantation) revealed that similar to d3.5pc, localization of Cripto protein is limited to the implantation sites. At this time-point, Cripto protein was observed in decidual cells in PDZ and differentiating stromal cells in SDZ (Figure 2.S2).

Immunohistological evaluations on d3.5pc and d5.5pc also revealed perivascular localization of Cripto in pregnant uteri. This localization was very prominent around the mesometrial vasculature (Figure 2.S3, A and C) and although present, showed less intensity around the vascular structures in myometrium and stroma (Figure 2.S3, B and D). This perivascular localization of Cripto was not limited to implantation sites as it was also visible in inter-implantation spaces.

Cripto conditional knockout females are subfertile.

Cripto null mutants are embryonically lethal, therefore, a tissue-specific conditional knockout (cK.O) of Cripto in the maternal reproductive tract using a Cre-loxP recombinase system was employed. The Cre-recombinase in this mouse model is driven under the progesterone receptor (PR) promoter, thereby creating a specific deletion of Cripto in female reproductive tissues (Figure 2.2 A). Gross morphology and histology of the uterus in Cripto cK.O mice was observed to be normal. By means of IHC, Cripto deletion was confirmed by the absence of expression on d3.5pc at the implantation sites where Cripto localization is expected in the luminal epithelium and stromal cells (Figure 2.2 B-C'). Interestingly, as expected, Cripto was still detected in the

embryo at this stage (Figure 2.2 C'). On d5.5pc, Cripto expression was also absent in decidual cells in PDZ and differentiating stromal cells in SDZ (Figure 2.2 D-E').

Figure 2.2. Conditional deletion of Cripto in the mouse uterus. The Cre-recombinase is driven under the progesterone receptor (PR) promoter, thereby creating a specific deletion of Cripto in reproductive tissues of mice bearing loxP insertions before exon 3 after exon 5 of Cripto gene (A). By IHC, Cripto deletion was confirmed in the implantation sites where Cripto localization (brown) is expected in luminal epithelium and stromal cells on d3.5pc (B-C') and in decidual cells and differentiating stromal cells on d5.5pc (D-E'). In B', although there is no sign of Cripto expression in the uterus, the localization of Cripto in the embryo present within the uterine lumen is quite evident which further confirms the successful deletion if Cripto in the maternal tissues. B', C', D' and E' are higher magnification of the fields defined by black boxes in B, C, D and E respectively. AM, antimesometrial pole; De, decidual cells; Em, embryo; GE, glandular epithelium; LE, luminal epithelium; Lu, lumen; M, mesometrial pole; My, myometrium; St, Stroma. (Scale bar: B, C, D and E: 250 µm; B' and C': 50 µm; D' and E': 25 µm)

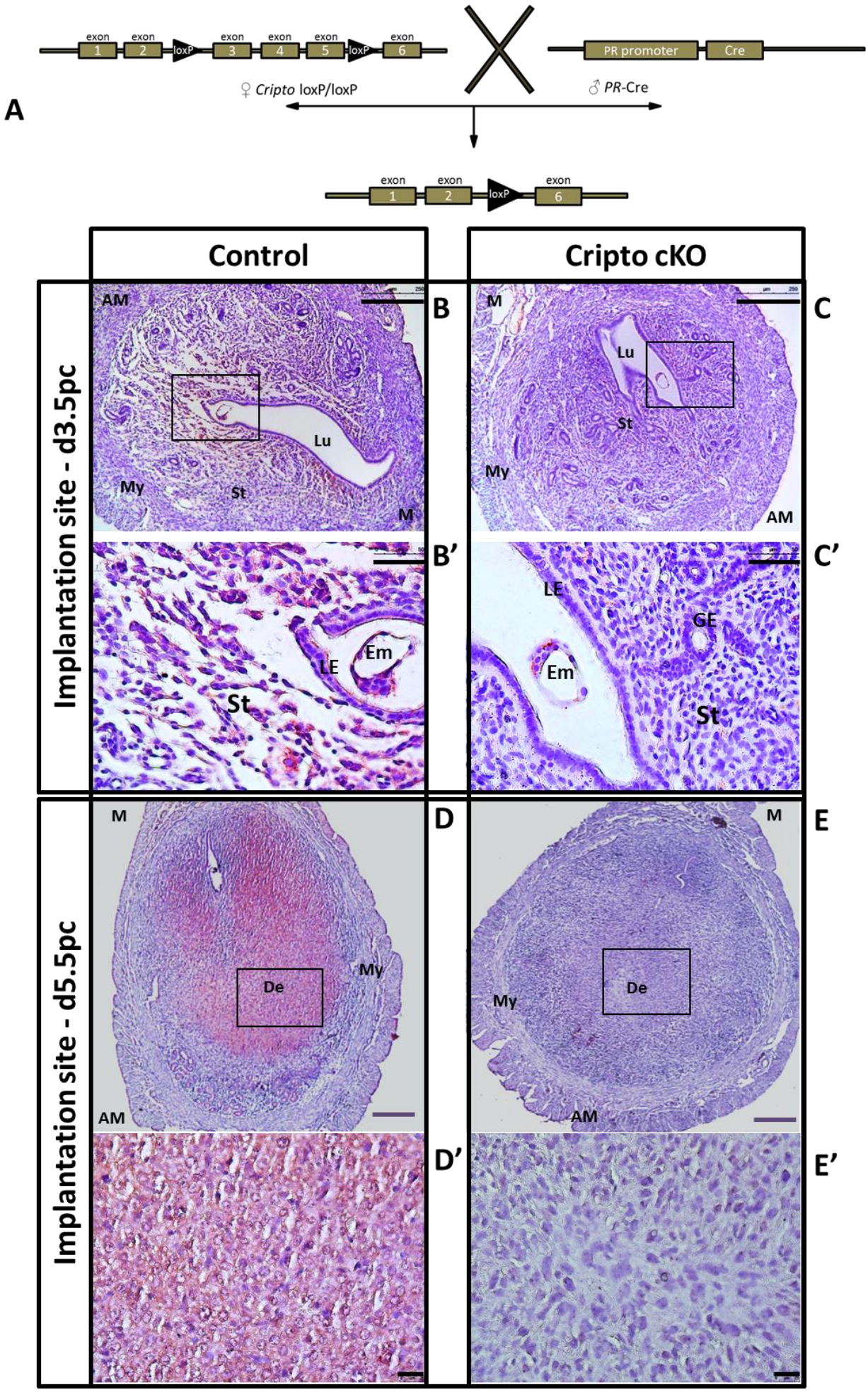
A
exon
1
2
loxP
3
4
5
loxP
6
♀ Cripto loxP/loxP
PR promoter
Cre
♂ PR-Cre
Control
Cripto cKO
Implantation site - d3.5pc
Implantation site - d5.5pc
AM
M
Lu
St
My
LE
Em
GE
De
B
B'
C
C'
D
D'
E
E'

To assess fertility, we mated 6-8 weeks old virgin Cripto conditional heterozygous (Cripto cHet), Cripto cK.O and control females with proven fertile wildtype CD1 males and plugged females were enrolled in the study. A successful pregnancy was defined by delivery of live pups after the recorded mating. In this trial, only 62% of mated Cripto cK.O females gave birth to pups (had a successful pregnancy) which was significantly lower than Cripto cHet (94%) and Control (100%) females ($P<0.05$) (Table 1). Furthermore, in this trial, a slightly but statistically significant fewer number of pups per litter was observed in Cripto cK.O females as compared to cHet and controls (7.68 pups/litter in cK.O vs. 9.52 in cHets and 9.71 in Control; $p<0.05$) (Table 1). As Cripto cHets mice showed similar fertility parameters to Controls, we continued our study only with Cripto cK.O and Control mice.

Table1. Overall and pre-implantation fertility assessments in Cripto cK.O versus Control females. (*) shows statistically significant difference.

Table 1.	Cripto Control	Cripto cKO	Cripto cHet
Overal fertility rate (%)	100% (7 of 7)	62.5% (15 of 24)*	94.4% (17 of 18)
No. of pups/litter	9.71 ± 0.36	7.68 ± 0.59*	9.52 ± 0.62
Percent of plugged mice with embryos on d2.5pc	100% (10 of 10)	100% (7 of 7)	NA
No. of embryos/dam retrieved on d2.5 pc	10.3 ± 0.73	9.28 ± 0.86	NA
Percent of plugged mice with embryos on d3.5pc	100% (9 of 9)	100% (10 of 10)	NA
No. of embryos/dam retrieved on d3.5 pc	7.22 ± 0.7	7 ± 0.78	NA

In another approach, we enrolled Cripto cKO and Control females in a 5 months-long breeding trial to assess and compare their fertility indices over time. Four Cripto cKO and four Control

females were caged individually with fertile wildtype males and were monitored regularly for 5 months. At the end of this trial, the 4 control females totally gave birth to 219 pups from 21 litters where Cripto cKO females together gave birth to only 101 pups from 19 litters. Although after 5 months of breeding, the average number of litters per female was not different between groups (5.25 ± 0.75 litters/Control female vs 4.75 ± 0.25 litters/Cripto cKO female) but the average number of pups per litter was significantly lower ($P < 0.0001$) in Cripto cKO group (5.32 ± 0.64 pups/litter) compared to Control group (10.42 ± 0.54 pups/litter) (Figure 2.S4). Another interesting observation was the obvious decline in the average number of pups per litter over time in Cripto cKO females in contrast to control females which showed a rather consistent number of pups per litter over 5 months of breeding trial (Figure 2.S4).

In order to identify the reason for the decreased pregnancy rate in Cripto cK.O females, we first examined cycling, ovulation and fertilization and did not observe any difference between Cripto cK.O and controls (data not shown). We next examined the embryos isolated at d2.5pc and d3.5pc. A similar number of embryos were retrieved from Cripto cK.O and Control groups (Table 1) and no morphological differences were observed between embryos from either groups (data not shown). To evaluate the post-implantation period, Cripto cK.O and Control females were sacrificed on d5.5pc and d8.5pc for the assessment of their pregnancy status. Females with visible implantation sites were considered as pregnant. The number of implantation sites (decidua), average decidual size, number of resorption sites and incidence of full litter resorption was compared between groups (Table 2). Our assessments showed that although around 60% of Cripto cK.O females established pregnancy and had similar fertility parameters with Control females until d8.5pc (Table 2 and Figure 2.3 A), approximately 20% of

Cripto cK.O females never establish pregnancy, showing no signs of any growing decidua, even though a mating plug was observed and corpora lutea were present on their ovaries (data not shown). Furthermore, an additional 20% of Cripto cK.O females established pregnancy but failed to maintain their pregnancy and lost their entire litter between d5.5pc and d8.5pc (Table 2 and Figure 2.3 A). Together, these two latter groups contributed to the observed overall 40% infertility in Cripto cK.O females.

To assess the possibility of implantation failure, the uteri of d5.5pc mated but non-pregnant Cripto cK.O females were processed and embedded in paraffin blocks. Serial sectioning and Hematoxylin and Eosin staining were done, and the slides were analyzed using bright-field microscopy. No sign of embryo attachment/implantation and decidualization initiation was observed (data not shown) confirming implantation failure in these mice.

Table 2. Assessment of pregnancy status on d5.5pc and d8.5pc in Cripto cK.O versus Control females.

Table 2.	d5.5 pc		d8.5 pc	
	Cripto Control	Cripto cKO	Cripto Control	Cripto cKO
Pregnancy rate	100% (9of9)	78.5% (11of14)	100% (5of5)	50% (5of10)
No. of mice with implantation failure	0 (0%)	3 (21.43%)	0 (0%)	2 (20%)
No. of mice with full litter resorption	NA	NA	0 (0%)	3 (30%)
No. of implantation sites/pregnant mouse	10.56 ± 0.5	10.27 ± 0.72	9.8 ± 0.2	9.75 ± 0.62
No. of resorption sites/pregnant mouse	0	0	0.4 ± 0.4	1.5 ± 0.64
Decidual area (mm^2)	NA	NA	13.89 ± 0.25	13.69 ± 0.3

Uterine decidualization is compromised in Cripto cK.O females.

The pattern of Cripto protein localization and findings on early pregnancy failure in Cripto cK.O females suggested that Cripto might play a role in the process of decidualization during the early stages of pregnancy. We therefore performed artificial decidualization within a single uterine horn of pseudo-pregnant Cripto cK.O and control females and used the contralateral horn as the internal control. Interestingly, all control females responded and significant decidualization was observed in the induced uterine horn, while none of the Cripto cK.O females had any response (Figure 2.3 B and C). This result strongly suggests that Cripto is involved in the process of decidualization.

As progesterone (P4) from the ovaries is the major regulator of uterine receptivity as well as initiation and maintenance of uterine stromal decidualization, we evaluated the level of progesterone in blood circulation of Cripto cK.O females and compared them to Controls. No difference in the level of circulating progesterone was observed between d7.5pc Control and Cripto cK.O females (including all 3 categories described earlier) and all animals had the minimum required concentration of blood P4 for that gestational age (Table S1) [30].

Looking for the cause of compromised decidualization ability in Cripto cK.O females, we evaluated the expression level of some of the important factors known to affect uterine decidualization including Ihh, Cox2, Hoxa10, Hoxa11, Wnt4 and BMP2 [1] in d5.5pc pregnant Control, d5.5pc pregnant Cripto cK.O and d5.5pc non-pregnant Cripto cK.O mice. While the expression of Ihh, Cox2, Hoxa10 and Hoxa11 showed no difference between groups (Figure 2.S5), the expression of Bmp2 and Wnt4 was significantly lower in d5.5pc non-pregnant Cripto

cK.O mice compared to the pregnant d5.5pc cK.O and Controls. The expression of Wnt4 was also significantly lower in pregnant d5.5pc cK.O compared to pregnant d5.5pc Controls (Figure 2.3 D and E). To assess whether P4 supplementation can improve the pregnancy rate, Cripto cK.O females were mated with fertile wild-type CD1 males and on d3.5pc half of them were supplemented with subcutaneous P4 implants. On d7.5pc, mice were sacrificed, and pregnancy status was determined based on observation of decidua. No difference was observed between the 2 groups suggesting that P4 supplementation cannot compensate for the lack of uterine CRIPTO in terms of pregnancy rate (data not shown).

In order to evaluate the differentiation status of decidualizing stromal cells in pregnant Cripto cK.O females vs controls, Alkaline phosphatase (ALP) staining was performed on histological sections of d5.5pc implantation sites. Interestingly the level of ALP activity was drastically lower in Cripto cK.O females compared to Controls indicating compromised differentiation of decidual cells in the former group (Figure 2.3 F).

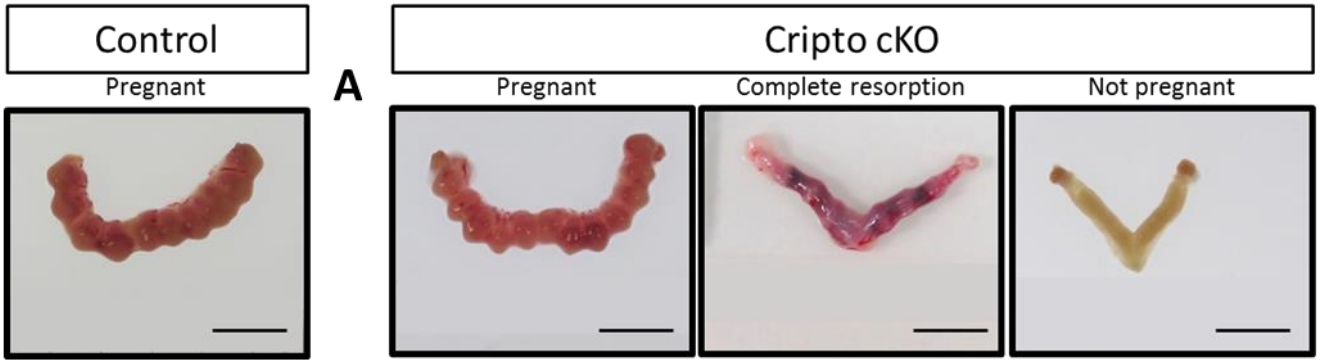
Control
Pregnant
A
Cripto cKO
Pregnant
Complete resorption
Not pregnant

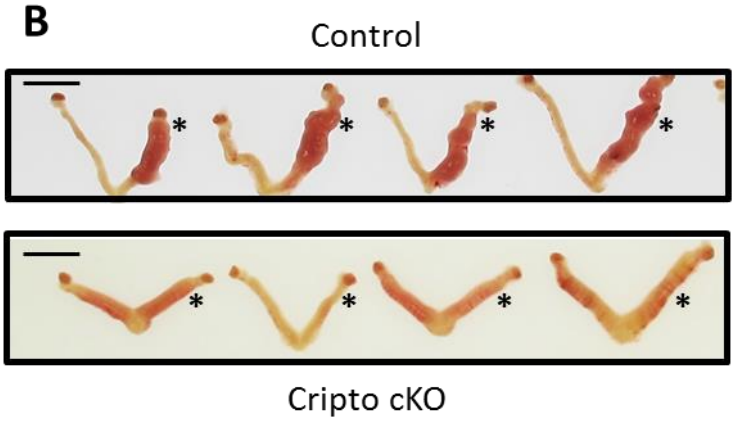
B
Control
Cripto cKO

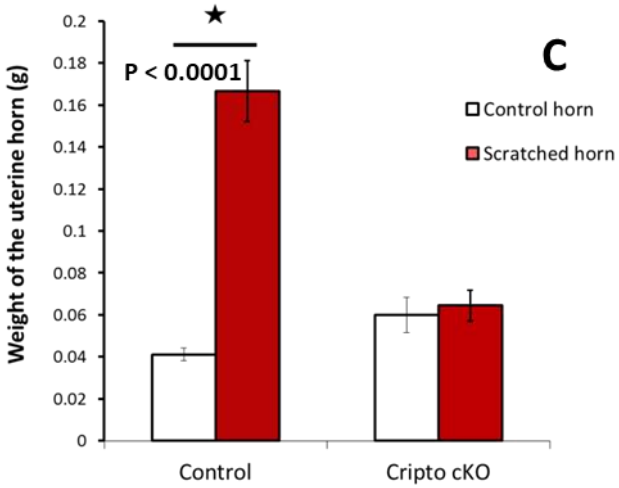
C
★
P < 0.0001
Weight of the uterine horn (g)
Control horn
Scratched horn
Control
Cripto cKO

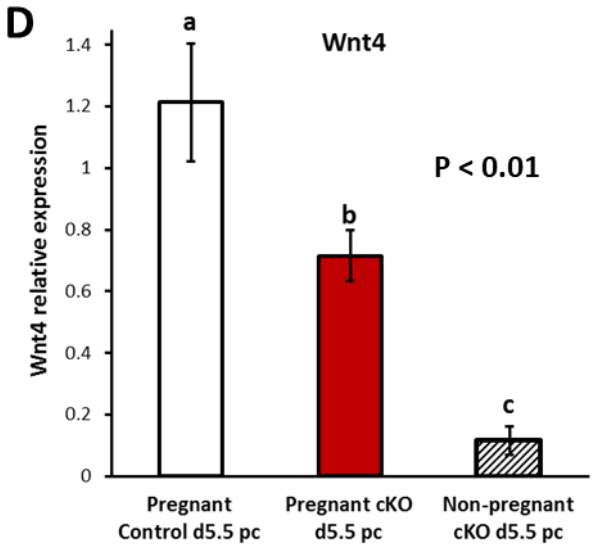
D
Wnt4
P < 0.01
Wnt4 relative expression
a
b
c
Pregnant Control d5.5 pc
Pregnant cKO d5.5 pc
Non-pregnant cKO d5.5 pc

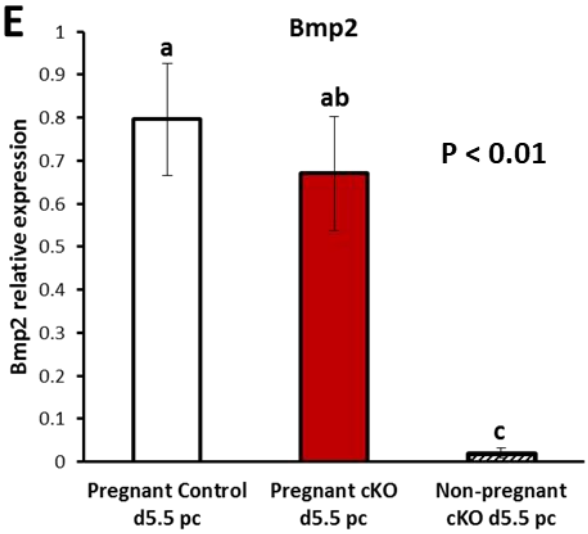
E
Bmp2
P < 0.01
Bmp2 relative expression
a
ab
c
Pregnant Control d5.5 pc
Pregnant cKO d5.5 pc
Non-pregnant cKO d5.5 pc

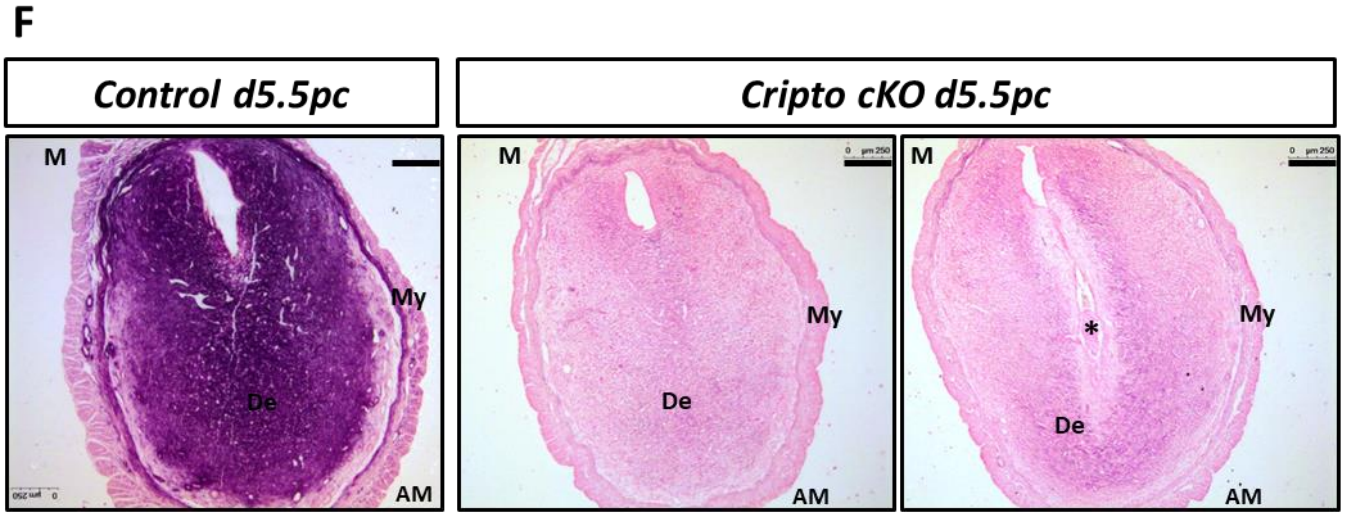
F
Control d5.5pc
Cripto cKO d5.5pc
M
My
De
AM
*

Figure 2.3. Impaired decidualization in Cripto cKO females. (A) On d8.5pc Cripto cK.O females are either pregnant (left image) with pregnancy parameters comparable to Control group, or they have established pregnancy but have gone through full litter loss (middle image) or have failed to established pregnancy at all (right image). (B) Uterine decidualization ability was assessed by artificial induction of decidualization in pseudo-pregnant females on d3.5pc. while all Control females (9 of 9) positively responded to this experiment by decidualization of the scratched uterine horn, none of the Cripto cKO females (0 of 9) had any response. (C) The decidualization response was also quantified by comparing the weight of scratched horn (marked by star) versus non-scratched horn (internal control) on d7.5pc which was 4 days after the procedure. (D and E) Relative expression level of *Wnt4* and *BMP2* on d5.5pc was measured by quantitative real-time PCR (pregnant Control d5.5pc, n= 6-8 females; pregnant Cripto cKO d5.5pc, n= 8-10 females and non-pregnant Cripto cKO d5.5pc, n = 5-6 females). (C. D and E) P-values for significant differences are included in each panel and different letters or asterisks define the groups which are significantly different. (F) Alkaline phosphatase (ALP) staining and nuclear fast red counterstain on d5.5pc implantation sites. High levels of ALP activity in decidual cells in Control females resulted in development of strong purple color whereas the staining is very weak in the case of Cripto cK.O females. AM, antimesometrial pole; De, decidual cells; M, mesometrial pole; My, myometrium; embryo in the section is marked by star (Scale bar: 250 μm).

Abnormal implantation crypt and incomplete uterine luminal closure in pregnancy of Cripto cK.O females

During the peri-implantation period, proper remodeling of uterine lumen and stroma is critical for successful implantation. This process starts around d3.5pc and results in formation of single longitudinal implantation crypt which is oriented along the anti-mesometrial/mesometrial (AM/M) axis of the uterus. The embryo implants at the AM pole of the implantation crypt. With the start of the implantation process, decidualization and remodeling of decidualizing stroma leads to complete closure of the uterine lumen at the implantation sites and is critical for

proper placentation later in the course of pregnancy [3]. Abnormal implantation crypt on d3.5pc (irregular shape with presence of extra branch versus the expected single longitudinal AM/M oriented crypt, Figure 2.2 B and C, Figure 2.4 A and B) and incomplete luminal closure on d4.5pc and d7.5pc (Figure 2.4 D-E and Figure 2.5) were observed in histological analysis of the implantation sites in Cripto cK.O females but not the controls, suggesting impaired remodeling of uterine lumen and stroma in the former group.

We evaluated the proliferative status of stroma and luminal epithelium on d3.5pc and d4.5pc using IHC against proliferative cell nuclear antigen (PCNA). On d3.5pc the number of proliferating cells in the uterine stroma of Cripto cK.O females seemed to be lower whereas the proliferation level in glandular epithelium was clearly stronger compared to Controls (Figure 2.4 A and B). On d4.5pc, very strong PCNA staining in uterine stromal cells of Cripto cK.O females indicates high level of proliferation in this compartment which was much higher than in the Control group. Although the number of proliferative cells in the luminal epithelium was low as is expected for this timepoint, it still seemed to be more than what was observed in Control females (Figure 2.4 C and D).

Notch signaling pathway components are known to be involved in uterine luminal closure and stromal remodeling during decidualization [16, 31, 32] and Cripto has been shown to modulate the activity of this pathway [33]. Considering disrupted Notch signaling as a possible cause of the observed impaired uterine remodeling in Cripto cK.O females, the expression of components of Notch signaling pathway in the uteri of pregnant Cripto cK.O and Control mice was assessed on d5.5pc. Interestingly we observed that the expression of Notch1, Notch4 and

Dll4 are significantly lower in Cripto cK.O females compared to Controls (Figure 2.4 F). Thus, Cripto cK.O females have reduced expression of Notch receptor and ligand which can account for the observed disruption in luminal closure and stromal remodeling in pregnancy of these mice.

Figure 2.4. impaired peri-implantation uterine remodeling in Cripto cK.O females accompanied by downregulation of Notch signaling components. (A-D) IHC against proliferative cell nuclear antigen (PCNA, brown, nuclear localization) for evaluation the proliferative status of stroma and luminal epithelium on d3.5pc and d4.5pc. On d3.5pc the number of proliferating cells in the uterine stroma of Cripto cK.O females (B) is lower whereas the proliferation level in glandular epithelium is clearly stronger compared to Controls (A). On d4.5pc, very strong PCNA staining in uterine stromal cells of Cripto cK.O females (D and E) indicates high level of proliferation in this compartment and much higher than in the Control group (C). Failure of uterine luminal closure and presence of extra branch can also be noticed in D and E in contrast to C. (F) Relative expression level of Notch4, Notch1 and Dll4 on d5.5pc was measured by quantitative real-time PCR (pregnant Control d5.5pc, n= 6-8 females and pregnant Cripto cKO d5.5pc, n= 8-10 females). P-values for significant differences are included in each panel and different letters in each panel define the groups with significant difference. AM, antimesometrial pole; GE, glandular epithelium; LE, luminal epithelium; Lu, lumen; M, mesometrial pole; My, myometrium; St, Stroma. (Scale bar, A-E main panels: 250 µm; A-E magnified panels: 75 µm)

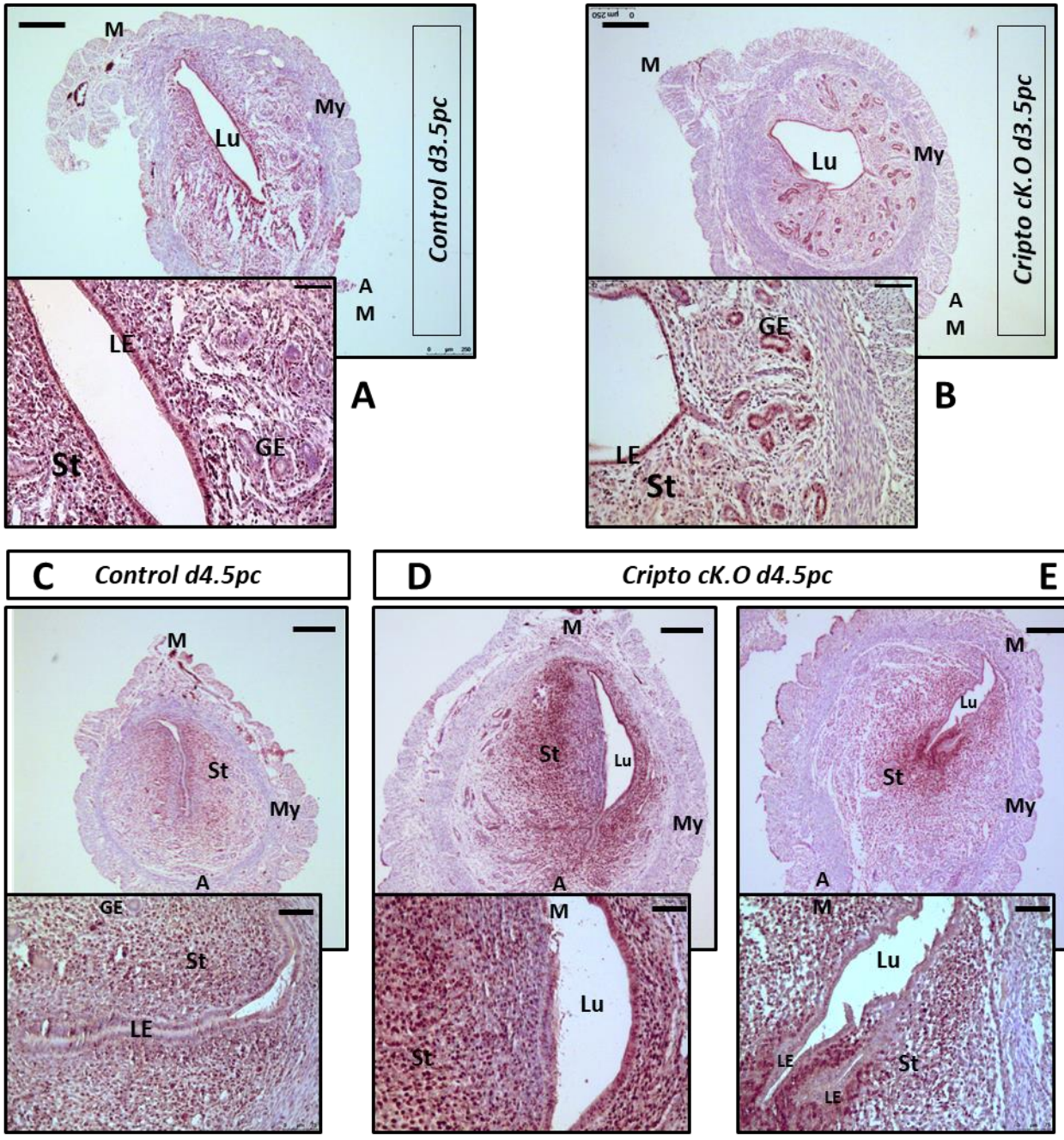
M
Lu
My
Control d3.5pc
A
M
LE
GE
St
A
Cripto cK.O d3.5pc
B
C
Control d4.5pc
D
Cripto cK.O d4.5pc
E

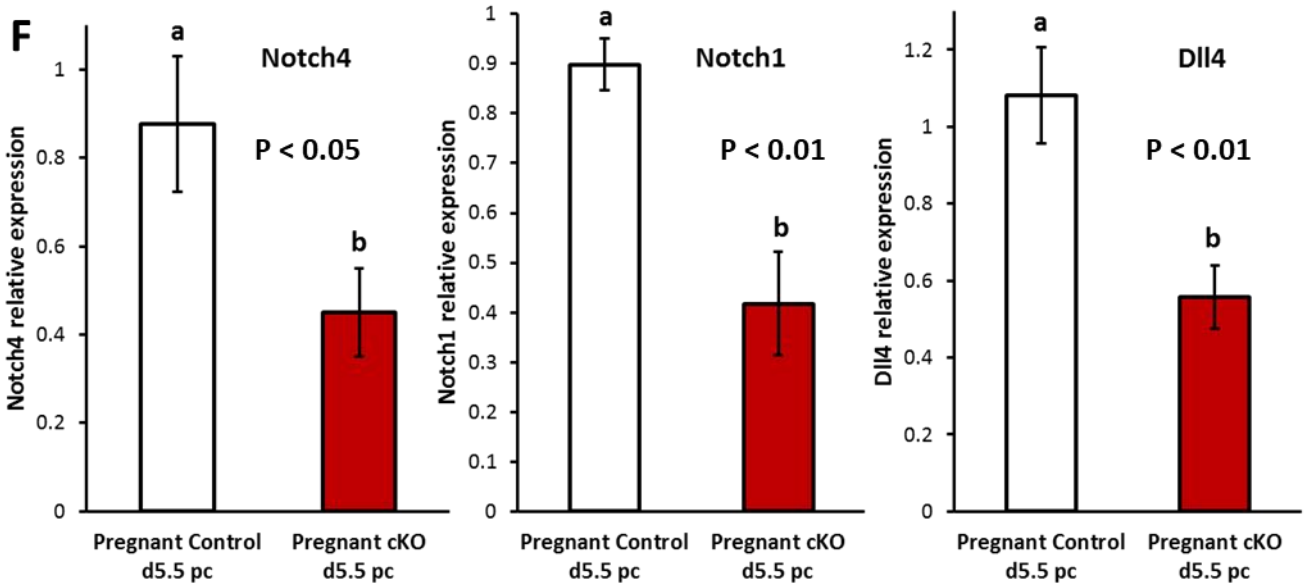
F
Notch4
P < 0.05
Notch4 relative expression
Notch1
P < 0.01
Notch1 relative expression
Dll4
P < 0.01
Dll4 relative expression
a
b
Pregnant Control d5.5 pc
Pregnant cKO d5.5 pc

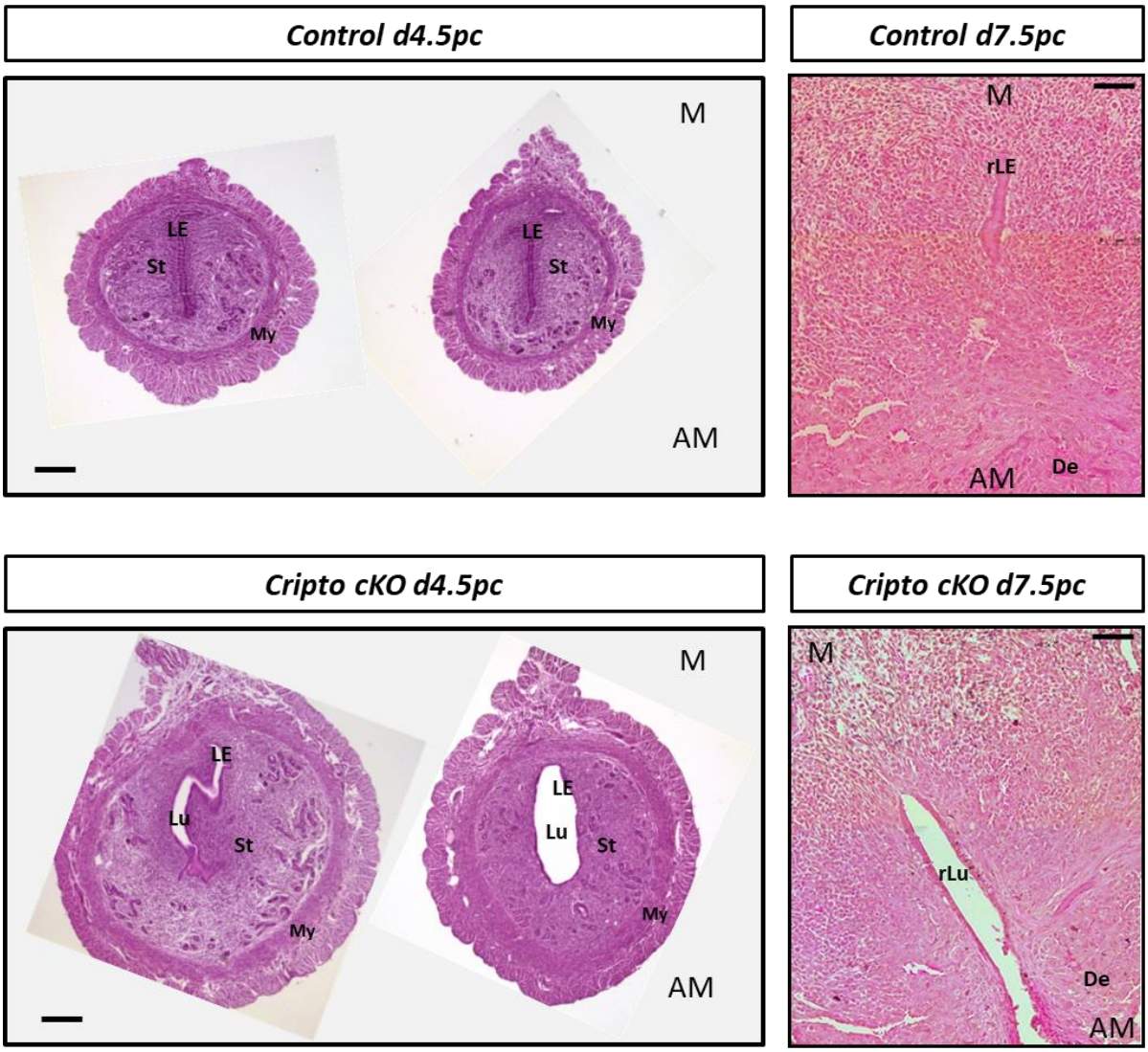

Figure 2.5. Failure of implantation associated uterine luminal closure in Cripto cK.O females. Hematoxylin and Eosin (H&E) stained sections from d4.5pc and d7.5pc implantation sites in Cripto cK.O females and Controls. On d4.5pc in Control group, uterine lumen in implantation sites is completely closed in contrast to cK.O females. on d7.5pc, in implantation site of Control uterus, residues of closed uterine lumen can be seen whereas in many implantation sites from Cripto cKO females, failure of uterine luminal closure is still quite evident. AM, antimesometrial pole; De, Decidual cells; LE, luminal epithelium; Lu, lumen; M, mesometrial pole; My, myometrium; rLE, residual luminal epithelium; rLu, residual lumen; St, Stroma (Scale bar, d4.5pc: 250 µm; d7.5pc: 75 µm).

Discussion

Currently, how Cripto is involved in female reproduction is not well understood. In our study, we have shown that Cripto is expressed in the uterus during critical stages of early pregnancy and its deletion results in subfertility due to of implantation failure, impaired peri-implantation uterine remodeling and impaired uterine decidualization.

Most of the literature concerning the mechanisms by which CRIPTO influences gene expression and cellular processes comes from studies of the Nodal signaling pathway. Nodal signal is mediated by binding to an extracellular membrane-bound receptor complex comprised of type I (ALK4/ALK7, mainly ALK4) and type II (ActRIIA/ActRIIB) Activin receptors, along with an EGF-CFC co-receptor (Cripto/Cryptic, mainly Cripto). Activation of the receptor complex results in phosphorylation of the transcription factors SMAD2 and SMAD3. Phosphorylated SMAD2/3 binds to SMAD4, which allows for the nuclear translocation of the SMAD2/3/4 complex. These SMADs then associate with additional transcription factors, such as FoxH1, Mixer and p53 to facilitate DNA binding and regulation of downstream target genes [34]. It is known, however, that besides being a co-receptor for Nodal, Cripto can activate Smad-independent signaling elements such as PI3K/Akt and MAPK and also facilitate signaling through the canonical Wnt/ß-catenin and Notch/Cbf-1 pathways by functioning as a chaperone protein for LRP5/6 and Notch, respectively [25].

Among the components of Nodal-Cripto-Alk4-Smad dependent pathway, the uterine expression pattern and/or reproductive consequences of uterine deletion of Nodal [10, 11], ALK4 [18], Smad3 [12], Smad2 and Smad4 [20, 35] have been studied. Deletion of Cripto in the female

reproductive tract does not phenocopy uterine specific deletion of Nodal or Alk4. Some physiologic events are disrupted in Nodal cK.O mice but seem to be normal, impaired with less severity or impaired with a different phenotype in Cripto cK.O and/or Alk4 cK.O mice. A conditional deletion of Nodal in the mouse uterus, using a similar loxP-Cre system, resulted in a dramatic reduction in fertility of Nodal conditional homozygous knockout (cK.O) and conditional heterozygous females due to impaired implantation, decidualization and placentation [11]. Unlike Cripto cK.Os and Alk4 cK.Os however, Nodal cK.Os are prone to pre-term delivery on d17.5pc as opposed to term birth at d19.5pc [11] and both Nodal cK.O and Nodal cHet females showed significantly higher sensitivity to infection-induced inflammation which causes them to deliver prematurely [17]. Even though ovulation, fertilization and early embryo development are normal in Cripto, Nodal and Alk4 cK.O mouse models, considerable implantation failure is observed in Nodal cK.O mice; this phenotype is very mild in Cripto cK.O and Alk4 cK.O females however [18]. This observation can be justified with these 2 possibilities: 1) Nodal role in regulating implantation is exerted through Cripto/Alk4/Smad-independent pathways and/or 2) Nodal target cells in the uterus during peri-implantation period are those that do not express progesterone receptor (most probably immune cells); Therefore, Cripto or Alk4 would not be deleted in these cells and the required pathway will remain active.

Comparative analysis of decidualization in Nodal, Cripto and Alk4 conditional K.O female mice suggests that Nodal and Cripto, but not Alk4, are required for stromal decidualization. Evaluated by means of artificial decidualization, while both Cripto cK.O (shown in the present study) and Nodal cK.O females (Park CB, Dufort D; manuscript in preparation) show a compromised decidualization ability in response to artificial trigger of decidualization, Alk4 cK.O

females reveal no defect in decidualization as they react completely similar to control females [18]. This observation can suggest that Nodal and Cripto are involved in uterine decidualization probably through Alk4/Smad-independent pathways.

We have assessed the level of some critical factors in uterine decidualization including the serum level of progesterone (P4) on d7.5pc and expression of Cox2, IHH, Hoxa10, Hoxa11, Bmp2, Wnt4 and Notch signaling pathway components on d5.5pc uteri of Cripto cK.O and Control females. While the level of P4 on d7.5pc and the expression of Ihh, Cox2, Hoxa10 and Hoxa11 on d5.5pc showed no difference between groups, the expression of Bmp2 and Wnt4 were significantly lower in d5.5pc non-pregnant Cripto cKO mice compared to the pregnant d5.5pc Cripto cKO and Controls. The expression of Wnt4 was also significantly lower in pregnant d5.5pc Cripto cKO compared to pregnant d5.5pc Controls. In a study by Farah et. Al. in 2017 [36] it was shown that in the uteri of porcupine cK.O females in which signaling by all Wnts is disrupted, on d5.5pc the level of Wnt4 expression is significantly decreased and these females have impaired uterine decidualization. As mentioned before, Cripto enhances canonical Wnt signaling [37], therefore a possible cause for the lowered levels of Wnt4 in Cripto cK.O females might be a potential decrease in canonical Wnt signaling activity.

BMP2 [9] and Wnt4 [38] which are both critical decidualization elements are suggested to be involved more in differentiation of decidual cells rather than the proliferation phase [29]. We evaluated the differentiation state of decidual cells in d5.5pc pregnant Cripto cKO females versus Controls using a staining for tissue Alkaline phosphatase activity. Differentiated decidual cells should have a high level of alkaline phosphatase enzyme which results in a strong staining.

Interestingly this experiment showed that decidual cell differentiation is indeed compromised in Cripto cKO females.

The Notch signaling pathway and its components such as Notch1 and Rbpj have been shown to be critical for uterine stromal decidualization [31, 32], stromal remodeling and uterine luminal closure [16]. We have seen a significant decrease in the expression of Notch1, Notch4 and Dll4 in the uteri of pregnant d5.5pc Cripto cK.O compared to Control females. In addition, histological analysis during the post-implantation period, abnormal implantation crypts and failure of uterine luminal closure were frequently observed in Cripto cK.O females in contrast to controls. These findings are very similar to phenotypes observed in the case of disruption of Notch signaling pathway [16]. Cripto has been shown to be implicated in enhancing of Notch signaling [33]. Impaired decidualization and uterine luminal closure process in Cripto cK.O mice can therefore be the result of decreased activity of Notch signaling which in turn results in lowered expression of Notch receptors [39] leading to additional decrease in the activity of Notch signaling pathway and worsening of the condition.

Conclusion

We have characterized the expression pattern of Cripto during early mouse pregnancy and studied the effects of deleting Cripto in the female reproductive tract which results in subfertility in the forms of lower pregnancy rate and smaller litter size. We have also shown that the presence of defective peri-implantation uterine remodeling, decidualization and luminal closure in Cripto cK.O females are the underlying causes for their subfertility. Although we have not shown precisely but based on findings of this study, we suggest that Cripto exerts

functions in female reproduction that can be both related and independent of Nodal signaling. We have introduced a mouse model to better understand the regulation of female reproduction by TGF-β related signaling which also can be considered a good tool to study the pathogenesis of pregnancy-related issues in humans aiming towards the development of new treatments for female infertility and pregnancy complications.

Acknowledgment

This work was supported by grants from the Canadian Institutes of Health Research PJT-159788 and a March of Dimes grnt #21-FY14-130 to D.D. S.S. was supported by a scholarship from the Faculty of Medicine, Division of Experimental Medicine of McGill University and the RI-MUHC.

References

1. Dey, S.K., et al., Molecular cues to implantation. Endocrine Reviews, 2004. 25(3): p. 341-373.

2. Wang, H.B. and S.K. Dey, Roadmap to embryo implantation: clues from mouse models. Nature Reviews Genetics, 2006. 7(3): p. 185-199.

3. Cha, J.Y., X.F. Sun, and S.K. Dey, Mechanisms of implantation: strategies for successful pregnancy. Nature Medicine, 2012. 18(12): p. 1754-1767.

4. Matzuk, M.M., T.R. Kumar, and A. Bradley, DIFFERENT PHENOTYPES FOR MICE DEFICIENT IN EITHER ACTIVINS OR ACTIVIN RECEPTOR-TYPE-II. Nature, 1995. 374(6520): p. 356-360.

5. Dong, J.W., et al., Growth differentiation factor-9 is required during early ovarian folliculogenesis. Nature, 1996. 383(6600): p. 531-535.

6. Elvin, J.A., et al., Paracrine actions of growth differentiation factor-9 in the mammalian ovary. Molecular Endocrinology, 1999. 13(6): p. 1035-1048.

7. Brown, C.W., et al., Insertion of Inhbb into the Inhba locus rescues the Inhba-null phenotype and reveals new activin functions. Nature Genetics, 2000. 25(4): p. 453-457.

8. Jorgez, C.J., et al., Granulosa cell-specific inactivation of follistatin causes female fertility defects. Molecular Endocrinology, 2004. 18(4): p. 953-967.

9. Lee, K.Y., et al., Bmp2 is critical for the murine uterine decidual response. Molecular and Cellular Biology, 2007. 27(15): p. 5468-5478.

10. Park, C.B. and D. Dufort, Nodal Expression in the Uterus of the Mouse Is Regulated by the Embryo and Correlates with Implantation. Biology of Reproduction, 2011. 84(6): p. 1103-1110.

11. Park, C.B., et al., NODAL in the Uterus Is Necessary for Proper Placental Development and Maintenance of Pregnancy. Biology of Reproduction, 2012. 86(6).

12. Zhao, K.Q., et al., Maternal Smad3 deficiency compromises decidualization in mice. Journal of Cellular Biochemistry, 2012. 113(10): p. 3266-3275.

13. Clementi, C., et al., Activin-Like Kinase 2 Functions in Peri-implantation Uterine Signaling in Mice and Humans. Plos Genetics, 2013. 9(11).

14. Nagashima, T., et al., BMPR2 is required for postimplantation uterine function and pregnancy maintenance. Journal of Clinical Investigation, 2013. 123(6): p. 2539-2550.

15. Park, C.B. and D. Dufort, NODAL signaling components regulate essential events in the establishment of pregnancy. Reproduction, 2013. 145(2): p. R55-R64.

16. Zhang, S., et al., Uterine Rbpj is required for embryonic-uterine orientation and decidual remodeling via Notch pathway-independent and -dependent mechanisms. Cell Research, 2014. 24(8): p. 925-942.

17. Heba, T., C. Park, and D. Dufort, DECIPHERING THE ROLE OF THE NODAL SIGNALING PATHWAY IN PRETERM BIRTH. Placenta, 2015. 36(9): p. A59-A59.

18. Peng, J., et al., Uterine Activin-Like Kinase 4 Regulates Trophoblast Development During Mouse Placentation. Molecular Endocrinology, 2015. 29(12): p. 1684-1693.

19. Peng, J., et al., Uterine activin receptor-like kinase 5 is crucial for blastocyst implantation and placental development. Proceedings of the National Academy of Sciences of the United States of America, 2015. 112(36): p. E5098-E5107.

20. Rodriguez, A., et al., SMAD Signaling Is Required for Structural Integrity of the Female Reproductive Tract and Uterine Function During Early Pregnancy in Mice. Biology of Reproduction, 2016. 95(2).

21. Ni, N. and Q.L. Li, TGF beta superfamily signaling and uterine decidualization. Reproductive Biology and Endocrinology, 2017. 15.

22. Strizzi, L., et al., Cripto-1: A multifunctional modulator during embryogenesis and oncogenesis. Oncogene, 2005. 24(37): p. 5731-5741.

23. Jin, J.Z. and J.X. Ding, Cripto is required for mesoderm and endoderm cell allocation during mouse gastrulation. Developmental Biology, 2013. 381(1): p. 170-178.

24. Ding, J.X., et al., Cripto is required for correct orientation of the anterior-posterior axis in the mouse embryo. Nature, 1998. 395(6703): p. 702-707.

25. Klauzinska, M., et al., The multifaceted role of the embryonic gene Cripto-1 in cancer, stem cells and epithelial-mesenchymal transition. Seminars in Cancer Biology, 2014. 29: p. 51-58.

26. Papageorgiou, I., et al., Expression of nodal signalling components in cycling human endometrium and in endometrial cancer. Reproductive Biology and Endocrinology, 2009. 7.

27. Bandeira, C.L., et al., Tumorigenic Factor CRIPTO-1 Is Immunolocalized in Extravillous Cytotrophoblast in Placenta Creta. Biomed Research International, 2014.

28. Dela Cruz, C., et al., Expression of Nodal, Cripto, SMAD3, Phosphorylated SMAD3, and SMAD4 in the Proliferative Endometrium of Women With Endometriosis. Reproductive Sciences, 2015. 22(5): p. 527-533.

29. Ramathal, C.Y., et al., Endometrial Decidualization: Of Mice and Men. Seminars in Reproductive Medicine, 2010. 28(1): p. 17-26.

30. Milligan, S.R. and C.A. Finn, Minimal progesterone support required for the maintenance of pregnancy in mice. Human Reproduction, 1997. 12(3): p. 602-607.

31. Afshar, Y., et al., Notch1 mediates uterine stromal differentiation and is critical for complete decidualization in the mouse. Faseb Journal, 2012. 26(1): p. 282-294.

32. Strug, M.R., et al., RBPJ mediates uterine repair in the mouse and is reduced in women with recurrent pregnancy loss. Faseb Journal, 2018. 32(5): p. 2452-2466.

33. Watanabe, K., et al., Enhancement of Notch receptor maturation and signaling sensitivity by Cripto-1. Journal of Cell Biology, 2009. 187(3): p. 343-353.

34. Schier, A.F., Nodal Morphogens. Cold Spring Harbor Perspectives in Biology, 2009. 1(5).

35. Liu, G., et al., Expression of Smad2 and Smad4 in mouse uterus during the oestrous cycle and early pregnancy. Placenta, 2004. 25(6): p. 530-537.

36. Farah, O., et al., Regulation of porcupine-dependent Wnt signaling is essential for uterine development and function. Reproduction, 2018. 155(1): p. 93-102.

37. Nagaoka, T., et al., Cripto-1 enhances the canonical Wnt/beta-catenin signaling pathway by binding to LRP5 and LRP6 co-receptors. Cellular Signalling, 2013. 25(1): p. 178-189.

38. Franco, H.L., et al., WNT4 is a key regulator of normal postnatal uterine development and progesterone signaling during embryo implantation and decidualization in the mouse. Faseb Journal, 2011. 25(4): p. 1176-1187.

39. Artavanis-Tsakonas, S., M.D. Rand, and R.J. Lake, Notch signaling: Cell fate control and signal integration in development. Science, 1999. 284(5415): p. 770-776.

40. Soyal, S.M., et al., Cre-mediated recombination in cell lineages that express the progesterone receptor. Genesis, 2005. 41(2): p. 58-66.

Supplemental material

Figure 2.S1. Cripto localization in pregnant uterus corresponds with implantation sites. Localization of Cripto (brown) is shown by Immunohistochemistry. On d1.5pc, Cripto protein expression (arrows) is very low and is limited to a few stromal cells adjacent to the luminal epithelium and in a few cells within the luminal epithelium (A and B). On d3.5pc, Cripto protein expression is quite prominent in the uterine stromal cells and to a less extent in the luminal epithelium only at future implantation site (C, C' and C") but not at inter-implantation space (D, D' and D", sections are from the same pregnant uterus). Gradient pattern of Cripto protein expression in the stromal cells at the implantation site is also noticeable (C-C") where the expression is highest in the stromal cells adjacent to the luminal epithelium and decreases with distance from the luminal epithelium toward the periphery of the uterus. Cripto protein expression is also visible in the embryo within uterine lumen (C"). C', C", D' and D" are higher magnification of the fields defined by boxes in C and D. AM, antimesometrial pole; Em, embryo; GE, glandular epithelium; LE, luminal epithelium; Lu, lumen; M, mesometrial pole; My, myometrium; St, stroma. (Scale bar: A, 75 µm; B, C and D, 50 µm; C', C", D' and D", 250 µm)

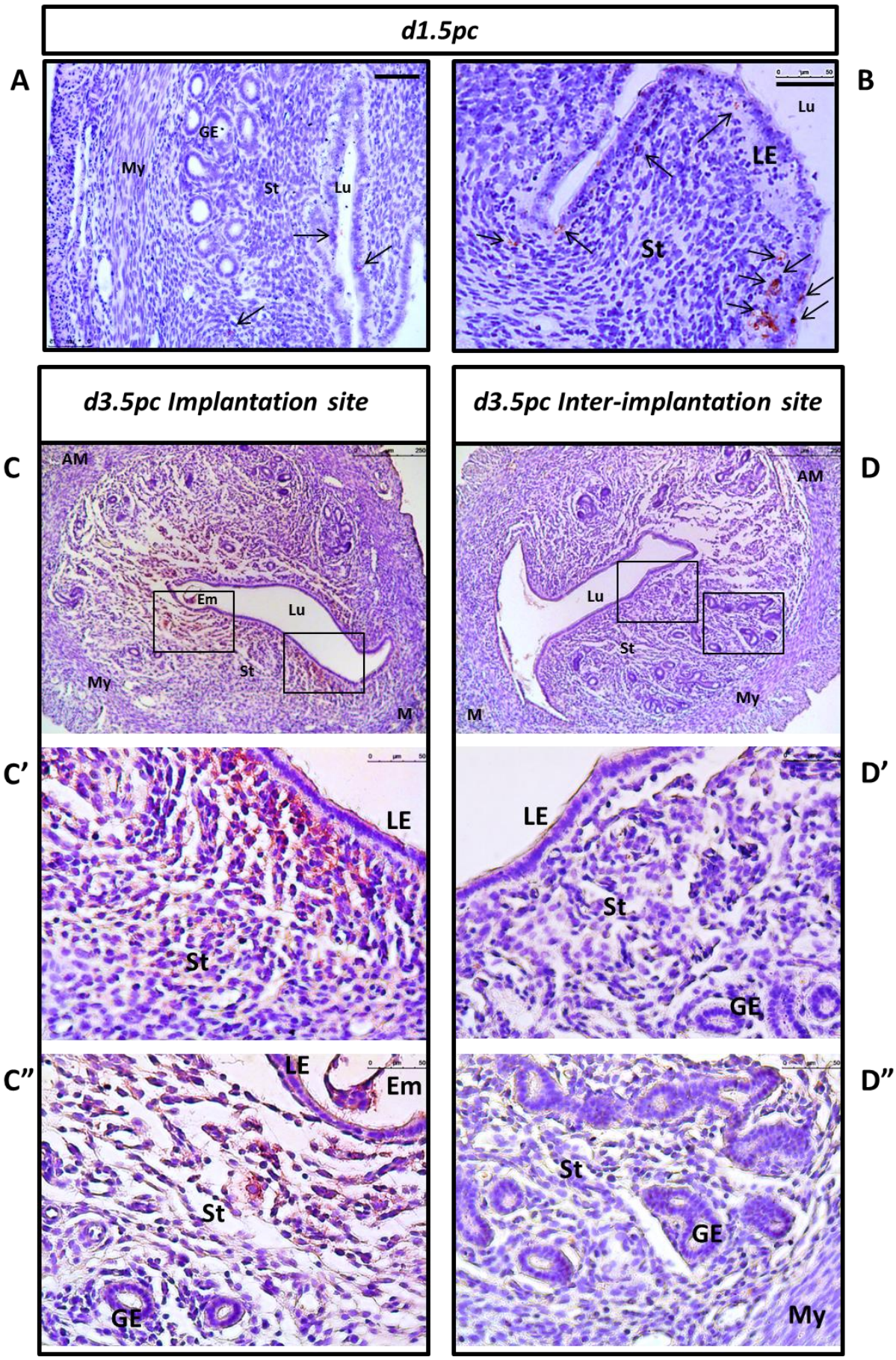
d1.5pc
A
GE
My
St
Lu
B
Lu
LE
St
d3.5pc Implantation site
d3.5pc Inter-implantation site
C
AM
Em
Lu
St
My
M
D
AM
Lu
St
My
M
C'
LE
St
D'
LE
St
GE
C''
LE
Em
St
GE
D''
St
GE
My

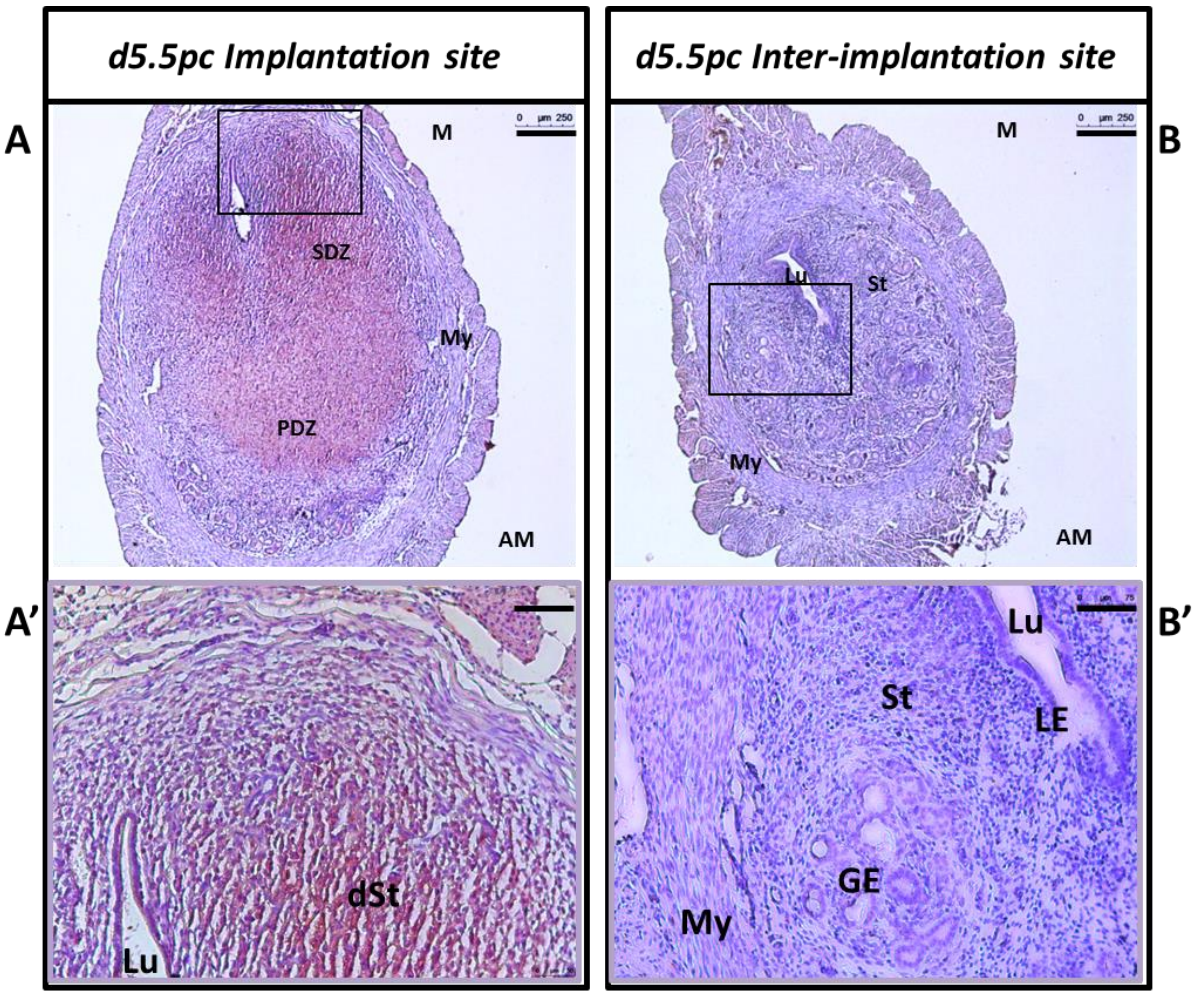

Figure 2.S2. Cripto protein is highly expressed in uterine decidual cells and differentiating stromal cells after implantation. Immunohistochemistry against Cripto (brown) on d5.5pc (1 day after implantation) comparing implantation site (A and A') and inter-implantation site (B and B') in the same pregnant uterus. Localization of Cripto protein is limited to the implantation sites (A) and is observed in decidual cells and differentiating stromal cells (A'). Cripto is not detectable at inter-implantation spaces (B and B'). A' and B' are higher magnification of the fields defined by black boxes in A and B. AM, antimesometrial pole; dSt, differentiating stromal cells; GE, glandular epithelium; LE, luminal epithelium; Lu, lumen; M, mesometrial pole; My, myometrium; PDZ, primary decidual zone; SDZ, secondary decidual zone; St, Stroma. (Scale bar, A' and B': 75 µm; A and B: 250 µm)

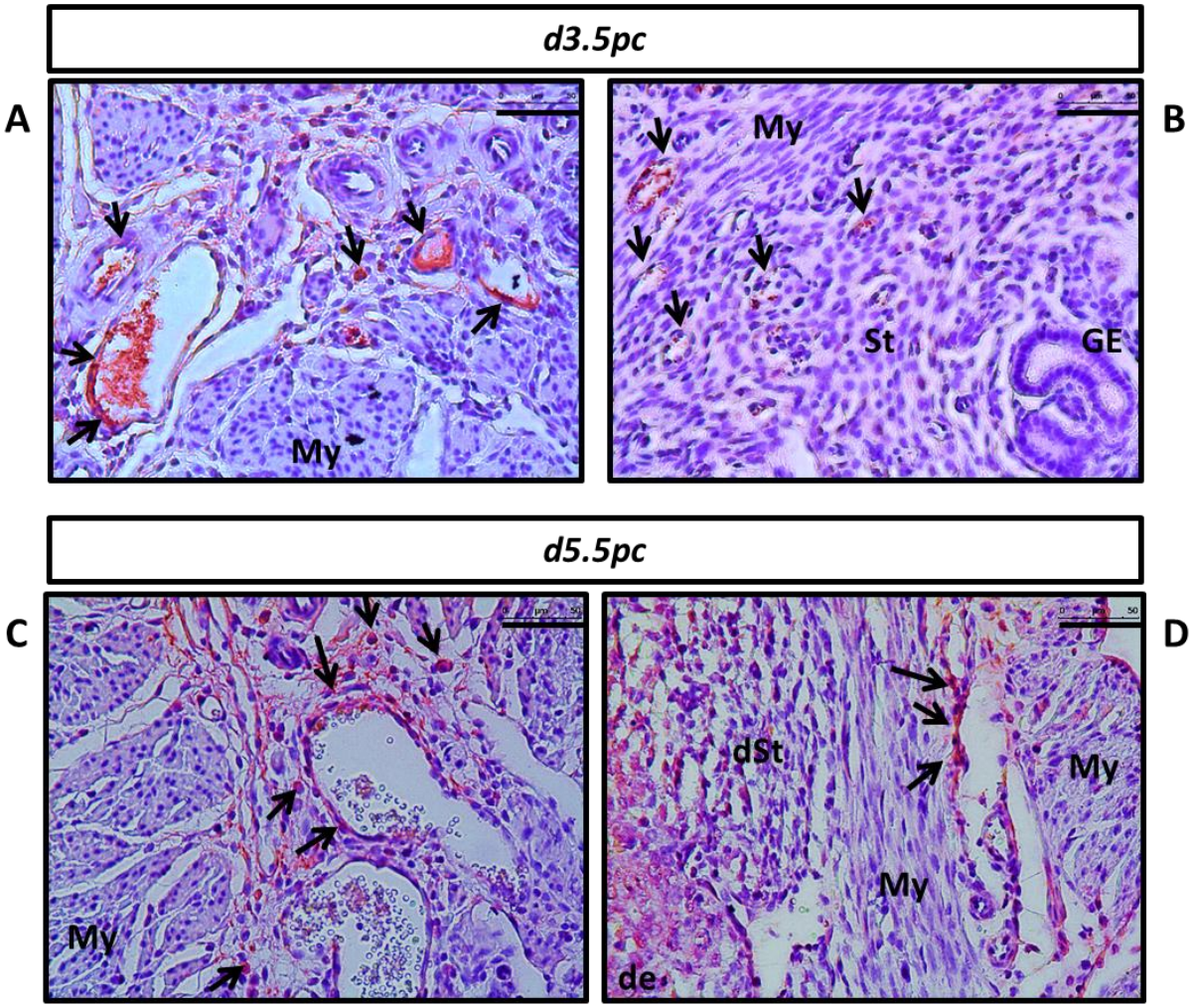

Figure 2.S3. Cripto protein is localized around the uterine vasculature during peri-implantation and post –implantation period. Immunohistological evaluations on d3.5pc and d5.5pc revealed perivascular localization of Cripto (brown, marked with arrows) around mesometrial (A and C) and myometrial/stromal vascular structures (B and D). De, decidual cells; GE, glandular epithelium; My, myometrium; dSt, differentiating stroma. (Scale bar: 50 µm)

Figure 2.S4

A

	Control females (n=4)	Cripto cKO females (n=4)
Total no. of pups-first month	32 pups/4 litter	10 pups/1 litter
Total no. of pups-second month	35 pups/3 litters	48 pups/7 litters
Total no. of pups-third month	55 pups/5 litters	22 pups/4 litters
Total no. of pups-forth month	55 pups/5 litters	7 pups/2 litters
Total no. pups-fifth month	42 pups/4 litters	14 pups/5 litters
Total no. of pups over 5 months	219 pups	101 pups
Total no. of litters over 5 months	21 litters	19 litters

B

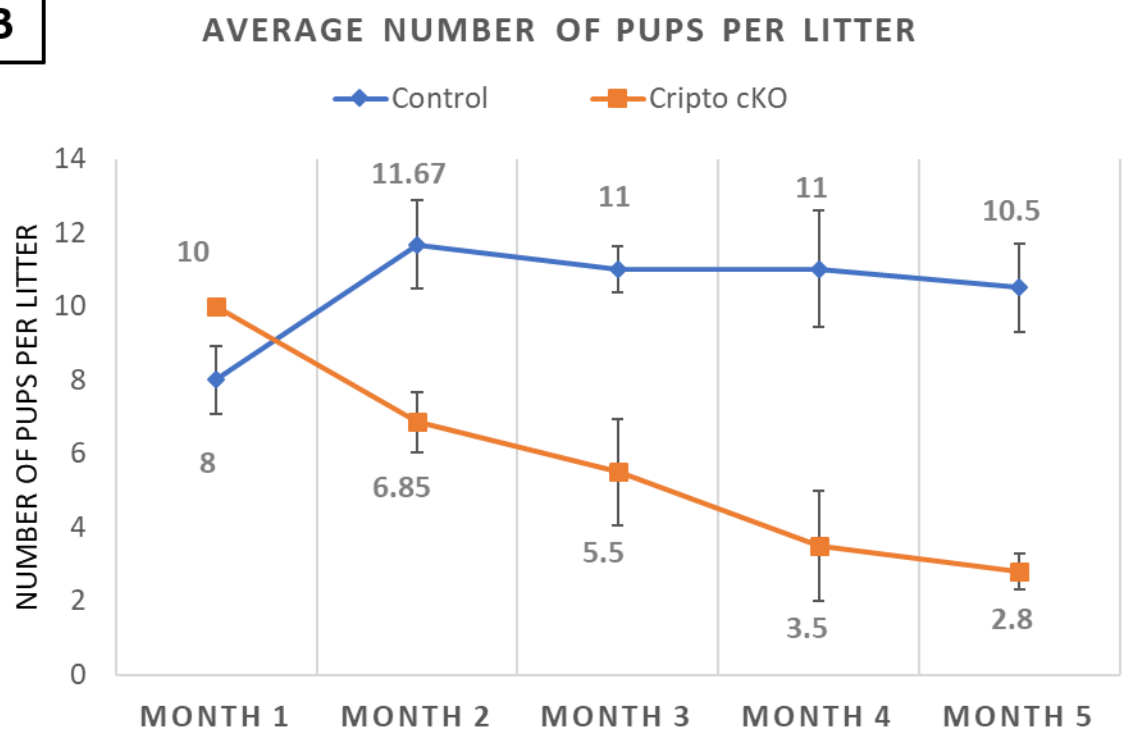

Figure 2.S4. Assessment of fertility in a 5 months-long breeding trial. (A), the number of pups and litters produced by Control and Cripto cKO females during every month of the trial. (B), the changes in the average number of pups per litter over time is shown in Cripto cKO females compared to Controls.

Figure 2.S5

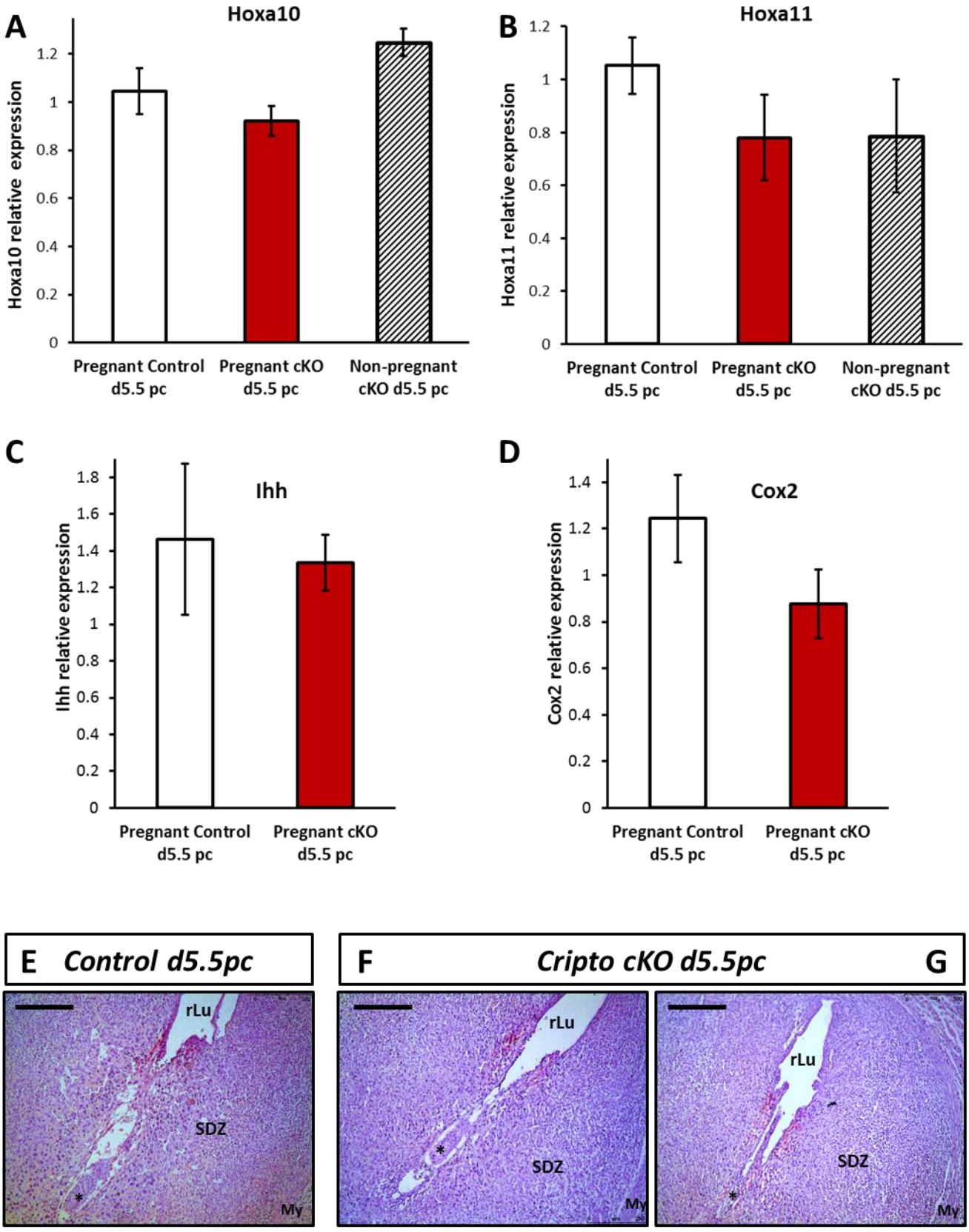
A
Hoxa10
Hoxa10 relative expression
1.2
1
0.8
0.6
0.4
0.2
0
Pregnant Control d5.5 pc
Pregnant cKO d5.5 pc
Non-pregnant cKO d5.5 pc
B
Hoxa11
Hoxa11 relative expression
1.2
1
0.8
0.6
0.4
0.2
0
Pregnant Control d5.5 pc
Pregnant cKO d5.5 pc
Non-pregnant cKO d5.5 pc
C
Ihh
Ihh relative expression
1.8
1.6
1.4
1.2
1
0.8
0.6
0.4
0.2
0
Pregnant Control d5.5 pc
Pregnant cKO d5.5 pc
D
Cox2
Cox2 relative expression
1.4
1.2
1
0.8
0.6
0.4
0.2
0
Pregnant Control d5.5 pc
Pregnant cKO d5.5 pc
E Control d5.5pc
F Cripto cKO d5.5pc
G
rLu
SDZ
My
rLu
SDZ
My
rLu
SDZ
My

Figure 2.S5. Normal expression level of *Ihh, Cox2, Hoxa10* and *Hoxa11* in Cripto cK.O females. (A-D) Relative expression of *Ihh, Cox2, Hoxa10* and *Hoxa11* on d5.5pc was measured by quantitative real-time PCR (pregnant Control d5.5pc, n= 6-8 females; pregnant Cripto cKO d5.5pc, n= 8-10 females and non-pregnant Cripto cKO d5.5pc, n = 5-6 females). (E-G) IHC staining against Cox2 on d5.5pc implantation site shows that localization of Cox2 protein (brown) in Cripto cK.O females is similar to Control. (G) Presence of an extra branch in the implantation crypt is also visible. My, myometrium; rLu, residual lumen; SDZ, secondary decidual zone; embryos in the sections are marked by stars (Scale bar: 250 μm).

Table S1. Level of serum Progesterone on d7.5pc in Cripto cK.O females versus Controls.

Table S1	Pregnancy status on d7.5 pc	Level of serum Progesterone on d7.5 pc * (ng/ml)
Cripto cKO	Pregnant-9 decidua	>42.00
Cripto cKO	Pregnant-11 decidua	>42.00
Cripto cKO	Not pregnant	>42.00
Cripto cKO	Not pregnant	>42.00
Cripto cKO	Pregnant-8 decidua	29.81
Cripto cKO	Pregnant-13 decidua	>42.00
Cripto cKO	Pregnant-10 decidua	>42.00
Cripto cKO	Pregnant-9 decidua	>42.00
Cripto cKO	Complete litter resorption (7 resorption sites)	39.05
Cripto Control	Pregnant-9 decidua	>42.00
Cripto Control	Pregnant-8 decidua	>42.00
Cripto Control	Pregnant-12 decidua	>42.00
Cripto Control	Pregnant-9 decidua	>42.00

* minimum required level of Progesterone on d7.5pc of pregnancy: 12.5-15.5 ng/ml

Chapter 3: MANUSCRIPT II

Title

Maternal Cripto is critical for proper development of placental vasculature by affecting the level of VEGF and Notch signaling pathway components

Shiva Shafiei,[1,2] Daniel Dufort [1,2,3,4]

1 Division of Experimental Medicine, McGill University Health Centre, Montreal, Canada
2 Child Health and Human Development Program, Research Institute of the McGill University Health Centre, Montreal, Canada
3 Department of Obstetrics and Gynecology, McGill University Health Centre, Montreal, Canada
4 Department of Biology, McGill University, McGill University Health Centre, Montreal, Canada

Corresponding Author: Daniel Dufort

Program Leader, Child Health and Human Development program
Director of the Division of Translational Research in OBGYN
Research Institute of the McGill University Health Centre
1001 boul Décarie
CHHD EM03230
Montréal, QC, H4A 3J1
Canada
Daniel.dufort@mcgill.ca
Tel: (514) 934-1934 ext. 34743

Keywords: Cripto, Placenta, placental vasculature, Notch signaling, IUGR, immune cells at

maternal-fetal interface

Preface

In Manuscript I (Chapter 2), we showed that Cripto is expressed in the mouse uterus during early stages of pregnancy and loss of uterine Cripto results in subfertility in the form of lower pregnancy rate and fewer number of pups per litter. In Manuscript I (Chapter 2) we also showed that the cause of the lower pregnancy rate is implantation failure, impaired peri-implantation uterine remodeling and defective stromal decidualization.

Here, in Manuscript II (Chapter 3), we asked ***why Cripto cKO female give birth to fewer number of pups per litter with possibility of fetal death due to placentation defects in our mind***. In this chapter we were mainly focused on the ***period of placental development and late pregnancy***. The expression pattern of Cripto at maternal-fetal interface during placentation period was evaluated. Furthermore, the structure of placenta, viability and growth of the fetuses, as well as maternal immune cell composition at the placentation site were analyzed in pregnancy of Cripto cKO females in comparison with Controls.

Abstract

The growth and survival of the mammalian fetus is dependent on the placenta, which is the interface between the maternal and fetal blood circulation that is essential for the exchange of nutrients, gas and elimination of fetal wastes. Several research groups including our lab have demonstrated the involvement of different transforming growth factor-beta (TGFβ) superfamily members and their related receptors in placentation. Cripto is a member of the epidermal growth factor-Cripto1/FRL1/Cryptic protein family and plays a critical role in embryonic development, stem cell maintenance and tumor progression through TGFβ-dependent and independent pathways. Several studies have suggested that Cripto may also have a role in female reproduction and pregnancy maintenance, but its specific role remains elusive. We have previously created a uterine-specific conditional knockout of Cripto and have shown that Cripto cKO females are subfertile due to compromised uterine remodeling and decidualization. Our previous findings also suggested that deletion of Cripto from the uterus resulted in placental defects or insufficiency, leading to fetal death. Here, we showed that Cripto is expressed at maternal-fetal interface during the placentation period by a variety of cell types including different maternal immune cells and fetal trophoblast cells. We found that loss of maternal Cripto in uterine stromal, epithelial and decidual cells during early pregnancy eventually results in defective placentation, altered immune cell composition at maternal-fetal interface, decreased vascularization within maternal decidua and more interestingly in the placental labyrinth. We further demonstrated that components of the VEGF and Notch signaling pathways are downregulated in Cripto cKO decidua and placenta potentially contributing to defects in the development of the vasculature at maternal-fetal interface. These findings

suggest that maternal Cripto is part of the maternal-fetal communications required for proper development of placenta and placental vasculature.

Introduction

The growth and survival of the mammalian fetus depends on the placenta which is the interface between the maternal and fetal blood circulation, essential for the exchange of nutrients, gas and elimination of fetal wastes [1]. The placenta also forms a barrier that protects the fetus against the maternal immune system. Furthermore, the placenta is the source of hormones that changes the maternal physiology required for adaptation to pregnancy [2]. Although there are some differences in the details of the human and mouse placental structures, the overall architecture of placenta and the molecular mechanisms controlling placental development are similar [3]. This similarity has led to the increasing use of mouse models for studying the essential elements of placental development.

The mature placenta in both humans and rodents has three main layers: the maternal layer which is composed of uterine decidual cells, maternal vasculature and maternal immune cells, a junctional layer composed of fetal trophoblast cells that are responsible for attachment of the fetal compartments of placenta to the maternal compartment by invading the uterine wall and maternal vessels; and the third layer which is composed of vastly branched villi [3]. Placenta in primates and rodents is of the hemochorial type in which fetal blood is surrounded by fetal

endothelial cell-lined vessels but the maternal blood is in contact with specific types of trophoblast cells [4].

In mice, at embryonic day 8.0 (E8.0), extraembryonic mesoderm (allantois), which subsequently will give rise to the fetal vascular compartment of the placenta [2], extends from the posterior end of the embryo and at E8.5, in a process called chorioallantoic attachment (or fusion), the chorion and the allantois locate closely and join together. Shortly after, the chorion starts to fold toward the mesometrial pole, eventually forming the chorionic villi, which creates spaces for the allantois-derived fetal blood vessels to grow into [2]. Concomitantly, the differentiation of chorionic villi trophoblast cells into labyrinth cell types begins. Syncytiotrophoblasts are multinucleated cells that surround the endothelium of the fetal capillaries within the labyrinth and are formed by the fusion of trophoblast cells. The maternal blood sinuses within the labyrinth are lined by a mononuclear trophoblast cell type termed sinusoidal trophoblast giant cells. The labyrinth trophoblast cells, and fetal vasculature together form the structure of the highly branched mouse placental labyrinth villi. The labyrinth grows and becomes more extensively branched with progress of pregnancy until birth which in mice is E18.5 to 19.5 [5]. Labyrinth of the placenta is the placental compartment where the maternal and fetal blood are in very close proximity for the purpose of nutrients, gas and fetal waste transport. The countercurrent direction of maternal and fetal blood flow within the labyrinth maximizes the efficiency of this transport [5]. Any developmental defect such as aberrant or inadequate vascularization, branching or dilation of the labyrinth can result in impaired placental perfusion and insufficient oxygen and nutrient diffusion which negatively affects fetal growth and survival [6].

Several research groups including our lab, have demonstrated the involvement of different transforming growth factor-beta (TGFβ) superfamily members and their related receptors in placentation (e.g. Nodal [7, 8], BMPR2 [9], ALK4 [10] and ALK5 [11]) as well as other fundamental reproductive events [7-24]. Cripto is a member of the epidermal growth factor-Cripto1/FRL1/Cryptic (EGF-CFC) protein family that acts as a co-receptor in the TGF-β signaling pathways (Nodal, GDF1 and GDF3) and plays a critical role in embryonic development [25, 26]. Cripto null mice are embryonic lethal (between d7.5pc and d10.5pc) because of major gastrulation and heart developmental defects [27]. In addition to be a co-receptor in the TGF-β signaling pathway, Cripto can activate Smad-independent signaling pathways such as PI3K/Akt and MAPK and facilitate signaling through the canonical Wnt/ß-catenin and Notch/Cbf-1 signaling pathways [28]. Through these various mechanisms, Cripto is implicated in early embryogenesis, embryonic stem cell maintenance, facilitating epithelial-mesenchymal transitions and significantly enhancing tumor cell migration, invasion and angiogenesis [28].

Several studies in the literature suggest that, in addition to the aforementioned functions, Cripto may also have a role in female reproduction and pregnancy maintenance. Cripto mRNA is consistently detected in endometrial samples from healthy women during the menstrual cycle [29]. The expression of Cripto is also dysregulated in specific human placental and endometrial pathologies such as placenta creta, [30] and endometriosis [31]. The specific role of maternal Cripto in female reproduction and pregnancy remains elusive however, as no study has yet been conducted that presents an in-depth analysis of its function in the endometrium. We have previously created a uterine-specific conditional knockout (cKO) of Cripto and have shown that Cripto cKO females are subfertile due to compromised uterine remodeling and decidualization

(Shafiei et al, manuscript submitted). Our previous findings also suggested that deletion of Cripto from the uterus results in placental defects or insufficiency leading to fetal death. In the present study, we showed that Cripto is expressed at maternal-fetal interface during the placentation period and that maternal Cripto plays a key role in normal placental development.

Materials and methods

Generation and maintenance of Cripto cK.O and Control Mice

Experimental protocols in this study are in accordance with regulations established by the Canadian Council on Animal Care and were reviewed and approved by the Animal Care Committee of the McGill University Health Centre. Mice with loxP sites flanking exon 3-5 of the Cripto gene (Criptofloxed/floxed or Cripto f/f) on a C57BL6 background were purchased from The Jackson Laboratory (Stock Number: 016539, Strain Name: STOCKTdgf1tm2.2Mms/J). The generation of these mice has been previously described [32]. Progesterone receptor-Cre mice (PgrCre/+) were generously donated by F. J. DeMayo and J. P. Lydon [33] and maintained on a CD1 background in our lab. Both strains have previously been reported to be healthy and demonstrated normal fertility. PgrCre/+ mice have been used in numerous studies to investigate uterine-specific gene function.

Homozygous Criptof/f females were crossed with heterozygous PgrCre/+ males and the offspring were genotyped by tail snip digestion and PCR. The Cripto floxed (~ 300 bp) and Cripto wildtype (178 bp) alleles were amplified by touch-down PCR (94 °C 30 Sec, 58-55 °C 30 Sec, 72 °C 30 Sec) for 7 cycles decreasing the annealing temperature 0.5 °C in every cycle; then 30

cycles of (94 °C 30 Sec, 55 °C 30 Sec, 72 °C 30 Sec) using the following primers: Forward 5'-TGG TGA TCC AGA GTC ATT GG-3' and Reverse 5'-GGG GTC ATT CCT CTC CTA GC-3'. The Pgr-Cre (550 bp) and Pgr-wildtype (300 bp) alleles were amplified by standard PCR (94 °C 1 min, 60 °C 1 min, 72 °C 2 min) for 30 cycles using the following primers: 5'-ATGTTTAGCTGGCCCAAATG-3'; 5'-TATACCGATCTCCCTGGACG-3'; 5'-CCCAAAGAGACACCAGGAAG-3').

In the first generation, half of the offspring are heterozygous for both genes (Criptof/+ PgrCre/+). The Criptof/+ PgrCre/+ males were crossed with Criptof/f females in order to generate the required genotypes. Then the Cripto f/f, PgrCre/+ males were crossed with Criptof/f,Pgr +/+ females to produce the littermates used in our experiments: Cripto conditional knockout females (Cripto cK.O: Cripto f/f, PgrCre/+), and Control females (Criptof/f,Pgr +/+).

Mating and sample collection

To assess fertility, 6-12 weeks-old virgin females (Control and Cripto cK.O) were mated with sexually mature fertile wild-type CD1 males. Mating was confirmed by observation of a vaginal plug. Females were then separated from males after mating and the date of mating was recorded (d0.5pc). Mice were sacrificed on specific gestational ages, uteri were dissected, and the gross morphology was assessed, photographs were taken and then further required analysis was done.

Measurements of the conceptus site size

Using ImageJ software, the area of each conceptus site was measured in the photographs taken from whole mount pregnant uteri of Control and Cripto cK.O females at different time-points of pregnancy.

Tissue processing, paraffin embedding, sectioning and H&E staining

Dissected samples (Uterus or placenta) were collected in PBS, fixed overnight at 4 °C in 4% paraformaldehyde (PFA)/PBS or 10% neutral buffered formalin, dehydrated in increasing ethanol series (25%, 50%, 75%, and 100%, 20 min each) and cleared in xylenes (2×, 15 min). The tissue was incubated overnight in melted paraffin wax (TissueTek) at 60 °C in a vacuum oven then embedded at room temperature, and the blocks were placed on a cold plate for 1 hour to solidify slowly then transferred to −20 °C freezer overnight before sectioning. Seven-micrometer sections were cut with the Leica RM2145 microtome, mounted on Fisherbrand Superfrost plus slides and dried overnight. Slides were then either used for immunofluorescence, immunohistochemistry (described later) or stained with Hematoxylin and Eosin (H&E).

Immunofluorescence

As described earlier, uteri (Non-pregnant or d0.5pc to d4.5pc pregnant) were dissected, dehydrated, cleared, embedded in paraffin blocks and sectioned. Slides were then washed in

xylenes (2x 10 min), rehydrated with a decreasing ethanol gradient (100%, 95%, 85%, 75%, 50%, 20%; 2 min each). Antigen retrieval was done in 10mM sodium citrate solution (+ 0.05% Tween 20, pH 6) at 95 °C for 20 min. Sections then were permeabilized with PBT (0.2% BSA, 2.5% Triton X-100 in PBS for 15 min), blocked for 1 h at room temperature (10% heat-inactivated serum and 1% BSA in PBT) then incubated with the primary antibody (Table S2) at 4 °C overnight. Following several washes in 0.1% PBS-Tween 20, slides were incubated with the secondary antibody (Table S2) for 1 h at room temperature. Slides were then washed, counterstained with DAPI (1:5000) and mounted with Mowiol 4–88 [Sigma].

Immunohistochemistry

As described earlier, uteri were dissected, dehydrated, cleared, embedded in paraffin blocks and sectioned. Slides were then washed in xylenes (2x 10 min), rehydrated with a decreasing ethanol gradient (100%, 95%, 85%, 75%, 50%, 20%; 2 min each). Antigen retrieval was done in 10mM sodium citrate solution (+ 0.05% Tween 20, pH 6) at 95 °C for 20 min. Sections then were permeabilized with TBT (0.2% BSA, 2.5% TritonX-100 in TBS for 15 min), blocked for 1 h at room temperature (10% heat-inactivated serum and 1% BSA in TBS). Following washes in TBS-0.025 % Tween 20 (TBST), slides were incubated with primary antibody (Table S2) at 4 °C overnight. After washes with TBST, 0.3 % H_2O_2 in TBS was used for blocking endogenous peroxidase activity following by incubation with an appropriate (Table S2) secondary HRP antibody (1:500) for 1 h at room temperature. For antigen visualization, DAB Substrate Kit (Abcam ab64238) was used based on recommended instructions provided by the manufacturer. Then Slides were

counterstained with Hematoxylin solution, Gill no. 2 (Sigma-Aldrich) and mounted with Richard-Allan Scientific™ Mounting Medium (Thermo Fisher Scientific).

Reverse transcription and Real-time PCR

RNA extraction was done using Trizol and RNeasy Mini Kit [Qiagen Cat. No. 74104]. QuantiTect Reverse Transcription Kit [Qiagen Cat. No. 205311] was then used for cDNA synthesis. Real-time PCR was performed using the Rotor-Gene SYBR Green PCR Kit [Qiagen Cat. No. 204074] following the manufacturer's protocol. The primers are listed in Table S3.

Flow cytometry

Flow cytometry was used to investigate the decidual leukocyte populations present at maternal-fetal interface on d10.5pc of pregnancy. Females were sacrificed, uteri were dissected, and implantation sites were cut individually to remove the inter-implantation spaces. Embryo and fetal membranes were removed from each implantation site and the remaining tissues of 5 implantation sites from every pregnant female were combined, cut finely using surgical blades and then digested with an enzymatic cocktail (100 µl 1mg/ml of Liberase TM Research Grade (Sigma Roche, 5401119001), 9.9 ml HBSS (Sigma-Aldrich), 10 µl of 30 mg/ml DNase I (Sigma-Aldrich)) for 45 minutes in 37˚C with occasional pipetting to help with cell dissociation. Isolated cells were passed through 70-micron cell strainer, blocked for 10 minutes on ice with FC block (10 µl Purified Rat Anti-Mouse CD16/CD32 (Mouse BD Fc Block, Clone 2.4G2 BD 553141) in 990 µl FACS buffer) and were incubated with the designed panel of

antibodies (Table S4) for 30 min on ice. Then cells were washed 3 times with FACS buffer (495 ml PBS, 5 g BSA and 5 ml 0.5 M pH 8 EDTA) by centrifugation for 4 min at 800g, then fixed with 4% PFA for 10 minutes in ice. After 3 more washes, the supernatant was removed, and the cells were resuspended in 300 µl FACS buffer for flow cytometric analysis. To determine live vs dead cells a Fixable viability dye (Table S4) was used in the panel of antibodies. Analysis was carried out using the BD LSR Fortessa-X20 and data were collected using BD FACSDiva software and analyzed using FlowJo software version10.

For analysis of Cripto expression by immune cells, first similar process was performed with the same panel of antibodies. Then, instead of fixation with 4% PFA, a Fixation/Permeabilization Kit was used based on manufacturer's recommendation (eBioscience FoxP3/Transcription Factor Staining Buffer Set" Invitrogen 00-5523-00). After permeabilization, cells were incubated for 30 minutes on ice in the dark with Cripto antibody diluted in permeabilization buffer. Then cells were washed twice with permeabilization buffer by centrifuge at 500g for 5 minutes, resuspended in 300 µl of FACS buffer and moved to flow tubes for analysis by BD LSR Fortessa-X20.

Statistics

Data are presented as the mean ± SEM of independent samples. Statistical analysis comparing experimental groups was performed using two-tailed Student t-test for independent samples, Student t-test for correlated samples and F-test for the comparison of the difference between the variances of the two samples. P-values less than 0.05 were considered statistically significant.

Results

Fetal death and intrauterine growth restriction are observed in pregnancy of Cripto cKO mice during placentation and post-placentation period

We have previously shown (Shafiei et al, manuscript submitted) that although around 40% of Cripto cKO mice either fail to establish pregnancy or undergo embryo resorbsion between d5.5pc and d8.5pc, about 60% of the females do establish and maintain pregnancy with a similar number and size of implantation sites as in control females until the initiation of the placentation process (i.e. d8.5pc). However, by d10.5pc, 2 days after the start of placental development, the average size of implantation sites in Cripto cK.O females is significantly lower than that of controls ($P<0.0001$)(Figure 3.1 A and B). On d16.5pc, a significantly higher number of resorption sites (i.e. fetal death) and fewer number of decidua per pregnancy were observed in Cripto cK.O females compared to Controls (Figure 3.1 C and D). Furthermore, the average fetal weight was significantly lower ($P<0.0001$) in Cripto cK.O mothers compared to Controls (i.e. intra-uterine growth restriction; IUGR). Variations in fetal weight was also significantly higher in Cripto cK.O mothers compared to Controls (p value for difference of variances <0.0001) (Figure 3.1 E and F).

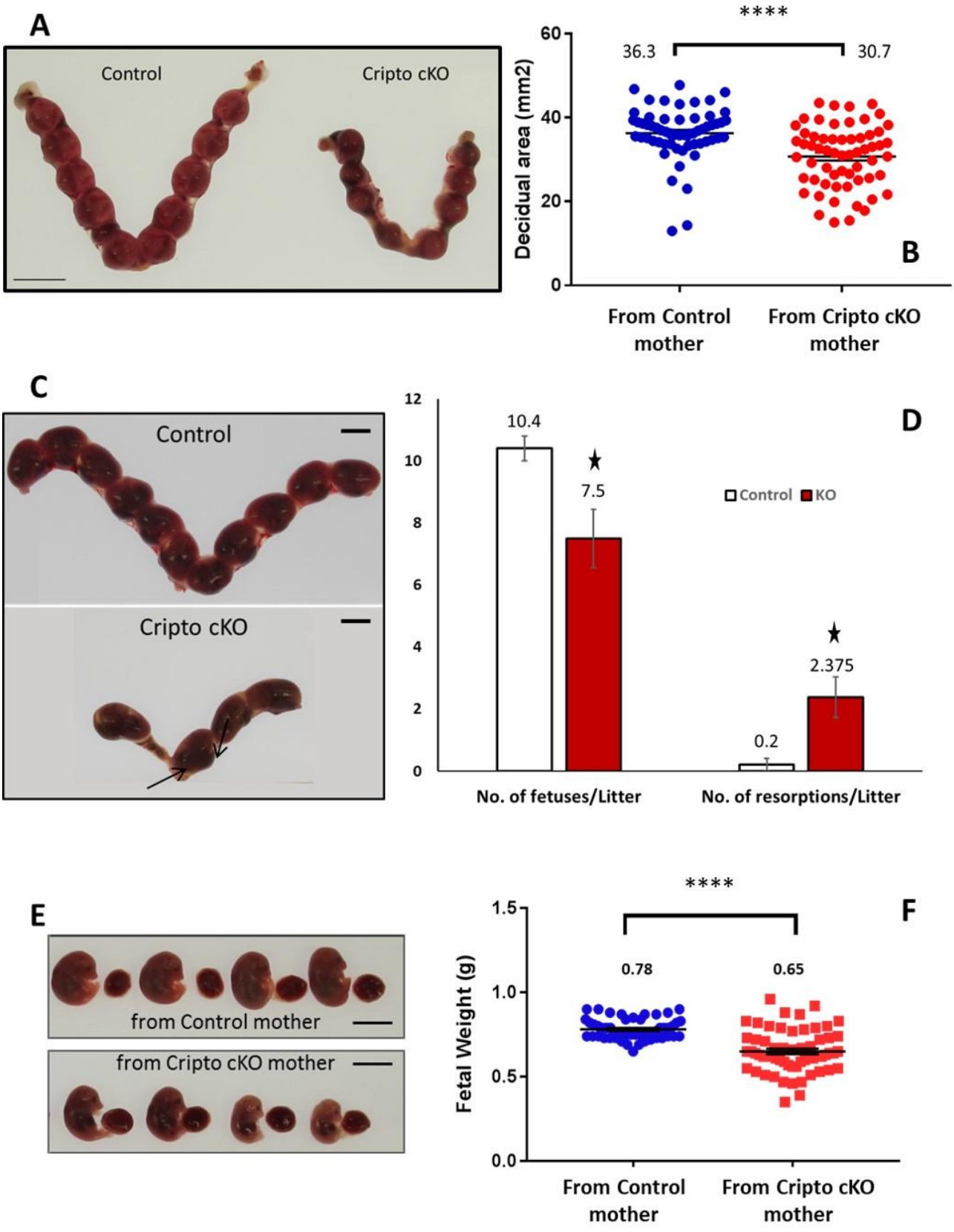
A
Control
Cripto cKO
****
36.3
30.7
Decidual area (mm2)
60
40
20
0
B
From Control mother
From Cripto cKO mother
C
Control
Cripto cKO
D
12
10
8
6
4
2
0
10.4
7.5
Control
KO
2.375
0.2
No. of fetuses/Litter
No. of resorptions/Litter
E
from Control mother
from Cripto cKO mother
****
F
1.5
1.0
0.5
0.0
Fetal Weight (g)
0.78
0.65
From Control mother
From Cripto cKO mother

Figure 3.1. Intrauterine growth restriction and fetal death in pregnancy of Cripto cKO females during placentation period. (A) Whole mount d10.5pc pregnant uteri from Cripto cKO and Control females. Although at this timepoint, no significant difference was observed in the average number of implantation and resorption sites per pregnancy (data not shown); (B) the size of implantation sites, evaluated by measurement of implantation site area (i.e. decidual area; mm2) was significantly smaller (P<0.0001) in Cripto cKO females (n= 61 decidua from 6 females) compared to controls (n= 61 decidua from 5 females). (C) Whole mount d16.5pc pregnant uteri from Cripto cKO and Control females. (D) On d16.5pc, significantly higher (P< 0.05) number of fetal resorptions (i.e. fetal death) and significantly lower (P< 0.05) number of viable fetuses per litter are observed in Cripto cKO females (n= 8 females) compared to Controls (n= 5 females). (E and F) Furthermore, average fetal weight (grams, g) on d16.5pc is significantly lower (P < 0.0001) in Cripto cKO mice (n= 60 fetuses from 8 females) compared to controls (n= 52 fetuses from 5 females). Fetal weight variation is also significantly higher at this timepoint pregnancy in Cripto cKO mothers compared to Controls. (Scale bar: 1 cm)

Mild to severe positional and developmental placental defects are evident in pregnancy of Cripto cKO females

The observed fetal IUGR and fetal death suggested the presence of placental defects or incompetency where more severe defects probably causing fetal death and less severe problems resulting in varying degrees of IUGR. To address this hypothesis we performed histological analysis of placentas from Cripto cK.O and Control mothers.

On d10.5, embryos extracted from the Cripto cK.O uteri showed considerable degrees of variation in size within a litter and generally smaller in contrast to embryos from Control mothers (Figure 3.2 A-C). At this timepoint of pregnancy, we evaluated the histological structure of placentas from Control mothers and placentas related to fetuses with different growth retardation status coming from Cripto cK.O mothers. H&E staining showed that although placentas related to the more normal size fetuses (Figure 3.2 E) in Cripto cK.O females

are almost similar to placentas from Control mothers (Figure 3.2 D), but placentas related to growth retarded embryos have severe structural and/or positional defects (Figure 3.2 F-H). These placentas were not developed at the appropriate position on the mesometrial pole of the uterine axis and were positionally “tilted” to either sides along with obvious abnormal organization and/or size of the fetal compartments in these placentas. The abnormal position of developing placenta can potentially compromise the maternal-fetal cell communications required for directing proper development of placenta and efficient maternal-fetal blood association. These severely defective placentas may eventually result in death of the corresponding fetuses in Cripto cK.O mothers.

To better assess the initial development and organization of fetal compartments of placenta, on d10.5pc we performed IF staining against a specific marker for spongiotrophoblast layer of placenta called trophoblast specific protein A (TpbpA). Using this staining we were able to visualize the junctional zone of placenta which separates the maternal decidua and the labyrinth of placenta. We were therefore able to evaluate the overall size and organization of each placental compartment. We observed that at this timepoint, in placentas related to more normal sized embryos in Cripto cK.O mothers, all compartments of placenta are present and the size of every compartment is almost comparable to placentas from Control mothers (Figure 3.2 I and J).

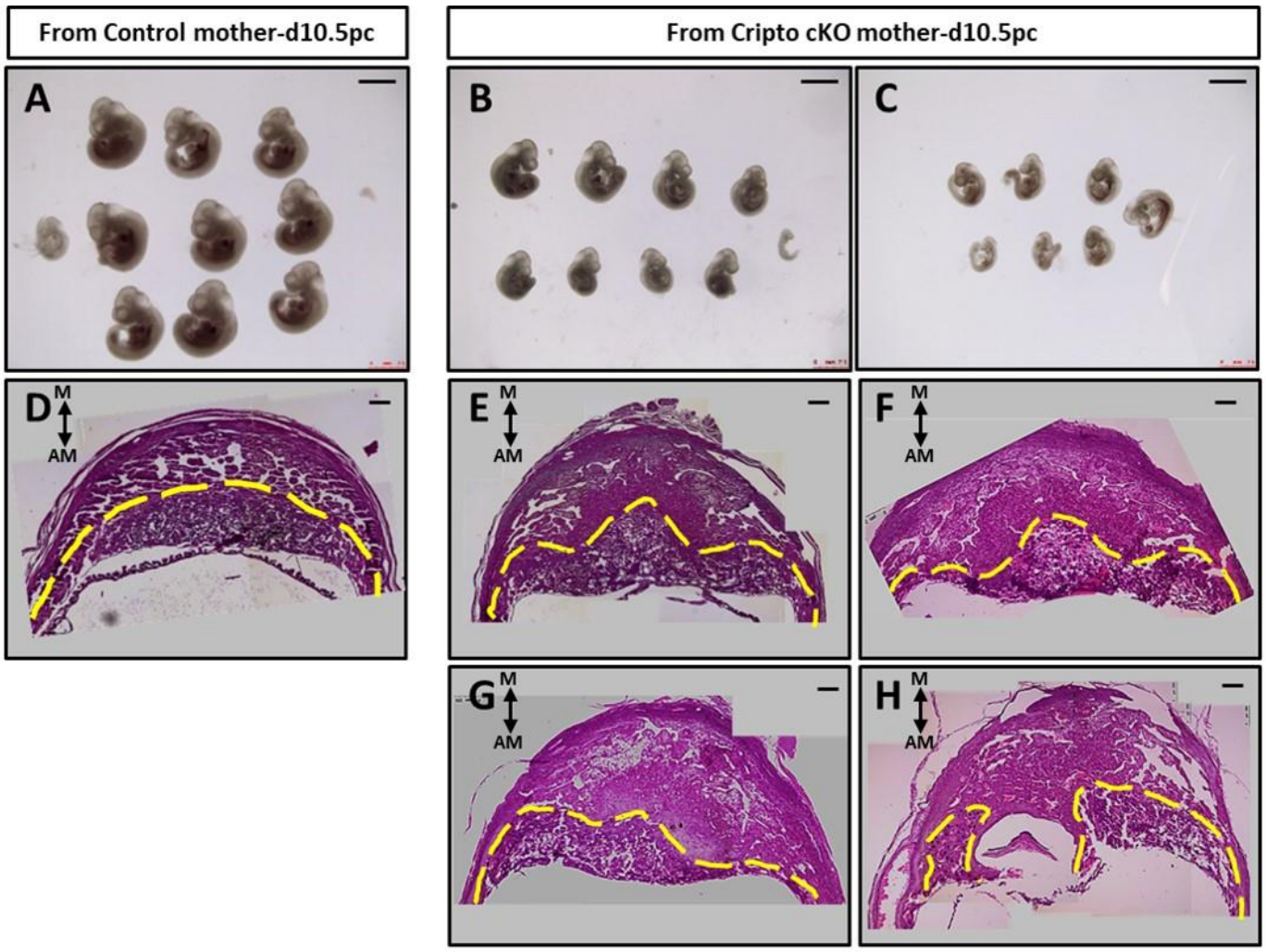
From Control mother-d10.5pc
From Cripto cKO mother-d10.5pc
A
B
C
D
E
F
G
H
M
AM

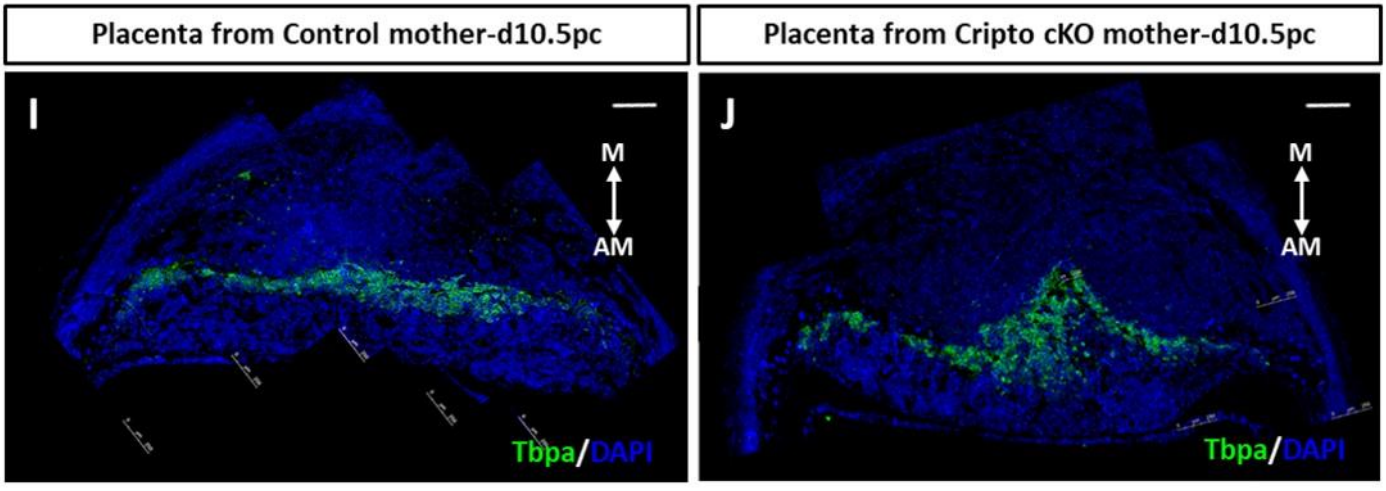
Placenta from Control mother-d10.5pc
Placenta from Cripto cKO mother-d10.5pc
I
J
M
AM
Tbpa/DAPI

Figure 3.2. positional and developmental placental defects in pregnancy of Cripto cKO females. (A-C) On d10.5, embryos extracted from the Cripto cK.O uteri showed considerable degrees of variation in size within a litter in contrast to embryos from Control mothers and were also smaller compared to embryos from control mothers. Hematoxylin and Eosin (H&E) stained sections of d10.5pc placentas from Cripto cK.O (E-H) and Control (D) females. Dashed yellow line shows the position of parietal giant cell layer demarking the border between maternal and fetal compartments of placenta. Placentas in F-H are positionally "tilted" to either sides (relative to uterine M-AM axis) and the overall size of fetal compartments of placenta is also smaller compared to placenta from Control mother (D). (I and J) IF staining against TpbpA visualizing Spongiotrophoblast layer of the placenta which separates the maternal decidua and the labyrinth of placenta. At this timepoint, in placentas related to more normal sized embryos (represented by E in H&E) in Cripto cK.O mothers (J), all compartments of placenta are present and the size of every compartment is almost comparable to placentas from Control mothers (I). AM, antimesometrial pole; (Scale bar, A-C: 2 mm; D-J: 250 µm).

As previously mentioned, on d16.5pc, the "surviving" fetuses in Cripto cK.O mothers were significantly growth restricted which again suggests the presence of a placental defect. While the average placental weight (Figure 3.3 A) and the overall size of placental compartments (Figure 3.3 B) in d16.5pc pregnant Cripto cK.O and Control females did not show any difference, histological analysis showed a placental labyrinth defect in which increased cell density and limited blood-filled spaces in the labyrinth of the placenta was evident (Figure 3.3 C and D). This defect was still present on d18.5pc, almost a day before delivery of the pups (Figure 3.3 E and F). As the labyrinth of placenta is the site of close proximity between maternal and fetal blood for the exchange of nutrients, waste and O2/CO2, the low vascularized labyrinth can describe the observed IUGR in surviving fetuses of Cripto cK.O mothers.

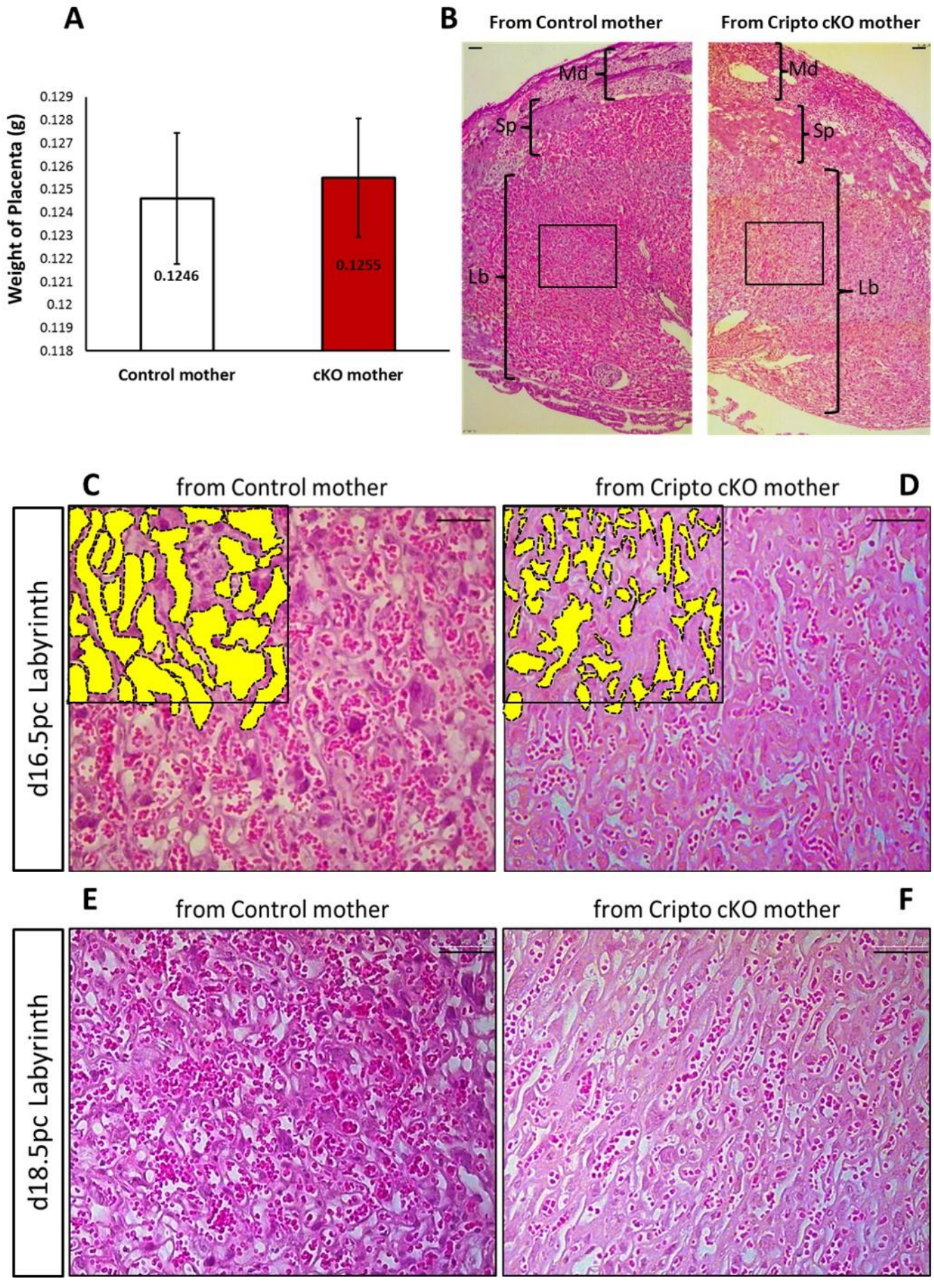
A
Weight of Placenta (g)
0.129
0.128
0.127
0.126
0.125
0.124
0.123
0.122
0.121
0.12
0.119
0.118
0.1246
0.1255
Control mother
cKO mother
B
From Control mother
From Cripto cKO mother
Md
Sp
Lb
C
from Control mother
from Cripto cKO mother
D
d16.5pc Labyrinth
E
from Control mother
from Cripto cKO mother
F
d18.5pc Labyrinth

Figure 3.3. labyrinth defect in placentas from Cripto cKO mothers. The average size of the placenta (measured by weight, g) obtained from d16.5pc pregnant Cripto cKO (n= 60 placentas from 8 females) and Control females (n= 52 placentas from 5 females) did not show any difference (A). In our preliminary histological analysis by H&E staining on placentas from d16.5pc pregnant mice, while all layers of a mature placenta are recognizable in placentas from both Cripto cKO and Control mothers (B), a placental labyrinth defect is evident in placentas from Cripto cKO mothers in which blood-filled spaces are limited compared to Controls. (C and D, higher magnification of the area defined by boxes in the labyrinth of placentas shown in B). We also showed that this defect is still present on d18.5pc, almost a day before delivery of the pups (D and E, d18.5pc placental labyrinth). In C and D all of the blood-filled spaces within the defined area (on the upper left corner of each image) are filled with yellow color to better show the difference between the labyrinth of placenta from Cripto cKO and Control mothers. Md, maternal decidua; Sp, spongiotrophoblast and Lb, labyrinth. (Scale bar: B, 75 µm; C-F, 50 µm)

Fetal vascularization in placental labyrinth is significantly reduced in Cripto cK.O mothers

To better describe the observed labyrinth defect, we asked whether the diminished blood spaces in the labyrinth is the result of a decrease in size of the maternal blood sinuses, or decreased fetal vasculature development or possibly both. To answer this question, we evaluated the labyrinth of the placenta on day 12.5pc. Because of the distinct appearance of fetal and maternal red blood cells (RBC) at this stage (Figure 3.4 A and B), it is easy to distinguish fetal vasculature and maternal blood sinuses from each other with a simple H&E stain. We took images of 5 microscopic fields at certain positions within labyrinth of every placenta (defined in Figure 3.4 C) and using Image-J software quantified the nonvascular area of the labyrinth (occupied by different labyrinth cell types), the area filled with fetal RBC and the area filled with maternal RBC (Figure 3.4 D). The results showed significant increase in nonvascular area and significant decrease in area allocated to fetal vasculature within the

labyrinth of placentas from Cripto cKO mothers compared to Controls while the area correlated to maternal blood sinuses was comparable between Control and Cripto cKO groups (Figure 3.4 E).

Because in the placentas from Cripto cKO mothers, the overall size of labyrinth compartment is not reduced, and the size of maternal blood sinuses is not expanded (both characteristic features of decreased branching morphogenesis of chorionic villi), we concluded that chorionic villi branching is normal and the observed decreased fetal vasculature within the labyrinth is directly caused by reduced fetal vascularization.

Figure 3.4. Lower fetal vascular development in placental labyrinth in pregnancy of Cripto cK.O mice. (A and B) Histological analysis of d12.5pc placental labyrinth by H&E staining. At this stage fetal RBC (green arrows) are larger and still have their nucleus versus maternal RBC (black arrows) which are very small with no nucleus which makes it easy to distinguish fetal vasculature and maternal blood sinuses from each other with a simple H&E staining. (C and D) Images of 5 microscopic fields at certain positions within labyrinth of every placenta were analyzed using Imag-J software to quantify the nonvascular area of the labyrinth (occupied by different labyrinth cell types), the area filled with fetal RBC (red) and the area filled with maternal RBC (blue). (E) The results showed significant increase in nonvascular area and significant decrease in area allocated to fetal vasculature within the labyrinth of placentas from Cripto cKO mothers compared to Controls while the area correlated to maternal blood sinuses was comparable between Control and Cripto cKO groups (p values are defined in each panel, Cripto cKO group, n= 8 placenta from 3 females; Cripto Control group, n= 9 Placenta from 3 females). (Scale bar: A and B, 25 μm).

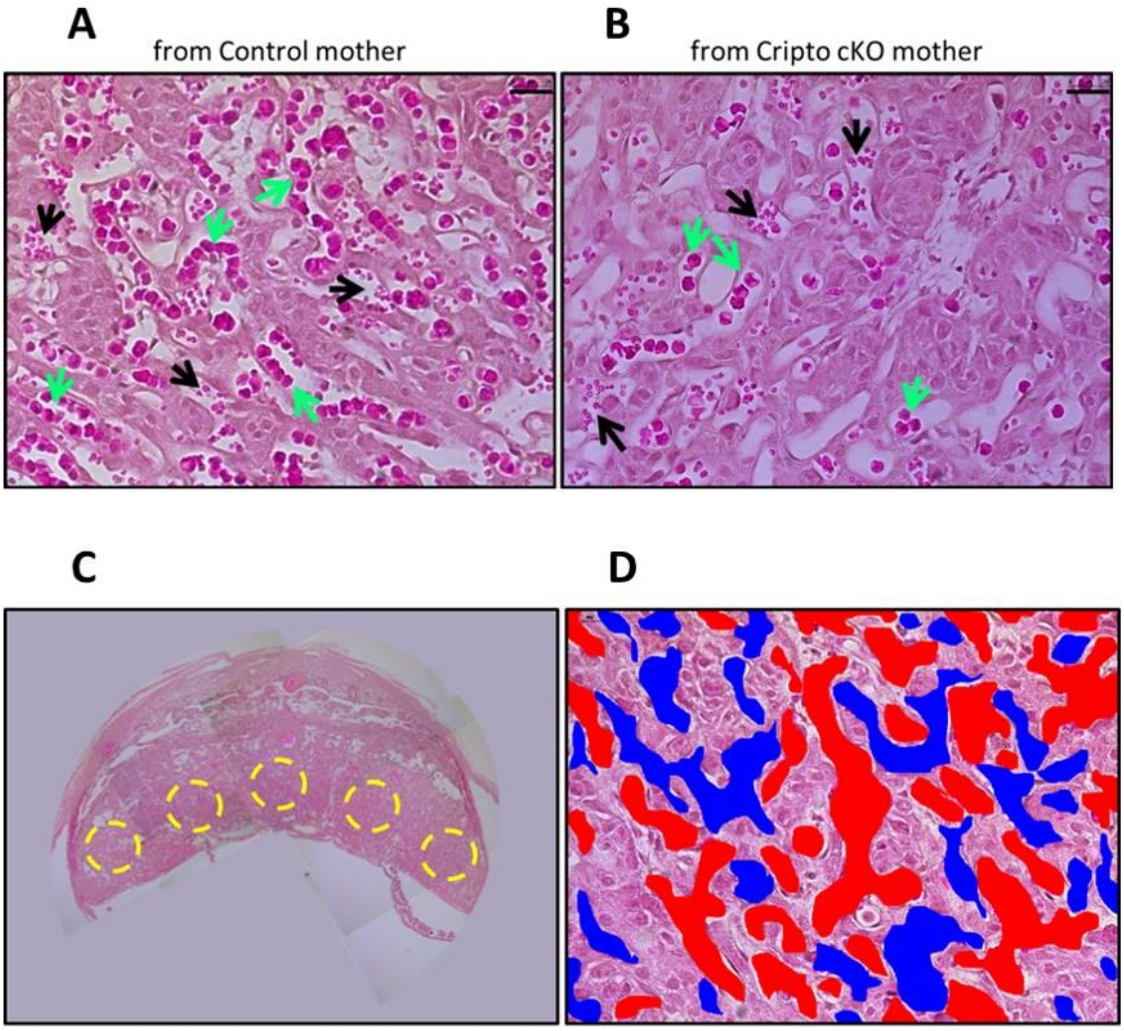
A
from Control mother
B
from Cripto cKO mother
C
D

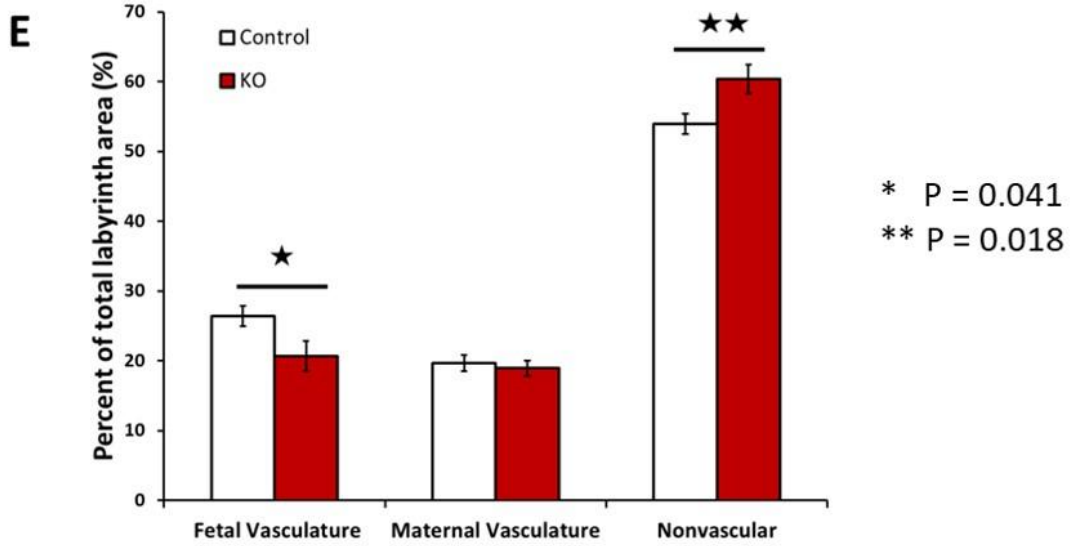
E
Control
KO
Percent of total labyrinth area (%)
70
60
50
40
30
20
10
0
★
★★
Fetal Vasculature
Maternal Vasculature
Nonvascular
* P = 0.041
** P = 0.018

Down-regulation of VEGF, VEGFR2 and different components of Notch signaling pathway in maternal and fetal compartments of placenta in Cripto cKO mothers

Looking for the cause for the decreased fetal vascularization in the labyrinth layer of placenta, we measured the expression level of some general angiogenic factors (Vegf and its receptor Vegfr2 [34]) and also factors known to be specifically critical for the development of the fetal vasculature in placental labyrinth (Esx1 [35] and components of Notch signaling pathway [36-39]).

To do so, females were sacrificed on d12.5pc and uteri were dissected, and fetal components of placenta were separated from maternal decidua. The vascularization factors were then measured in uterine wall/maternal decidua (Figure 3.5) and in fetal compartment of placenta (Figure 3.6). We observed that expression of Vegf, Vegfr2 and several components of Notch signaling pathway (Dll4, Notch1, Notch4, Hey1, Hey2, and Hes1) were significantly lower in uterine wall/maternal decidua of Cripto cKO females compared to Controls. However, the expression of Wnt4 did not show any difference between groups (Figure 3.5). In the fetal compartments of placenta, the expression of Vegf and Notch4 was significantly lower and the expression of Hes1 was significantly higher in Cripto cKO group compared to Control. The expression of Wnt4 and Esx1 did not show any difference between groups (Figure 3.6). These findings suggest that down-regulation of both general and specific vascularization factors contributes to decreased fetal vasculature development of placental labyrinth in Cripto cKO mothers.

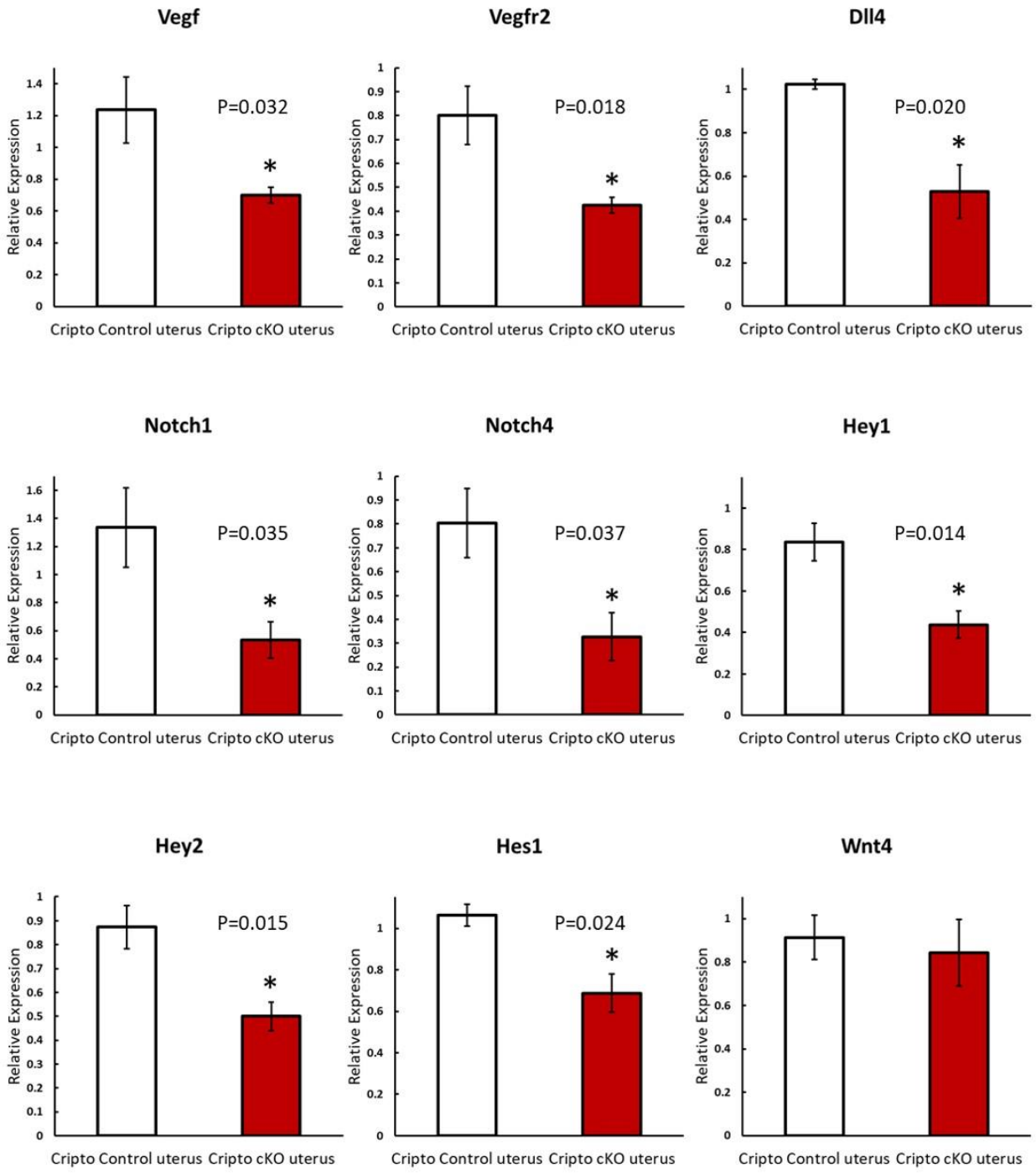

Figure 3.5. Decreased expression level of angiogenic factors in uterus and maternal decidua in pregnancy of Cripto cK.O females. Relative expression level of Vegf, Vegfr2, Notch4, Notch1, Dll4, Hey1, Hey2, Hes1 and Wnt4 on d12.5pc was measured by quantitative real-time PCR (Control, n= 3 females and Cripto cKO, n= 4 females). P-values for significant differences are included in each panel along with an asterisk.

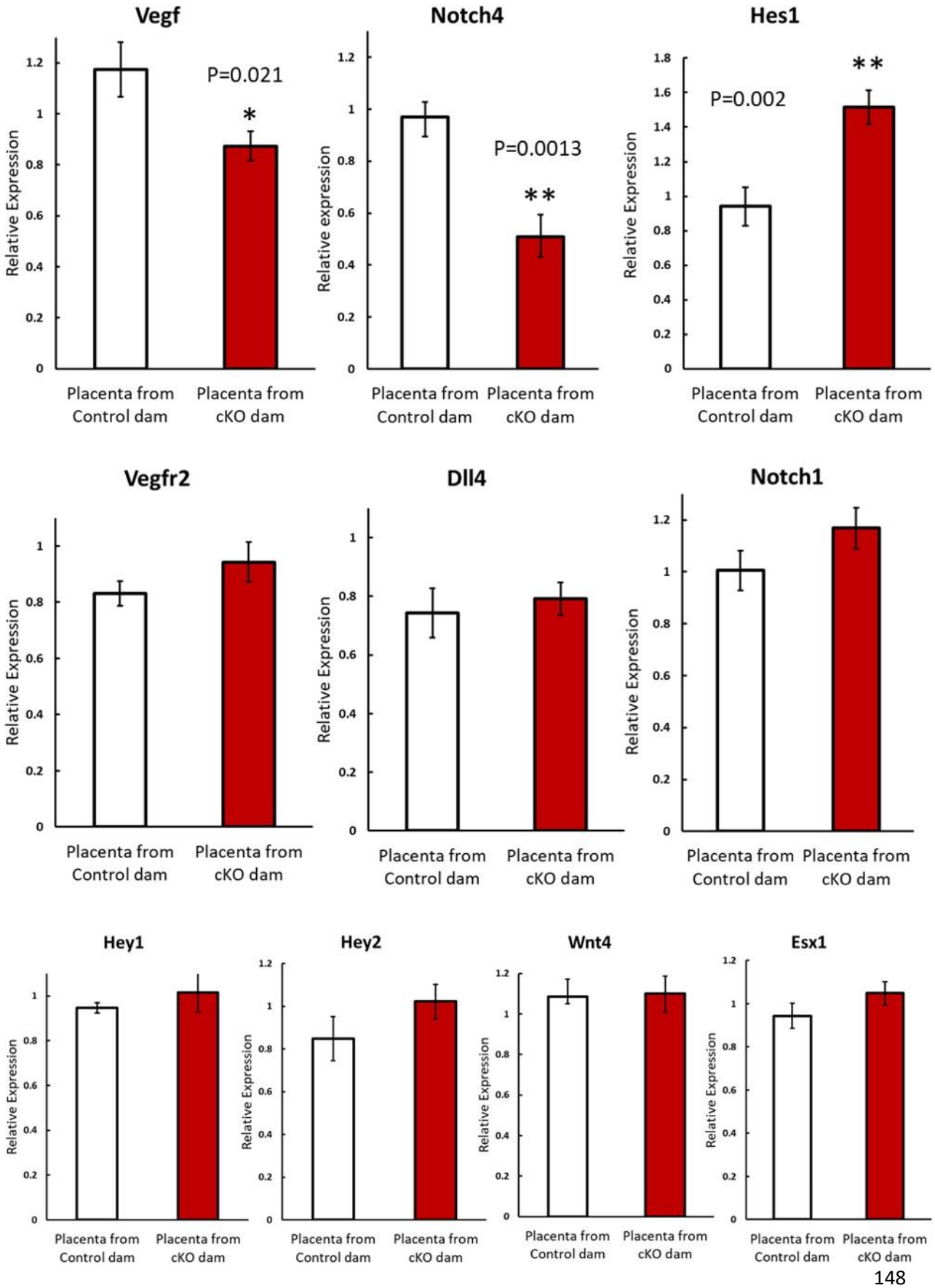
Vegf
P=0.021
*
Relative Expression
Placenta from Control dam
Placenta from cKO dam
Notch4
P=0.0013
**
Relative expression
Hes1
P=0.002
**
Vegfr2
Dll4
Notch1
Hey1
Hey2
Wnt4
Esx1

Figure 3.6. Decreased expression level of angiogenic factors in fetal parts of placenta in pregnancy of Cripto cK.O females. Relative expression level of Vegf, Vegfr2, Notch4, Notch1, Dll4, Hey1, Hey2, Hes1, Esx1 and Wnt4 on d12.5pc was measured by quantitative real-time PCR (Control, n= 6 placentas from 3 females and Cripto cKO, n= 8 placentas from 4 females). P-values for significant differences are included in each panel along with an asterisk.

Mid-gestation maternal angiogenesis required for the formation of the lateral vascular sinuses at maternal-fetal interface, is compromised in Cripto cK.O mothers

Since the level of vasculogenic factors was found to be down regulated on d12.5pc of pregnancy in the maternal decidua of Cripto cKO females compared to Controls, we evaluated the development of maternal vasculature at implantation sites by means of immunohistochemical staining (IHC) against CD31, a marker for endothelial cells.

On d5.5pc, maternal endothelial cells within implantation sites showed similar pattern of localization between Cripto cKO and Control females where they were mostly localized around the embryo on the anti-mesometrial pole (Figure 3.7 A and B). Although the intensity of staining appeared to be reduced in Cripto cKO females, the level of Vegf was comparable between 2 groups at this timepoint (Figure 3.S1). We previously demonstrated that the level of Notch1, Notch4 and Dll4 was significantly lower in Cripto cKO females compared to Controls on d5.5pc. However, at this timepoint the level of downstream targets of Notch signaling pathways, Hey1, Hey2 and Hes1, which are known to be involved in the process of angiogenesis, was similar between groups (Figure 3.S1).

On d7.5pc, the pattern of maternal endothelial cell localization within implantation sites appeared different between the two groups. In the case of Cripto cKO females in contrast to Controls, the staining against CD31 was still prominent toward anti-mesometrial pole (Figure 3.7 D-G). Furthermore, lateral vascular sinuses (which are formed by fusion of maternal vascular network on the mesometrial pole and in histology appear as empty spaces within maternal decidua) appeared smaller and less developed in Cripto cKO group compared to Control on d7.5pc (Figure 3.7 C-F) as well as d10.5 pc (Figure 3.2 D-H, Figure 3.10 A and D).

These findings suggest that although the initial maternal angiogenesis within implantation sites of Cripto cKO females are similar to Controls, the pattern and level of angiogenesis eventually becomes abnormal. Therefore, around the time of placentation, the maternal vascular network at maternal-fetal interface is less developed in Cripto cKO females. This defect can adversely affect the process of placentation and the growth of the fetus.

Figure 3.7. Reduced maternal angiogenesis on the antimesometrial pole of the implantation sites. (A-F) IHC staining against CD31 (brown), an endothelial cell marker. Slides were counter-stained with Hematoxylin. On d5.5pc, strong staining is observed on the mesometrial pole of the implantation site in both Control (A) and Cripto cKO (B) groups. On d7.5pc, in the case of Cripto cKO (D and F) in contrast to Control (C and E), the staining against CD31 is still prominent toward anti-mesometrial pole. Furthermore, lateral vascular sinuses (appear as empty spaces within maternal decidua, marked by arrows) are smaller and less developed in Cripto cKO group (D and F) compared to Control (C and E). AM, antimesometrial pole; M, mesometrial pole; asterisk, embryo within the section. (Scale bar: 250 μm)

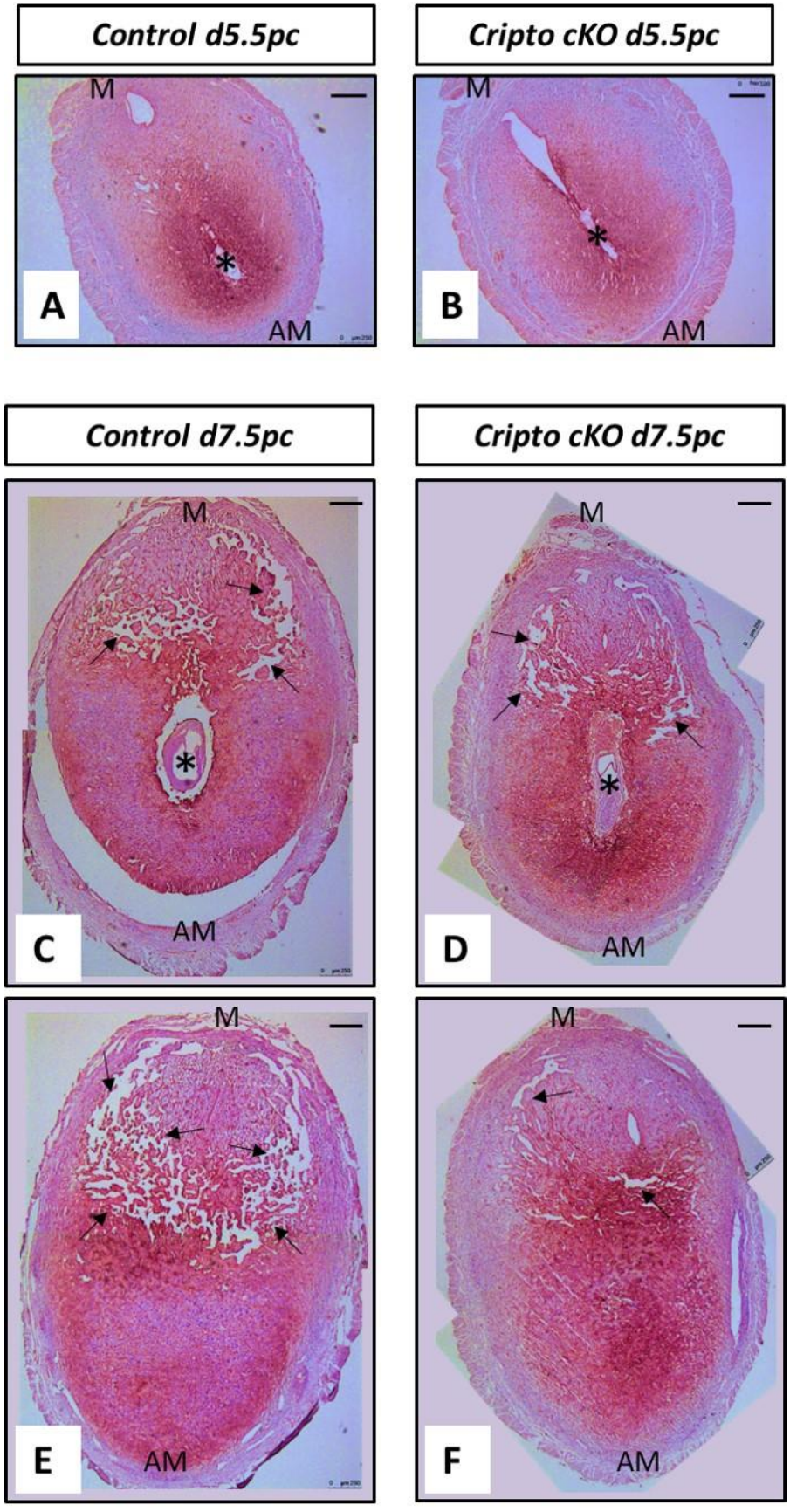
Control d5.5pc
Cripto cKO d5.5pc
Control d7.5pc
Cripto cKO d7.5pc
M
AM
A
B
C
D
E
F

Altered immune cell composition at maternal-fetal interface in pregnancy of Cripto cKO mice

Studies have shown that interactions between fetal trophoblasts, maternal decidual cells, maternal immune cells and endothelial cells are critical for angiogenesis and vascular remodeling at implantation site [40, 41]. Furthermore, it has been shown that immune cells at maternal-fetal interface (mainly Macrophages and uNK cells) also produce angiogenic factors [42, 43].

By means of flow cytometry we investigated whether the composition of immune cells at maternal-fetal interface is normal at mid-gestation in Cripto cKO females. Using specific markers for different immune cell types and gating strategy, which is described in Figure 3.S2, we defined the frequency of B cells, T cells, Macrophages, Monocytes and uNK cells at maternal-fetal interface in d10.5pc of pregnancy in both Cripto cKO and Control females. No significant difference was observed between Cripto cKO and Control group in abundance of total immune cells at maternal-fetal interface. Macrophages (Control 6.13% and cKO 4.97%) and uNK cells (Control 6.25% and cKO 6.58%) also showed similar proportions of total immune cells in Cripto cKO and Control mice (Figure 3.8 and Figure 3.S3). However, the frequency of T cells was significantly lower ($p<0.05$) in Cripto cKO (2.54%) compared to Control group (3.22%). Furthermore, the frequency of Monocytes was significantly higher ($p< 0.01$) in Cripto cKO group (11.07%) compared to Control (7.2%) (Figure 3.8 and Figure 3.S3). Although the proportion of B cells among immune cells was less than half in Cripto cKO group (6.16%) compared to Control (12.43%), the difference was not statistically significant (Figure 3.8 and Figure 3.S3).

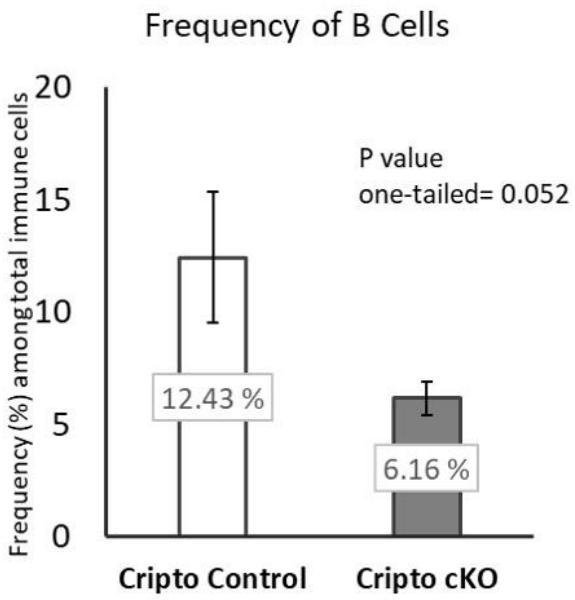
Frequency of B Cells
Frequency (%) among total immune cells
20
15
10
5
0
P value
one-tailed= 0.052
12.43 %
6.16 %
Cripto Control
Cripto cKO

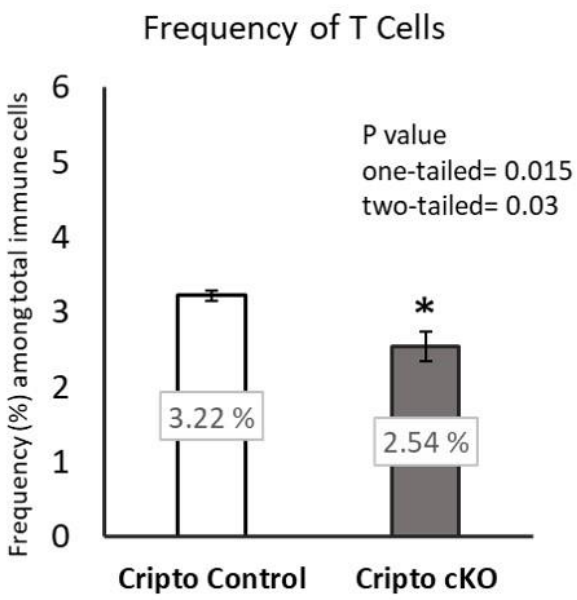
Frequency of T Cells
Frequency (%) among total immune cells
6
5
4
3
2
1
0
P value
one-tailed= 0.015
two-tailed= 0.03
*
3.22 %
2.54 %
Cripto Control
Cripto cKO

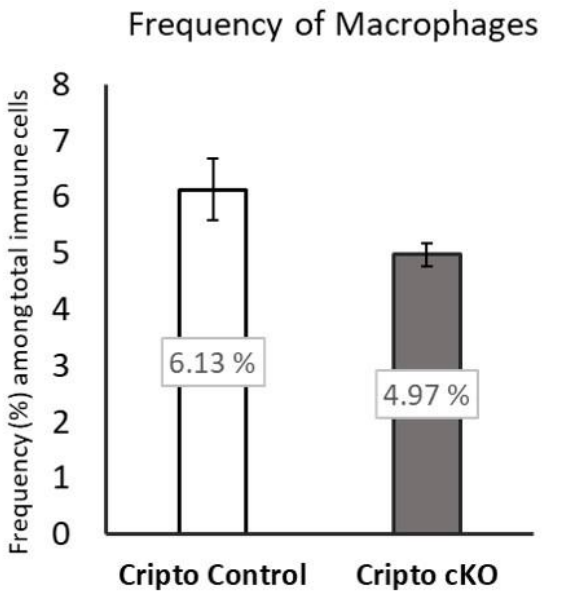
Frequency of Macrophages
Frequency (%) among total immune cells
8
7
6
5
4
3
2
1
0
6.13 %
4.97 %
Cripto Control
Cripto cKO

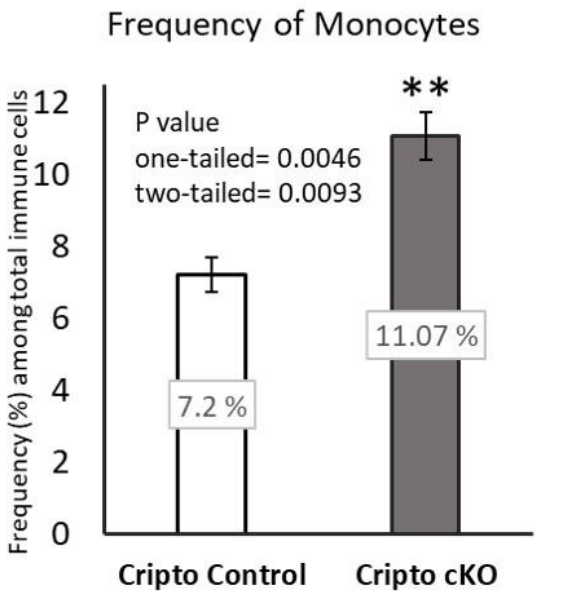
Frequency of Monocytes
Frequency (%) among total immune cells
12
10
8
6
4
2
0
**
P value
one-tailed= 0.0046
two-tailed= 0.0093
7.2 %
11.07 %
Cripto Control
Cripto cKO

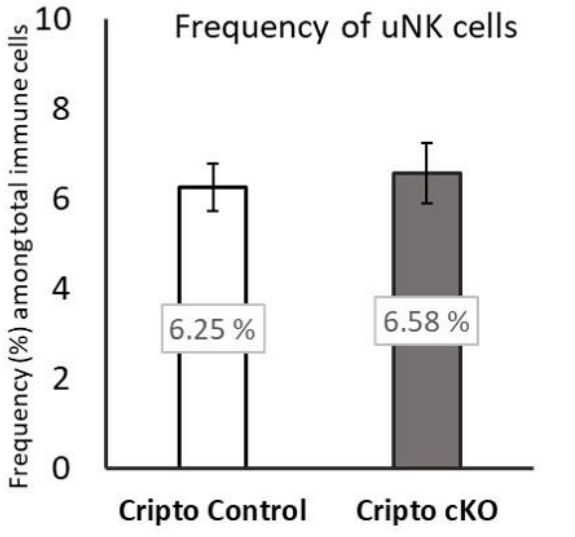
Frequency of uNK cells
Frequency (%) among total immune cells
10
8
6
4
2
0
6.25 %
6.58 %
Cripto Control
Cripto cKO

Figure 3.8. Comparison of different leukocyte populations in d10.5pc implantation sites of pregnant Control and Cripto cKO females by flow cytometric analysis. Frequency of B cells, T cells, Macrophages, Monocytes and uNK cells among immune cells in d10.5pc implantation sites was measured by flow cytomeric analysis. Macrophages as well as uNK cells showed similar proportions of total immune cells between pregnant Cripto cKO and pregnant Control mice. Frequency of T cells among immune cells was significantly lower and frequency of Monocytes among immune cells was significantly higher in Cripto cKO compared to Control group. Although the proportion of B cells among immune cells was less than half in Cripto cKO group compared to Control, the difference was not statistically significant because of the high variation observed within the control group and small number of samples. Control group n = 3 females, Cripto cKO group n = 3 females. Frequency of each immune cell type in each group and the p values for significant differences are shown in each panel.

It is known that during the course of pregnancy, from implantation to placentation as well as parturition; maternal immune cell composition and their functions changes dynamically to fit the various phases of pregnancy [44-46]. Our findings showed that immune cell composition is altered at maternal-fetal interface of Cripto cKO females during placentation period (d10.5). We also evaluated the expression level of some immune cell markers within the implantation sites of Cripto cKO and Controls females on d5.5pc (early post-implantation period) to determine if the immune cell composition was affected earlier during the pregnancy as well. While the expression of CD45, a marker for all immune cells, and NKp46 a specific marker for all subsets of NK cells did not show any difference, the expression of F4/80 and CD11b, markers for Macrophage and Monocytes, was significantly higher (more than double) in Cripto cK.O group compared to control (Figure 3.9 A). Immunofluorescence staining against F4/80 on d5.5pc also

showed presence of higher number of F4/80 positive cells in the implantation sites of Cripto cK.O females compared to Controls (Figure 3.9 B-E).

Together these findings show that although the total number of immune cells seems to be normal at implantation sites/maternal-fetal interface of Cripto cKO females, the ratio of immune cell types is altered and therefore, this deviation in balance of immune cell composition can be considered as a contributor to placentation and vascular defects observed in pregnancy of Cripto cKO mice.

Figure 3.9. Significant increase in expression of Monocytes and Macrophages markers in d5.5pc implantation sites of Cripto cK.O females. (A) Relative expression level of CD45, NKp46, F4/80 and CD11b on d5.5pc was measured by quantitative real-time PCR (pregnant Control d5.5pc, n= 6-8 females and pregnant Cripto cKO d5.5pc, n= 8-10 females). P-values for significant differences are included in each panel. While the expression of CD45, a general marker for all immune cells, and specific NK cells marker NKp46 did not show any difference, the expression of F4/80 and CD11b, markers expressed by macrophages and Monocytes, was significantly higher in Cripto cK.O group compared to control. (B-E) Immunofluorescence staining against F4/80 (red) on d5.5pc reveals presence of higher number of cells expressing this marker in the implantation sites of Cripto cK.O females on d5.5pc compared to controls. AM, antimesometrial pole; My, myometrium; PDZ, primary decidual zone; embryos are marked by asterisks (Scale bar, B and C: 250 µm; D and E: 75 µm).

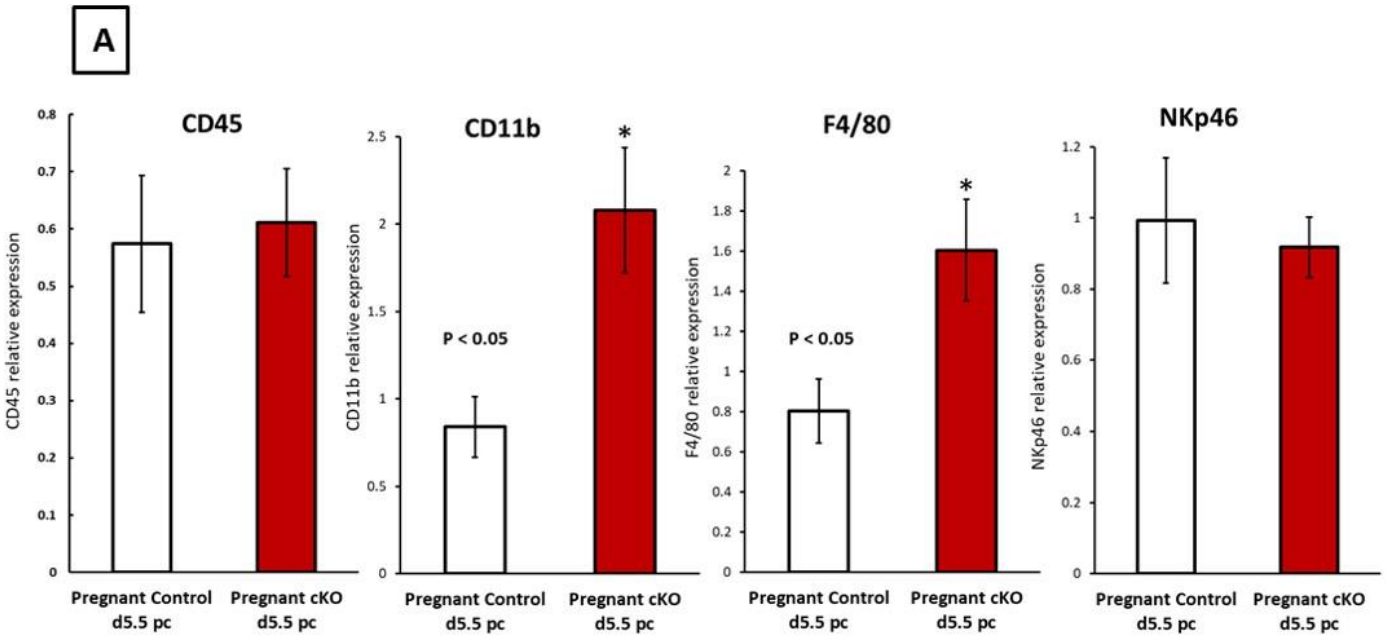
A
CD45
CD45 relative expression
Pregnant Control d5.5 pc
Pregnant cKO d5.5 pc
CD11b
CD11b relative expression
P < 0.05
*
F4/80
F4/80 relative expression
NKp46
NKp46 relative expression

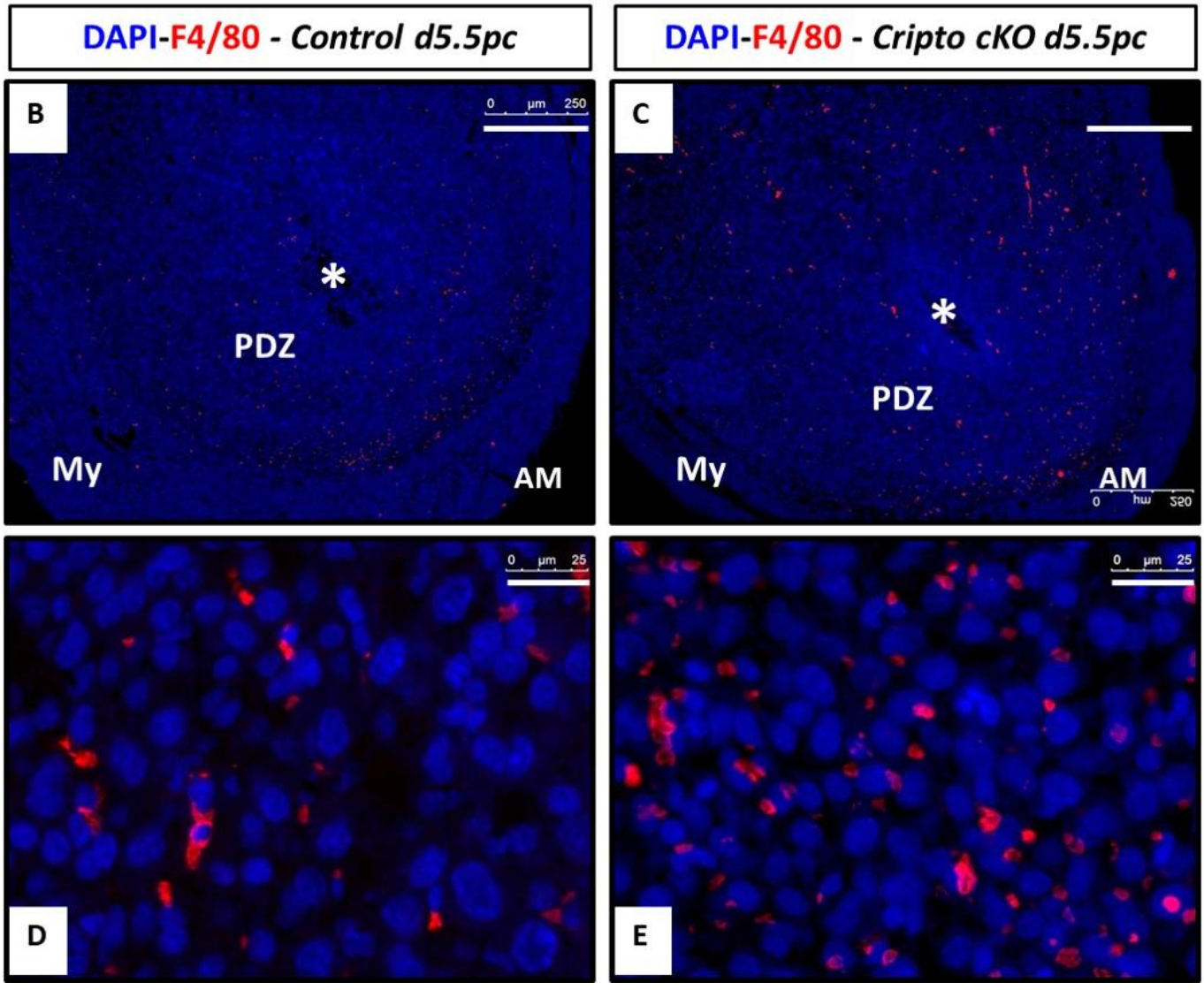
DAPI-F4/80 - Control d5.5pc
DAPI-F4/80 - Cripto cKO d5.5pc
B
C
PDZ
My
AM
D
E
0 µm 250
0 µm 25

Cripto protein is localized in both maternal and fetal compartments during early placentation period and its level declines post-placentation

We previously demonstrated that decidual cells are the major source of uterine Cripto during early post-implantation period. To understand the role of maternal Cripto in placentation, we assessed the tissue specific localization pattern of Cripto during the placentation period.

Using IHC staining, Cripto localization was observed in both maternal and fetal compartments on d10.5pc in control mice (Figure 3.10 A-C). However, by d12.5pc (Figure 3.11 A-C) and d16.5pc (Figure 3.S4 A), the localization of Cripto was drastically decreased and limited to some sparsely distributed cells in the maternal compartment of the placenta. Interestingly the pattern and level of Cripto expression in Cripto cKO was very similar to Controls on d10.5pc (Figure 3.10 D-F). However, on d12.5pc, Cripto protein was strongly expressed in the placental labyrinth and also in a population of cells just above the parietal TGC layer within the maternal compartment (Figure 3.11 D-F). Although on d12.5pc, the localization of Cripto protein was evidently stronger in both fetal and maternal compartments of placenta in Cripto cKO group compared to Control, at mRNA level there was no difference in expression of Cripto within fetal compartments of placenta and the mRNA expression level was significantly lower within maternal compartment of placenta in Cripto cKO group (Figure 3.11 G and H). On d16.5pc, similar to Controls, weak Cripto protein localization was visible only within the maternal decidua in placentas from Cripto cKO group as well (Figure 3.S4 B).

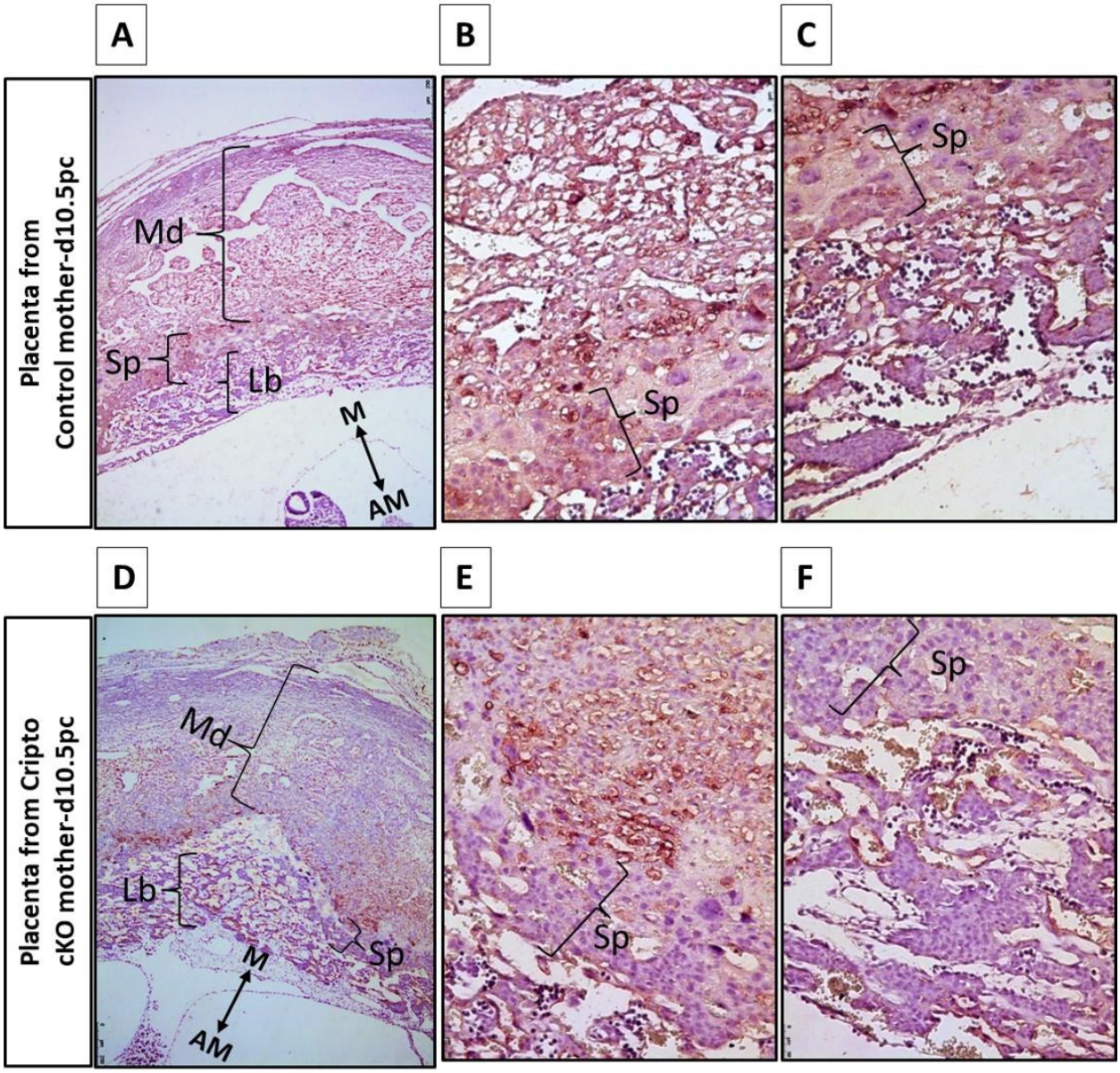

Figure 3.10. Cripto protein is highly expressed at maternal-fetal interface on d10.5pc of pregnancy. IHC against Cripto (brown) on d10.5pc comparing the maternal-fetal interface (developing placenta) within implantation sites of Control (A-C) and Cripto cKO females (D-F). Slides were counter-stained with Hematoxylin. Localization of Cripto protein is observed in both maternal compartment (Md in A and D, above Sp in B and E) and fetal compartments of placenta (Sp and Lb in A and D, whole section in C and F) in both Control and Cripto cKO groups. B and C are higher magnification of the fields from A. E and F are higher magnification of the fields from D. AM, antimesometrial pole; M, mesometrial pole; Md, maternal decidua; Sp, spongiotrophoblast and Lb, labyrinth. (Scale bar, A and D: 250 µm; B, C, E and F: 50 µm)

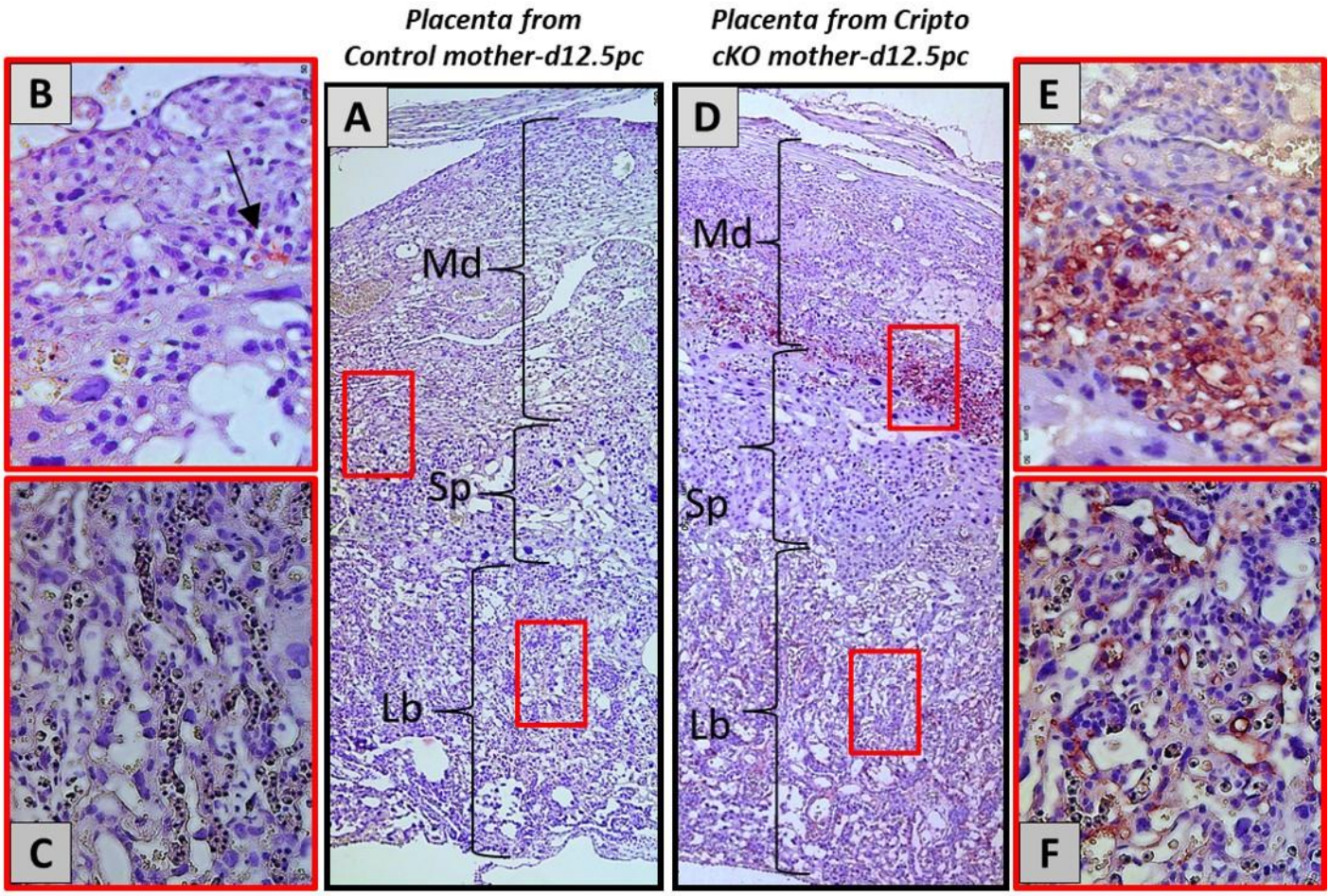
Placenta from Control mother-d12.5pc
Placenta from Cripto cKO mother-d12.5pc
A
B
C
D
E
F
Md
Sp
Lb
Md
Sp
Lb

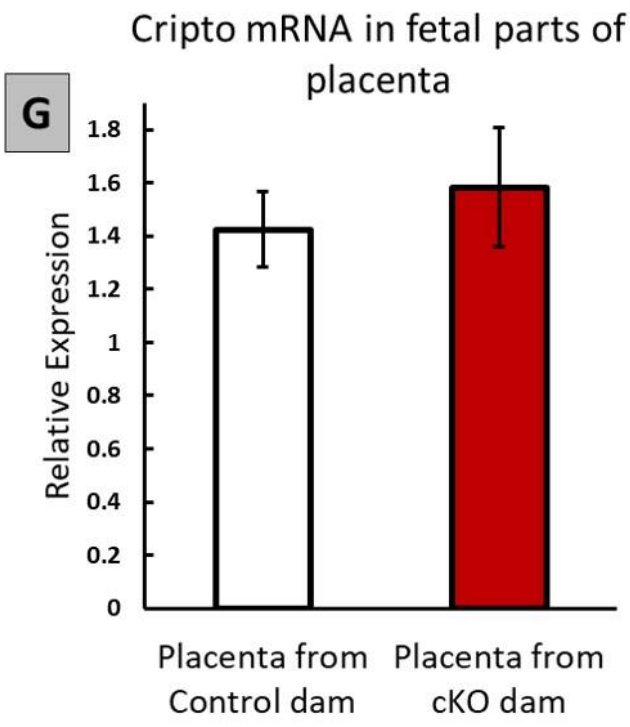
G
Cripto mRNA in fetal parts of placenta
Relative Expression
1.8
1.6
1.4
1.2
1
0.8
0.6
0.4
0.2
0
Placenta from Control dam
Placenta from cKO dam

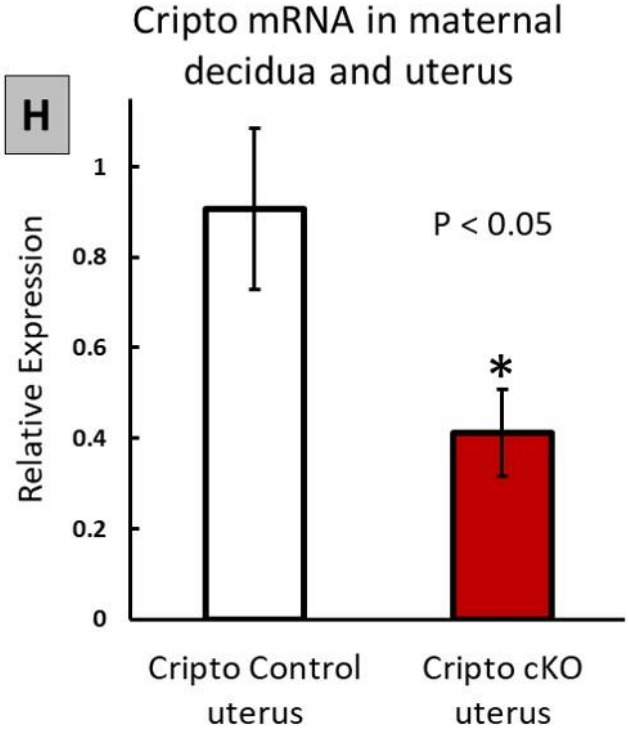
H
Cripto mRNA in maternal decidua and uterus
Relative Expression
1
0.8
0.6
0.4
0.2
0
P < 0.05
*
Cripto Control uterus
Cripto cKO uterus

Figure 3.11. Cripto protein is strongly expressed at maternal-fetal interface on d12.5pc of pregnancy in Cripto cKO females in contrast to Controls. IHC against Cripto (brown) on d12.5pc comparing the maternal-fetal interface (developing placenta) within implantation sites of Control (A-C) and Cripto cKO females (D-F). Slides were counter-stained with Hematoxylin. While low Cripto staining is detected only within maternal compartment of placenta (arrow at B) from Control females, Strong Cripto protein localization is observed both within maternal compartment (D and E) in a population of cells located adjacent to parietal trophoblast giant cells (large cells with very large nucleus evident in D at the border of Md and Sp) and also within labyrinth of the placenta (F and Lb in D). (G and H) relative expression of Cripto mRNA measured by quantitative PCR on d12.5 within maternal and fetal tissues separately. P values for statistically significant differences is indicated in the related panel along with an asterisk. (G) Control n= 6 placenta from 3 females, Cripto cKO n= 8 placentas from 4 females. (H) Control n= 3 females, Cripto cKO n= 4 females. (B and C) are higher magnification of the fields define in A. (E and F) are higher magnification of the fields defined in D. Md, maternal decidua; Sp, spongiotrophoblast and Lb, labyrinth. (Scale bar, A and D: 250 µm; B, C, E and F: 50 µm)

Labyrinth sinusoidal trophoblast giant cells (TGCs), some Spongiotrophoblast cells and different maternal immune cells express Cripto protein at maternal-fetal interface during placentation

We attempted to define the exact fetal and maternal cell types that produce Cripto during placentation. By interpreting the histological position of Cripto localization inplacenta, performing IHC and IF staining against Cripto and specific placental compartment markers for visualization of co-localization and also by using flow cytometry; we were able to determine some of maternal and fetal Cripto producing cell types on d10.pc.

IF staining against Cripto and Tpbpa (Spongiotrophoblasts marker) showed that in both Cripto cKO and Control groups, some cells within the spongiotrophoblast compartment of the placenta expressed Cripto protein (Figure 3.12). Furthermore, Cripto protein localization within the labyrinth of placenta showed a very specific and organized pattern (Figure 3.13 A and B). By using IHC staining against Cripto in order to have a better visualization of histology, we were able to show that within the labyrinth, Cripto protein is expressed by sinusoidal trophoblast giant cells, which are those cell types within the placental labyrinth that directly surround maternal blood sinuses (Figure 3.13 C-E). This specific labyrinth localization of Cripto protein seemed to be lower in placentas from Cripto cKO mothers on d10.5pc (Figure 3.13 C and D) and was evidently higher on d12.5pc compared to Controls (Figure 3.11 C and F).

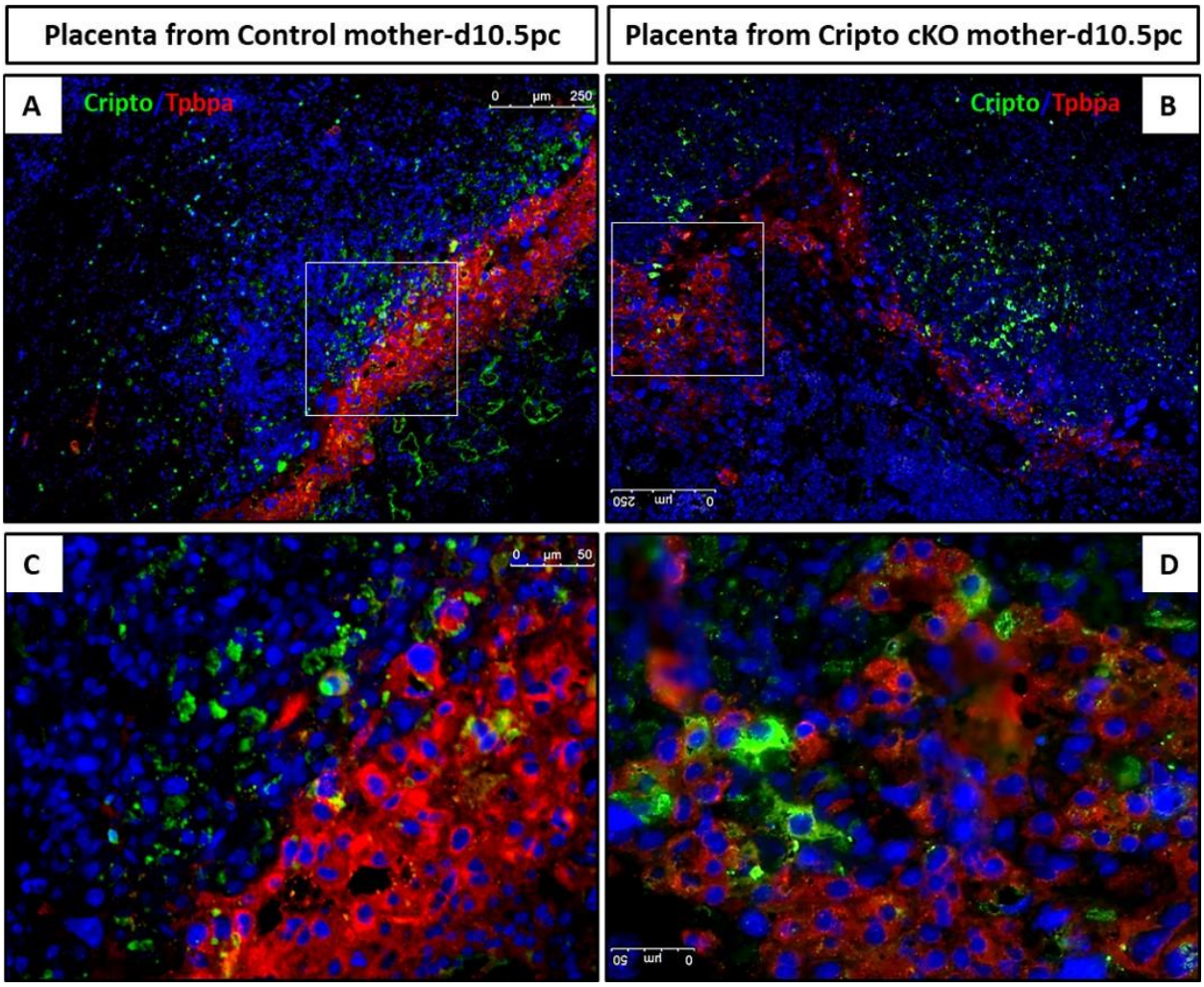

Figure 3.12. Cripto protein is expressed by some cells of spongiotrophoblast compartment of developing placenta on d10.5pc. IF staining against Cripto (green) and Tpbpa (red) on d10.5pc comparing the developing placenta of Control (A and C) and Cripto cKO females (B and D). Slides were also stained with DAPI to visualize the cells nuclei. Co-localization of Cripto and Tpbpa is observed within some cells of Spongiotrophoblast layer. C and D are higher magnification of the fields defined in A and B respectively. (Scale bar, A and B: 250 µm; C and D: 100 µm)

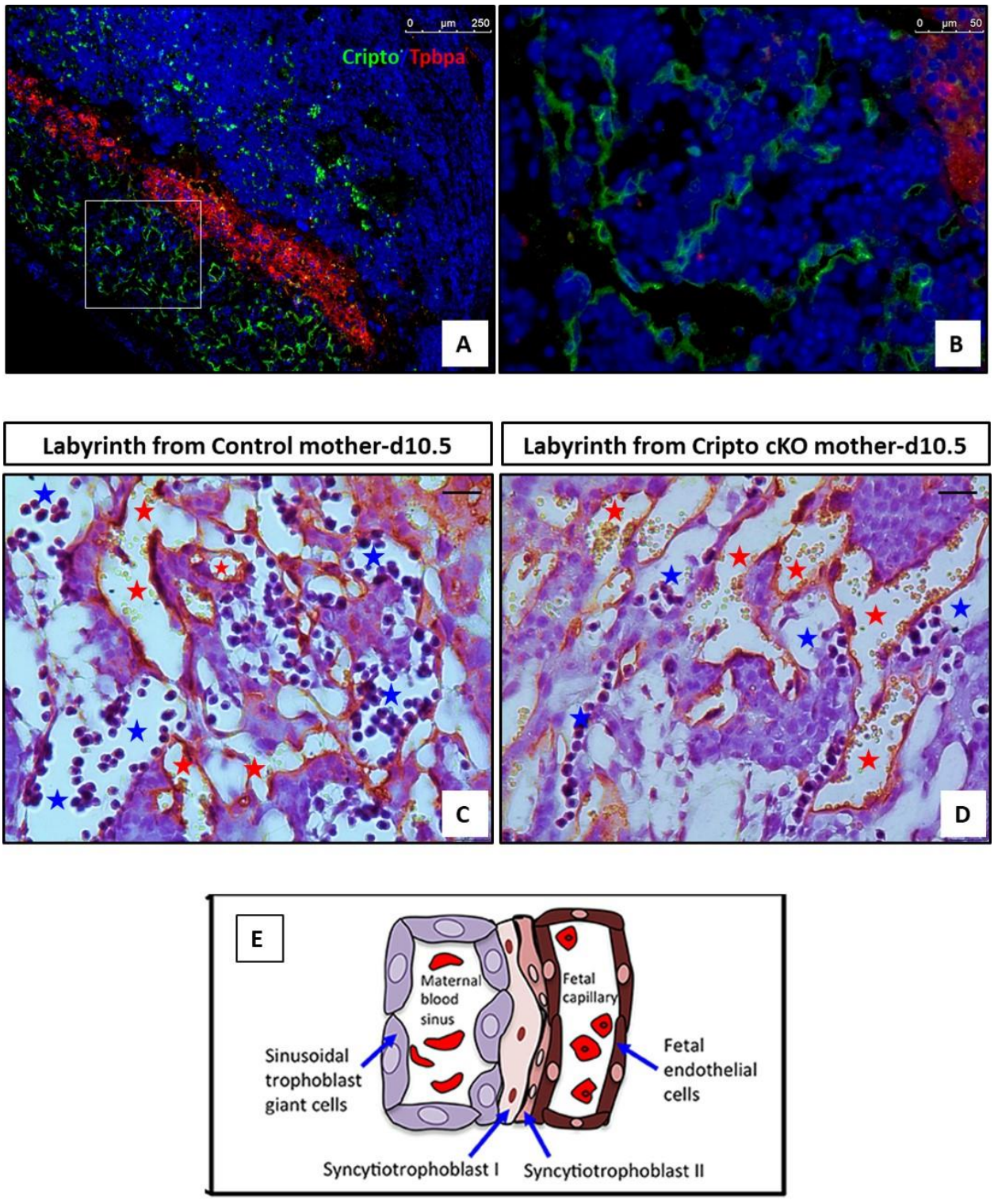

Figure 3.13. Cripto protein is expressed by sinusoidal trophoblast giant cells within labyrinth of developing placenta on d10.5pc. (A) IF staining against Cripto (green) and Tpbpa (red) on d10.5pc showed a very specific pattern of localization for Cripto within labyrinth of placenta (B,

magnification of the defined field in A). Slides were also stained with DAPI to visualize the cells nuclei. (C and D) IHC staining against Cripto (reddish brown) and counter-staining with Hematoxylin shows that within placental labyrinth, Cripto protein localization is only limited to those cells surrounding the maternal blood (red asterisks). These cells are sinusoidal trophoblast giant cells (E, adapted and modified from reference [73]). Red asterisk, maternal blood; Blue asterisk, fetal blood. (Scale bar, A: 250 μm; B: 50 μm; C and D: 25 μm)

As we have previously confirmed the successful deletion of Cripto in the uterus (Shafiei et al, Manuscript submitted), we speculated that those Cripto expressing cells residing in maternal compartment of placenta (seen in both Control and Cripto cKO groups) must be the cell types which do not express progesterone receptor (PR), therefore Cripto is not deleted in these cells. Immune cells were potential candidate cell types which are present at maternal-fetal interface and do not express PR. We employed flow cytometry using appropriate antibodies against Cripto and several markers for different immune cells types to determine whether any immune cell type possibly expresses Cripto (Figure 3.14). We observed that on d10.5pc, around 30% of all cells at maternal-fetal interface express Cripto. Intrestingly, out of these Cripto expressing cells, a little more than 50% were CD45 positive cells (immune cells). These Cripto positive immune cells make up around 28% of all immune cells at maternal-fetal interface on d10.5pc. Further gating of these Cripto positive immune cells for specific markers showed that around 20% of them are Macrophages, 7% are Monocytes and 13% are uNK cells. Expression of Cripto on B cells and T cells was not detected (Figure 3.14). We emphasize that these results are preliminary and in order to have a more precise estimation of the abundance of each immune

cell type that expresses Cripto, we need to analyze more samples and use more specific markers as we were only able to define the type of 40% of these Cripto positive immune cells.

To confirm the results obtained by flow cytometry, IF staining against Cripto and Dolichos Biflorus Agglutinin (DBA) lectin (which is specifically expressed by a subset of uNK cells at maternal-fetal interface) was employed. We were able to show that on d10.pc, Cripto is detected in some DBA positive uterine NK cells at maternal fetal interface in both Control and Cripto cKO females (Figure 3.15).

Figure 3.14. Flow cytometric analysis of leukocytes that express Cripto protein in d10.5pc implantation sites. This figure shows the gating scheme to identify total immune cells and several immune cells types present at d10.5pc implantation sites which express Cripto protein. Cells were chosen apart from debris and particles within the sample using gating for forward scatter area (FSC-A, representing the size) and side scatter area (SSC-A, representing the complexity). Single cells (singlets) were selected versus doublets using FSC-A and FSC-H (height). A Fixable Viability Dye (FVD efour506) was used to mark the dead cells. Live singlets were first gated for Cripto to select all the live single cell which express Cripto protein within the samples. Fluorescent Minus One control (FMO) for Cripto antibody showed the high specificity of the signal perceived in the sample. Cripto positive single cells were then gated for CD45 to select the population of all Cripto positive leukocytes. The selected population was further gated and some of immune cell types were defined as follows: uterine Natural Killer cells (uNK cells): CD45 pos, Ly6c neg-int, F4/80 neg, CD11b pos, CD11c pos. B cells: CD45 pos, Ly6c neg, CD3 neg, CD19 pos. T cells: CD45 pos, Ly6c neg, CD3 pos, CD19 neg. Macrophages: CD45 pos, CD11b pos, CD11c neg, Ly6c neg-int, F4/80 pos. Monocytes: CD45 pos, CD11b pos, CD11c neg, Ly6c hi, F4/80 neg-pos. Within Cripto positive immune cell population, we were able to define Monocytes (~ 7%), Macrophages (~ 20%), uNK cells (~ 13%) but no B cells or T cells (less than 1%). pos: positive, neg: negative, int: intermediate, hi: high, via: viability.

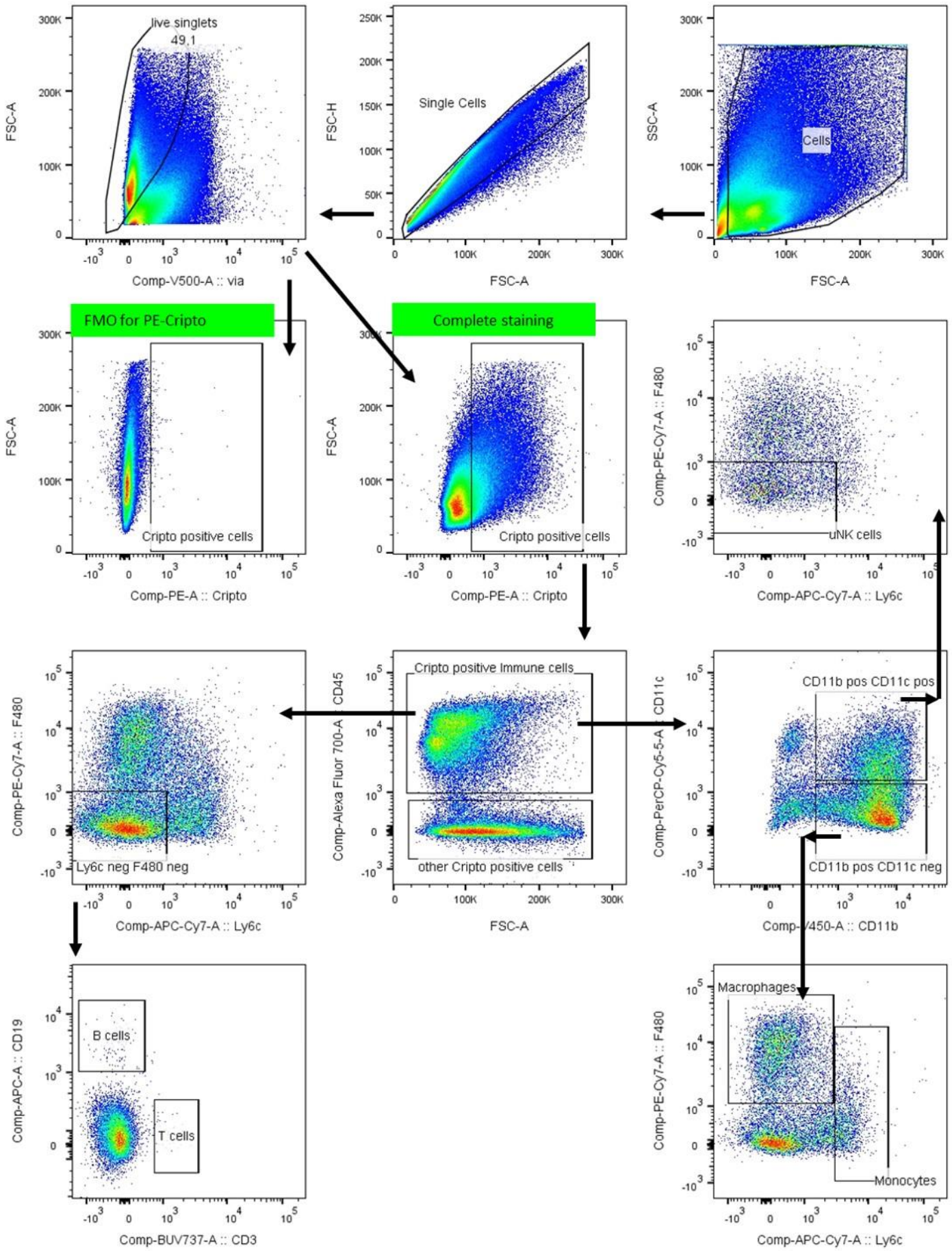
live singlets
49,1
FSC-A
Comp-V500-A :: via
Single Cells
FSC-H
FSC-A
Cells
SSC-A
FSC-A
FMO for PE-Cripto
Cripto positive cells
Comp-PE-A :: Cripto
Complete staining
Cripto positive cells
Comp-PE-A :: Cripto
uNK cells
Comp-PE-Cy7-A :: F480
Comp-APC-Cy7-A :: Ly6c
Cripto positive Immune cells
Comp-Alexa Fluor 700-A :: CD45
other Cripto positive cells
FSC-A
CD11b pos CD11c pos
CD11b pos CD11c neg
Comp-PerCP-Cy5-5-A :: CD11c
Comp-V450-A :: CD11b
Ly6c neg F480 neg
Comp-PE-Cy7-A :: F480
Comp-APC-Cy7-A :: Ly6c
B cells
T cells
Comp-APC-A :: CD19
Comp-BUV737-A :: CD3
Macrophages
Monocytes
Comp-PE-Cy7-A :: F480
Comp-APC-Cy7-A :: Ly6c

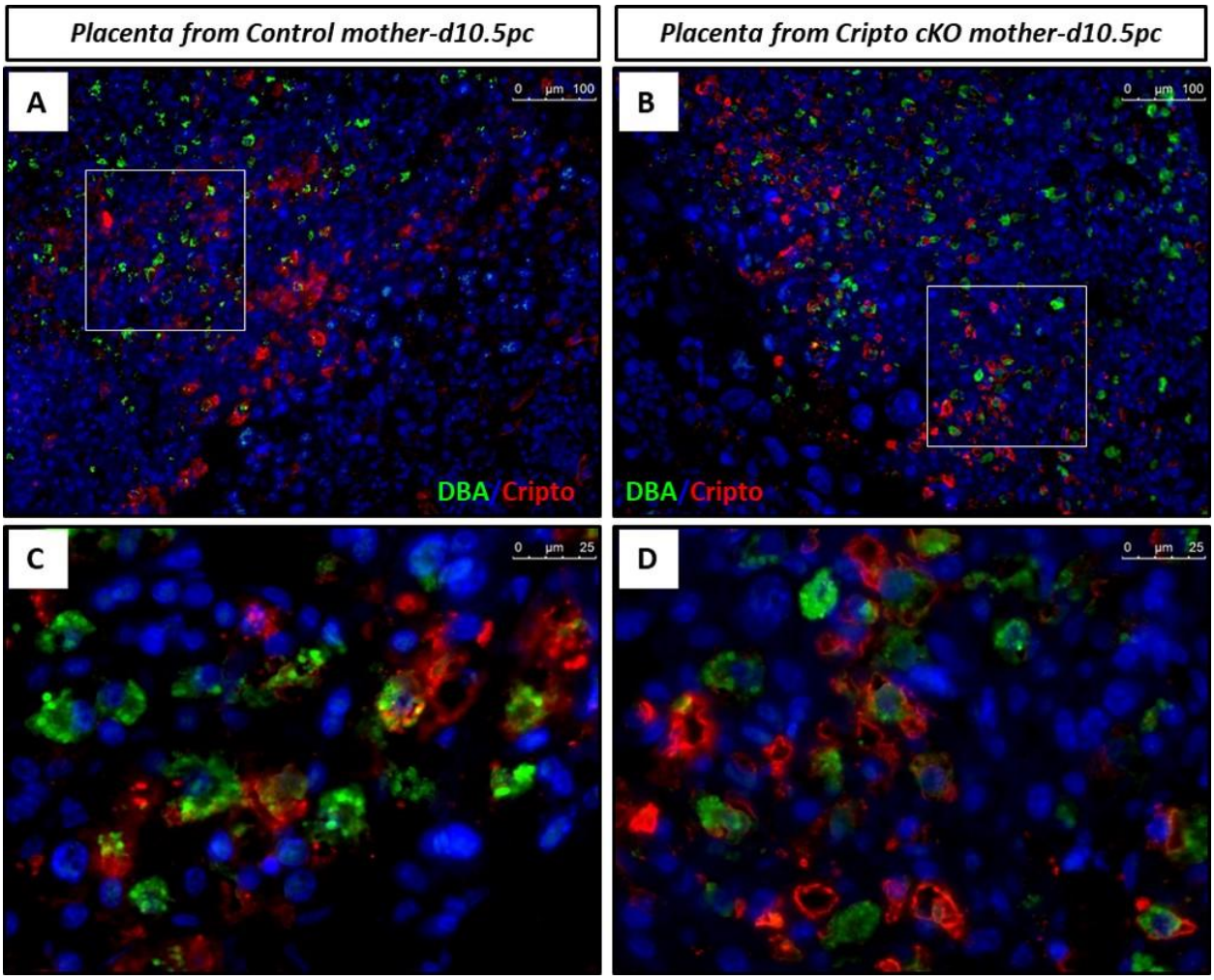

Figure 3.15. Cripto protein is expressed by some uNK cells within maternal decidual compartment of developing placenta on d10.5pc. IF staining against Cripto (Red) and DBA (Green) on d10.5pc comparing the developing placenta of Control (A and C) and Cripto cKO females (B and D). Slides were also stained with DAPI to visualize the cells nuclei. expression of Cripto is observed in some DBA positive uNK cells within maternal decidua. C and D are higher magnification of the fields defined in A and B respectively. (Scale bar, A and B: 100 µm; C and D: 25 µm)

Discussion

We have previously demonstrated that Cripto cKO females are sub-fertile as around 40% of them fail to give birth to any pups although they have normal estrous cycles, ovulation and fertilization (Shafiei et al. manuscript submitted). Furthermore, the Cripto cKO females that became pregnant, despite having similar number and size of implantation sites as control littermates at the start of the placentation process, eventually gave birth to significantly fewer number of pups per litter suggesting a loss of embryos during later developmental stages. In this study we assessed the implantation site, fetal size and placental structure from early placentation until a few days prior to delivery. On d10.5pc, the average decidual and embryo size in Cripto cKO females was already significantly lower than that of controls with significant variations in fetal size within a litter from Cripto cKO female in contrast to Control. On d16.5pc, a significantly higher number of fetal resorptions (i.e. fetal death) was observed in Cripto cK.O females which explained why these mice give birth to fewer numbers of pups per litter. Furthermore, fetal weight was more variable within a litter and the average fetal weight was also significantly lower in Cripto cK.O mice compared to controls (i.e. intra-uterine growth restriction; IUGR). The observed fetal IUGR and fetal death suggested the presence of placental defects or incompetency.

Histological and markers analysis for different compartments of the placenta demonstrated that some placentas from Cripto cKO females have severe structural and positional defects. These placentas were positionally “tilted” to either sides of the mesometrial-antimesometrial axis along with obvious abnormal organization and size of the fetal placental compartments. This tilted position of placentation most probably originates from incomplete uterine luminal

closure and the presence of extra luminal branches which results in defective crypt formation (Shafiei et al. manuscript submitted). Abnormal position of the developing placenta can potentially compromise maternal-fetal cell communications that are required for directing the proper development of placenta and efficient maternal-fetal blood association, leading to development of severely defective placentas eventually resulting in death of the corresponding fetuses in Cripto cK.O mothers. Interestingly, surviving fetuses in Cripto cKO females at d16.5pc were growth restricted suggesting further placental defects at this stage. While the average placental weight and the overall size of placental compartments in d16.5pc pregnant Cripto cK.O and Control females did not show any difference, histological analysis showed a placental labyrinth defect in which increased cell density and limited blood-filled spaces in the labyrinth of the placenta is evident. This defect was still present on d18.5pc, almost a day before delivery. As the labyrinth of the placenta is the site for maternal- fetal exchange of nutrients, waste and O2/CO2, this defect is most likely the underlying cause of fetal IUGR in Cripto cK.O mothers.

We also showed that this defect in the labyrinth layer of the placenta was the result of a significant decrease in fetal vasculature within the labyrinth and a significant increase in the area occupied by labyrinth trophoblast cells; whereas the area of the maternal blood sinuses within the labyrinth had remained normal. In our study, we observe a cell dense labyrinth with less blood spaces, a phenotype mostly associated with defective branching morphogenesis of the placental labyrinth [1], however, as the overall size of placental labyrinth was not smaller and the size of maternal blood sinuses were not increased in placentas from Cripto cKO mothers compared to Controls (neither on d12.5pc nor on d16.5pc), we concluded that

chorionic villi branching must be normal and the primary defect is in the process of fetal vascularization into the chorionic villi. This phenotype is similar to what has been observed only in a few mouse mutant models including Esx1 and some components of the Notch signaling pathway [35-39].

Along with the fetal vasculature defect, we also observed that the development of maternal vasculature at the placentation site is decreased in pregnancy of Cripro cKO females compared to Controls. This defect was first observed starting on d7.5pc and was also evident on d10.5pc. To determine the cause of decreased vascularization within maternal decidua and labyrinth, we measured the expression of general angiogenic factor Vegf and its receptor Vegfr2 and two known primary fetal allantoic vascularization factors, Esx1 and components of Notch signaling pathway in uterus/maternal decidua and fetal parts of placenta separately. We observed that expression of Vegf, Vegfr2 and all components of Notch signaling pathway, Dll4, Hey1, Hey2, Hes1, Notch1 and Notch4, was significantly lower in uterus/maternal decidua of Cripto cKO females compared to Controls. Furthermore, the expression of Vegf and Notch4 in fetal parts of placenta was also significantly lower in Cripto cKO group compared to Control.

VEGF signaling through Its receptors (mostly VEGFR2) is the main pathway involved in development of vascular structures [34, 47]. Furthermore, different Components of Notch signaling pathway including Notch1, Notch4, Dll1, Dll4, Hey1, Hey2 and Rbpj are critical for vascular development in different organs as well as fetal vasculature of placental labyrinth [37-39, 48-51]. Notch signaling has been shown to affect vasculogenesis both through interaction with VEGF signaling and also independent of it [48, 49, 51-55]. Interestingly, Cripto has been

shown to enhance the Notch signaling pathway activity [56], thus, the loss of Cripto can potentially results in less activity of Notch and VEGF signaling resulting in lower vasculogenesis. Furthermore, it has been suggested that Cripto itself has angiogenic effects which are independent of VEGF [57]. It is worth to mention that we observed strong localization of Cripto protein around the vascular structures of the pregnant uterus both before and after implantation (Shafiei et al, manuscript submitted). Therefore, a significant decrease in the level of Cripto in maternal tissues in our cKO mouse model, may result in decreased vascular development both directly and also through Notch and VEGF signaling pathways.

We showed that the level of Cripto expression is not different in fetal compartments of placenta in Cripto cKO dams compared to Controls. However, the level of Notch4 and VEGF were significantly lower in fetal parts of placentas from Cripto cKO mothers compared to Controls. We speculate that loss of Cripto in maternal uterine tissues results in altered maternal-fetal cell communications where the required signal from maternal cells for regulating the function of fetal trophoblasts (e.g. level of VEGF and Notch4 expression) is probably missing.

We have previously demonstrated that decidual cells are the major source of uterine Cripto during the early post-implantation period. To understand the role of maternal Cripto in early placentation and how the loss of Cripto in maternal tissues results in placentation defects, we assessed the tissue specific localization pattern of Cripto in Control uteri during placentation period.

IHC staining on d10.5 showed that during the early placentation period, Cripto was localized in both maternal and fetal compartments of placenta in Control. Interestingly, Cripto was also found to be localized in both maternal and fetal compartments of placenta in Cripto cKO. As we had previously confirmed the successful deletion of Cripto in the uterus (Shafiei et al, manuscript submitted), we speculated that those Cripto expressing cells residing in maternal compartment of placenta must be the cell types which do not express progesterone receptor, therefore Cripto is not deleted in these cells. Immune cells and fetal trophoblast cells were our best candidate cell types as these calls are present at maternal-fetal interface and do not express progesterone receptor. Interestingly, our preliminary results using flow cytometry and IF staining showed that Cripto is indeed expressed by maternal immune cells at maternal-fetal interface during early placentation period. Although we did not determine the type of all these Cripto positive immune cells, we were able to define populations of Macrophages, Monocytes and uNK cells that express Cripto at maternal-fetal interface. Furthermore, using flow cytometry we showed that although the abundance of total immune cell population at maternal-fetal interface is similar between Control and Cripto cKO females, the composition of immune cell types is different and there are significantly more Monocytes and fewer T cells in Cripto cKO females compared to Controls. Many studies have brought attention to the importance of maternal immune cells for proper vascular development and remodeling during placentation [42, 44-46, 58-67]. It is suggested that there are extensive interactions between certain immune cell types, decidual cells, vascular endothelial cells and fetal trophoblast cells which are believed to be of critical importance for proper placental development. Furthermore, different subsets with specific functions have been defined in the population of Macrophages

[42, 68] and uNK cells [69-73] which are the most abundant immune cell types at maternal-fetal interface during placental development. For example, there are different subsets of NK cells at maternal-fetal interface with quite different inhibitory and stimulatory functions including production of angiogenic factors and involvement in remodeling of maternal vasculature (both critical for proper placentation) [43, 72]. Based on our results, we speculate that loss of Cripto in decidual cells could have possibly rendered them defective in directing the formation of proper immune cell composition at maternal fetal interface which is highly critical for normal development of placenta and placental vasculature.

In summary, in this study we have shown the localization pattern of Cripto at maternal-fetal interface during placentation period of mouse pregnancy. We found that a variety of different cell types are the source of Cripto during this period including different maternal immune cells, fetal spongiotrophoblast cells and fetal labyrinth sinusoidal giant cells. Our study suggests that although maternal immune cells and fetal trophoblast cells are the source of Cripto during placentation period, the presence of Cripto in maternal uterine structural cells (uterine luminal epithelium, stroma and decidual cells) during early stages of pregnancy is critical for proper development of placenta, placental vasculature, and balanced immune cell composition at maternal-fetal interface later during the course of pregnancy. We observed that loss of Cripto in maternal uterine structural cells leads to defective placentation which leads to fetal IUGR and fetal death. Our results also suggest that the role of Cripto in vascularization during placentation period is most likely exerted through VEGF and Notch signaling pathway.

Our study brings many interesting questions into the mind such as “how uterine Cripto during early stages of pregnancy is linked to the composition of maternal immune cells later on during the placentation period?”, “what are the different immune cell types and subtypes that express Cripto within maternal-fetal interface?”, “What is the role of Cripto in these immune cells?”, “does Cripto acts as a co-receptor for TGF-beta signaling in these immune cells and makes them specific target cells for TGF-beta ligands or it acts as a secreted ligand itself that is produced by these immune cells and will affect its own target cells?”, etc. More studies are required to answer these interesting questions.

Acknowledgment

This work was supported by grants from the Canadian Institutes of Health Research PJT-159788 and a March of Dimes grnt #21-FY14-130 to D.D. S.S. was supported by a scholarship from the Faculty of Medicine, Division of Experimental Medicine of McGill University and the RI-MUHC.

References

1. Watson, E.D. and J.C. Cross, Development of structures and transport functions in the mouse placenta. Physiology, 2005. 20: p. 180-193.

2. Cross, J.C., D.G. Simmons, and E.D. Watson, Chorioallantoic morphogenesis and formation of the placental villous tree. Ann N Y Acad Sci, 2003. 995: p. 84-93.

3. Rossant, J. and J.C. Cross, Placental development: Lessons from mouse mutants. Nature Reviews Genetics, 2001. 2(7): p. 538-548.

4. Rai, A. and J.C. Cross, Development of the hemochorial maternal vascular spaces in the placenta through endothelial and vasculogenic mimicry. Developmental Biology, 2014. 387(2): p. 131-141.

5. Adamson, S.L., et al., Interactions between trophoblast cells and the maternal and fetal circulation in the mouse placenta. Dev Biol, 2002. 250(2): p. 358-73.

6. Pardi, G., A.M. Marconi, and I. Cetin, Placental-fetal interrelationship in IUGR fetuses--a review. Placenta, 2002. 23 Suppl A: p. S136-41.

7. Park, C.B., et al., NODAL in the Uterus Is Necessary for Proper Placental Development and Maintenance of Pregnancy. Biology of Reproduction, 2012. 86(6).

8. Park, C.B. and D. Dufort, NODAL signaling components regulate essential events in the establishment of pregnancy. Reproduction, 2013. 145(2): p. R55-R64.

9. Nagashima, T., et al., BMPR2 is required for postimplantation uterine function and pregnancy maintenance. Journal of Clinical Investigation, 2013. 123(6): p. 2539-2550.

10. Peng, J., et al., Uterine Activin-Like Kinase 4 Regulates Trophoblast Development During Mouse Placentation. Molecular Endocrinology, 2015. 29(12): p. 1684-1693.

11. Peng, J., et al., Uterine activin receptor-like kinase 5 is crucial for blastocyst implantation and placental development. Proceedings of the National Academy of Sciences of the United States of America, 2015. 112(36): p. E5098-E5107.

12. Matzuk, M.M., T.R. Kumar, and A. Bradley, DIFFERENT PHENOTYPES FOR MICE DEFICIENT IN EITHER ACTIVINS OR ACTIVIN RECEPTOR-TYPE-II. Nature, 1995. 374(6520): p. 356-360.

13. Dong, J.W., et al., Growth differentiation factor-9 is required during early ovarian folliculogenesis. Nature, 1996. 383(6600): p. 531-535.

14. Elvin, J.A., et al., Paracrine actions of growth differentiation factor-9 in the mammalian ovary. Molecular Endocrinology, 1999. 13(6): p. 1035-1048.

15. Brown, C.W., et al., Insertion of Inhbb into the Inhba locus rescues the Inhba-null phenotype and reveals new activin functions. Nature Genetics, 2000. 25(4): p. 453-457.

16. Jorgez, C.J., et al., Granulosa cell-specific inactivation of follistatin causes female fertility defects. Molecular Endocrinology, 2004. 18(4): p. 953-967.

17. Lee, K.Y., et al., Bmp2 is critical for the murine uterine decidual response. Molecular and Cellular Biology, 2007. 27(15): p. 5468-5478.

18. Park, C.B. and D. Dufort, Nodal Expression in the Uterus of the Mouse Is Regulated by the Embryo and Correlates with Implantation. Biology of Reproduction, 2011. 84(6): p. 1103-1110.

19. Zhao, K.Q., et al., Maternal Smad3 deficiency compromises decidualization in mice. Journal of Cellular Biochemistry, 2012. 113(10): p. 3266-3275.

20. Clementi, C., et al., Activin-Like Kinase 2 Functions in Peri-implantation Uterine Signaling in Mice and Humans. Plos Genetics, 2013. 9(11).

21. Zhang, S., et al., Uterine Rbpj is required for embryonic-uterine orientation and decidual remodeling via Notch pathway-independent and -dependent mechanisms. Cell Research, 2014. 24(8): p. 925-942.

22. Heba, T., C. Park, and D. Dufort, DECIPHERING THE ROLE OF THE NODAL SIGNALING PATHWAY IN PRETERM BIRTH. Placenta, 2015. 36(9): p. A59-A59.

23. Rodriguez, A., et al., SMAD Signaling Is Required for Structural Integrity of the Female Reproductive Tract and Uterine Function During Early Pregnancy in Mice. Biology of Reproduction, 2016. 95(2).

24. Ni, N. and Q.L. Li, TGF beta superfamily signaling and uterine decidualization. Reproductive Biology and Endocrinology, 2017. 15.

25. Strizzi, L., et al., Cripto-1: A multifunctional modulator during embryogenesis and oncogenesis. Oncogene, 2005. 24(37): p. 5731-5741.

26. Jin, J.Z. and J.X. Ding, Cripto is required for mesoderm and endoderm cell allocation during mouse gastrulation. Developmental Biology, 2013. 381(1): p. 170-178.

27. Ding, J.X., et al., Cripto is required for correct orientation of the anterior-posterior axis in the mouse embryo. Nature, 1998. 395(6703): p. 702-707.

28. Klauzinska, M., et al., The multifaceted role of the embryonic gene Cripto-1 in cancer, stem cells and epithelial-mesenchymal transition. Seminars in Cancer Biology, 2014. 29: p. 51-58.

29. Papageorgiou, I., et al., Expression of nodal signalling components in cycling human endometrium and in endometrial cancer. Reproductive Biology and Endocrinology, 2009. 7.

30. Bandeira, C.L., et al., Tumorigenic Factor CRIPTO-1 Is Immunolocalized in Extravillous Cytotrophoblast in Placenta Creta. Biomed Research International, 2014.

31. Dela Cruz, C., et al., Expression of Nodal, Cripto, SMAD3, Phosphorylated SMAD3, and SMAD4 in the Proliferative Endometrium of Women With Endometriosis. Reproductive Sciences, 2015. 22(5): p. 527-533.

32. Chu, J.H., et al., Non-cell-autonomous role for Cripto in axial midline formation during vertebrate embryogenesis. Development, 2005. 132(24): p. 5539-5551.

33. Soyal, S.M., et al., Cre-mediated recombination in cell lineages that express the progesterone receptor. Genesis, 2005. 41(2): p. 58-66.

34. Douglas, N.C., et al., Vascular Endothelial Growth Factor Receptor 2 (VEGFR-2) Functions to Promote Uterine Decidual Angiogenesis during Early Pregnancy in the Mouse. Endocrinology, 2009. 150(8): p. 3845-3854.

35. Li, Y. and R.R. Behringer, Esx1 is an X-chromosome-imprinted regulator of placental development and fetal growth. Nat Genet, 1998. 20(3): p. 309-11.

36. Duarte, A., et al., Dosage-sensitive requirement for mouse Dll4 in artery development. Genes Dev, 2004. 18(20): p. 2474-8.

37. Fischer, A., et al., The Notch target genes Hey1 and Hey2 are required for embryonic vascular development. Genes Dev, 2004. 18(8): p. 901-11.

38. Krebs, L.T., et al., Haploinsufficient lethality and formation of arteriovenous malformations in Notch pathway mutants. Genes Dev, 2004. 18(20): p. 2469-73.

39. Krebs, L.T., et al., Notch signaling is essential for vascular morphogenesis in mice. Genes Dev, 2000. 14(11): p. 1343-52.

40. Lima, P.D.A., et al., Leukocyte driven-decidual angiogenesis in early pregnancy. Cellular & molecular immunology, 2014. 11(6): p. 522-537.

41. Laws, M.J., et al., Gap junction communication between uterine stromal cells plays a critical role in pregnancy-associated neovascularization and embryo survival. Development, 2008. 135(15): p. 2659-2668.

42. Faas, M.M. and P. de Vos, Uterine NK cells and macrophages in pregnancy. Placenta, 2017. 56: p. 44-52.

43. Ratsep, M.T., et al., Uterine natural killer cells: supervisors of vasculature construction in early decidua basalis. Reproduction, 2015. 149(2): p. R91-102.

44. Mor, G., et al., Inflammation and pregnancy: The role of the immune system at the implantation site. Annals of the New York Academy of Sciences, 2011. 1221: p. 80-7.

45. Racicot, K., et al., Understanding the complexity of the immune system during pregnancy. Am J Reprod Immunol, 2014. 72(2): p. 107-16.

46. Li, Y., et al., Decidual-Placental Immune Landscape During Syngeneic Murine Pregnancy. Frontiers in Immunology, 2018. 9(2087).

47. Kim, M., et al., VEGF-A regulated by progesterone governs uterine angiogenesis and vascular remodelling during pregnancy. Embo Molecular Medicine, 2013. 5(9): p. 1415-1430.

48. Hellstrom, M., et al., Dll4 signalling through Notch1 regulates formation of tip cells during angiogenesis. Nature, 2007. 445(7129): p. 776-780.

49. Harrington, L.S., et al., Regulation of multiple angiogenic pathways by D114 and Notch in human umbilical vein endothelial cells. Microvascular Research, 2008. 75(2): p. 144-154.

50. Kim, H., et al., Notch ligand Delta-like 1 promotes in vivo vasculogenesis in human cord blood-derived endothelial colony forming cells. Cytotherapy, 2015. 17(5): p. 579-592.

51. Shawber, C.J., et al., Vascular Notch proteins and Notch signaling in the peri-implantation mouse uterus. Vascular Cell, 2015. 7: p. 17.

52. Lobov, I.B., et al., Delta-like ligand 4 (DII4) is induced by VEGF as a negative regulator of angiogenic sprouting. Proceedings of the National Academy of Sciences of the United States of America, 2007. 104(9): p. 3219-3224.

53. Shawber, C.J., et al., Notch alters VEGF responsiveness in human and murine endothelial cells by direct regulation of VEGFR-3 expression. Journal of Clinical Investigation, 2007. 117(11): p. 3369-3382.

54. Garcia-Pascual, C.M., et al., Inhibition of Delta-like 4 mediated signaling induces abortion in mice due to deregulation of decidual angiogenesis. Placenta, 2014. 35(7): p. 501-508.

55. Thomas, J.-L., et al., Interactions between VEGFR and Notch signaling pathways in endothelial and neural cells. Cellular and molecular life sciences : CMLS, 2013. 70(10): p. 1779-1792.

56. Watanabe, K., et al., Enhancement of Notch receptor maturation and signaling sensitivity by Cripto-1. J Cell Biol, 2009. 187(3): p. 343-53.

57. Bianco, C., et al., Role of human cripto-1 in tumor angiogenesis. Journal of the National Cancer Institute, 2005. 97(2): p. 132-141.

58. Bulmer, J.N., P.J. Williams, and G.E. Lash, Immune cells in the placental bed. Int J Dev Biol, 2010. 54(2-3): p. 281-94.

59. Schumacher, A., et al., Immune Cells at the Fetomaternal Interface: How the Microenvironment Modulates Immune Cells To Foster Fetal Development. The Journal of Immunology, 2018. 201(2): p. 325.

60. van den Heuvel, M.J., et al., Trafficking of circulating pro-NK cells to the decidualizing uterus: regulatory mechanisms in the mouse and human. Immunol Invest, 2005. 34(3): p. 273-93.

61. Wu, X., et al., Human first-trimester trophoblast cells recruit CD56brightCD16- NK cells into decidua by way of expressing and secreting of CXCL12/stromal cell-derived factor 1. J Immunol, 2005. 175(1): p. 61-8.

62. Yadi, H., et al., Unique receptor repertoire in mouse uterine NK cells. J Immunol, 2008. 181(9): p. 6140-7.

63. Lash, G.E., et al., Expression of angiogenic growth factors by uterine natural killer cells during early pregnancy. J Leukoc Biol, 2006. 80(3): p. 572-80.

64. Naruse, K., et al., The urokinase plasminogen activator (uPA) system in uterine natural killer cells in the placental bed during early pregnancy. Placenta, 2009. 30(5): p. 398-404.

65. Robson, A., et al., Uterine natural killer cells initiate spiral artery remodeling in human pregnancy. Faseb j, 2012. 26(12): p. 4876-85.

66. Ratsep, M.T., et al., Uterine natural killer cells: supervisors of vasculature construction in early decidua basalis. Reproduction, 2015. 149(2): p. R91-R102.

67. Felker, A.M. and B.A. Croy, Promotion of Early Pregnancy Events in Mice and Humans by Uterine Natural Killer Cells. NeoReviews, 2016. 17(2): p. e93-e101.

68. Svensson, J., et al., Macrophages at the fetal-maternal interface express markers of alternative activation and are induced by M-CSF and IL-10. J Immunol, 2011. 187(7): p. 3671-82.

69. Croy, B.A., et al., Analysis of uterine natural killer cells in mice. Methods Mol Biol, 2010. 612: p. 465-503.

70. Chen, Z., et al., DBA-lectin reactivity defines mouse uterine natural killer cell subsets with biased gene expression. Biol Reprod, 2012. 87(4): p. 81.

71. Lima, P.D., et al., Heterogeneity in composition of mouse uterine natural killer cell granules. J Leukoc Biol, 2012. 92(1): p. 195-204.

72. Sojka, D.K., L.P. Yang, and W.M. Yokoyama, Uterine natural killer cells: To protect and to nurture. Birth Defects Research, 2018. 110(20): p. 1531-1538.

73. Sojka, D.K., L.P. Yang, and W.M. Yokoyama, Uterine Natural Killer Cells. Frontiers in Immunology, 2019. 10.

Supplementary material

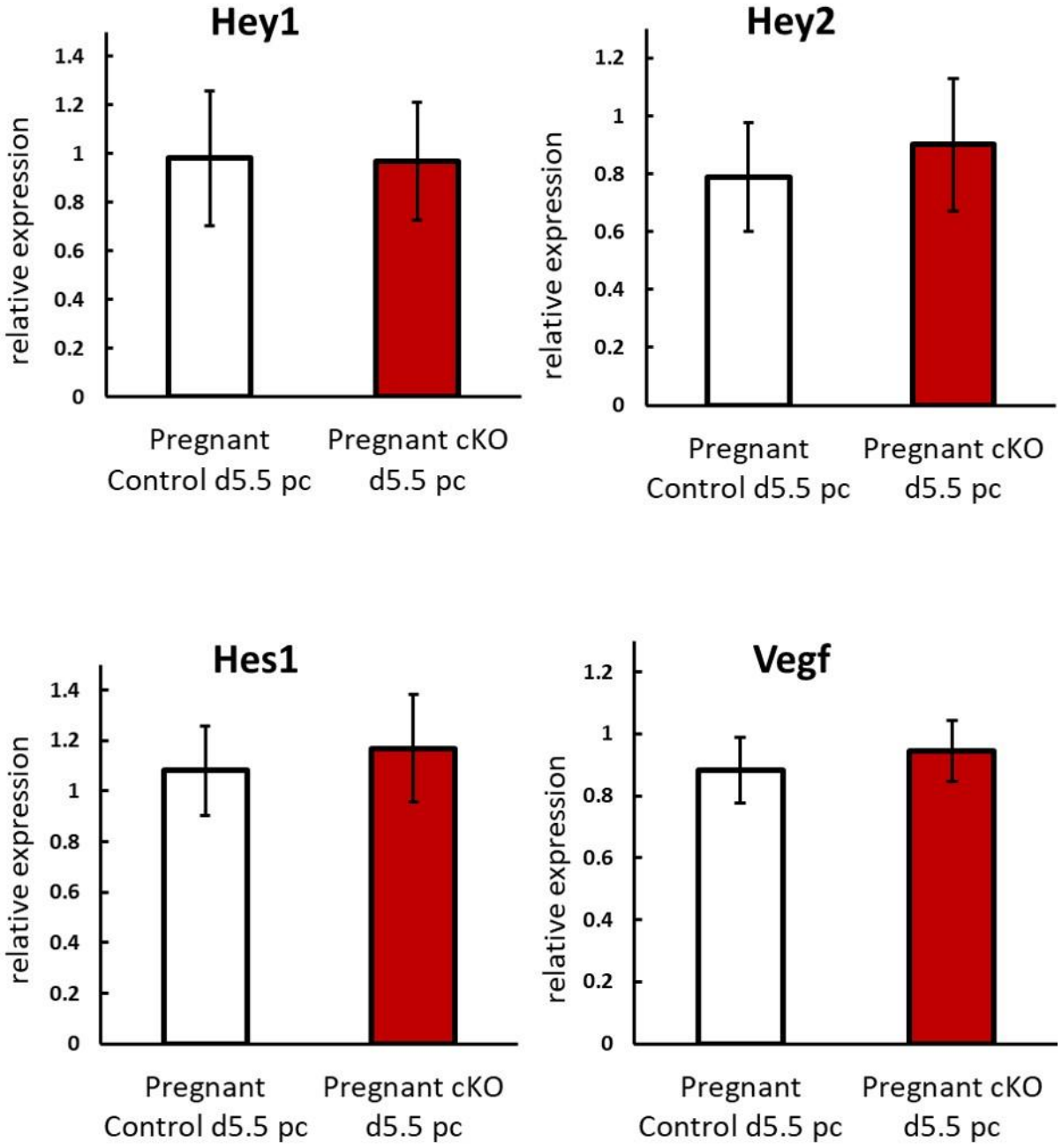

Figure 3.S1. Expression level of downstream targets of Notch signaling pathway involved in angiogenesis during early post-implantation. Similar relative expression level of *Vegf, Hey1, Hey2 and Hes1,* on d5.5pc measured by quantitative real-time PCR was observed in Control (n= 4 females) and Cripto cKO (n= 5 females) groups.

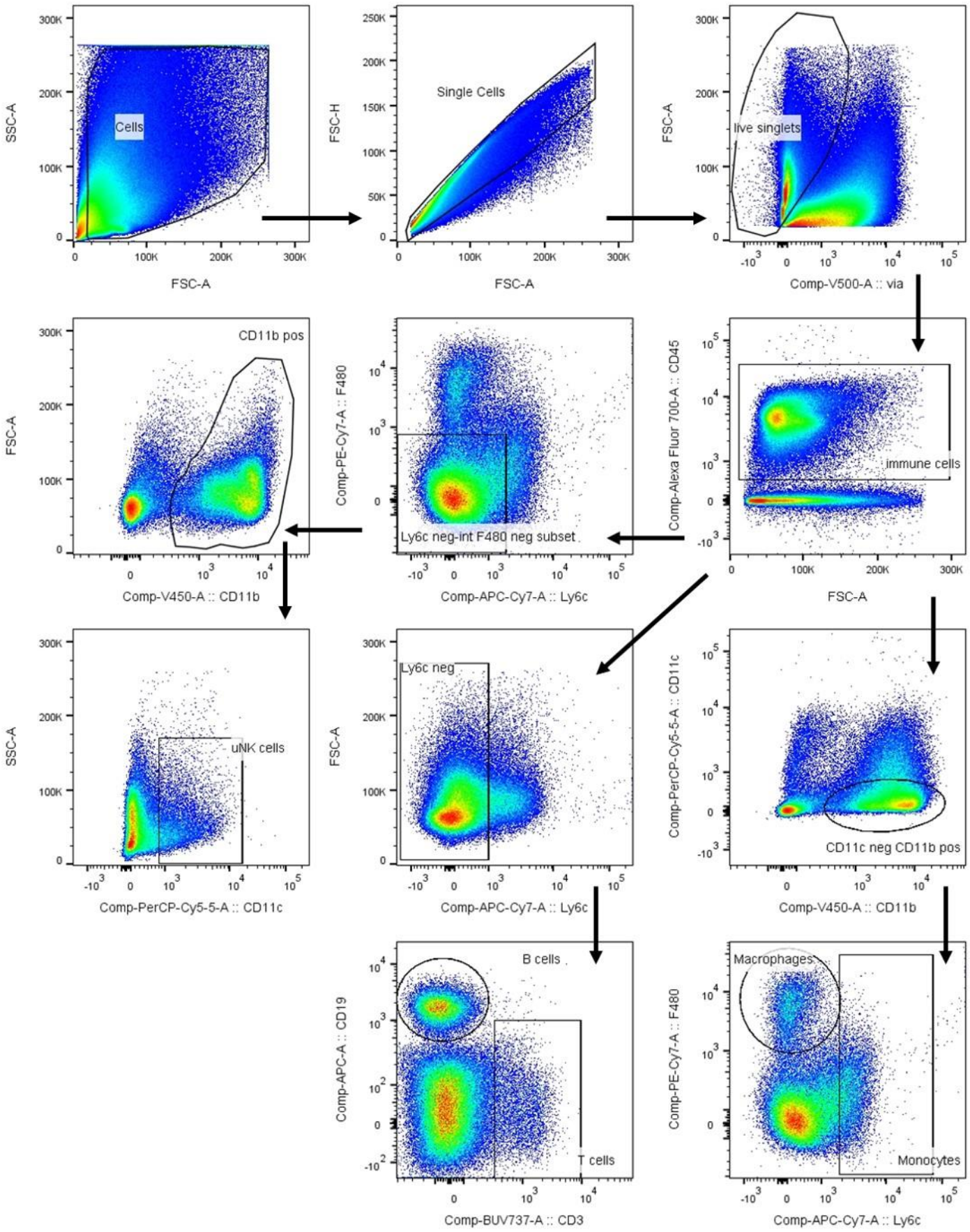
Cells
SSC-A
FSC-A
Single Cells
FSC-H
FSC-A
live singlets
FSC-A
Comp-V500-A :: via
immune cells
Comp-Alexa Fluor 700-A :: CD45
FSC-A
Ly6c neg-int F480 neg subset
Comp-PE-Cy7-A :: F480
Comp-APC-Cy7-A :: Ly6c
CD11b pos
FSC-A
Comp-V450-A :: CD11b
uNK cells
SSC-A
Comp-PerCP-Cy5-5-A :: CD11c
Ly6c neg
FSC-A
Comp-APC-Cy7-A :: Ly6c
CD11c neg CD11b pos
Comp-PerCP-Cy5-5-A :: CD11c
Comp-V450-A :: CD11b
B cells
T cells
Comp-APC-A :: CD19
Comp-BUV737-A :: CD3
Macrophages
Monocytes
Comp-PE-Cy7-A :: F480
Comp-APC-Cy7-A :: Ly6c

Figure 3.S2. Flow cytometric analysis of leukocytes in d10.5pc implantation sites. The figure shows the gating scheme to identify total immune cells and several immune cells types present at d10.5pc implantation sites. Cells were chosen apart from debris and particles within the sample using gating for forward scatter area (FSC-A, representing the size) and side scatter area (SSC-A, representing the complexity). Single cells (singlets) were selected versus doublets using FSC-A and FSC-H (height). A Fixable Viability Dye (FVD efour506) was used to mark the dead cells. Live singlets were gated for CD45 to define the population of all leukocytes. Some of immune cell types were defined as follows: **uterine Natural Killer cells (uNK cells):** *CD45 pos, Ly6c neg-int, F4/80 neg, CD11b pos, CD11c pos.* **B cells:** *CD45 pos, Ly6c neg, CD3 neg, CD19 pos.* **T cells:** *CD45 pos, Ly6c neg, CD3 pos, CD19 neg.* **Macrophages:** *CD45 pos, CD11b pos, CD11c neg, Ly6c neg-int, F4/80 pos.* **Monocytes:** *CD45 pos, CD11b pos, CD11c neg, Ly6c hi, F4/80 neg-pos.* pos: positive, neg: negative, int: intermediate, hi: high, via: viability.

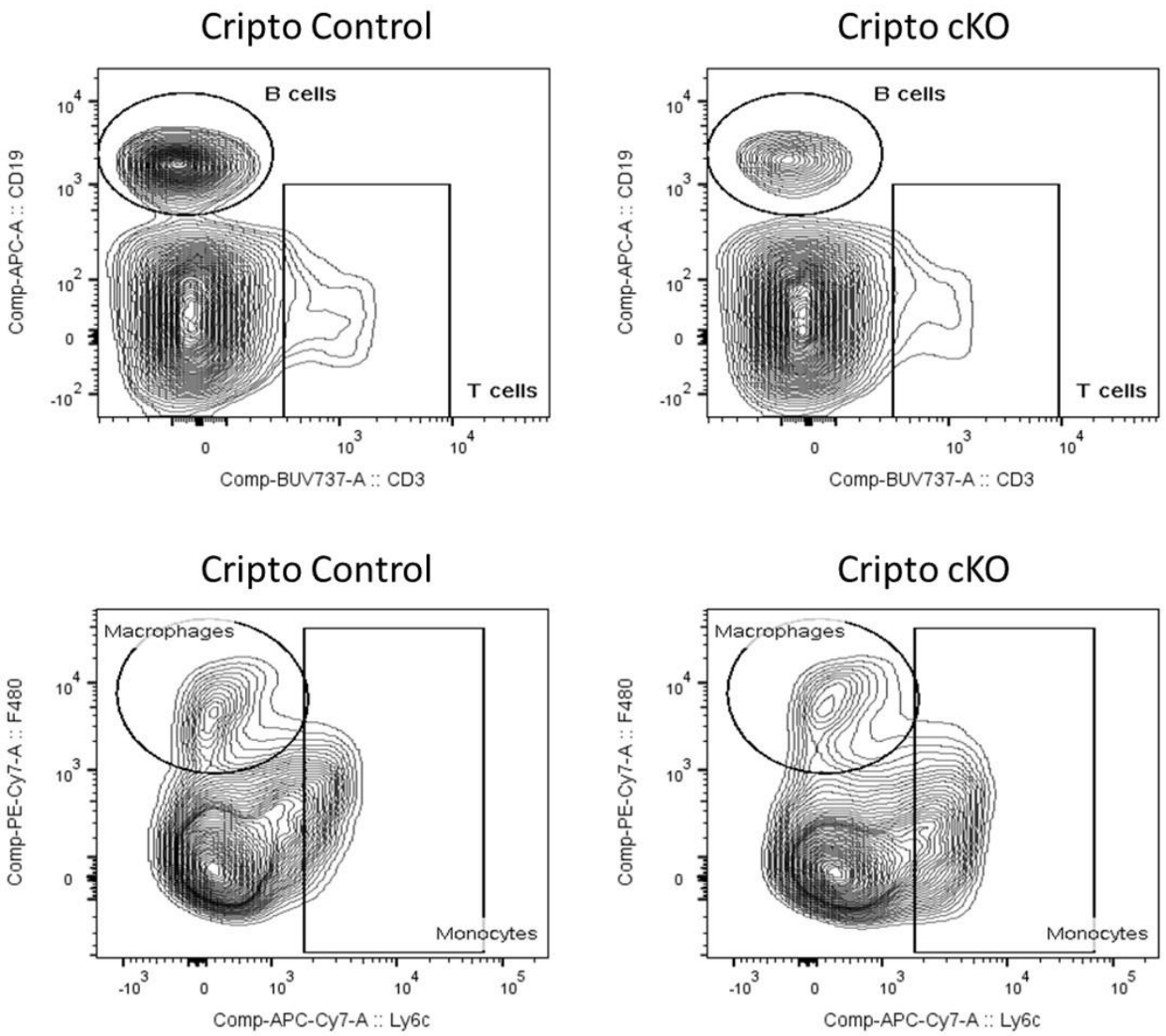

Figure 3.S3. Representative flow cytometry contour plots showing the clustering scheme of different immune cell subsets in d10.5pc implantation sites. The plots created by FlowJo software (version 10) show how B cells, T cells, Monocytes and Macrophages, obtained from implantation sites of Control and Cripto cKO females on d10.5pc of pregnancy, cluster after flow cytometric analysis. Each line in the graphs represent 2% of the whole population present in the graph. Smaller population of T cells and B cells, and larger population of Monocytes can be appreciated in graphs related to Cripto cKO compared to Control.

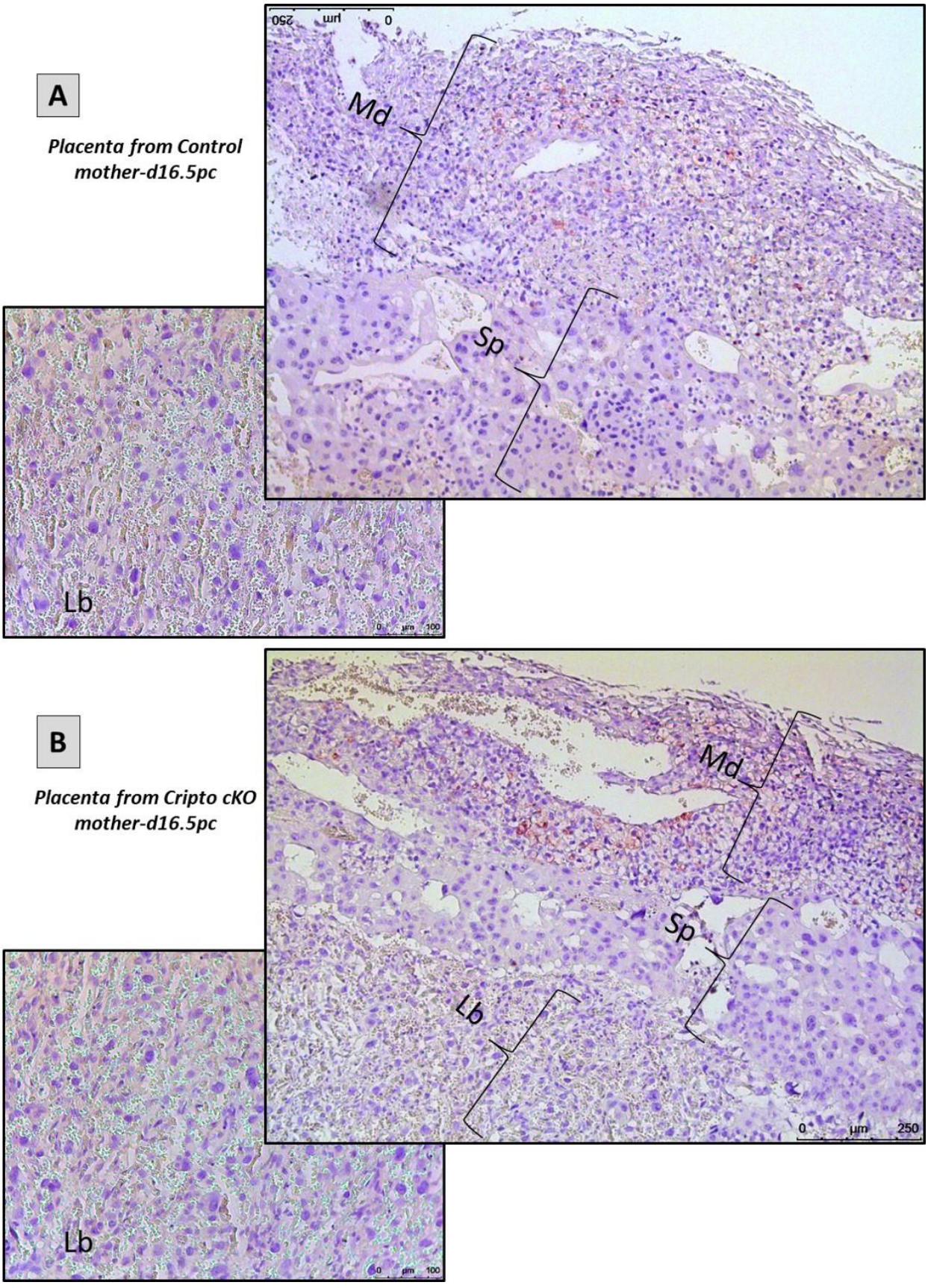
A
Placenta from Control mother-d16.5pc
Md
Sp
Lb
B
Placenta from Cripto cKO mother-d16.5pc
Md
Sp
Lb
0
µm
250

Figure 3.S4. Cripto protein is weakly expressed only within maternal compartment of mature placenta. IHC against Cripto (brown) on d16.5pc comparing the mature placenta of Control (A) and Cripto cKO females (B). Slides were counter-stained with Hematoxylin. In both groups low Cripto staining is detected only within maternal compartment of placenta (Md). Smaller panels in each section show higher magnification of placental labyrinth. Md, maternal decidua; Sp, spongiotrophoblast and Lb, labyrinth. (Scale bar, larger panels: 250 µm; smaller panels: 100 µm)

Antibody	Host animal	Company	Concentration
Cripto	Goat	Santa Cruz sc-17188	1:100
CD31	Rabbit	Abcam-ab28364	1:100
Tpbpa	Rabbit	Abcam-ab104401	1:100
DBA-FITC conjugated		bioWORD- 21761015-1	1:300
F4/80	Rat	Invitrogen eBiosciences 14-4801-82	1:50
HRP-anti Rabbit	mouse	Santa Cruz- sc-2357	1:250
HRP-anti Goat	Donkey	Santa Cruz- sc-2020	1:250
Alexa Fuor 594 anti Rabbit	Donkey	Molecular probes	1:250
Alexa Fluor 488 anti Goat	Donkey	Life Technologies	1:250
Alexa Fluor 546 anti Goat	Donkey	Invitrogen	1:300
Rhodamine Red-X anti Rat	Goat	Invitrogen-molecular probes	1:300

Table S2

Gene Name	Q-PCR primer-Forward	Q-PCR primer-Reverse
Cripto	5′- GACCAGAAAGAACCTGCCGT -3′	5′- AGGATAGACCCACAGTGCTCTT -3′
Wnt4	5′-AACGGAACCTTGAGGTGATG-3′	5′-TCACAGCCACATTCTCCAG-3′
Notch4	5′-TTGGCTGAGCAGAAGTCTCG-3′	5′-CCTCACTTCTCCTGCACCTG-3′
Notch1	5′-TCACTCTCACAGTTGCGACC-3′	5′-AGTGGCCCTAATTGCCAGAC-3′
Dll4	5′-TTCTTGCACGGAGAGTGGTG-3′	5′-CAACACGACACCGGAACAAAC-3′
GAPDH	5′-AACTTTGGCATTGTGGAAGG-3′	5′-ACACATTGGGGGTAGGAACA-3′
F4/80	5′- GCTGCCTCCCTGACTTTCAA-3′	5′- GCTGTATCTGCTCACTTTGGAG-3′
CD11b	5′- GAGGCCCCCAGGACTTTAAC-3′	5′- CTTCTTGGTGAGCGGGTTCT-3′
NKp46	5′-TGGTCTTTTCCCAGTGAGCC -3′	5′-AGTAGGGTCGGTAGGTGCAA-3′
Hey1	5′-GCCGACGAGACCGAATCAA-3′	5′-CCCCAAACTCCGATAGTCCA-3′
Hey2	5′-TCCAGGCTACAGGGGGTAAA-3′	5′-AGATGAGAGACAAGGCGCAC-3′
Hes1	5′-CAACACGACACCGGACAAAC-3′	5′-TTGGAATGCCGGGAGCTATC-3′
Esx1	5′-TGGAGCAGTGAAGGAGGAAAC-3′	5′-GCTTCTTCCAGAAACATGGAGT-3′
Vegfr2	5′-TGTGCCTGAGAACTGGGCTC-3′	5′-GTCTTTCTGTGTGCTGAGCTTG-3′
Vegf	5′-ACTGGACCCTGGCTTTCATG-3′	5′-GCTTCGCTGGTAGACATCCA-3′
Nodal	5′-TGGCGTACATGTTGAGCCTCT-3′	5′-TGAAAGTCCAGTTCTGTCCGG-3′
CD45	5′-GAGATGCAGGGTCCACCTAC-3′	5′-GGCCTTTTGCTCCCAGATCA-3′

Table S3

Antibody	Fluorochrome	Company
Fixable Viability Dye	eFluor 506	Invitrogen eBio. (65-0866-14)
CD45	Alexa Fluor 700	Biolegend (103127)
CD3	BUV 737	BD (17a2 612803)
CD19	APC	Invitrogen eBio. (1d3 17-0193-80)
Ly6c	APC-Cy7	BD (AL-21 560596)
CD11b	V450	Invitrogen (M1/70 48-0112-80)
CD11c	PerCp-Cy5.5	BD (HL3 560584)
F4/80	PE-Cy7	eBiosciences (BM8 25-4801-82)
Cripto	PE	Novus (NB100-1598)

Table S4

Chapter 4: DISCUSSION and CONCLUSION

Discussion

Currently, it is not well understood how Cripto is involved in female reproduction. In the studies conducted in this thesis, we investigated whether Cripto is present in the mouse uterus during pregnancy and if it played a role in physiologic events of female reproduction such as implantation, uterine decidualization and placentation. We generated a conditional knockout mouse model in which Cripto was deleted in all cell types expressing progesterone receptor, including the uterus. We showed that these mice are subfertile due to abnormalities observed in decidualization, uterine remodeling and luminal closure as well as defective placental development.

Our lab had previously generated a conditional deletion of Nodal in the mouse uterus, using a similar loxP-Cre system, resulted in a dramatic reduction in fertility of Nodal conditional homozygous knockout (cKO) and conditional heterozygous (cHet) females due to impaired implantation, decidualization and placentation (Park CB, 2012, Park CB, manuscript in preparation). In addition, Nodal cKO were prone to spontaneous pre-term delivery on d17.5pc as opposed to term birth at d19.5pc (Park CB, 2012) and both Nodal cKO and Nodal cHet females showed significantly higher sensitivity to infection induced inflammation which causes them to deliver prematurely (Heba T. and Dufort D., manuscript accepted in Biology of Reproduction). Nodal signals through an extracellular membrane-bound receptor complex comprised of type I (ALK4/ALK7) and type II (ActRIIA/ActRIIB) Activin receptors and an EGF-CFC (Cripto/Cryptic) co-receptor. Activation of the receptor complex results in the phosphorylation of the transcription factors SMAD2 and SMAD3. Phosphorylated SMAD2/3 bind to SMAD4, which allows the complex to undergo nuclear translocation. These SMADs then associate with

additional transcription factors, such as FoxH1, Mixer and p53 to facilitate DNA binding and regulate downstream target genes (Schier AF, 2009). Besides Smad-dependent pathway, Nodal can also function through Smad-independent pathways such as ERK/JNK/P38-MAPK and PI3/Akt pathways (Zhang YE., 2010).

The present study was part of our lab's main goal to elucidate the precise mechanisms of Nodal action with regards to female reproduction. In order to activate the Alk4-Smad2/3 signaling, Nodal depends highly on the EGF-CFC proteoglycan family; Cripto in particular (Blanchet AH, 2008). However, other studies have indicated that Nodal can also bind ActRIIA/B and Alk4 (its receptor complex) independent of Cripto (BenHaim N, 2006). It has been shown that besides being a co-receptor for Nodal, Cripto can activate Smad-independent signaling elements such as PI3K/Akt and MAPK and also facilitate signaling through the canonical Wnt/ß-catenin and Notch/Cbf-1 pathways by functioning as a chaperone protein for LRP5/6 and Notch, respectively (Klauzinska, Castro et al. 2014).

Among different components of the Nodal-Cripto-Alk4-Smad dependent pathway, the uterine expression pattern and/or reproductive consequences of uterine deletion of Nodal (Park CB, 2012; Park CB, manuscript in preparation), Cripto (this study), ALK4 (Peng J. et al, 2015), Smad3 (Zhao, K.Q. et al, 2012), Smad2 and Smad4 (Liu G. et al 2003, Rodriguez, A. 2016) have been studied. Although all these components have been detected in the mouse uterus during early pregnancy, they show different spatiotemporal pattern of expression. Similar to what we have observed for Cripto, Nodal (Park CB 2012) and Smad3 (Zhao, K.Q. 2012) are not expressed in non-pregnant uterus while ALK4 protein expression was detected in luminal epithelium,

glandular epithelium, stroma, and myometrium (Peng J. et al, 2015), and Smad2 and Smad4 mRNA was found to be predominantly present in the luminal and glandular epithelium of non-pregnant mouse uterus (Liu G. et al 2003).

We have shown that Cripto expression starts weakly after mating and increases gradually till it becomes prominent on d3.5pc only at future implantation sites in the subluminal uterine stromal cells and luminal epithelium and is not present at the inter-implantation spaces. Similarly, on d5.5pc (1 day after implantation) localization of Cripto protein is limited to the implantation sites in decdidual cells, differentiating stromal cells and some glandular epithelium. During this period (d0.5pc-d5.5pc) Smad3 shows a very similar expression pattern to Cripto (Zhao, K.Q. 2012). Nodal, Smad2 and smad4 were shown to be present in luminal epithelium and glandular epithelium from d0.5pc-d4.5pc. On the day of implantation, Smad2 and Smad4 are also detectable in the subluminal stroma around the implanting blastocysts then on d5.5pc and d6.5pc in primary and secondary decidual zone in decidual cells whereas, the expression of Nodal becomes limited only to inter-implantation spaces on d4.5pc till d6.5pc (Park CB 2012, Liu G. et al 2003). In the study by Peng J. et al, 2015 however, localization of Alk4 was not assessed during early pregnancy. They reported that on d5.5pc ALK4 protein expression is almost undetectable in uterus at the implantation sites (the possibility of ALK4 expression in the inter-implantation sites like that of Nodal at this timepoint of pregnancy has not been assessed). ALK4 expression was reported in the antimesometrial stroma near the embryo at around d7.5pc and reached its peak at d8.5pc, with the highest expression observed at the antimesometrial pole of the implantation site which is the site of placental development (Peng J. et al, 2015). On d8.5pc both Nodal and its receptor ALK4 are present on the

stroma/decidual cells in the antimesometrial aspect of the conceptus site. Then expression of ALK4 decreases and becomes undetectable by d10.5pc whereas Nodal continues to have a dynamic expression in a distinct thin layer of the decidua parietalis from d8.5pc untill d12.5pc shifting from antimesometrial to the lateral and mesometrial aspects of conceptus and continues to be expressed till the end of pregnancy (Park CB, 2012, Peng J. et al, 2015). These dynamic patterns of expression of the components of Nodal Smad-dependent pathway during pregnancy is very interesting and suggest complex and extensive communications between embryonic cells and uterine cells at implantation as well as inter-implantation spaces.

Our studies have shown that the outcomes of deleting Cripto in the female reproductive tract are not similar with what happens in the case of the uterine specific deletion of Nodal or Alk4. Some physiologic events are disrupted in Nodal cKO mice but seem to be completely normal, impaired with less severity or impaired with a different phenotype in Cripto cKO and/or Alk4 cKO mice. While ovulation, fertilization and early embryo development are normal in these 3 cKO mouse model, considerable implantation failure is observed in Nodal cKO females (Park and Dufort, manuscript in preparation) while this phenotype is very mild in Cripto cKO (present study) and Alk4 cKO females (Peng J. et al, 2015). This observation can be justified with these 2 possibly: 1) Nodal role in regulating implantation is exerted through Smad-independent pathways and/or 2) Nodal target cells in the uterus during peri-implantation period are those that do not express progesterone receptor (such as immune cells); Therefore, Cripto or Alk4 will not be deleted in these cells and required pathway will remain active.

While both Cripto cKO females (present study) and Nodal cKO mice (Park and Dufort, manuscript in preparation) showed compromised decidualization ability, Alk4 cKO females have been shown to not have any defects in decidualization (Peng J. et al, 2015). This observation suggests that Nodal and Cripto are involved in uterine decidualization through Alk4/Smad-independent pathways and although we have not yet tested this directly, their involvement in uterine decidualization is probably not redundant. Creating a conditional knockout mouse model with deletion of both Nodal and Cripto from the uterus is required for understanding whether Nodal and Cripto exert their roles in the process of decidualization independently or through the same pathway.

We have assessed the level of some critical factors in uterine decidualization including the serum level of progesterone as well as the expression of Ihh, Cox2, Hoxa10, Hoxa11, Bmp2, Wnt4 and Notch signaling pathway components in uteri of pregnant cKO and Control females. A significant decrease was observed in the expression of Wnt4 and Bm2 in the uteri of d5.5pc Cripto cKO compared to Control females. BMP2 (Lee, Jeong et al. 2007) and Wnt4 (Franco, Dai et al. 2011) which are both critical decidualization elements are suggested to be involved more in differentiation of decidual cells rather than the proliferation phase (Ramathal, Bagchi et al. 2010). We also evaluated the differentiation state of decidual cells in d5.5pc pregnant Cripto cKO females versus Controls using staining for tissue Alkaline phosphatase activity. Differentiated decidual cells have a high level of alkaline phosphatase enzyme which results in a strong staining. Interestingly this experiment showed that decidual cell differentiation is indeed compromised in Cripto cKO females.

The Notch signaling pathway and its components such as Notch1 and Rbpj have been shown to be critical for uterine stromal decidualization (Ramathal, Bagchi et al. 2010, Afshar, Jeong et al. 2012), stromal remodeling and uterine luminal closure (Zhang, Kong et al. 2014). We have seen a significant decrease in the expression of Notch1, Notch4 and Dll4 in the uteri of pregnant d5.5pc Cripto cK.O compared to Control females. In addition, abnormal implantation crypts and failure of uterine luminal closure were frequently observed in Cripto cK.O females in contrast to controls. These findings are very similar to phenotypes observed in the case of disruption of Notch signaling pathway (Zhang, Kong et al. 2014). As described earlier, Cripto has been shown to be implicated in enhancing of Notch signaling (Watanabe, Nagaoka et al. 2009). Impaired decidualization and uterine luminal closure process in Cripto cK.O mice can therefore at least partly be the result of decreased activity of Notch signaling which in turn results in lowered expression of Notch receptors (Artavanis-Tsakonas, Rand et al. 1999) leading to additional decrease in the activity of Notch signaling pathway and worsening of the condition.

We observed fetal death and IUGR in pregnancy of Cripto cKO females which are also the phenotypes seen in Nodal cKO and Alk4 cKO females all due to placental defects. The characteristics of the defective placentas however, is not completely similar in these three cKO mouse models. We showed that in placentas from Cripto cKO females, all placental compartments including maternal decidua, junctional zone (spongiotrophoblast and trophoblast giant cells), and labyrinth are present, and each layer seems to have a normal overall size as analyzed on d16.5pc in our study. However, we have observed that the labyrinth layer of the placenta in Cripto cKO females was cell dense and had significantly less blood-filled spaces due to significant decrease in development of fetal vasculature. As the overall size of the

labyrinth was not diminished and labyrinth maternal blood sinuses showed normal size, this phenotype was concluded to be the result of normal villi branching but impaired labyrinth fetal vascularization, a defective labyrinth phenotype which is also observed in mutants of Notch signaling pathway components and Esx1 (Li and Behringer 1998, Krebs, Xue et al. 2000, Duarte, Hirashima et al. 2004, Fischer, Schumacher et al. 2004, Krebs, Shutter et al. 2004). Interestingly we observed that the expression of several components of Notch signaling pathway (Dll4, Hey1, Hey2, Hes1, Notch1 and Notch4) along with Vegf and its receptor Vegfr2 was significantly lower in uterus/maternal decidua of Cripto cKO females compared to Controls. Furthermore, the expression of Vegf and Notch4 in fetal parts of placenta was also significantly lower in Cripto cKO group compared to Control. These findings suggest that maternal Cripto could be a part of the maternal-fetal communications required for proper development of the placenta and of the placental vasculature. Our results also suggest that the role of Cripto in the development of vasculature at maternal-fetal interface is at least partly through VEGF and Notch signaling pathways.

In comparison, pregnancy of Nodal cKO females showed a drastic decrease in the maternal decidual compartment of placenta and an expansion of the trophoblast giant cell layer and spongiotrophoblast layer but overall size of labyrinth did not seem to be changed (Park C.B., 2012). In Alk4 cKO mice, although all layers of placenta are present, the normal organization is disrupted in the form of an expansion of the trophoblast giant cells layer (similar to Nodal cKO females) and a reduction in size of spongiotrophoblast and labyrinth layers. The size of the maternal decidua, however, is not affected in Alk4 cKO mice as severely as it is seen in placenta of Nodal cKO females. Together, these studies including our data suggest that the required

pathway for the maintenance of maternal decidua compartment of placenta during late pregnancy, is either Nodal Smad-independent pathways or Nodal Smad-dependent pathway in the target cells that do not express PR (such as immune cells). It can be also speculated that Nodal signaling through Alk4 is probably active in regulation of giant cells and trophoblast cells at the fetal-maternal interface as impaired organization of giant cell and spongiotrophoblast layers are observed in placentas in both Nodal and Alk4 cKO females. This defect is not observed in Cripto cKO mouse model which can possibly suggest that either Nodal signaling through Alk4 might function independently of EGF-CFC co-receptors (Cripto or Cryptic), which is supported by studies indicating that Nodal can bind ActRIIA/B and Alk4 independently of Cripto (BenHaim N, 2006) or that there is functional redundancy between the two EGF-CFC genes, Cripto and Cryptic. Despite the non-overlapping expression of Cripto and Cryptic prior to gastrulation in the developing embryo, in a study using double Cripto/Cryptic mutants, Chu J. and Shen M. in 2010 showed some partially redundant functions between these proteins in early mouse development (Chu and Shen 2010). The expression of Cryptic in mouse uterus has not been elucidated yet. Our preliminary results of Real-Time quantitative PCR suggest that in uteri of wild type mice during estrous cycle (estrus and diestrus) and early pregnancy from d0.5pc to d5.5pc, Cryptic expression is generally very low (data not shown). The definite answer will be reached by creating a double Cripto/Cryptic uterine cKO mutant which is beyond the scope of the present study.

In this study, no incidence of preterm delivery in Cripto cKO females was observed, similar to Alk4 cKO and in contrast to Nodal cKO females. Again, these data suggest that for maintenance of pregnancy to full-term, Nodal possibly either signals through Cripto/ALK4/Smad-independent

pathways and/or Nodal Smad-dependent pathway is required in target cells that do not express PR (such as immune cells). Interestingly, our preliminary results using flow cytometric analysis showed that indeed during the placentation period, a population of maternal immune cells at maternal-fetal interface express Cripto and these cells are most likely the target cells of Nodal and may be involved in modulating pregnancy maintenance and/or timing of parturition.

Conclusion

In summary, in this study we have shown the spatiotemporal localization pattern of Cripto in the uterus and at the maternal-fetal interface during the course of mouse pregnancy for the first time. We have defined that depending on gestational age, different cell types produce Cripto including uterine luminal epithelium, uterine stroma, decidual cells, uterine immune cells, embryonic trophectoderm, trophoblast giant cells, spongiotrophoblast cells and labyrinth sinusoidal giant cells. Deletion of Cripto in the female reproductive system (maternal sources of Cripto) leads to subfertility in the forms of lower pregnancy rate and smaller litter size. We have shown that implantation failure, compromised uterine remodeling and luminal closure, impaired uterine decidualization, as well as placentation defects in Cripto cKO females are the underlying causes for this subfertility. Based on findings in this study, we suggest that Cripto exerts functions in female reproduction that can be both dependent and independent of Nodal signaling. We have introduced a mouse model to better understand regulation of female reproduction by TGF-β related signaling which also can be considered a good tool to study pathogenesis of pregnancy related issues in humans, aiming towards the development of new treatments for female infertility.

Chapter 5: REFERENCES

Adamson, S. L., Y. Lu, K. J. Whiteley, D. Holmyard, M. Hemberger, C. Pfarrer and J. C. Cross (2002). "Interactions between trophoblast cells and the maternal and fetal circulation in the mouse placenta." Dev Biol **250**(2): 358-373.

Afshar, Y., J. W. Jeong, D. Roqueiro, F. DeMayo, J. Lydon, F. Radtke, R. Radnor, L. Miele and A. Fazleabas (2012). "Notch1 mediates uterine stromal differentiation and is critical for complete decidualization in the mouse." Faseb Journal **26**(1): 282-294.

Albertsson, P., M. H. Kim, L. E. Jonges, R. P. Kitson, P. J. Kuppen, B. R. Johansson, U. Nannmark and R. H. Goldfarb (2000). "Matrix metalloproteinases of human NK cells." In Vivo **14**(1): 269-276.

Andersson, O., P. Bertolino and C. F. Ibanez (2007). "Distinct and cooperative roles of mammalian Vg1 homologs GDF1 and GDF3 during early embryonic development." Dev Biol **311**(2): 500-511.

Andersson, O., E. Reissmann, H. Jornvall and C. F. Ibanez (2006). "Synergistic interaction between Gdf1 and Nodal during anterior axis development." Dev Biol **293**(2): 370-381.

Ansell, J. D., P. W. Barlow and A. McLaren (1974). "Binucleate and polyploid cells in the decidua of the mouse." J Embryol Exp Morphol **31**(1): 223-227.

Armant, D. R. and S. Kameda (1994). "Mouse trophoblast cell invasion of extracellular matrix purified from endometrial tissue: a model for peri-implantation development." J Exp Zool **269**(2): 146-156.

Artavanis-Tsakonas, S., M. D. Rand and R. J. Lake (1999). "Notch signaling: Cell fate control and signal integration in development." Science **284**(5415): 770-776.

Ashton, S. V., G. S. Whitley, P. R. Dash, M. Wareing, I. P. Crocker, P. N. Baker and J. E. Cartwright (2005). "Uterine spiral artery remodeling involves endothelial apoptosis induced by extravillous trophoblasts through Fas/FasL interactions." Arterioscler Thromb Vasc Biol **25**(1): 102-108.

ASSHETON, R. (1894). "On the Cause which lead to the Attachment of the Mammalian Embryo to the Walls of the Uterus." Quarterly Journal of Microscopical Science **s2-37**(146): 173-190.

Bamford, R. N., E. Roessler, R. D. Burdine, U. Saplakoglu, J. dela Cruz, M. Splitt, J. A. Goodship, J. Towbin, P. Bowers, G. B. Ferrero, B. Marino, A. F. Schier, M. M. Shen, M. Muenke and B. Casey (2000). "Loss-of-function mutations in the EGF-CFC gene CFC1 are associated with human left-right laterality defects." Nat Genet **26**(3): 365-369.

Bandeira, C. L., A. U. Borbely, R. P. V. Francisco, R. Schultz, M. Zugaib and E. Bevilacqua (2014). "Tumorigenic Factor CRIPTO-1 Is Immunolocalized in Extravillous Cytotrophoblast in Placenta Creta." Biomed Research International.

Barrientos, G., I. Tirado-Gonzalez, B. F. Klapp, K. Karimi, P. C. Arck, M. G. Garcia and S. M. Blois (2009). "The impact of dendritic cells on angiogenic responses at the fetal-maternal interface." J Reprod Immunol **83**(1-2): 85-94.

Behrens, A. N., Y. Ren, A. Ferdous, D. J. Garry and C. M. Martin (2012). "Nkx2-5 Regulates Tdgf1 (Cripto) Early During Cardiac Development." J Clin Exp Cardiolog **Suppl 11**: 1-4.

Bendall, S. C., C. Hughes, J. L. Campbell, M. H. Stewart, P. Pittock, S. Liu, E. Bonneil, P. Thibault, M. Bhatia and G. A. Lajoie (2009). "An enhanced mass spectrometry approach reveals human embryonic stem cell growth factors in culture." Mol Cell Proteomics **8**(3): 421-432.

Berezowsky, J., I. Zbieranowski, J. Demers and D. Murray (1995). "DNA ploidy of hydatidiform moles and nonmolar conceptuses: a study using flow and tissue section image cytometry." Mod Pathol **8**(7): 775-781.

Bevilacqua, E. M. and P. A. Abrahamsohn (1988). "Ultrastructure of trophoblast giant cell transformation during the invasive stage of implantation of the mouse embryo." J Morphol **198**(3): 341-351.

Bianco, C., H. B. Adkins, C. Wechselberger, M. Seno, N. Normanno, A. De Luca, Y. Sun, N. Khan, N. Kenney, A. Ebert, K. P. Williams, M. Sanicola and D. S. Salomon (2002). "Cripto-1 activates nodal- and ALK4-dependent and -independent signaling pathways in mammary epithelial Cells." Mol Cell Biol **22**(8): 2586-2597.

Bianco, C., N. P. Castro, C. Baraty, K. Rollman, N. Held, M. C. Rangel, H. Karasawa, M. Gonzales, L. Strizzi and D. S. Salomon (2013). "Regulation of human Cripto-1 expression by nuclear receptors and DNA promoter methylation in human embryonal and breast cancer cells." J Cell Physiol **228**(6): 1174-1188.

Bianco, C., C. Cotten, E. Lonardo, L. Strizzi, C. Baraty, M. Mancino, M. Gonzales, K. Watanabe, T. Nagaoka, C. Berry, A. E. Arai, G. Minchiotti and D. S. Salomon (2009). "Cripto-1 Is Required for Hypoxia to Induce Cardiac Differentiation of Mouse Embryonic Stem Cells." American Journal of Pathology **175**(5): 2146-2158.

Bianco, C., M. C. Rangel, N. P. Castro, T. Nagaoka, K. Rollman, M. Gonzales and D. S. Salomon (2010). "Role of Cripto-1 in Stem Cell Maintenance and Malignant Progression." The American Journal of Pathology **177**(2): 532-540.

Bianco, C., L. Strizzi, A. Ebert, C. Chang, A. Rehman, N. Normanno, L. Guedez, R. Salloum, E. Ginsburg, Y. P. Sun, N. Khan, M. Hirota, B. Wallace-Jones, C. Wechselberger, B. K. Vonderhaar, G. Tosato, W. G. Stetler-Stevenson, M. Sanicola and D. S. Salomon (2005). "Role of human cripto-1 in tumor angiogenesis." Journal of the National Cancer Institute **97**(2): 132-141.

Bianco, C., L. Strizzi, N. Normanno, N. Khan and D. S. Salomon (2005). Cripto-1: An oncofetal gene with many faces. Current Topics in Developmental Biology, Vol 67. G. P. Schatten. **67:** 85-133.

Bianco, C., L. Strizzi, A. Rehman, N. Normanno, C. Wechselberger, Y. Sun, N. Khan, M. Hirota, H. Adkins, K. Williams, R. U. Margolis, M. Sanicola and D. S. Salomon (2003). "A Nodal- and ALK4-independent signaling pathway activated by Cripto-1 through Glypican-1 and c-Src." Cancer Res **63**(6): 1192-1197.

Bianco, C., C. Wechselberger, A. Ebert, N. I. Khan, Y. Sun and D. S. Salomon (2001). "Identification of Cripto-1 in human milk." Breast Cancer Res Treat **66**(1): 1-7.

Brown, C. W., D. E. Houston-Hawkins, T. K. Woodruff and M. M. Matzuk (2000). "Insertion of Inhbb into the Inhba locus rescues the Inhba-null phenotype and reveals new activin functions." Nature Genetics **25**(4): 453-457.

Bulmer, J. N., L. Morrison, M. Longfellow, A. Ritson and D. Pace (1991). "Granulated lymphocytes in human endometrium: histochemical and immunohistochemical studies." Hum Reprod **6**(6): 791-798.

Bulmer, J. N., D. Pace and A. Ritson (1988). "Immunoregulatory cells in human decidua: morphology, immunohistochemistry and function." Reprod Nutr Dev **28**(6b): 1599-1613.

Bulmer, J. N., P. J. Williams and G. E. Lash (2010). "Immune cells in the placental bed." Int J Dev Biol **54**(2-3): 281-294.

Burney, R. O. and L. C. Giudice (2012). "Pathogenesis and pathophysiology of endometriosis." Fertil Steril **98**(3): 511-519.

Cha, J. and S. K. Dey (2014). "Cadence of procreation: Orchestrating embryo-uterine interactions." Seminars in Cell & Developmental Biology **34**: 56-64.

Cha, J. Y., X. F. Sun and S. K. Dey (2012). "Mechanisms of implantation: strategies for successful pregnancy." Nature Medicine **18**(12): 1754-1767.

Chakraborty, D., M. A. Rumi, T. Konno and M. J. Soares (2011). "Natural killer cells direct hemochorial placentation by regulating hypoxia-inducible factor dependent trophoblast lineage decisions." Proc Natl Acad Sci U S A **108**(39): 16295-16300.

Chen, F., S. K. Hou, H. J. Fan and Y. F. Liu (2014). "MiR-15a-16 represses Cripto and inhibits NSCLC cell progression." Mol Cell Biochem **391**(1-2): 11-19.

Chen, Q., Y. Zhang, D. Elad, A. J. Jaffa, Y. Cao, X. Ye and E. Duan (2013). "Navigating the site for embryo implantation: biomechanical and molecular regulation of intrauterine embryo distribution." Mol Aspects Med **34**(5): 1024-1042.

Chen, X., G. C. W. Man, Y. Liu, F. Wu, J. Huang, T. C. Li and C. C. Wang (2017). "Physiological and pathological angiogenesis in endometrium at the time of embryo implantation." Am J Reprod Immunol **78**(2).

Chen, Z., J. Zhang, K. Hatta, P. D. Lima, H. Yadi, F. Colucci, A. T. Yamada and B. A. Croy (2012). "DBA-lectin reactivity defines mouse uterine natural killer cell subsets with biased gene expression." Biol Reprod **87**(4): 81.

Chu, J. H. and M. M. Shen (2010). "Functional redundancy of EGF-CFC genes in epiblast and extraembryonic patterning during early mouse embryogenesis." Developmental Biology **342**(1): 63-73.

Ciccodicola, A., R. Dono, S. Obici, A. Simeone, M. Zollo and M. G. Persico (1989). "Molecular characterization of a gene of the 'EGF family' expressed in undifferentiated human NTERA2 teratocarcinoma cells." Embo j **8**(7): 1987-1991.

Clementi, C., S. K. Tripurani, M. J. Large, M. A. Edson, C. J. Creighton, S. M. Hawkins, E. Kovanci, V. Kaartinen, J. P. Lydon, S. A. Pangas, F. J. DeMayo and M. M. Matzuk (2013). "Activin-Like Kinase 2 Functions in Peri-implantation Uterine Signaling in Mice and Humans." Plos Genetics **9**(11).

Colas, J.-F. and G. C. Schoenwolf (2000). "Subtractive hybridization identifies chick-cripto, a novel EGF–CFC ortholog expressed during gastrulation, neurulation and early cardiogenesis." Gene **255**(2): 205-217.

Cross, J. C. (2010). "Trophoblast function in normal and preeclamptic pregnancy." Fetal and Maternal Medicine Review **8**(2): 57-66.

Cross, J. C., D. Baczyk, N. Dobric, M. Hemberger, M. Hughes, D. G. Simmons, H. Yamamoto and J. C. P. Kingdom (2003). "Genes, development and evolution of the placenta." Placenta **24**(2-3): 123-130.

Cross, J. C., M. Hemberger, Y. Lu, T. Nozaki, K. Whiteley, M. Masutani and S. L. Adamson (2002). "Trophoblast functions, angiogenesis and remodeling of the maternal vasculature in the placenta." Mol Cell Endocrinol **187**(1-2): 207-212.

Cross, J. C., D. G. Simmons and E. D. Watson (2003). "Chorioallantoic morphogenesis and formation of the placental villous tree." Ann N Y Acad Sci **995**: 84-93.

Cross, J. C., Z. Werb and S. J. Fisher (1994). "IMPLANTATION AND THE PLACENTA - KEY PIECES OF THE DEVELOPMENT PUZZLE." Science **266**(5190): 1508-1518.

Croy, B. A., A. A. Ashkar, K. Minhas and J. D. Greenwood (2000). "Can murine uterine natural killer cells give insights into the pathogenesis of preeclampsia?" J Soc Gynecol Investig **7**(1): 12-20.

Croy, B. A., Z. Chen, A. P. Hofmann, E. M. Lord, A. L. Sedlacek and S. A. Gerber (2012). "Imaging of vascular development in early mouse decidua and its association with leukocytes and trophoblasts." Biol Reprod **87**(5): 125.

Croy, B. A., J. Zhang, C. Tayade, F. Colucci, H. Yadi and A. T. Yamada (2010). "Analysis of uterine natural killer cells in mice." Methods Mol Biol **612**: 465-503.

Daikoku, T., J. Cha, X. Sun, S. Tranguch, H. Xie, T. Fujita, Y. Hirota, J. Lydon, F. DeMayo, R. Maxson and S. K. Dey (2011). "Conditional deletion of Msx homeobox genes in the uterus inhibits blastocyst implantation by altering uterine receptivity." Dev Cell **21**(6): 1014-1025.

Daikoku, T., H. Song, Y. Guo, A. Riesewijk, S. Mosselman, S. K. Das and S. K. Dey (2004). "Uterine Msx-1 and Wnt4 signaling becomes aberrant in mice with the loss of leukemia inhibitory factor or Hoxa-10: evidence for a novel cytokine-homeobox-Wnt signaling in implantation." Mol Endocrinol **18**(5): 1238-1250.

Das, S. K., X. N. Wang, B. C. Paria, D. Damm, J. A. Abraham, M. Klagsbrun, G. K. Andrews and S. K. Dey (1994). "Heparin-binding EGF-like growth factor gene is induced in the mouse uterus temporally by the blastocyst solely at the site of its apposition: a possible ligand for

interaction with blastocyst EGF-receptor in implantation." Development **120**(5): 1071-1083.

de la Cruz, J. M., R. N. Bamford, R. D. Burdine, E. Roessler, A. J. Barkovich, D. Donnai, A. F. Schier and M. Muenke (2002). "A loss-of-function mutation in the CFC domain of TDGF1 is associated with human forebrain defects." Hum Genet **110**(5): 422-428.

Degaki, K. Y., Z. Chen, A. T. Yamada and B. A. Croy (2012). "Delta-like ligand (DLL)1 expression in early mouse decidua and its localization to uterine natural killer cells." PLoS One **7**(12): e52037.

Dela Cruz, C., H. L. Del Puerto, A. L. L. Rocha, I. K. Cavallo, A. D. Clarizia, F. Petraglia and F. M. Reis (2015). "Expression of Nodal, Cripto, SMAD3, Phosphorylated SMAD3, and SMAD4 in the Proliferative Endometrium of Women With Endometriosis." Reproductive Sciences **22**(5): 527-533.

Delgado, S. R., B. A. McBey, S. Yamashiro, J. Fujita, Y. Kiso and B. A. Croy (1996). "Accounting for the peripartum loss of granulated metrial gland cells, a natural killer cell population, from the pregnant mouse uterus." J Leukoc Biol **59**(2): 262-269.

Demott, R. P. and S. S. Suarez (1992). "HYPERACTIVATED SPERM PROGRESS IN THE MOUSE OVIDUCT." Biology of Reproduction **46**(5): 779-785.

Dey, S. K., H. Lim, S. K. Das, J. Reese, B. C. Paria, T. Daikoku and H. B. Wang (2004). "Molecular cues to implantation." Endocrine Reviews **25**(3): 341-373.

Ding, J. X., L. Yang, Y. T. Yan, A. Chen, N. Desai, A. Wynshaw-Boris and M. M. Shen (1998). "Cripto is required for correct orientation of the anterior-posterior axis in the mouse embryo." Nature **395**(6703): 702-707.

Dong, J. W., D. F. Albertini, K. Nishimori, T. R. Kumar, N. F. Lu and M. M. Matzuk (1996). "Growth differentiation factor-9 is required during early ovarian folliculogenesis." Nature **383**(6600): 531-535.

Dono, R., L. Scalera, F. Pacifico, D. Acampora, M. G. Persico and A. Simeone (1993). "The murine cripto gene: expression during mesoderm induction and early heart morphogenesis." Development **118**(4): 1157-1168.

Douglas, N. C., H. Y. Tang, R. Gomez, B. Pytowski, D. J. Hicklin, C. M. Sauer, J. Kitajewski, M. V. Sauer and R. C. Zimmermann (2009). "Vascular Endothelial Growth Factor Receptor 2 (VEGFR-2) Functions to Promote Uterine Decidual Angiogenesis during Early Pregnancy in the Mouse." Endocrinology **150**(8): 3845-3854.

Duarte, A., M. Hirashima, R. Benedito, A. Trindade, P. Diniz, E. Bekman, L. Costa, D. Henrique and J. Rossant (2004). "Dosage-sensitive requirement for mouse Dll4 in artery development." Genes Dev **18**(20): 2474-2478.

Edgar, B. A. and T. L. Orr-Weaver (2001). "Endoreplication cell cycles: More for less." Cell **105**(3): 297-306.

Elvin, J. A., A. T. Clark, P. Wang, N. M. Wolfman and M. M. Matzuk (1999). "Paracrine actions of growth differentiation factor-9 in the mammalian ovary." Molecular Endocrinology **13**(6): 1035-1048.

Erlebacher, A. (2013). Immunology of the Maternal-Fetal Interface. Annual Review of Immunology, Vol 31. D. R. Littman and W. M. Yokoyama. Palo Alto, Annual Reviews. **31:** 387-411.

Farah, O., S. Biechele, J. Rossant and D. Dufort (2017). "Porcupine-dependent Wnt activity within the uterine epithelium is essential for fertility." Biology of Reproduction **97**(5): 688-697.

Farah, O., S. Biechele, J. Rossant and D. Dufort (2017). "Porcupine-dependent Wnt signaling controls stromal proliferation and endometrial gland maintenance through the action of distinct WNTs." Developmental Biology **422**(1): 58-69.

Farah, O., S. Biechele, J. Rossant and D. Dufort (2018). "Regulation of porcupine-dependent Wnt signaling is essential for uterine development and function." Reproduction **155**(1): 93-102.

Fazleabas, A. T. (2007). "Physiology and pathology of implantation in the human and nonhuman primate - Preface." Seminars in Reproductive Medicine **25**(6): 405-409.

Felker, A. M., Z. Chen, W. G. Foster and B. A. Croy (2013). "Receptors for non-MHC ligands contribute to uterine natural killer cell activation during pregnancy in mice." Placenta **34**(9): 757-764.

Fest, S., P. B. Aldo, V. M. Abrahams, I. Visintin, A. Alvero, R. Chen, S. L. Chavez, R. Romero and G. Mor (2007). "Trophoblast-macrophage interactions: a regulatory network for the protection of pregnancy." Am J Reprod Immunol **57**(1): 55-66.

Fischer, A., N. Schumacher, M. Maier, M. Sendtner and M. Gessler (2004). "The Notch target genes Hey1 and Hey2 are required for embryonic vascular development." Genes Dev **18**(8): 901-911.

Fisher, S. J. (2004). "The placental problem: linking abnormal cytotrophoblast differentiation to the maternal symptoms of preeclampsia." Reprod Biol Endocrinol **2**: 53.

Fortune, J. E. (1994). "OVARIAN FOLLICULAR-GROWTH AND DEVELOPMENT IN MAMMALS." Biology of Reproduction **50**(2): 225-232.

Fox, D. T. and R. J. Duronio (2013). "Endoreplication and polyploidy: insights into development and disease." Development **140**(1): 3-12.

Franco, H. L., D. Dai, K. Y. Lee, C. A. Rubel, D. Roop, D. Boerboom, J. W. Jeong, J. P. Lydon, I. C. Bagchi, M. K. Bagchi and F. J. DeMayo (2011). "WNT4 is a key regulator of normal postnatal uterine development and progesterone signaling during embryo implantation and decidualization in the mouse." Faseb Journal **25**(4): 1176-1187.

Garcia-Pascual, C. M., H. Ferrero, R. C. Zimmermann, C. Simon, A. Pellicer and R. Gomez (2014). "Inhibition of Delta-like 4 mediated signaling induces abortion in mice due to deregulation of decidual angiogenesis." Placenta **35**(7): 501-508.

Gasperowicz, M., C. Surmann-Schmitt, Y. Hamada, F. Otto and J. C. Cross (2013). "The transcriptional co-repressor TLE3 regulates development of trophoblast giant cells lining maternal blood spaces in the mouse placenta." Dev Biol **382**(1): 1-14.

Gray, P. C. and W. Vale (2012). "Cripto/GRP78 modulation of the TGF-beta pathway in development and oncogenesis." FEBS Lett **586**(14): 1836-1845.

Greenwood, J. D., K. Minhas, J. P. di Santo, M. Makita, Y. Kiso and B. A. Croy (2000). "Ultrastructural studies of implantation sites from mice deficient in uterine natural killer cells." Placenta **21**(7): 693-702.

Hamada, S., K. Watanabe, M. Hirota, C. Bianco, L. Strizzi, M. Mancino, M. Gonzales and D. S. Salomon (2007). "beta-Catenin/TCF/LEF regulate expression of the short form human Cripto-1." Biochem Biophys Res Commun **355**(1): 240-244.

Hanna, J., O. Wald, D. Goldman-Wohl, D. Prus, G. Markel, R. Gazit, G. Katz, R. Haimov-Kochman, N. Fujii, S. Yagel, A. Peled and O. Mandelboim (2003). "CXCL12 expression by invasive trophoblasts induces the specific migration of CD16- human natural killer cells." Blood **102**(5): 1569-1577.

Harrington, L. S., R. C. A. Sainson, C. K. Williams, J. M. Taylor, W. Shi, J. L. Li and A. L. Harris (2008). "Regulation of multiple angiogenic pathways by D114 and Notch in human umbilical vein endothelial cells." Microvascular Research **75**(2): 144-154.

Harris, L. K. (2010). "Review: Trophoblast-vascular cell interactions in early pregnancy: how to remodel a vessel." Placenta **31 Suppl**: S93-98.

Hazan, A. D., S. D. Smith, R. L. Jones, W. Whittle, S. J. Lye and C. E. Dunk (2010). "Vascular-leukocyte interactions: mechanisms of human decidual spiral artery remodeling in vitro." Am J Pathol **177**(2): 1017-1030.

Heba, T., C. Park and D. Dufort (2015). "DECIPHERING THE ROLE OF THE NODAL SIGNALING PATHWAY IN PRETERM BIRTH." Placenta **36**(9): A59-A59.

Hellstrom, M., L. K. Phng, J. J. Hofmann, E. Wallgard, L. Coultas, P. Lindblom, J. Alva, A. K. Nilsson, L. Karlsson, N. Gaiano, K. Yoon, J. Rossant, M. L. Iruela-Arispe, M. Kalen, H. Gerhardt and C. Betsholtz (2007). "Dll4 signalling through Notch1 regulates formation of tip cells during angiogenesis." Nature **445**(7129): 776-780.

Henderson, T. A., P. T. Saunders, A. Moffett-King, N. P. Groome and H. O. Critchley (2003). "Steroid receptor expression in uterine natural killer cells." J Clin Endocrinol Metab **88**(1): 440-449.

Hentschke, M., I. Kurth, U. Borgmeyer and C. A. Hubner (2006). "Germ cell nuclear factor is a repressor of CRIPTO-1 and CRIPTO-3." J Biol Chem **281**(44): 33497-33504.

Hess, A. P., N. R. Nayak and L. C. Giudice (2006). Oviduct and Endometrium: Cyclic Changes in the Primate Oviduct and Endometrium.

Hirota, M., K. Watanabe, S. Hamada, Y. Sun, L. Strizzi, M. Mancino, T. Nagaoka, M. Gonzales, M. Seno, C. Bianco and D. S. Salomon (2008). "Smad2 functions as a co-activator of canonical Wnt/beta-catenin signaling pathway independent of Smad4 through histone acetyltransferase activity of p300." Cell Signal **20**(9): 1632-1641.

Hoshida, M. S., R. Gorjao, C. Lima, S. Daher, R. Curi and E. Bevilacqua (2007). "Regulation of gene expression in mouse trophoblast cells by interferon-gamma." Placenta **28**(10): 1059-1072.

Hough, S. R., A. L. Laslett, S. B. Grimmond, G. Kolle and M. F. Pera (2009). "A continuum of cell states spans pluripotency and lineage commitment in human embryonic stem cells." PLoS One **4**(11): e7708.

Hu, D. and J. C. Cross (2010). "Development and function of trophoblast giant cells in the rodent placenta." International Journal of Developmental Biology **54**(2-3): 341-354.

Hu, D. and J. C. Cross (2011). "Ablation of Tpbpa-positive trophoblast precursors leads to defects in maternal spiral artery remodeling in the mouse placenta." Dev Biol **358**(1): 231-239.

Huet-Hudson, Y. M., G. K. Andrews and S. K. Dey (1989). "Cell type-specific localization of c-myc protein in the mouse uterus: modulation by steroid hormones and analysis of the periimplantation period." Endocrinology **125**(3): 1683-1690.

Jiang, L. L., X. Y. Wu, J. Y. Yan, R. X. Chen, Q. Han and Q. J. Zhang (2019). "Expression of Cripto-1 in the placenta and its role in placenta accreta and placenta previa." Ginekologia Polska **90**(2): 86-92.

Jin, J. Z. and J. X. Ding (2013). "Cripto is required for mesoderm and endoderm cell allocation during mouse gastrulation." Developmental Biology **381**(1): 170-178.

Jorgez, C. J., M. Klysik, S. P. Jamin, R. R. Behringer and M. M. Matzuk (2004). "Granulosa cell-specific inactivation of follistatin causes female fertility defects." Molecular Endocrinology **18**(4): 953-967.

Kelber, J. A., A. D. Panopoulos, G. Shani, E. C. Booker, J. C. Belmonte, W. W. Vale and P. C. Gray (2009). "Blockade of Cripto binding to cell surface GRP78 inhibits oncogenic Cripto signaling via MAPK/PI3K and Smad2/3 pathways." Oncogene **28**(24): 2324-2336.

Kenney, N. J., R.-P. Huang, G. R. Johnson, J.-X. Wu, D. Okamura, W. Matheny, E. Kordon, W. J. Gullick, G. Plowman, G. H. Smith, D. S. Salomon and E. D. Adamson (1995). "Detection and location of amphiregulin and Cripto-1 expression in the developing postnatal mouse mammary gland." Molecular Reproduction and Development **41**(3): 277-286.

Kim, H., L. Huang, P. J. Critser, Z. Y. Yang, R. J. Chan, L. Wang, N. Carlesso, S. L. Voytik-Harbin, I. D. Bernstein and M. C. Yoder (2015). "Notch ligand Delta-like 1 promotes in vivo

vasculogenesis in human cord blood-derived endothelial colony forming cells." Cytotherapy **17**(5): 579-592.

Kim, M., H. J. Park, J. W. Seol, J. Y. Jang, Y. S. Cho, K. R. Kim, Y. Choi, J. P. Lydon, F. J. DeMayo, M. Shibuya, N. Ferrara, H. K. Sung, A. Nagy, K. Alitalo and G. Y. Koh (2013). "VEGF-A regulated by progesterone governs uterine angiogenesis and vascular remodelling during pregnancy." Embo Molecular Medicine **5**(9): 1415-1430.

Kingdom, J. C. and P. Kaufmann (1997). "Oxygen and placental villous development: origins of fetal hypoxia." Placenta **18**(8): 613-621; discussion 623-616.

Kinoshita, N., J. Minshull and M. W. Kirschner (1995). "The identification of two novel ligands of the fgf receptor by a yeast screening method and their activity in xenopus development." Cell **83**(4): 621-630.

Klauzinska, M., N. P. Castro, M. C. Rangel, B. T. Spike, P. C. Gray, D. Bertolette, F. Cuttitta and D. Salomon (2014). "The multifaceted role of the embryonic gene Cripto-1 in cancer, stem cells and epithelial-mesenchymal transition." Seminars in Cancer Biology **29**: 51-58.

Kopcow, H. D., D. S. Allan, X. Chen, B. Rybalov, M. M. Andzelm, B. Ge and J. L. Strominger (2005). "Human decidual NK cells form immature activating synapses and are not cytotoxic." Proc Natl Acad Sci U S A **102**(43): 15563-15568.

Krebs, C., L. M. Macara, R. Leiser, A. W. Bowman, I. A. Greer and J. C. Kingdom (1996). "Intrauterine growth restriction with absent end-diastolic flow velocity in the umbilical artery is associated with maldevelopment of the placental terminal villous tree." Am J Obstet Gynecol **175**(6): 1534-1542.

Krebs, L. T., N. Iwai, S. Nonaka, I. C. Welsh, Y. Lan, R. Jiang, Y. Saijoh, T. P. O'Brien, H. Hamada and T. Gridley (2003). "Notch signaling regulates left-right asymmetry determination by inducing Nodal expression." Genes Dev **17**(10): 1207-1212.

Krebs, L. T., J. R. Shutter, K. Tanigaki, T. Honjo, K. L. Stark and T. Gridley (2004). "Haploinsufficient lethality and formation of arteriovenous malformations in Notch pathway mutants." Genes Dev **18**(20): 2469-2473.

Krebs, L. T., Y. Xue, C. R. Norton, J. R. Shutter, M. Maguire, J. P. Sundberg, D. Gallahan, V. Closson, J. Kitajewski, R. Callahan, G. H. Smith, K. L. Stark and T. Gridley (2000). "Notch signaling is essential for vascular morphogenesis in mice." Genes Dev **14**(11): 1343-1352.

Kumar, N. M. and N. B. Gilula (1996). "The gap junction communication channel." Cell **84**(3): 381-388.

Lash, G. E., B. Schiessl, M. Kirkley, B. A. Innes, A. Cooper, R. F. Searle, S. C. Robson and J. N. Bulmer (2006). "Expression of angiogenic growth factors by uterine natural killer cells during early pregnancy." J Leukoc Biol **80**(3): 572-580.

Laws, M. J., R. N. Taylor, N. Sidell, F. J. DeMayo, J. P. Lydon, D. E. Gutstein, M. K. Bagchi and I. C. Bagchi (2008). "Gap junction communication between uterine stromal cells plays a critical

role in pregnancy-associated neovascularization and embryo survival." Development **135**(15): 2659-2668.

Lee, K. Y., J. W. Jeong, J. R. Wang, L. J. Ma, J. F. Martin, S. Y. Tsai, J. P. Lydon and F. J. DeMayo (2007). "Bmp2 is critical for the murine uterine decidual response." Molecular and Cellular Biology **27**(15): 5468-5478.

Lei, T., H. P. Hohn, R. Behr and H. W. Denker (2007). "Influences of extracellular matrix and of conditioned media on differentiation and invasiveness of trophoblast stem cells." Placenta **28**(1): 14-21.

Levine, A. J. and A. H. Brivanlou (2006). "GDF3 at the crossroads of TGF-beta signaling." Cell Cycle **5**(10): 1069-1073.

Li, Q. X., A. Kannan, W. Wang, F. J. DeMayo, R. N. Taylor, M. K. Bagchi and I. C. Bagchi (2007). "Bone morphogenetic protein 2 functions via a conserved signaling pathway involving Wnt4 to regulate uterine decidualization in the mouse and the human." Journal of Biological Chemistry **282**(43): 31725-31732.

Li, Y. and R. R. Behringer (1998). "Esx1 is an X-chromosome-imprinted regulator of placental development and fetal growth." Nat Genet **20**(3): 309-311.

Lim, H., R. A. Gupta, W. G. Ma, B. C. Paria, D. E. Moller, J. D. Morrow, R. N. DuBois, J. M. Trzaskos and S. K. Dey (1999). "Cyclo-oxygenase-2-derived prostacyclin mediates embryo implantation in the mouse via PPARdelta." Genes & development **13**(12): 1561-1574.

Lim, H., B. C. Paria, S. K. Das, J. E. Dinchuk, R. Langenbach, J. M. Trzaskos and S. K. Dey (1997). "Multiple female reproductive failures in cyclooxygenase 2-deficient mice." Cell **91**(2): 197-208.

Lim, H. J. and H. B. Wang (2010). "Uterine disorders and pregnancy complications: insights from mouse models." Journal of Clinical Investigation **120**(4): 1004-1015.

Lima, P. D., B. A. Croy, K. Y. Degaki, C. Tayade and A. T. Yamada (2012). "Heterogeneity in composition of mouse uterine natural killer cell granules." J Leukoc Biol **92**(1): 195-204.

Lin, H., T. R. Mosmann, L. Guilbert, S. Tuntipopipat and T. G. Wegmann (1993). "Synthesis of T helper 2-type cytokines at the maternal-fetal interface." J Immunol **151**(9): 4562-4573.

Lobov, I. B., R. A. Renard, N. Papadopoulos, N. W. Gale, G. Thurston, G. D. Yancopoulos and S. J. Wiegand (2007). "Delta-like ligand 4 (DII4) is induced by VEGF as a negative regulator of angiogenic sprouting." Proceedings of the National Academy of Sciences of the United States of America **104**(9): 3219-3224.

Loh, Y. H., Q. Wu, J. L. Chew, V. B. Vega, W. W. Zhang, X. Chen, G. Bourque, J. George, B. Leong, J. Liu, K. Y. Wong, K. W. Sung, C. W. H. Lee, X. D. Zhao, K. P. Chiu, L. Lipovich, V. A. Kuznetsov, P. Robson, L. W. Stanton, C. L. Wei, Y. J. Ruan, B. Lim and H. H. Ng (2006). "The Oct4 and Nanog transcription network regulates pluripotency in mouse embryonic stem cells." Nature Genetics **38**(4): 431-440.

MacAuley, A., J. C. Cross and Z. Werb (1998). "Reprogramming the cell cycle for endoreduplication in rodent trophoblast cells." Mol Biol Cell **9**(4): 795-807.

Mancino, M., L. Strizzi, C. Wechselberger, K. Watanabe, M. Gonzales, S. Hamada, N. Normanno, D. S. Salomon and C. Bianco (2008). "Regulation of human Cripto-1 gene expression by TGF-beta1 and BMP-4 in embryonal and colon cancer cells." J Cell Physiol **215**(1): 192-203.

Maruyama, T. and Y. Yoshimura (2008). "Molecular and Cellular Mechanisms for Differentiation and Regeneration of the Uterine Endometrium." Endocrine Journal **55**(5): 795-810.

Matsumoto, H., W. G. Ma, T. Daikoku, X. M. Zhao, B. C. Paria, S. K. Das, J. M. Trzaskos and S. K. Dey (2002). "Cyclooxygenase-2 differentially directs uterine angiogenesis during implantation in mice." Journal of Biological Chemistry **277**(32): 29260-29267.

Matzuk, M. M., T. R. Kumar and A. Bradley (1995). "DIFFERENT PHENOTYPES FOR MICE DEFICIENT IN EITHER ACTIVINS OR ACTIVIN RECEPTOR-TYPE-II." Nature **374**(6520): 356-360.

Maynard, S., F. H. Epstein and S. A. Karumanchi (2008). "Preeclampsia and angiogenic imbalance." Annual Review of Medicine **59**: 61-78.

Meno, C., Y. Ito, Y. Saijoh, Y. Matsuda, K. Tashiro, S. Kuhara and H. Hamada (1997). "Two closely-related left-right asymmetrically expressed genes, lefty-1 and lefty-2: their distinct expression domains, chromosomal linkage and direct neuralizing activity in Xenopus embryos." Genes Cells **2**(8): 513-524.

Miharada, K., G. Karlsson, M. Rehn, E. Rorby, K. Siva, J. Cammenga and S. Karlsson (2011). "Cripto regulates hematopoietic stem cells as a hypoxic-niche-related factor through cell surface receptor GRP78." Cell Stem Cell **9**(4): 330-344.

Minchiotti, G., G. Manco, S. Parisi, C. T. Lago, F. Rosa and M. G. Persico (2001). "Structure-function analysis of the EGF-CFC family member Cripto identifies residues essential for nodal signalling." Development **128**(22): 4501-4510.

Minchiotti, G., S. Parisi, G. Liguori, M. Signore, G. Lania, E. D. Adamson, C. T. Lago and M. G. Persico (2000). "Membrane-anchorage of Cripto protein by glycosylphosphatidylinositol and its distribution during early mouse development." Mech Dev **90**(2): 133-142.

Morkel, M., J. Huelsken, M. Wakamiya, J. Ding, M. van de Wetering, H. Clevers, M. M. Taketo, R. R. Behringer, M. M. Shen and W. Birchmeier (2003). "Beta-catenin regulates Cripto- and Wnt3-dependent gene expression programs in mouse axis and mesoderm formation." Development **130**(25): 6283-6294.

Nagaoka, T., H. Karasawa, N. P. Castro, M. C. Rangel, D. S. Salomon and C. Bianco (2012). "An evolving web of signaling networks regulated by Cripto-1." Growth Factors **30**(1): 13-21.

Nagaoka, T., H. Karasawa, T. Turbyville, M. C. Rangel, N. P. Castro, M. Gonzales, A. Baker, M. Seno, S. Lockett, Y. E. Greer, J. S. Rubin, D. S. Salomon and C. Bianco (2013). "Cripto-1 enhances the canonical Wnt/beta-catenin signaling pathway by binding to LRP5 and LRP6 co-receptors." Cellular Signalling **25**(1): 178-189.

Nagashima, T., Q. L. Li, C. Clementi, J. P. Lydon, F. J. DeMayo and M. M. Matzuk (2013). "BMPR2 is required for postimplantation uterine function and pregnancy maintenance." Journal of Clinical Investigation **123**(6): 2539-2550.

Naruse, K., G. E. Lash, J. N. Bulmer, B. A. Innes, H. A. Otun, R. F. Searle and S. C. Robson (2009). "The urokinase plasminogen activator (uPA) system in uterine natural killer cells in the placental bed during early pregnancy." Placenta **30**(5): 398-404.

Ni, N. and Q. L. Li (2017). "TGF beta superfamily signaling and uterine decidualization." Reproductive Biology and Endocrinology **15**.

Nusse, R., C. Fuerer, W. Ching, K. Harnish, C. Logan, A. Zeng, D. ten Berge and Y. Kalani (2008). "Wnt signaling and stem cell control." Cold Spring Harb Symp Quant Biol **73**: 59-66.

Paffaro, V. A., Jr., M. C. Bizinotto, P. P. Joazeiro and A. T. Yamada (2003). "Subset classification of mouse uterine natural killer cells by DBA lectin reactivity." Placenta **24**(5): 479-488.

Papageorgiou, I., P. K. Nicholls, F. Wang, M. Lackmann, Y. Makanji, L. A. Salamonsen, D. M. Robertson and C. A. Harrison (2009). "Expression of nodal signalling components in cycling human endometrium and in endometrial cancer." Reproductive Biology and Endocrinology **7**.

Pardi, G., A. M. Marconi and I. Cetin (2002). "Placental-fetal interrelationship in IUGR fetuses--a review." Placenta **23 Suppl A**: S136-141.

Paria, B. C., Y. M. Huet-Hudson and S. K. Dey (1993). "Blastocyst's state of activity determines the "window" of implantation in the receptive mouse uterus." Proc Natl Acad Sci U S A **90**(21): 10159-10162.

Paria, B. C., Y. M. Huethudson and S. K. Dey (1993). "BLASTOCYSTS STATE OF ACTIVITY DETERMINES THE WINDOW OF IMPLANTATION IN THE RECEPTIVE MOUSE UTERUS." Proceedings of the National Academy of Sciences of the United States of America **90**(21): 10159-10162.

Paria, B. C., W. Ma, J. Tan, S. Raja, S. K. Das, S. K. Dey and B. L. Hogan (2001). "Cellular and molecular responses of the uterus to embryo implantation can be elicited by locally applied growth factors." Proc Natl Acad Sci U S A **98**(3): 1047-1052.

Paria, B. C., J. Reese, S. K. Das and S. K. Dey (2002). "Deciphering the cross-talk of implantation: Advances and challenges." Science **296**(5576): 2185-2188.

Park, C. B., F. J. DeMayo, J. P. Lydon and D. Dufort (2012). "NODAL in the Uterus Is Necessary for Proper Placental Development and Maintenance of Pregnancy." Biology of Reproduction **86**(6).

Park, C. B. and D. Dufort (2011). "Nodal Expression in the Uterus of the Mouse Is Regulated by the Embryo and Correlates with Implantation." Biology of Reproduction **84**(6): 1103-1110.

Park, C. B. and D. Dufort (2013). "NODAL signaling components regulate essential events in the establishment of pregnancy." Reproduction **145**(2): R55-R64.

Peel, S. (1989). "Granulated metrial gland cells." Adv Anat Embryol Cell Biol **115**: 1-112.

Peng, J., P. T. Fullerton, D. Monsivais, C. Clementi, G. H. Su and M. M. Matzuk (2015). "Uterine Activin-Like Kinase 4 Regulates Trophoblast Development During Mouse Placentation." Molecular Endocrinology **29**(12): 1684-1693.

Peng, J., D. Monsivais, R. You, H. Zhong, S. A. Pangas and M. M. Matzuk (2015). "Uterine activin receptor-like kinase 5 is crucial for blastocyst implantation and placental development." Proceedings of the National Academy of Sciences of the United States of America **112**(36): E5098-E5107.

Plaisier, M. (2011). "Decidualisation and angiogenesis." Best Practice & Research Clinical Obstetrics & Gynaecology **25**(3): 259-271.

Postovit, L. M., E. A. Seftor, R. E. Seftor and M. J. Hendrix (2007). "Targeting Nodal in malignant melanoma cells." Expert Opin Ther Targets **11**(4): 497-505.

Psychoyos, A. (1973). "Hormonal control of ovoimplantation." Vitam Horm **31**: 201-256.

Qiu, X., L. Zhu and J. W. Pollard (2009). "Colony-stimulating factor-1-dependent macrophage functions regulate the maternal decidua immune responses against Listeria monocytogenes infections during early gestation in mice." Infect Immun **77**(1): 85-97.

Rabbani, M. L. M. and P. A. W. Rogers (2001). "Role of vascular endothelial growth factor in endometrial vascular events before implantation in rats." Reproduction **122**(1): 85-90.

Rai, A. and J. C. Cross (2014). "Development of the hemochorial maternal vascular spaces in the placenta through endothelial and vasculogenic mimicry." Developmental Biology **387**(2): 131-141.

Ramathal, C. Y., I. C. Bagchi, R. N. Taylor and M. K. Bagchi (2010). "Endometrial Decidualization: Of Mice and Men." Seminars in Reproductive Medicine **28**(1): 17-26.

Raya, A., Y. Kawakami, C. Rodriguez-Esteban, D. Buscher, C. M. Koth, T. Itoh, M. Morita, R. M. Raya, I. Dubova, J. G. Bessa, J. L. de la Pompa and J. C. Izpisua Belmonte (2003). "Notch activity induces Nodal expression and mediates the establishment of left-right asymmetry in vertebrate embryos." Genes Dev **17**(10): 1213-1218.

Rendi, M. H., A. Muehlenbachs, R. L. Garcia and K. L. Boyd (2011). FEMALE REPRODUCTIVE SYSTEM. San Diego, Elsevier Academic Press Inc.

Reya, T. and H. Clevers (2005). "Wnt signalling in stem cells and cancer." Nature **434**(7035): 843-850.

Rimon-Dahari, N., L. Yerushalmi-Heinemann, L. Alyagor and N. Dekel (2016). Ovarian Folliculogenesis. Molecular Mechanisms of Cell Differentiation in Gonad Development. R. P. Piprek. **58:** 167-190.

Robboy, S. J., T. Kurita, L. Baskin and G. R. Cunha (2017). "New insights into human female reproductive tract development." Differentiation **97**: 9-22.

Robson, A., L. K. Harris, B. A. Innes, G. E. Lash, M. M. Aljunaidy, J. D. Aplin, P. N. Baker, S. C. Robson and J. N. Bulmer (2012). "Uterine natural killer cells initiate spiral artery remodeling in human pregnancy." Faseb j **26**(12): 4876-4885.

Rocha, A. L. L., P. Carrarelli, R. Novembri, L. Sabbioni, S. Luisi, F. M. Reis and F. Petraglia (2011). "Altered expression of activin, cripto, and follistatin in the endometrium of women with endometrioma." Fertility and Sterility **95**(7): 2241-2246.

Rockwell, L. C., S. Pillai, C. E. Olson and R. D. Koos (2002). "Inhibition of vascular endothelial growth factor/vascular permeability factor action blocks estrogen-induced uterine edema and implantation in rodents." Biology of Reproduction **67**(6): 1804-1810.

Rodriguez-Esteban, C., J. Capdevila, Y. Kawakami and J. C. Izpisua Belmonte (2001). "Wnt signaling and PKA control Nodal expression and left-right determination in the chick embryo." Development **128**(16): 3189-3195.

Rodriguez, A., S. K. Tripurani, J. C. Burton, C. Clementi, I. Larina and S. A. Pangas (2016). "SMAD Signaling Is Required for Structural Integrity of the Female Reproductive Tract and Uterine Function During Early Pregnancy in Mice." Biology of Reproduction **95**(2).

Rossant, J. and J. C. Cross (2001). "Placental development: Lessons from mouse mutants." Nature Reviews Genetics **2**(7): 538-548.

Rossant, J. and P. P. Tam (2004). "Emerging asymmetry and embryonic patterning in early mouse development." Dev Cell **7**(2): 155-164.

Sachs, L. and M. C. Shelesnyak (1955). "THE DEVELOPMENT AND SUPPRESSION OF POLYPLOIDY IN THE DEVELOPING AND SUPPRESSED DECIDUOMA IN THE RAT." Journal of Endocrinology **12**(2): 146-&.

Saloman, D. S., C. Bianco, A. D. Ebert, N. I. Khan, M. De Santis, N. Normanno, C. Wechselberger, M. Seno, K. Williams, M. Sanicola, S. Foley, W. J. Gullick and G. Persico (2000). "The EGF-CFC family: novel epidermal growth factor-related proteins in development and cancer." Endocr Relat Cancer **7**(4): 199-226.

Schier, A. F. (2009). "Nodal Morphogens." Cold Spring Harbor Perspectives in Biology **1**(5).

Schiffer, S. G., S. Foley, A. Kaffashan, X. Hronowski, A. E. Zichittella, C. Y. Yeo, K. Miatkowski, H. B. Adkins, B. Damon, M. Whitman, D. Salomon, M. Sanicola and K. P. Williams (2001). "Fucosylation of Cripto is required for its ability to facilitate nodal signaling." J Biol Chem **276**(41): 37769-37778.

Sengupta, J., P. G. L. Lalitkumar, A. R. Najwa, D. S. Charnock-Jones, A. L. Evans, A. M. Sharkey, S. K. Smith and D. Ghosh (2007). "Immunoneutralization of vascular endothelial growth factor inhibits pregnancy establishment in the rhesus monkey (Macaca mulatta)." Reproduction **133**(6): 1199-1211.

Shani, G., W. H. Fischer, N. J. Justice, J. A. Kelber, W. Vale and P. C. Gray (2008). "GRP78 and Cripto form a complex at the cell surface and collaborate to inhibit transforming growth factor beta signaling and enhance cell growth." Mol Cell Biol **28**(2): 666-677.

Shawber, C. J., Y. Funahashi, E. Francisco, M. Vorontchikhina, Y. Kitamura, S. A. Stowell, V. Borisenko, N. Feirt, S. Podgrabinska, K. Shiraishi, K. Chawengsaksophak, J. Rossant, D. Accili, M. Skobe and J. Kitajewski (2007). "Notch alters VEGF responsiveness in human and

murine endothelial cells by direct regulation of VEGFR-3 expression." Journal of Clinical Investigation **117**(11): 3369-3382.

Shawber, C. J., L. Lin, M. Gnarra, M. V. Sauer, V. E. Papaioannou, J. K. Kitajewski and N. C. Douglas (2015). "Vascular Notch proteins and Notch signaling in the peri-implantation mouse uterus." Vascular Cell **7**: 17.

Shen, M. M. and A. F. Schier (2000). "The EGF-CFC gene family in vertebrate development." Trends in Genetics **16**(7): 303-309.

Shen, M. M., H. Wang and P. Leder (1997). "A differential display strategy identifies Cryptic, a novel EGF-related gene expressed in the axial and lateral mesoderm during mouse gastrulation." Development **124**(2): 429-442.

Shuya, L. L., E. M. Menkhorst, J. Yap, P. Li, N. Lane and E. Dimitriadis (2011). "Leukemia inhibitory factor enhances endometrial stromal cell decidualization in humans and mice." PLoS One **6**(9): e25288.

Simmons, D. G., A. L. Fortier and J. C. Cross (2007). "Diverse subtypes and developmental origins of trophoblast giant cells in the mouse placenta." Dev Biol **304**(2): 567-578.

Smith, L. J. (1980). "Embryonic axis orientation in the mouse and its correlation with blastocyst relationships to the uterus. Part 1. Relationships between 82 hours and 4 1/4 days." J Embryol Exp Morphol **55**: 257-277.

Smith, L. J. (1985). "Embryonic axis orientation in the mouse and its correlation with blastocyst relationships to the uterus. II. Relationships from 4 1/4 to 9 1/2 days." J Embryol Exp Morphol **89**: 15-35.

Sonderegger, S., J. Pollheimer and M. Knöfler (2010). "Wnt Signalling in Implantation, Decidualisation and Placental Differentiation - Review." Placenta **31**: 839-847.

Song, H., H. Lim, B. C. Paria, H. Matsumoto, L. L. Swift, J. Morrow, J. V. Bonventre and S. K. Dey (2002). "Cytosolic phospholipase A2alpha is crucial [correction of A2alpha deficiency is crucial] for 'on-time' embryo implantation that directs subsequent development." Development **129**(12): 2879-2889.

Spike, B. T., J. A. Kelber, E. Booker, M. Kalathur, R. Rodewald, J. Lipianskaya, J. La, M. He, T. Wright, R. Klemke, G. M. Wahl and P. C. Gray (2014). "CRIPTO/GRP78 signaling maintains fetal and adult mammary stem cells ex vivo." Stem Cell Reports **2**(4): 427-439.

Strizzi, L., C. Bianco, N. Normanno and D. Salomon (2005). "Cripto-1: A multifunctional modulator during embryogenesis and oncogenesis." Oncogene **24**(37): 5731-5741.

Svensson, J., M. C. Jenmalm, A. Matussek, R. Geffers, G. Berg and J. Ernerudh (2011). "Macrophages at the fetal-maternal interface express markers of alternative activation and are induced by M-CSF and IL-10." J Immunol **187**(7): 3671-3682.

Tabibzadeh, S. and A. Hemmati-Brivanlou (2006). "Lefty at the crossroads of "stemness" and differentiative events." Stem Cells **24**(9): 1998-2006.

Tan, J., S. Raja, M. K. Davis, O. Tawfik, S. K. Dey and S. K. Das (2002). "Evidence for coordinated interaction of cyclin D3 with p21 and cdk6 in directing the development of uterine stromal cell decidualization and polyploidy during implantation." Mechanisms of Development **111**(1-2): 99-113.

Tao, Q., C. Yokota, H. Puck, M. Kofron, B. Birsoy, D. Yan, M. Asashima, C. C. Wylie, X. Lin and J. Heasman (2005). "Maternal wnt11 activates the canonical wnt signaling pathway required for axis formation in Xenopus embryos." Cell **120**(6): 857-871.

Thaxton, J. E. and S. Sharma (2010). "Interleukin-10: a multi-faceted agent of pregnancy." Am J Reprod Immunol **63**(6): 482-491.

Tian, M. and W. P. Schiemann (2009). "The TGF-beta paradox in human cancer: an update." Future Oncol **5**(2): 259-271.

Torres, P. B., P. Florio, L. Galleri, F. M. Reis, L. E. Borges and F. Petraglia (2009). "Activin A, Activin Receptor Type II, Nodal, and Cripto mRNA Are Expressed by Eutopic and Ectopic Endometrium in Women With Ovarian Endometriosis." Reproductive Sciences **16**(8): 727-733.

Torry, D. S., J. Leavenworth, M. Chang, V. Maheshwari, K. Groesch, E. R. Ball and R. J. Torry (2007). "Angiogenesis in implantation." Journal of assisted reproduction and genetics **24**(7): 303-315.

Tranguch, S., J. Cheung-Flynn, T. Daikoku, V. Prapapanich, M. B. Cox, H. Xie, H. Wang, S. K. Das, D. F. Smith and S. K. Dey (2005). "Cochaperone immunophilin FKBP52 is critical to uterine receptivity for embryo implantation." Proc Natl Acad Sci U S A **102**(40): 14326-14331.

Tranguch, S., D. F. Smith and S. K. Dey (2006). "Progesterone receptor requires a co-chaperone for signalling in uterine biology and implantation." Reprod Biomed Online **13**(5): 651-660.

Trundley, A. and A. Moffett (2004). "Human uterine leukocytes and pregnancy." Tissue Antigens **63**(1): 1-12.

Vacca, P., M. C. Mingari and L. Moretta (2013). "Natural killer cells in human pregnancy." J Reprod Immunol **97**(1): 14-19.

van den Heuvel, M. J., S. Chantakru, X. Xuemei, S. S. Evans, F. Tekpetey, P. A. Mote, C. L. Clarke and B. A. Croy (2005). "Trafficking of circulating pro-NK cells to the decidualizing uterus: regulatory mechanisms in the mouse and human." Immunol Invest **34**(3): 273-293.

Vercellini, P., P. Vigano, E. Somigliana and L. Fedele (2014). "Endometriosis: pathogenesis and treatment." Nat Rev Endocrinol **10**(5): 261-275.

Wang, B., J. Yan, Z. Peng, J. Wang, S. Liu, X. Xie and X. Ma (2011). "Teratocarcinoma-derived growth factor 1 (TDGF1) sequence variants in patients with congenital heart defect." Int J Cardiol **146**(2): 225-227.

Wang, H. B. and S. K. Dey (2006). "Roadmap to embryo implantation: clues from mouse models." Nature Reviews Genetics **7**(3): 185-199.

Wang, Z., Y. Li, S. Banerjee and F. H. Sarkar (2009). "Emerging role of Notch in stem cells and cancer." Cancer Lett **279**(1): 8-12.

Watanabe, K., S. Hamada, C. Bianco, M. Mancino, T. Nagaoka, M. Gonzales, V. Bailly, L. Strizzi and D. S. Salomon (2007). "Requirement of glycosylphosphatidylinositol anchor of Cripto-1 for trans activity as a Nodal co-receptor." J Biol Chem **282**(49): 35772-35786.

Watanabe, K., M. J. Meyer, L. Strizzi, J. M. Lee, M. Gonzales, C. Bianco, T. Nagaoka, S. S. Farid, N. Margaryan, M. J. C. Hendrix, B. K. Vonderhaar and D. S. Salomon (2010). "Cripto-1 Is a Cell Surface Marker for a Tumorigenic, Undifferentiated Subpopulation in Human Embryonal Carcinoma Cells." Stem Cells **28**(8): 1303-1314.

Watanabe, K., T. Nagaoka, J. M. Lee, C. Bianco, M. Gonzales, N. P. Castro, M. C. Rangel, K. Sakamoto, Y. Sun, R. Callahan and D. S. Salomon (2009). "Enhancement of Notch receptor maturation and signaling sensitivity by Cripto-1." J Cell Biol **187**(3): 343-353.

Watson, E. D. and J. C. Cross (2005). "Development of structures and transport functions in the mouse placenta." Physiology **20**: 180-193.

Whiteside, E. J., M. M. Jackson, A. C. Herington, D. R. Edwards and M. B. Harvey (2001). "Matrix metalloproteinase-9 and tissue inhibitor of metalloproteinase-3 are key regulators of extracellular matrix degradation by mouse embryos." Biol Reprod **64**(5): 1331-1337.

Whitley, G. S. and J. E. Cartwright (2009). "Trophoblast-mediated spiral artery remodelling: a role for apoptosis." J Anat **215**(1): 21-26.

Wimsatt, W. A. (1975). "Some comparative aspects of implantation." Biol Reprod **12**(1): 1-40.

Wu, M. Y. and C. S. Hill (2009). "Tgf-beta superfamily signaling in embryonic development and homeostasis." Dev Cell **16**(3): 329-343.

Wu, X., L. P. Jin, M. M. Yuan, Y. Zhu, M. Y. Wang and D. J. Li (2005). "Human first-trimester trophoblast cells recruit CD56brightCD16- NK cells into decidua by way of expressing and secreting of CXCL12/stromal cell-derived factor 1." J Immunol **175**(1): 61-68.

Xu, C., G. Liguori, M. G. Persico and E. D. Adamson (1999). "Abrogation of the Cripto gene in mouse leads to failure of postgastrulation morphogenesis and lack of differentiation of cardiomyocytes." Development **126**(3): 483-494.

Yadi, H., S. Burke, Z. Madeja, M. Hemberger, A. Moffett and F. Colucci (2008). "Unique receptor repertoire in mouse uterine NK cells." J Immunol **181**(9): 6140-6147.

Yan, Y. T., J. J. Liu, Y. Luo, C. E, R. S. Haltiwanger, C. Abate-Shen and M. M. Shen (2002). "Dual roles of Cripto as a ligand and coreceptor in the nodal signaling pathway." Mol Cell Biol **22**(13): 4439-4449.

Yang, Y. (2012). "Wnt signaling in development and disease." Cell Biosci **2**(1): 14.

Yokota, C., M. Kofron, M. Zuck, D. W. Houston, H. Isaacs, M. Asashima, C. C. Wylie and J. Heasman (2003). "A novel role for a nodal-related protein; Xnr3 regulates convergent extension movements via the FGF receptor." Development **130**(10): 2199-2212.

Yoshinaga, K. (1988). "Uterine receptivity for blastocyst implantation." Ann N Y Acad Sci **541**: 424-431.

Zhang, J., Z. Chen, J. H. Fritz, Y. Rochman, W. J. Leonard, J. L. Gommerman, A. W. Plumb, N. Abraham and B. A. Croy (2012). "Unusual timing of CD127 expression by mouse uterine natural killer cells." J Leukoc Biol **91**(3): 417-426.

Zhang, J., W. S. Talbot and A. F. Schier (1998). "Positional cloning identifies zebrafish one-eyed pinhead as a permissive EGF-related ligand required during gastrulation." Cell **92**(2): 241-251.

Zhang, J. H., A. T. Yamada and B. A. Croy (2009). "DBA-lectin reactivity defines natural killer cells that have homed to mouse decidua." Placenta **30**(11): 968-973.

Zhang, Q. and J. Yan (2016). "Update of Wnt signaling in implantation and decidualization." Reproductive Medicine and Biology **15**(2): 95-105.

Zhang, S., S. B. Kong, B. Y. Wang, X. H. Cheng, Y. J. Chen, W. W. Wu, Q. Wang, J. C. Shi, Y. Zhang, S. M. Wang, J. H. Lu, J. P. Lydon, F. DeMayo, W. S. Pear, H. Han, H. Y. Lin, L. Li, H. M. Wang, Y. L. Wang, B. Li, Q. Chen, E. K. Duan and H. B. Wang (2014). "Uterine Rbpj is required for embryonic-uterine orientation and decidual remodeling via Notch pathway-independent and -dependent mechanisms." Cell Research **24**(8): 925-942.

Zhang, S., H. Lin, S. Kong, S. Wang, H. Wang, H. Wang and D. R. Armant (2013). "Physiological and molecular determinants of embryo implantation." Mol Aspects Med **34**(5): 939-980.

Zhao, K. Q., H. Y. Lin, C. Zhu, X. Yang and H. M. Wang (2012). "Maternal Smad3 deficiency compromises decidualization in mice." Journal of Cellular Biochemistry **113**(10): 3266-3275.

Zhou, Y., O. Genbacev and S. J. Fisher (2003). "The human placenta remodels the uterus by using a combination of molecules that govern vasculogenesis or leukocyte extravasation." Ann N Y Acad Sci **995**: 73-83.

Zybina, E. V. and T. G. Zybina (1996). "Polytene chromosomes in mammalian cells." Int Rev Cytol **165**: 53-119.